

HelmholtzZentrum münchen
German Research Center for Environmental Health

Development and characterisation of an immunochemical test system for the determination of bacterial signal molecules (*N*-acylated homoserine lactones)



Dissertation der Fakultät für Biologie der Ludwig-Maximilians-
Universität München

vorgelegt von

Xiao Chen

November 2010, München

Ehrenwörtliche Erklärung

Hiermit erkläre ich, dass ich die vorliegende Dissertation selbständig und ohne unerlaubte Hilfe angefertigt habe. Ich habe weder anderweitig versucht, eine Dissertation einzureichen oder eine Doktorprüfung durchzuführen, noch habe ich diese Dissertation oder Teile derselben einer anderen Prüfungskommission vorgelegt.

Begutachter 1: Herr Prof. Dr. Anton Hartmann

Begutachter 2: Frau Prof. Dr. Elisabeth Weiss

Datum der Abgabe der Dissertation: 04 November 2010

Datum der mündlichen Prüfung: 10 Mai 2011

Lernen ist wie Rudern gegen den Strom. Hört man damit auf,
treibt man zurück.

----Laozi

INDEX OF CONTENTS

INDEX OF FIGURES.....	8
INDEX OF TABLES	10
INDEX OF ATTACHMENTS	11
ABBREVIATION	12
1 INTRODUCTION	14
1.1 Quorum sensing	14
1.1.1 Discovery of quorum sensing	14
1.1.2 Mechanism of quorum sensing	15
1.1.3 Gram-negative bacteria and AHL (HSL) quorum sensing molecules.....	18
1.1.3.1 <i>Burkholderia cepacia</i> and quorum sensing.....	20
1.1.3.2 <i>Pseudomonas aeruginosa</i> and quorum sensing	21
1.1.3.3 Interspecies communication between <i>P. aeruginosa</i> and <i>B. cepacia</i>	22
1.1.3.4 <i>Pseudomonas putida</i> and quorum sensing	22
1.1.3.5 Quorum sensing in biofilm communities and 1,2,4-trichlorobenzene (TCB) biomineralisation	24
1.2 Quorum quenching	25
1.2.1 Inhibition of AHL signal sensing.....	25
1.2.2 Limitation of signal accumulation-HSL degradation.....	26
1.2.2.1 Abiotic degradation.....	26
1.2.2.2 Enzymatic degradation.....	27
1.2.3 The biological functions of the AHLases.....	28
1.3 Current HSL analytical methods.....	28
1.3.1 Conventional chemical analysis.....	28
1.3.2 Bioreporters	30
1.4 Immunochemistry	31
1.4.1 Introduction of immunochemical techniques	31
1.4.2 Production of antibody.....	31
1.4.2.1 Antibody introduction.....	31
1.4.2.2 Target molecule selection	32
1.4.2.3 Hapten design	33
1.4.2.4 Hapten synthesis and conjugation to carrier molecules	33
1.4.2.5 Immunisation, fusion and hybridoma	34
1.4.3 Immunoassay and different formats.....	36
1.4.3.1 Enzyme-tracer format ELISA	37
1.4.3.2 Coating antigen format ELISA	37
1.4.3.3 Sandwich ELISA	37
1.4.4 Optimisation of immunoassays.....	37
1.4.4.1 Test sensitivity	37
1.4.4.2 Reagents.....	38
1.4.4.3 Hapten conjugates	38
1.4.4.4 Buffers and blocking systems	39
1.4.4.5 Immobilisation on the surface of microtiter plate	39
1.4.5 Immunoassay evaluation.....	39
1.4.6 Fluorescence in immunochemistry	40

1.4.6.1	Fluorescence	40
1.4.6.2	Fluorescent dye conjugation to antibody	41
1.4.6.3	Tyramide Signal Amplification (TSA)	42
1.4.7	Aqua-Optosensor (AOS).....	42
1.5	Outline of goal and tasks for this work	44
2	MATERIALS AND METHODS	45
2.1	Chemicals, standards and proteins.....	45
2.2	Instruments for hapten syntheses	46
2.3	Synthesis of HSL haptens	47
2.3.1	Synthesis of sebacic acid monobenzyl ester (1).....	47
2.3.2	Synthesis of N-(9-benzylcarboxyl-1-hydroxy)-Meldrum's acid (2)	48
2.3.3	Synthesis of N-(11-benzylcarboxy-3-oxoundecanoyl)-L-homoserine lactone (3).....	48
2.3.4	Synthesis of N-(11-carboxy-3-oxoundecanoyl)-L-homoserine lactone (HSL1) (4)	49
2.3.5	Synthesis of N-(5-carboxypentanoyl)-L-homoserine lactone (HSL2) (5).....	50
2.3.6	Synthesis of N-(11-benzylcarboxy-3-hydroxyundecanoyl)-L-homoserine lactone (6).....	51
2.3.7	Synthesis of N-(11-carboxy-3-hydroxyundecanoyl)-L-homoserine lactone (HSL3) (7)	51
2.3.8	Synthesis of N-(9-benzylcarboxy nonanoyl)-L-homoserine lactone (8)	52
2.3.9	Synthesis of N-(9-carboxynonanoyl)-L-homoserine lactone 8 (HSL 4)	53
2.4	Materials and instruments for ELISA	54
2.5	Preparation of hapten-protein conjugates for immunogens and coating antigens.....	54
2.6	Characterisation of hapten protein conjugates with UV absorbance spectra	57
2.7	Preparation of enzyme-tracers	57
2.8	Production of anti-HSL monoclonal antibodies	58
2.9	Determination of immunoglobulin type	59
2.10	Purification of monoclonal antibodies and determination of protein concentration	59
2.11	Characterisation of HSL antibodies (anti-HSL mAbs) with enzyme-linked immunosorbent assay (ELISA).....	59
2.11.1	Standard procedure of coating antigen format ELISA	60
2.11.2	ELISA in the enzyme-tracer format	61
2.11.3	Titration and screening against HSL substances	62
2.11.4	Binding test to a few possible HSL degradation substances	63
2.11.5	Standard curves.....	64
2.11.6	Determination of cross reactivity	65
2.12	Detection of HSLs in biological samples with ELISA	65
2.12.1	Standard curves in matrix: determination of matrix effects	66
2.12.2	Standard curves in ABC Medium: determination of HSL in <i>B. cepacia</i> LA3 supernatants	66
2.13	Preparation of biological samples.....	66
2.13.1	Preparation of <i>Burkholderia cepacia</i> culture supernatants	67
2.13.2	Preparation of <i>Pseudomonas putida</i> culture supernatants.....	67
2.13.3	Preparation of 1,2,4-TCB-mineralising bacterial biofilm community samples	68
2.14	HSL antibody characterisation with Aqua-Optosensor (AOS).....	68
2.15	Optimisation of fluorescent labelling	70
2.15.1	Antibody-dye conjugation	70

2.15.2	Determination of the label degree	71
2.15.3	Affinity test of fluorophore labelled antibodies	72
2.16	In situ experiments.....	72
2.16.1	<i>B. cepacia</i> biofilm in flow chamber system-ibidi slide.....	72
2.16.2	<i>Pseudomonas putida</i> IsoF on the root of barley.....	75
2.16.2.1	Preparation of the plant roots inoculated with <i>P. putida</i> IsoF.....	75
2.16.2.2	HSL antibody treatment on the barley root.....	75
3	RESULTS.....	76
3.1	Selection of hapten for immunisations	76
3.2	Hapten-protein conjugate characterisation with UV absorbance spectrum	77
3.3	Coating antigens and enzyme-tracers selection.....	82
3.4	Antibody screening	82
3.5	Antibody subclass determination and purification	86
3.6	Anti-HSL antibody characterisation with ELISAs	86
3.6.1	Comparison of ELISA in the coating antigen and in the enzyme-tracer formats.....	94
3.6.2	Difference in selectivities of anti-HSL1-, anti-HSL1/2-, and anti-HSL4 mAbs to HSL compounds	95
3.6.3	Recognition of HSL and HS	97
3.6.4	Recognition of HSL side chain length	97
3.6.5	Recognition of haptens	98
3.7	HSL detection in biological samples.....	99
3.7.1	<i>Burkholderia cepacia</i> isolate LA3	99
3.7.1.1	Matrix effects in ABC medium.....	99
3.7.1.2	Assay comparison with two mAbs and two setups with <i>B. cepacia</i> LA3 culture supernatants.....	100
3.7.1.3	Dilution control of <i>B. cepacia</i> LA3 culture supernatants.....	102
3.7.1.4	Hydrolysis and spiking experiments	103
3.7.2	HSL detection in <i>Pseudomonas putida</i> cultural supernatant.....	105
3.7.3	HSL detection in TCB degradation bacterial community	105
3.8	AOS results of mAb HSL1/2-2C10	106
3.9	Fluorophore labelled antibodies	109
3.10	In situ experiments.....	111
4	DISCUSSION	114
4.1	Selection of HSL haptens.....	114
4.2	Hapten conjugation and conjugates characterisation.....	114
4.3	HSL-protein and HSL-HRP conjugates selection for ELISAs	115
4.4	Antibody screening	115
4.5	Comparison of coating antigen and enzyme-tracer format assays	116
4.6	Comparison of ELISA and AOS.....	116
4.7	Antibody recognition of homoserine lactone (HSL) and homoserine (HS) compounds .	117

4.8	Biological relevance of HSL and HS.....	119
4.9	Development of QQ innovative biological tools.....	120
4.9.1	Immunotherapy.....	120
4.9.2	QQ bacterial strains as biocontrol agents.....	120
4.10	Comparison of the current methods for HSL and HS analysis	121
4.11	Matrix effects.....	124
4.12	Possible problems and suggestions of immunoassays	125
4.13	Difficulties and solutions of fluorescence based in situ experiments	125
5	SUMMARY	127
6	ZUSAMMENFASSUNG	129
7	REFERENCES	132
8	PUBLICATIONS.....	141
9	ACKNOWLEDGEMENTS	142
10	ATTACHMENTS	143
	CURRICULUM VITAE.....	164

Index of figures

Figure 1 Quorum sensing	15
Figure 2 Simplified quorum sensing mechanisms	17
Figure 3 Structures of some representative signal molecules	18
Figure 4 Dynamic curves of 3oxo-C10-HSL and 3oxo-C10-HS in <i>P. putida</i> culture supernatant	23
Figure 5 Quorum sensing inhibitors.....	26
Figure 6 HSL-degradation pathways and degradation products.	27
Figure 7 Structure of monoclonal antibody molecule.....	32
Figure 8 Monoclonal antibody production.....	35
Figure 9 Chemical structures of typical fluorescent dyes	41
Figure 10 Fluorescent dye conjugation using activated amino groups on lysine residues of proteins.....	42
Figure 11 Principle of the Aqua-Optosensor.....	43
Figure 12 Mass spectrum (LC-MS) of HSL3.....	52
Figure 13 Schematic protein conjugation process of HSL3.....	55
Figure 14 Scheme of coating antigen format ELISA.....	61
Figure 15 Scheme of enzyme-tracer format ELISA.....	62
Figure 16 A template example for titration in coating antigen format.....	63
Figure 17 Tested HSL/HS analogues	64
Figure 18 Aqua-Optosensor instruments.....	69
Figure 19 Chemical structure and fluorescent spectra and of Oyster-645	70
Figure 20 Antibody treatment of biofilm on ibidi slide	72
Figure 21 <i>In situ</i> experiment design with Oyster-645 labeled HSL antibody and Cy3-TSA ..	73
Figure 22 Antibody treatments of roots	74
Figure 23 HSL hapten structures (detailed chemical names see section 2.3)	76
Figure 24 UV spectra of HSL1 and HSL2 conjugates	78
Figure 25 UV spectra of HSL4 conjugates	79
Figure 26 UV spectra of HSL3 conjugates	80
Figure 27 HSL1/2-2C10 inhibition test against HSL substances in enzyme-tracer format.....	83
Figure 28 HSL4-5E12 inhibition tests against HSL substances in enzyme-tracer format.....	83
Figure 29 HSL1/2-2C10 coating antigen format standard curves.....	94
Figure 30 HSL1/2-2C10 enzyme-tracer format standard curve.....	95
Figure 31 HSL1-1A5 coating antigen format standard curves	96

Figure 32 HSL4-5H3 coating antigen format standard curves	97
Figure 33 HSL1/2-2C10 recognition of different chain length.....	98
Figure 34 Matrix effects in ABC medium.	100
Figure 35 Comparison of two ELISAs with different antibodies and set A and B of undiluted <i>B. cepacia</i> culture supernatants.....	101
Figure 36 HSLs detected with UPLC-MS in <i>B. cepacia</i> LA3 culture supernatant.....	102
Figure 37 Dilution controls in ELISA using mAb HSL1/2-2C10 (400 ng mL ⁻¹) and enzyme-tracer HSL3-HRP (1:600)	103
Figure 38 Hydrolysis and spiking experiments with 1:10 diluted <i>B. cepacia</i> culture supernatants.....	104
Figure 39 <i>P. putida</i> supernatants HSL detection with 24h inoculation time	105
Figure 40 HSL detection of TCB degradating bacterial communities	106
Figure 41 AOS peaks of Oyster-645 labelled mAb HSL1/2-2C10 without analyte	107
Figure 42 Standard curves of 3oxo-C10-HS with AOS	108
Figure 43 Standard curves of C10-HS with AOS	109
Figure 44 AOS affinity determination of HSL1-1A5 after fluorescent labelling	110
Figure 45 Inhibition 2D tests of HSL1-1A5+Oyster645 with coating antigen format ELISA	111
Figure 46 LSM-images of Oyster labeled mAb on <i>B. cepacia</i> LA3 biofilm in ibidi slide....	112
Figure 47 LSM-images of barley root with Oyster 645-labelled HSL1/2-2C10	113

Index of tables

Table 1 Quorum sensing bacteria and their signal molecules (an incomplete list).....	19
Table 2 Conventional AHL analytical methods	29
Table 3 Principal strategies for protein conjugates	34
Table 4 Commercially purchased HSL standards	45
Table 5 Preparation of hapten-protein conjugates for immunogens and coating antigens	56
Table 6 Concentration of haptens, proteins and conjugates for UV absorbance spectra	57
Table 7 Materials for enzyme-tracer production.....	58
Table 8 Spectra characteristics of the Oyster-645 (Ref: www.biolabels.com)	72
Table 9 Selected HSL1 and HSL1/2 antibodies and characterisation with coating antigen format	84
Table 10 Selected HSL4 antibodies and characterisation with coating antigen format	85
Table 11 Purified HSL antibodies	86
Table 12 Cross reactivity of mAbs in coating antigen format	88
Table 13 Cross reactivity of mAbs in enzyme- tracer format	90
Table 14 Test midpoints (IC_{50}) of main analytes using coating antigen format	92
Table 15 Test midpoints (IC_{50}) of main analytes using enzyme-tracer format	93
Table 16 IC_{50} and LOD comparison of ELISA and AOS	117
Table 17 Comparison of analytical methods for HSL compounds	122
Table 18 Matrix effects of different media	124

Index of attachments

Attach. 1 Chemicals for synthesis	143
Attach. 2 Buffers and media used in this study	144
Attach. 3 First screening of HSL1 and HSL1/2 antibodies with coating antigen format	147
Attach. 4 Characterisation of selected HSL4 mAbs with enzyme-tracer format	152
Attach. 5 HSL1-8E1 coating antigen format standard curves	155
Attach. 6 HSL4-5E12 coating antigen format standard curves	156
Attach. 7 HSL4-6D3 coating antigen format standard curves	157
Attach. 8 HSL4-4C9 coating antigen format standard curves	158
Attach. 9 AOS peaks of Oyster-645 labelled mAb HSL1/2-2C10 with analyte 3oxo-C10-HS concentration of [$55.5 \mu\text{g L}^{-1}$]	159
Attach. 10 AOS peaks of Oyster-645 labelled mAb HSL1/2-2C10 with analyte 3oxo-C10-HS concentration of [$123.3 \mu\text{g L}^{-1}$]	160
Attach. 11 HSL antibody recognition of DL and L HSL isomers in coating antigen format ELISA	161
Attach. 12 <i>P. putida</i> IsoF and strain KT2440 supernatants HSL detection with different sampling time	162
Attach. 13 HSL detection in extracted soil samples with inoculated TCB community	162
Attach. 14 LSM images of TSA and HSL mAb treated <i>B. cepacia</i> LA3 biofilm in ibidi slide	163
Attach. 15 HSL3 antibody list	163

Abbreviation

Ab: antibody

AI: autoinducer

ACN: acetonitrile

AHL (HSL): *N*-acylated homoserine lactone

AOS: Aqua-Opto sensor

Bcc: *Burkholderia cepacia* complex

Bn: benzyl

BSA: bovine serum albumin

CBs: chlorobenzenes

CF: Cystic Fibrosis

CONA: conalbumin

CR: cross reactivity

Da: dalton

DCC: 1,3-dicyclohexylcarbodiimide

DMF: dimethylformamide

RIA: radioimmunoassay

EA: ethyl acetate

EIAs: enzyme immunoassays

ELISA: enzyme-linked immunosorbent assay.

EW: evanescent wave

GAR: goat anti-rat

Gfp: green fluorescent protein

HRP: horseradish peroxidase

HS: homoserine

IA: immunoassay

IgG: immunoglobulin G

IgM: immunoglobulin M

IC₅₀: inhibitory concentration 50%, test midpoint of the standard curve

K_d: dissociation constant

KLH: Keyhole limpet hecocyenin

LC: liquid chromatography

LOD: limit of detection

mAb: monoclonal antibody

NaOH: sodium hydroxide

NHS: *N*-hydroxysuccinimide

NMR: nuclear magnetic resonance

MS: mass spectrometry

OD: optical density

OVA: ovalbumin

PBS: phosphate-buffered saline

PQS: *Pseudomonas* quinolone signal

PBST: phosphate-buffered saline with Tween 20

Protein G: protein G from *Streptococcus*

QS: quorum sensing

QQ: quorum quenching

RT: room temperature

SPR: surface plasmon resonance

TBAB: tetrabutyl ammonium bromide

TIRF: total internal reflectance fluorescence

TG: tyroglobulin

TMB: 3,3',5,5'-tetramethylbenzidine

TSA: tyramide signal amplification

PMMA: polymethyl methacrylate

HSL standards

C4-HSL: *N*-butyryl-L-homoserine lactone

3oxo-C4-HSL: *N*-3-oxo-butyryl-L-homoserine lactone

3OH-C4-HSL: *N*-3-hydroxy-butyryl-L-homoserine lactone

C6-HSL: *N*-hexanoyl-L-homoserine lactone

3oxo-C6-HSL: *N*-3-oxo-hexanoyl-L-homoserine lactone

3OH-C6-HSL: *N*-3-hydroxy-hexanoyl-L-homoserine lactone

C8-HSL: *N*-octanoyl-L-homoserine lactone

3oxo-C8-HSL: *N*-3-oxo-octanoyl-L-homoserine lactone

3OH-C8-HSL: *N*-3-hydroxy-octanoyl-L-homoserine lactone

C10-HSL: *N*-decanoyl-L-homoserine lactone

3oxo-C10-HSL: *N*-3-oxo-decanoyl-L-homoserine lactone

3OH-C10-HSL: *N*-3-hydroxy-decanoyl-L-homoserine lactone

C12-HSL: *N*-dodecanoyl-L-homoserine lactone

3oxo-C12-HSL: *N*-3-oxo-dodecanoyl-L-homoserine lactone

3OH-C12-HSL: *N*-3-hydroxy-dodecanoyl-L-homoserine lactone

1 Introduction

1.1 Quorum sensing

1.1.1 Discovery of quorum sensing

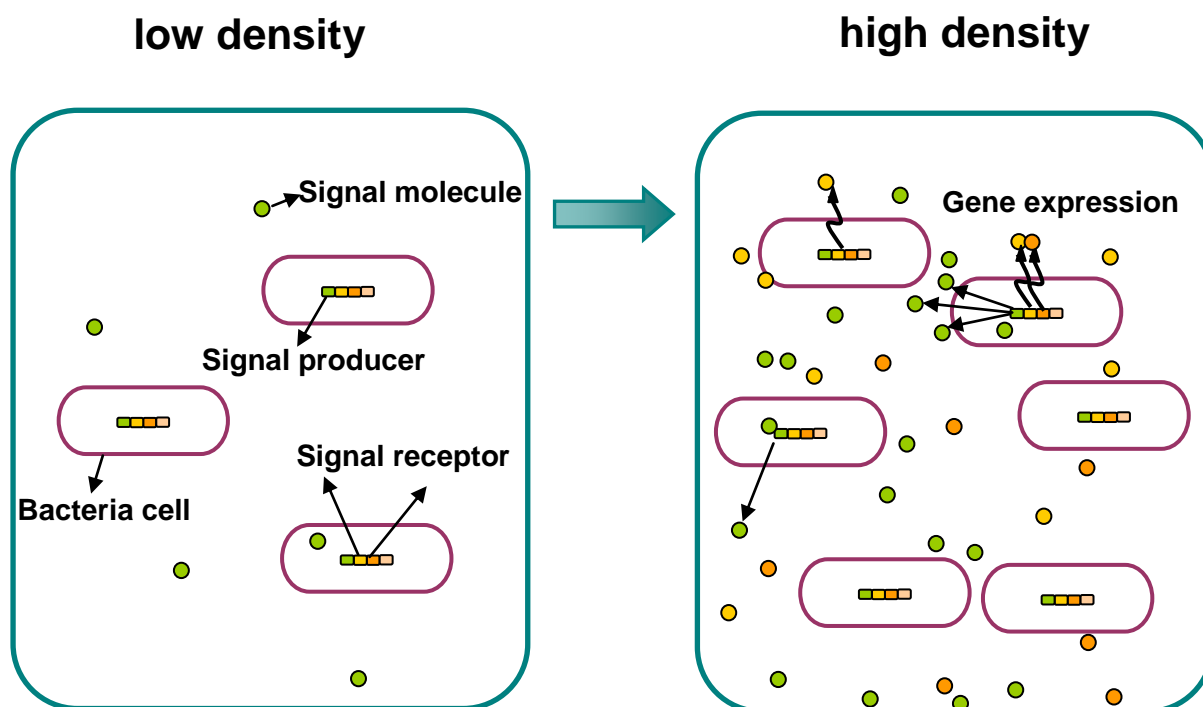
Quorum sensing has been an important topic only since a few decades. In the 300 years since van Leeuwenhoek's remarkable descriptions of the teeming world of microorganisms, bacteria have been regarded as deaf mutes going about their business without communicating with their neighbours (Bassler & Losick, 2006). It was not until the 1960s and 1970s, with the discovery of what is now called quorum sensing (QS), that it became evident that bacteria possess sophisticated systems of communication that enable them to send and receive chemical messages to and from other bacteria. In its simplest form, quorum sensing is a cell-cell communication mechanism by which bacteria count their own numbers by producing and detecting the accumulation of a signalling molecule that they export into their environment (Bassler & Losick, 2006). We now know that QS-mediated communication is more complicated than originally assumed and, furthermore, is one of several mechanisms bacteria use to interact with other cells. The concept of intercellular communication within a bacterial population originates for the discoveries of Tomasz (1965) on genetic competence in *Streptococcus pneumoniae* (then known as *Pneumococcus*) and Nealson *et al.* (1970) on bioluminescence in *Vibrio*. Competence is a physiological state in which bacteria are capable of taking up and undergoing genetic transformation by DNA molecules. In 1965, Tomasz reported that entry into the competent state is governed by an extracellular factor that is manufactured by *Streptococcus* itself (Tomasz, 1965). Thus, the competence factor, which was later shown to be a modified peptide, was described as a "hormone-like activator" that synchronises the behaviour of the bacterial population. In 1970, it was shown that two obscure species of bioluminescent marine bacteria, *Vibrio fischeri* and *Vibrio harveyi*, produced light at high cell density but not in dilute suspensions (Nealson *et al.*, 1970). Light production could be stimulated by the exogenous addition of cell-free culture fluids, and the component responsible, called the autoinducer (AI), was later identified as an acyl-homoserine lactone (Eberhard *et al.*, 1981; structures present in Figure 3). The combined findings of Tomasz (1965) and Nealson (1970) suggested that certain bacteria use the production, release, exchange, and detection of signalling molecules to measure their population density and to control their behaviour in response to variations in cell numbers. For nearly 20 years, these cell-cell signalling phenomena were considered unusual

occurrences restricted to a few specialised bacteria. It is now clear that intercellular communication is not the exception but, rather, is the norm in the bacterial world and that this process, called quorum sensing, is fundamental to all of microbiology (Bassler & Losick, 2006). In addition, bacterial AHL QS molecules are recognised by higher organisms, including plant and human. AHL-producing bacteria are associated with pathogenic, commensalic or even beneficial interactions (Hughes & Sprendio, 2008).

1.1.2 Mechanism of quorum sensing

Bacteria release a wide variety of small molecules including secondary metabolites such as antibiotics and siderophores (iron chelators), metabolic end products and cell-to-cell signalling molecules into the environment. In many instances, the latter are considered to provide the bacterial population with a means of determining its numerical size (or density). As the bacterial culture grows, signal molecules are released into the extracellular milieu and accumulate. Once a threshold concentration of the molecule (and consequently a specific population density) is achieved, a co-ordinated change in bacterial behaviour is initiated (illustrated in Figure 1, Williams *et al.*, 2007).

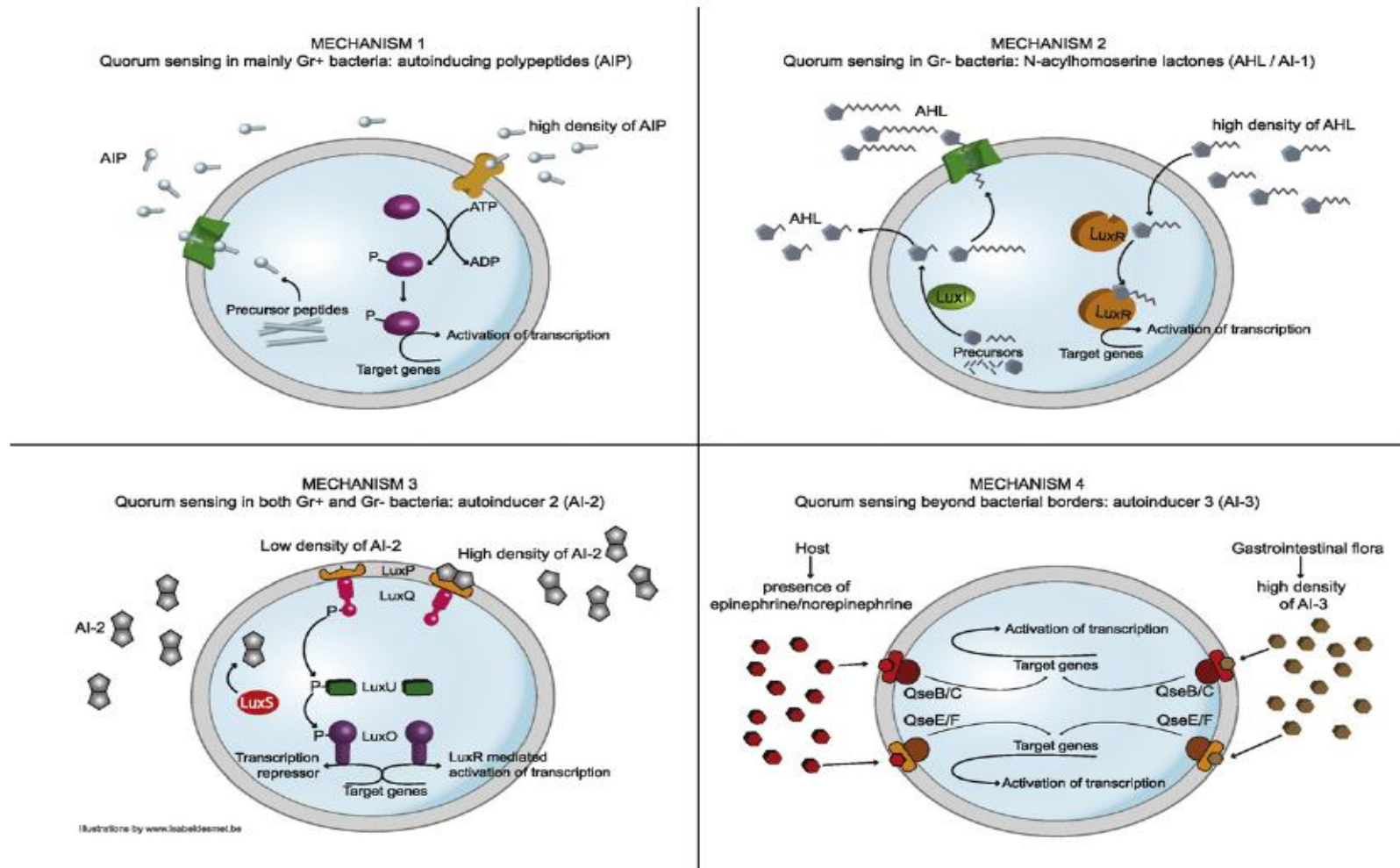
Figure 1 Quorum sensing



When the bacterial density is low (left), the concentration of signal molecules is also low. When the cell density (also the signal molecules) reaches a critical level, the bacteria start QS regulated gene expression (right).

Fuqua et al. (1994) firstly introduced the term 'quorum sensing' to describe this phenomenon. The term QS does not, however, adequately describe all situations where bacteria employ diffusible chemical signals. The size of the quorum, for example, is not fixed but will vary according to the relative rates of production and loss of signal molecule, i.e. it is dependent on the prevailing local environmental conditions (Hense *et al.*, 2007). It is also possible for a single bacterial cell to switch from the 'non-quorate' to the 'quorate' state as has been observed for *Staphylococcus aureus* trapped within an endosome in endothelial cells (Qazi *et al.*, 2001). In this context, 'diffusion sensing' or 'compartment sensing' are more appropriate terms since the signal molecule is supplying information with respect to the local environment rather than cell population density (Redfield, 2002; Winzer *et al.*, 2002). Quorum sensing might therefore be better considered as a special category of diffusion sensing where, in a given environment, the threshold concentration of signal molecule required to trigger a response can only be achieved by more than one cell (Redfield, 2002; Winzer *et al.*, 2002). Furthermore, it should be remembered that quorum sensing, as the determinant of cell population density, is only one of many different environmental signals (e.g. temperature, pH, osmolarity, oxidative stress, nutrient deprivation) which bacterial cells must integrate in order to determine their optimal survival strategy (Qazi *et al.*, 2001). Thus, QS is an integral component of the global gene regulatory networks which are responsible for facilitating bacterial adaptation to environmental stress (Hense *et al.*, 2007; Williams *et al.*, 2007).

Figure 2 Simplified quorum sensing mechanisms

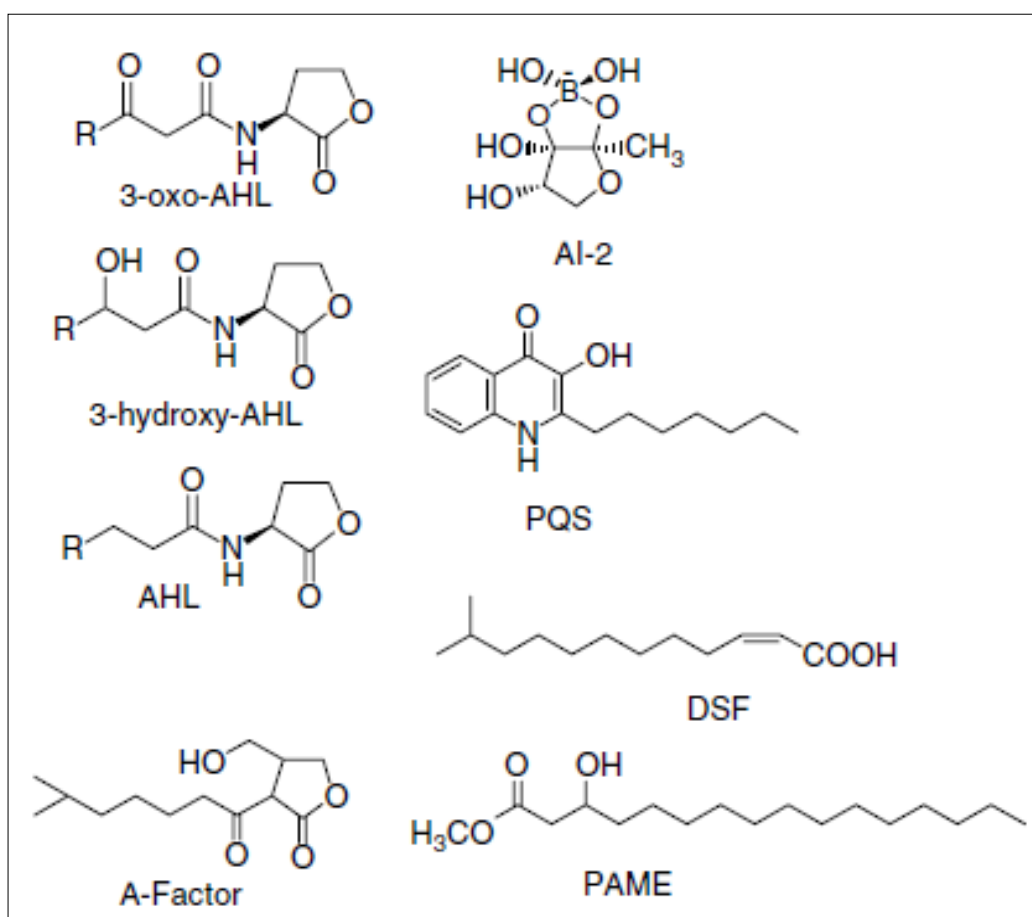


Mechanism 1 for quorum sensing in Gram-positive bacteria using polypeptide autoinducer; Mechanism 2 for Gram-positive bacteria employ *N*-acylated-homoserine lactones as signal molecules; Mechanism 3, quorum sensing in both Gram-positive and Gram-negative bacteria using autoinducer 2; Mechanism 4 describes quorum sensing beyond bacterial borders: autoinducer 3. Ref: (Boyen *et al.*, 2009)

1.1.3 Gram-negative bacteria and AHL (HSL) quorum sensing molecules

AHLs (HSLs) were the initially introduced QS molecules. However, they are not the only class of QS signal molecules. In Gram-negative bacteria, 4-quinolones, fatty acids and fatty acid methyl esters have been identified as QS signal molecules (Figure 3). Apart from γ -butyrolactones such as Khoklov's A-factor produced by *Streptomyces* (Figure 3), Gram-positive bacteria employ unmodified (e.g. the competence stimulating factors of *S. pneumoniae*) or post translationally modified peptides such as the staphylococcal cyclic peptides (not shown). Although no 'universal' bacterial quorum sensing system or signal molecule family has yet been discovered, many Gram-negative and Gram-positive bacteria produce 'autoinducer-2' (Figure 3), a collective term for a family of interconvertible furanone compounds (Williams *et al.*, 2007).

Figure 3 Structures of some representative signal molecules



3-oxo-AHL, 3-OH-AHL, and AHL (R ranges from C1 to C15). The acyl side chains may also contain one or more double bonds: A-factor, 2-isocapryloyl-3-hydroxymethyl-g-butyrolactone; AI-2, autoinducer-2, furanosyl borate ester form; PQS, *Pseudomonas* quinolone signal, 2-heptyl-3-hydroxy-4(1H)-quinolone; DSF, 'diffusible factor', methyl dodecenoic acid; PAME, hydroxyl-palmitic acid methyl ester. Ref: (Williams *et al.*, 2007).

Some examples of *LuxR/LuxI/AHL*-dependent quorum sensing systems in Gram-negative bacteria have been reviewed in (Williams *et al.*, 2007). The individual bacteria use different QS mechanism, different QS molecules and have different biological function. The details are listed in Table 1.

Table 1 Quorum sensing bacteria and their signal molecules (an incomplete list)

organism	major AHL(s)	LuxR	LuxI	phenotypes
<i>Aeromonas hydrophila</i>	C4-HSL	AhyR	AhyI	biofilms, exoproteases
<i>Aeromonas salmonicida</i>	C4-HSL	AsaR	AsaI	exoprotease
<i>Agrobacterium tumefaciens</i>	3-oxo-C8-HSL	TraR	TraI	plasmid conjugation
<i>Agrobacterium vitiae</i>	C14:1-HSL, 3-oxo-C16:1-HSL	AvsR	AvsI	virulence
<i>Burkholderia cenocepacia</i>	C6-HSL, C8-HSL	CepR, CciR	CepI, CciI	exoenzymes, biofilm formation, swarming motility, siderophore, virulence
<i>Burkholderia pseudomallei</i>	C8-HSL, C10-HSL, 3-hydroxy-C8-HSL, 3-hydroxy-C10-HSL, 3-hydroxy-C14-HSL	PmlIR1, BpmR2, BpmR3	PmlI1, PmlI2, PmlI3	virulence, exoprotease
<i>Burkholderia mallei</i>	C8-HSL, C10-HSL	BmaR1, BmaR3, BmaR4, BmaR5	BmaI1, BmaI3	Virulence
<i>Chromobacterium violaceum</i>	C6-HSL	CviR	CviI	exoenzymes, cyanide, pigment
<i>Erwinia carotovora</i> ssp. <i>carotovora</i>	3-oxo-C6-HSL	ExpR/CarR	CarI (ExpI)	carbapenem, exoenzymes, virulence
<i>Pantoea (Erwinia) stewartii</i>	3-oxo-C6-HSL	EsaR	EsaI	exopolysaccharide
<i>Pseudomonas aeruginosa</i>	C4-HSL; 3-oxo-C12-HSL	LasR, RhlR, QscR, VqsR	LasI, RhlI	exoenzymes, secretion, HCN, biofilms
<i>Pseudomonas aureofaciens</i>	C6-HSL	PhzR, CsaR	PhzI, CsaI	phenazines, protease, colony morphology, aggregation
<i>Pseudomonas putida</i>	3-oxo-C10-HSL, 3-oxo-C12-HSL	PpuR	PpuI	biofilm formation
<i>Pseudomonas chlororaphis</i>	C6-HSL	PhzR	PhzI	phenazine-1-carboxamide
<i>Pseudomonas syringae</i>	3-oxo-C6-HSL	AhIR	AhII	exopolysaccharide, swimming motility, virulence
<i>Rhizobium leguminosarum</i> bv <i>viciae</i>	7- <i>cis</i> -C14-HSL/C6-HSL/C7-HSL/C8-HSL, 3-oxo-C8-HSL, 3-hydroxy-C8-HSL	CinR, RhiR, RaiR, TraR, BisR, TriR	CinI, RhiI, RaiI	root nodulation/symbiosis, plasmid transfer, growth inhibition; stationary phase adaptation
<i>Rhodobacter sphaeroides</i>	7- <i>cis</i> -C14-HSL	CerR	CerI	aggregation
<i>Serratia</i> spp. ATCC 39006	C4-HSL	SmaR	SmaI	antibiotic, pigment, exoenzymes
<i>Serratia liquefaciens</i> MG1	C4-HSL	SwrR	SwrI	swarming motility, exoprotease, biofilm development, biosurfactant
<i>Serratia marcescens</i> SS-1	C6-HSL, 3-oxo-C6-HSL	SpnR	SpnI	sliding motility, biosurfactant, pigment, nuclease, transposition frequency
<i>Serratia proteamaculans</i> B5a	3-oxo-C6-HSL	SprR	SprI	exoenzymes
<i>Sinorhizobium meliloti</i>	C8-HSL, C12-HSL, 3-oxo-C14-HSL, 3-oxo-C16:1-HSL, C16:1-HSL, C18-HSL	SinR, ExpR, TraR	SinI	nodulation/symbiosis
<i>Vibrio fischeri</i>	3-oxo-C6-HSL	LuxR	LuxI	bioluminescence
<i>Yersinia enterocolitica</i>	C6-HSL, 3-oxo-C6-HSL, 3-oxo-C10-HSL, 3-oxo-C12-HSL, 3-oxo-C14-HSL	YenR, YenR2	YenI	swimming and swarming motility
<i>Yersinia pseudotuberculosis</i>	C6-HSL, 3-oxo-C6-HSL, C8-HSL	YpsR, YtbR	YpsI, YtbI	motility, aggregation

Ref: (Williams *et al.*, 2007)

1.1.3.1 *Burkholderia cepacia* and quorum sensing

The *Burkholderia cepacia* complex (Bcc) consists of seventeen closely related species (Vanlaere *et al.*, 2009), which were isolated from different natural habitats, such as plant rhizosphere, soil and river water (Chiarini *et al.*, 2006; Jha *et al.*, 2009). They were also found in some urban environments like playgrounds and athletic fields (Fries *et al.*, 1997; Bevivino *et al.*, 2000; Heungens & Parke, 2000; Fiore *et al.*, 2001; Miller *et al.*, 2002; Lee, 2003; Vermis *et al.*, 2003). Furthermore, they are able to promote plant growth, enhance plant disease resistance (Bevivino *et al.*, 1998; Peix *et al.*, 2001; Jha *et al.*, 2009) and were applied for bioremediation (Master *et al.*, 2002; Jiang *et al.*, 2008). However, the genus also contains primary pathogens for animals and humans. Disease in humans normally occurs in individuals who are frequently exposed to contaminated sites through bacterial infection of minor cuts or abrasions or inhalation of dusts (Dance, 2002). Bcc strains can cause life-threatening lung infections in patients requiring mechanical ventilation and in individuals with chronic granulomatous disease or cystic fibrosis (CF) (Eberl, 2006). In fact, over the past two decades, the number of human infections caused by *Burkholderia*-like bacteria has increased markedly. Polyphasic-taxonomic studies revealed that these organisms comprise a very heterogeneous group of strains, collectively referred to as the Bcc (Coenye & Vandamme, 2003). The Bcc species employ quorum sensing, using AHLs as autoinducers. Most members of the Bcc were found to use the *CepIR* QS system (Lewenza *et al.*, 1999). Numerous AHLs with different side chain length and functional groups at the C3 position were confirmed as AIs for Bcc species (Sokol *et al.*, 2007). Furthermore, the evidence of interspecies communication between *B. cepacia* and *Pseudomonas aeruginosa* in CF patients was also suggested to be related to QS and this correlation may cause a higher risk for the infected patients (McKenney *et al.*, 1995; Eberl, 2006).

Initial evidence for the production of signal molecules by a Bcc strain was obtained from cross-feeding experiments, which showed that AHL-containing culture supernatants of *P. aeruginosa* stimulated production of siderophores, protease and lipase in *B. cepacia* 10661 (McKenney *et al.*, 1995). The first QS genes in a Bcc strain were identified in a screen for transposon insertion mutants that hyperproduced siderophores on chrome azurol S agar (Lewenza *et al.*, 1999). This work showed that the QS system of *B. cenocepacia* K56-2 consists of the AHL synthase *CepI*, which directs the synthesis of *N*-octanoyl-homoserine lactone (C8-HSL) and, as a minor by-product, *N*-hexanoyl-homoserine lactone (C6-HSL), and the transcriptional regulator *CepR*. *CepR* was shown to tightly control expression of *cepI*,

likely through binding to a *lux* box-like sequence that partially overlaps the -35 region of the putative *cepI* promoter (Lewenza & Sokol, 2001). This positive feedback loop ensures that a very rapid increase in target gene expression occurs once the system has been triggered. Interestingly, *CepR* negatively controls its own regulation, i.e. is auto-regulated. A highly similar QS system was identified in a screen for mutants defective in biofilm formation of *B. cenocepacia* H111 (Gotschlich *et al.*, 2001; Huber *et al.*, 2001). Moreover, systematic surveys revealed that in fact representatives of all Bcc species contain the *CepI/CepR* QS system and produce mostly C8-HSL and the amount of AHLs produced by different Bcc strains varies dramatically with concentrations ranging from 10 nM to 1 mM for the abundant C8-HSL (Gotschlich *et al.*, 2001). Given that most *B. multivorans* and several *B. cenocepacia* strains produce extremely low amounts of C8-HSL (less than 1 nM), it has been suggested that additional regulatory factors may be present in these strains that silence *cepI* expression (Eberl, 2006).

B. cepacia LA3, an isolate from rice rhizosphere, produces mainly C10-HSL among C8-HSL at published concentration of 1.61 μ M (Li *et al.*, 2006). Using single drop microextraction (SDME), Malik *et al.* (2009) reported that both optical isomers of C10-HSL (D and L) were determined from the cell-free supernatant, while L-C10-HSL was dominant. The HSL detection of the *B. cepacia* LA3 supernatant with immunoassay and the *in situ* experiment with *B. cepacia* biofilm on ibidi slides will be introduced below.

1.1.3.2 *Pseudomonas aeruginosa* and quorum sensing

P. aeruginosa is an opportunistic human pathogen that causes chronic infection in CF patients. The pathogenicity of *P. aeruginosa* depends on multiple cell-associated factors such as alginate, pili, and lipopolysaccharide, and on extracellular virulence factors including proteases (elastase, alkaline protease, and *LasA* protease), hemolysins (rhamnolipid and phospholipase), and toxins (exoenzyme S and exotoxin A, Geisenberger *et al.*, 2000).

P. aeruginosa possesses two *N*-acylhomoserine lactone (AHL) dependent QS systems consisting of two pairs of *LuxRI* homologs, *LasRI* and *RhlRI*, respectively. *LasR* and *RhlR* are both *LuxR*-type transcriptional activators that are activated by AHLs synthesized via *LasI* (*N*-3-oxo-dodecanoyl-homoserine lactone) and *RhlI* (*N*-butanoyl-homoserine lactone), respectively (Diggle *et al.*, 2007). The *P. aeruginosa las* and *rhl* regulatory circuitry is linked to a second QS signalling system, which employs 2-heptyl-3-hydroxy-4(1H)-quinolone, the *Pseudomonas* quinolone signal (PQS; for structure, see Figure 3) (Pesci *et al.*, 1999; Diggle *et*

al., 2006). In common with the AHLs, PQS regulates the production of virulence determinants including elastase, rhamnolipids, the galactophilic lectin, LecA, and phycocyanin (a blue-green phenazine pigment) and have an influence on biofilm development (Pesci *et al.*, 1999; Diggle *et al.*, 2003). In contrast to the AHLs, when supplied exogenously, PQS overcomes the cell-population density-dependent production of *P. aeruginosa* exoproducts (Diggle *et al.*, 2003).

1.1.3.3 Interspecies communication between *P. aeruginosa* and *B. cepacia*

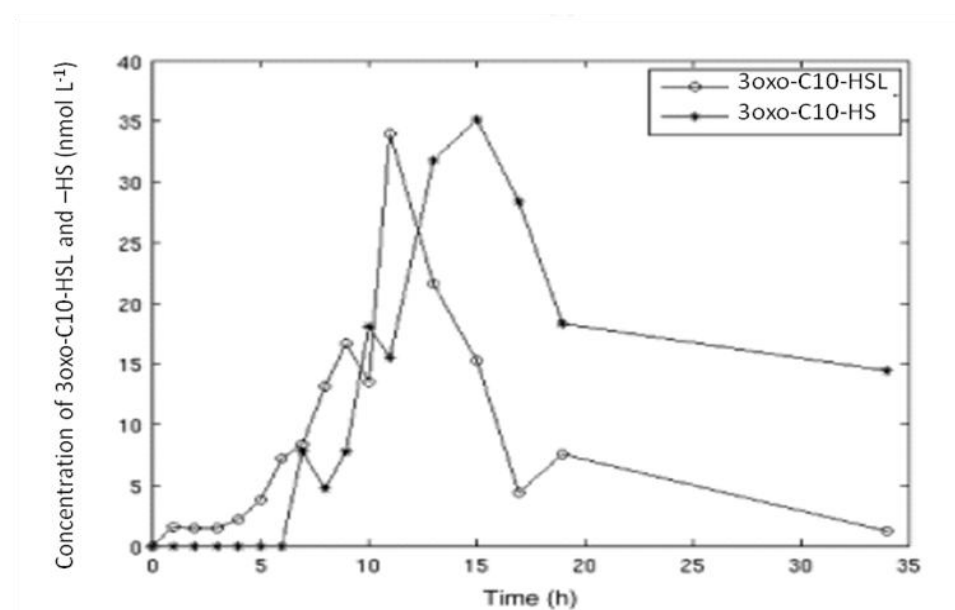
During chronic co-infection, *P. aeruginosa* and *B. cepacia* form mixed biofilms in the lungs of CF patients. Given that both bacteria utilize AHL signal molecules to control biofilm formation and expression of virulence factors, it appears likely that the two strains are not only capable of communicating with each other, but that these interactions may be of profound importance for the virulence of the mixed consortium (Geisenberger *et al.*, 2000). Using *gfp*-based biosensors it was possible to visualise AHL-mediated communication in mixed biofilms, which were cultivated either in artificial flow chambers or in alginate beads in mouse lung tissue (Riedel *et al.*, 2001). These investigations revealed that in both model systems *B. cepacia* is capable of perceiving the AHL signals produced by *P. aeruginosa*, while the latter strain did not respond to the molecules produced by *B. cepacia*, supporting the view of unidirectional communication between the two strains. The clinical importance of AHL-mediated cross-communication for the virulence of the mixed consortium during co-infection is subject of on-going investigations (Eberl, 2006).

1.1.3.4 *Pseudomonas putida* and quorum sensing

Another member of *Pseudomonas* family, *Pseudomonas putida* strains are frequently isolated from the rhizosphere of plants and many strains promote plant growth, exhibit antagonistic activities against plant pathogens and have the capacity to degrade pollutants (Arevalo-Ferro *et al.*, 2005). As previously described *Pseudomonas* species, *P. putida* also employs AHLs as QS molecules. Recent work demonstrated that the tomato rhizosphere isolate *P. putida* IsoF produces a wide spectrum of signal molecules including AHLs with side chain length from C6 to C14 with different substitutions (Steidle *et al.*, 2002; Fekete *et al.*, 2010). Therein, the 3oxo-decanoyl-homoserine lactone (3oxo-C10-HSL) was the most dominant HSL followed by 3oxo-dodecanoyl-homoserine lactone (3oxo-C12-HSL) and 3oxo-octanoyl-homoserine lactone (3oxo-C8-HSL). The remaining HSLs, e.g. the 3oxo-tetradecanoyl-homoserine

lactone (3oxo-C14-HSL), were determined in quite low amount (Fekete *et al.*, 2010). The QS system of this strain consists of *PpuI*, which directs the synthesis of AHL signal molecules and *PpuR*, which binds to the AHLs and regulates the *ppuI* expression in a positive feedback loop. While the wild type *P. putida* IsoF formed very homogenous unstructured biofilms that uniformly cover the surface, a *ppuI* mutant formed structured biofilms with characteristic microcolonies and water filled channels. When the medium was supplemented with AHL signal molecules, the mutant biofilm lost its structure and converted into an unstructured biofilm similar to the one formed by the wild type IsoF. These results suggest that the QS system influences biofilm structural development (Steidle *et al.*, 2001). For comparison, an AHL-negative mutant of *P. putida* IsoF, *P. putida* F117 and *P. putida* strain KT2440 were often used as negative controls of AHL-production. The mutant F117 is unable to produce AHLs but able to be activated by AHL autoinducers. Therefore, the mutant F117, which is deleted in AHL production, is used as AHL bioreporter using a green fluorescent protein (*gfp*) gene function (Steidle *et al.*, 2002). Consequently, the *P. putida* KT2440 is neither HSL producer nor AHL consumer (Steidle *et al.*, 2002).

Figure 4 Dynamics of 3oxo-C10-HSL and 3oxo-C10-HS in *P. putida* culture supernatant



The graph shows a comparison of the time-resolved concentrations of 3oxo-C10-HSL and 3oxo-C10-HS (as hydrolyzed product, being further degraded itself) from the beaker experiment. Ref: (Fekete, *et al.*, 2010).

Interestingly, Fekete *et al.* (2010) have recently demonstrated the dynamic regulation of AHL production and degradation in *P. putida* IsoF, which described the stage dependent HSL production and degradation process. Briefly, as showed in Figure 4, the concentration of the main autoinducer 3oxo-C10-HSL increased rapidly at the beginning of growth and reached its

maxima at 35 nM in 11 h followed by a rapid decline. A very similar dynamic was observed by 3oxo-C10-HS, the hydrolysed product of 3oxo-C10-HSL, just with a time delay of about 4 hours (Fekete *et al.*, 2010). The biological reason of the parallel production and degradation of HSL and HS is probably the occurrence of an AHL-hydrolysing enzyme, which is a very interesting aspect for further understanding of the QS (see also section 1.2).

1.1.3.5 Quorum sensing in biofilm communities and 1,2,4-trichlorobenzene (TCB) biomineralisation

Chlorobenzenes (CBs) are important basic materials and additives in the production of pesticides, dyes, pharmaceuticals, disinfectants, rubbers, plastics, and electric goods. Their occurrence in the environment is widespread and they were found in the atmosphere, water, soil sediments, vegetables, and biota (Wang *et al.*, 2007). Since CBs can be accumulated in the food chain, the elimination of these pollutants from the environment and from polluted sites is of great public interest. As chemical and photochemical degradation of CBs is very slow, biological degradation could be considered as a feasible process to eliminate these compounds from soil ecosystems (Wang *et al.*, 2007).

Biodegradation of 1,2,4-TCB in natural samples occurs in very low rates due to insufficient degradation capacity and slow adaptation of the indigenous microorganisms. In some cases, the biodegradation of 1,2,4-TCB in soil could be enhanced by inoculation with adapted bacteria like *Pseudomonas sp.* P51, *Burkholderia sp.* PS12 and *Burkholderia sp.* PS14 under laboratory conditions. Schroll *et al.*, (2004) showed an applicable method to considerably enhance the biodegradation of 1,2,4-TCB in a soil with low native degrading capacity by inoculating this soil with an adapted microbial community from a contaminated site via soil inoculum (Schroll *et al.*, 2004). Wang *et al.*, (2007) demonstrated that soil inoculation with a microbial community attached on clay particles resulted in a higher efficiency of 1,2,4-TCB mineralisation as compared with inoculating soil with the isolated key degrader or the microbial community in free liquid medium. Furthermore, the key organism *Bordetella sp.* of this degrading community was successfully isolated and identified (Wang *et al.*, 2007). The mechanism behind the very effective function of these “microbe-clay-particle complexes” is therefore very interesting but not understood yet. Since QS is widely employed by bacteria of intra- and inter- species’ communication, regulating their gene expressions, 1,2,4-TCB degradation might also be regulated by QS bacteria, e.g. *Pseudomonas spp.* or *Burkholderia spp.*. It was suggested, that biofilm forming bacteria on the clay particles may have several advantages that are not enjoyed by single cell bacteria. For example, organisms within

biofilms can withstand shear forces, nutrient deprivation, pH changes and antibiotics in a more pronounced manner; cells in biofilms have a better chance of survival especially in periods of stress as they are protected within a matrix and can utilize cooperative benefits in a community. However, this idea is so far only a hypothesis and up to date, no literature has been found to confirm the presence of QS in this particular community.

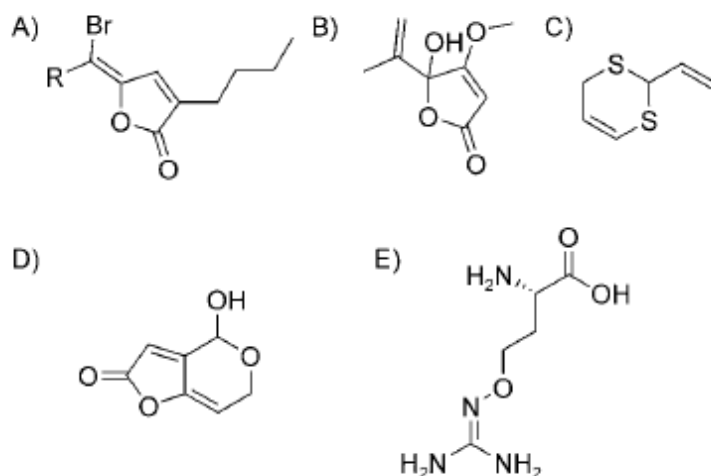
1.2 Quorum quenching

The term “quorum quenching” (QQ) was coined to describe all processes that interfere with QS (Dong *et al.*, 2001). QQ strategies do not aim to kill bacteria or limit their growth. Rather, they affect the expression or activity of a specific function. This is an important feature because these strategies exert a different selective pressure for microbial growth as compared to antibiotic/biocide treatments. This is a valuable trait for the development of sustainable biocontrol or therapeutic procedures in the present context of rising antibiotic resistance. Three steps of the AHL-based QS regulation mechanism could be targets for QQ procedures: 1) the production of signal molecules, 2) the signal molecule itself, and 3) sensing of the signal molecule by the cognate regulatory protein. The mechanisms that are involved could be either of abiotic or biotic origins (Uroz *et al.*, 2009).

1.2.1 Inhibition of AHL signal sensing

The first example of natural inhibition of AHL signal sensing involves AHLs themselves. *N*-decanoyl-HSL (C10-HSL) and *N*-3oxo-tetradecanoyl-HSL (3oxo-C14-HSL) were reported to inhibit the production of the antibiotic pigment violacein by *Chromobacterium violaceum*, a QS-dependent function controlled by *N*-hexanoyl-HSL (C6-HSL) (McClellan *et al.*, 1997). Similarly, the acyl length and the substitution of the acyl chain can perturb QS-regulated functions such as *V. fischeri* luminescence (Schaefer *et al.*, 1996) or conjugal transfer in *Agrobacterium tumefaciens* (Zhu *et al.*, 1998). Other natural compounds are capable of interfering with QS-regulated functions *in vivo* (Figure 5).

Figure 5 Quorum sensing inhibitors



A) Halogenated furanone from *Delisea pulchra*; B) Penicillic acid from *Penicillium*; C) Cyclic sulphur containing compound that was isolated from garlic; D) Patulin from *Penicillium* and E) L-canavanine from *Medicago truncatula*. Ref: (Uroz *et al.*, 2009)

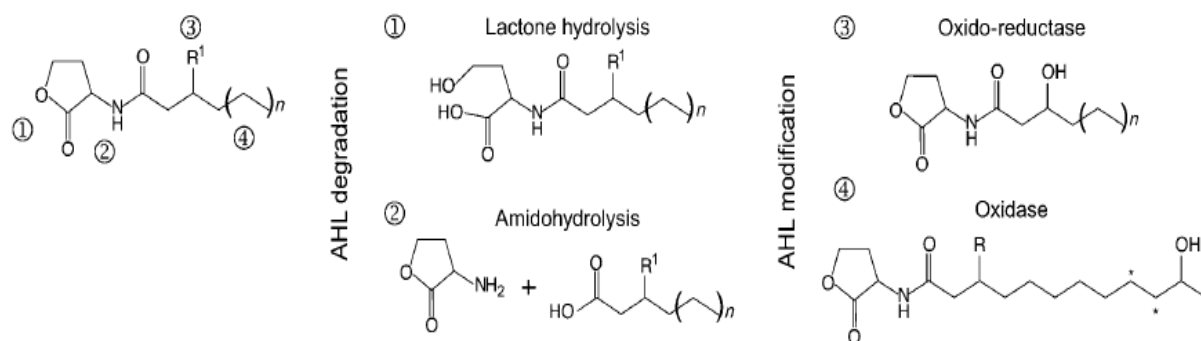
Their mode of action and chemical structure frequently remain unknown. These compounds often compete with AHL for binding to the *LuxR* like receptor. This prevents QS regulation from occurring (Uroz *et al.*, 2009).

1.2.2 Limitation of signal accumulation-HSL degradation

1.2.2.1 Abiotic degradation

N-acyl homoserine lactones are very sensitive to elevated temperatures. Yates *et al.*, (2002) reported that C4-HSL and C6-HSL were 3 and 1.5-times more rapidly degraded at 37°C than at 22°C, respectively. As they contain lactones, these molecules are also sensitive to alkaline pH. Schaefer *et al.*, (2000) estimated that the half-life (in days) of 3oxo-C6-HSL was $1/(1 \times 10^7 \times [\text{OH}^-])^{23}$. More recently, Byers *et al.*, (2002) demonstrated that the half-life of this molecule was 30 min at pH 8.5, while it was seven hours at pH 7.8. The mechanism involved in this degradation is chemical lactonolysis, which leads to the generation of acyl-homoserine. This reaction can be partially reversed by acidification of the medium, which allows the restoration of the QS signal molecule. In addition, AHL can undergo a spontaneous Claisen-like alkylation of the β -ketoamide moiety, which leads to the formation of tetramic acids. Tetramic acid derivatives of AHL do not function as QS signal molecules, but might act as antibiotics against Gram-positive bacteria (Kaufmann *et al.*, 2005).

Figure 6 HSL-degradation pathways and degradation products.



Degradation pathways: 1. lactone ring hydrolysis, 2. amidohydrolysis; or modification pathways: 3. oxido-reductase, 4. oxidase. Ref: (Uroz *et al.*, 2009)

1.2.2.2 Enzymatic degradation

Aside from abiotic factors, AHL stability is also affected by biotic activities. The enzymatic degradation of the AHL molecules appears to occur in a very broad range of organisms. Degradation of AHLs was first demonstrated in bacteria, and has been reported in members of nearly 20 genera. Several plants, including clover, lotus and yam bean were proven to prevent accumulation of AHLs with acyl chain length from C6 to C10 in their environment (Delalande *et al.*, 2005; Götz *et al.*, 2007). Three main enzymatic mechanisms have been discovered and were clearly described: lactone hydrolysis, amido hydrolysis (Figure 6.2) and oxido reduction (Figures 6.3 and 6.4).

AHL-lactonases catalyse the hydrolysis of the homoserine lactone ring of the AHLs; this leads to the generation of acyl homoserine. This hydrolysis is identical to the pH mediated lactonolysis, and as such, the reaction can be partially reversed by acidification of the medium. Lactonase activities have been demonstrated in several bacterial genera and also in eukaryotic cells (Uroz *et al.*, 2009).

AHL-acylases catalyse the complete and irreversible degradation of the AHLs through the hydrolysis of their amide bond; this releases homoserine lactone and the corresponding fatty acid (Figure 6.2). All of these AHL-acylases degrade long-chain AHLs more efficiently than short-chain forms.

To date, two occurrences of AHLases with oxidative or reducing activities have been reported, but only in bacteria. In contrast to the previous QQ enzymes, these activities do not

lead to the degradation of the AHL molecules into QS-inactive molecules. Instead, they catalyse a modification of the chemical structure of the signal.

1.2.3 The biological functions of the AHLases

A recent study revealed that rearrangement compounds arising from 3oxo-AHLs generated tetramic acids that are toxic to several Gram-positive strains, including *Bacillus sp.* Interestingly, numerous *Bacillus sp.* strains harbour on genes encoding AHL lactonases that are able to degrade AHLs. As a consequence, one role of the AiiA lactonase in *Bacillus* might be to detoxify the 3oxo-AHL derivatives, as proposed by Kaufmann *et al.* (2005).

Remarkably, degradation of AHLs also occurs in bacterial strains that produce these molecules. The best-described example is that of the plant pathogen *Agrobacterium tumefaciens*, for which Ti plasmid transfer and copy number are regulated by QS via the expression of the attKLM operon (Chevrot *et al.*, 2006). It was suggested that AHL degradation by bacteria and eukaryotes might not be the primary function of AHL degradation enzymes, but might play an important role in AHL turnover (Uroz *et al.*, 2009).

1.3 Current HSL analytical methods

Currently, arrays of different methods have been introduced for the detection and characterisation of AHL molecules. Generally speaking, one approach uses conventional analysis applying chromatography and mass spectrometry and the other was bioassays and bioreporters, which are inducible by AHL. Both of them have their advantages and disadvantages.

1.3.1 Conventional chemical analysis

The concentration of naturally produced AHL molecules can be quite low and they are difficult to be detected by conventional techniques. Furthermore, AHLs are difficult to analyse by liquid chromatography using traditional detectors, because their absorbance maxima are at low wavelengths and contain high background absorbance of solvents. Thus, the applicability of ultra violet (UV) detectors for AHLs analysis is very limited (Cataldi *et al.*, 2004). However many different analytical methods of AHLs have been developed and optimised in the last years. Shaw *et al.* (1997) developed detection method for AHLs in bacteria cultures using thin-layer chromatography (TLC). Frommberger *et al.* (2003) conducted partial filling micellar capillary electro-chromatography and nano LC with mass spectrometric detection.

Table 2 Conventional AHL analytical methods

Clean-up and pre-concentration		AHL structure identification		Quantification of AHLs
Liquid-Liquid Extraction (LLE)		Mass Spectrometry (MS)	Time Of Flight MS (TOF-MS)	Gas Chromatography (GC)
Normal Phase Liquid Chromatography (NPLC)			Fourier Transform Ion Cyclotron Resonance MS (FT-ICR-MS)	
Liquid Chromatography (LC)	Reversed Phase Liquid Chromatography (RPLC)	Nuclear Magnetic Resonance Spectroscopy (NMR)		High Performance Liquid Chromatography (HPLC)
	Ion Exchange Chromatography (IEC)			
	Thin Layer Chromatography (TLC)			
	(Semi) Preparative Liquid Chromatography	UV-VIS spectrophotometer		Ultra high Performance Liquid Chromatography (UPLC)
Solid Phase Extraction (SPE)	Capillary Electrophoresis (CE)			

Ref: (Fekete *et al.*, 2010)

Direct analysis of AHLs by gas chromatography (GC)/ mass spectrometry (MS) was demonstrated by Cataldi *et al.* (2004). Li *et al.* (2006) combined solid-phase extraction (SPE) and ultra high performance liquid chromatography (UPLC) detection methods. Conventional chemical analyses are the most accurate methods for identification of individual molecule

structures, though very resource and time consuming. Fekete *et al.* (2010) have recently reviewed the analytical methods for AHL molecule identification (listed in Table 2).

In summary, AHL containing samples need to be extracted, pre-concentrated and separated with chromatography and further identified with mass spectrometry. The quantification of the individual AHL needs a combination of chromatography and mass spectrometry (Table 2). Additionally, internal standards are always necessary for both identification and quantification; these are not always available.

1.3.2 Bioreporters

The principle of bioassay is that most of the autoinducer reporter strains are mutants that cannot synthesise their own AHLs; the wild type phenotype is only expressed upon the addition of exogenous AHLs. When the gene expression is induced, the production could be visualised directly or indirectly by the reaction of a reporter gene producing visible (light or fluorescence) signals. Brelles-Mariño & Bedmar, (2001) and Williams *et al.*, (2007) reviewed bioassays with different functions. Many autoinducer sensors are dependent upon the use of *lacZ* reporter fusions in an *E. coli* or *A. tumefaciens* genetic background or on the induction or inhibition of the purple pigment violacein in *Chromobacterium violaceum*. *lux*-based reporter assays include the recombinant reporter plasmid pSB315 that lacks a functional *luxI* homolog. *E. coli* cells transformed with pSB315 are dark unless supplied with an exogenous AHL and a long-chain fatty aldehyde such as dodecanal, which is an essential substrate for the light reaction (Swift *et al.*, 1993). In addition, a refined construct is available, pSB401, which does not require the addition of exogenous aldehyde and responds to a wide range of AHLs (Winson *et al.*, 1995). *E. coli* harbouring pSB401 responds most sensitively to 3-oxo-C6-HSL, which is the natural inductor, but it is less sensitive to AHLs with acyl side chains from 4 to 10 carbons in length, irrespective of the substituent at the 3-position. Other *lux*-based biosensors such as pSB406, are available in which *luxR* and the *luxI* promoter region are replaced with the *P. aeruginosa luxR* homolog. *lux*-based reporters detect most of the 3-oxo and alkanoyl standards, but do not detect *N*-butanoyl homoserine lactone or any of the 3-hydroxy forms. A broad range of AHLs (or AHL-like activities) can be detected by a set of *lux*-based reporters that differ in their sensitivity for specific AHLs (Winson *et al.*, 1998). Some microorganisms may produce signals that are not detected by one of the reporters or they may produce molecules at levels below the threshold of sensitivity of the reporter (Shaw *et al.*, 1997). Thus, the utilisation of several bioreporters with different sensitivities and specificities is highly recommended (Williams *et al.*, 2007).

1.4 Immunochemistry

1.4.1 Introduction of immunochemical techniques

Immunochemical techniques are analytical methods based on the interaction of antibodies (Abs) with antigens (Ags). Antibodies are polymers containing hundreds of individual amino acids arranged in a highly ordered secondary and tertiary structure sequence. These polypeptides are produced by immune system cells (B lymphocytes when exposed to antigenic substances or molecules). Abs contain in their structure recognition/binding sites for specific molecular structures of the Ag (see Figure 7). According to the 'key-lock' model an Ab interacts in a highly specific way with its unique Ag. The interaction is reversible, as determined by the law of mass action, and is based on electrostatic forces, hydrogen bonding and hydrophobic and Van der Waals interactions. This feature constitutes the key to the immunochemical techniques (Marco *et al.*, I, 1995).

Immunoassay technology originated in the late 1950s when Yalow and Berson (Nobel Prize awarded) published the development of a quantitative immunological assay which could detect human insulin at the pictogram level in small samples of body fluid. In the following years this technology found wide application in biochemistry, endocrinology and clinical chemistry. The reasons for these developments include the selectivity and sensitivity exhibited by the antibodies and the simplicity of performing the immunoassays (Marco *et al.*, I, 1995). Other immunochemical techniques like immunosensors are widely developed and used in different areas as well. However, small molecules are not able to produce an immune response, thus the small molecules need to be linked to a carrier, usually a protein, see also (1.4.2.3.).

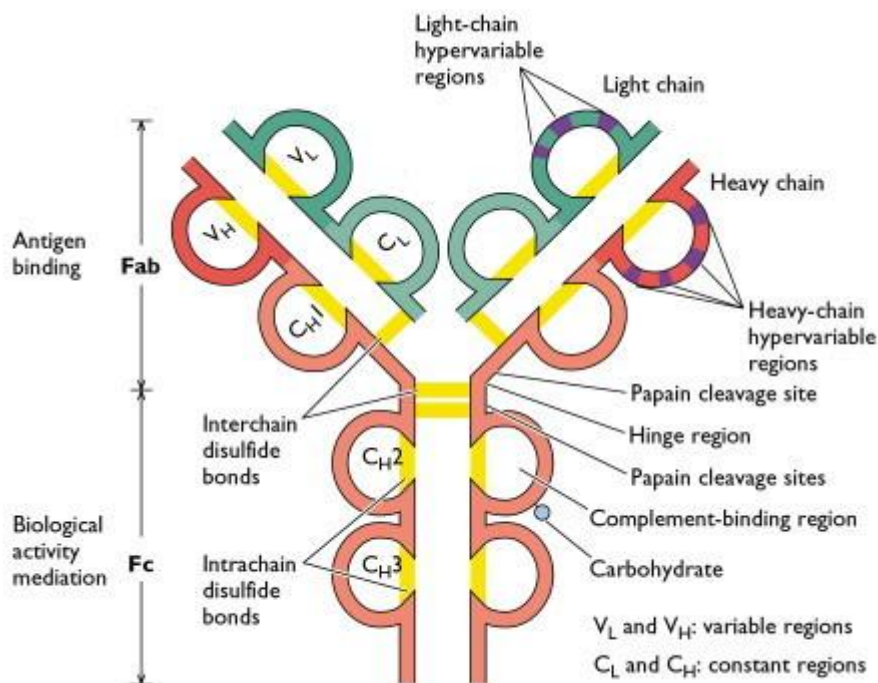
1.4.2 Production of antibody

1.4.2.1 Antibody introduction

Antibodies are large proteins produced by vertebrates and play an important role in identifying and eliminating foreign objects. The basic structural unit is composed of two heavy chains and two light chains, as shown in Figure 7. Antibodies bind other molecules known as antigens. Binding occurs in a small region near the ends of the heavy and light chain called the hypervariable region (labelled only on one arm in the figure). As the name implies, this region is extremely variable, which is why vertebrates can produce millions of antibodies that can bind many different antigens. The part of the antigen that is recognised by the antibody is known as an *epitope*.

There are five classes of immunoglobulins (Igs)—IgA, IgD, IgE, IgG, and IgM—defined by the amino acid sequence of the heavy chain. The Igs have different roles in immune responses (www.virology.ws).

Figure 7 Structure of IgG monoclonal antibody molecule



Ref: (www.virology.ws)

1.4.2.2 Target molecule selection

A good knowledge of the analytical target, its chemical structure, its stability and its degradation routes are required before assay development starts. Another important requirement is to establish the purpose of the analysis: is it to be class-selective or analyte selective? For use on an immunoaffinity column for some screening IAs a class-specific antibody may be more convenient than a very selective Ab, particularly with regard to the fact that many substances suffer degradation for biotransformation to other chemically related compounds. Finally, it is also important to know the kind of matrix to which the immunochemical analysis is going to be applied. Thus, metabolites or protein adducts may be the targets for Ab development when the aim of the analysis is biological monitoring of exposure to toxicants and/or pollutants (Marco *et al.*, II, 1995).

If the target compound contains functional groups such as NH₂, COOH, OH, SH, CO or CHO, direct covalent coupling to the carrier molecule can be performed. However, to avoid

masking essential groups for the Ab recognition, a hapten should be usually prepared. A hapten is a derivative of the target molecule that contains an appropriate group (linker or spacer arm) for attachment at a convenient place in the molecule (Marco *et al.*, II, 1995).

1.4.2.3 Hapten design

The term hapten is originally from Greek *haptain* and means to grasp. In immunochemistry, hapten is substance that acts as an antigen by combining with particular bonding sites on an antibody. A hapten conjugated to a carrier protein may cause an immune response (Mosby, 2009). Unlike a true antigen, it does not induce the formation of antibodies.

The design of a hapten is the most crucial step in the development of an immunochemical technique for all low-molecular-mass substances. The specificity and selectivity of immunochemical techniques are mainly determined by the Ab. A hapten should preserve as much as possible the chemical properties of the target molecules. However, characteristic portions of the molecules are sometimes sufficient to generate valuable antibodies. Exposure of the molecule to the immune system is greater for these sites placed further from the attachment point, thus determining the selectivity of the resulting antibodies. Using important functional groups of the target analyte leads to a reduction of the sites that could potentially help to stabilize the Ab-analyte immunocomplex. Antibodies with lower affinity may thus be obtained, leading to less sensitive assays. The length and structure should be chosen to reduce spacer recognition while maximising target exposure to the immune system. However, usually different haptens are used as immunogen and competitor. The length, size or/and chemical structure of the spacer arm is different in the immunogen and competitor. An optimal competitor hapten must be tested for every assay (Marco *et al.*, II, 1995).

1.4.2.4 Hapten synthesis and conjugation to carrier molecules

Haptens could be purchased commercially or synthesized in house. Table 3 shows a summary of some common coupling strategies. The functional group of the hapten governs the selection of the conjugation method to be used (Marco *et al.*, II, 1995). Keyhole limpet hemocyanin (KLH), tyroglobulin (TG), conalbumin (CONA), bovine serum albumin (BSA) or ovalbumin (OVA) are the carrier proteins most frequently used as either immunogens or coating Ags. As competitors, enzymes are the most commonly used labels in IA, but a variety of fluorescent labels are also available and increasingly being used.

Table 3 Principal strategies for protein conjugates

Principal strategies for preparing protein conjugates		
Protein P (reactive groups)	Hapten R (reactive groups)	Bond type
P-NH ₂ (lysine and N-amino terminal)	R-COOH (NHS esters or mixed anhydrides)	R-CO-NH-P
	R-N=C=S	R-NHCS-NH-P
	R-CHO	R-CH ₂ -NH-P ^a
	R-SO ₂ Cl	R-SO ₂ -NH-P
	R-CH ₂ -halogen	R-CH ₂ -NH-P
P-SH (cystine, cysteine and methionine)	R-COCH ₂ -halogen ^b	R-COCH ₂ -S-P
	R-maleimide ^c	R-succinimide-S-P ^d
	R-pyridyl-disulfide ^e	R-S-S-P
	R-halogen	R-CH ₂ -S-P
	R-NH ₂	R-NH-CO-P
P-COOH (glutamic and aspartic)	R-NH-NH ₂	R-NH-CO-P
	R-NH ₂	R-NH-CH ₂ -P ^a
P-CHO (periodate oxidation of carbohydrate residues)	R-NH-NH ₂	R-NH-CH ₂ -P ^a
	R-COOH	R-CO-O-P ^f
P-OH (tyrosine)	R-N ₂	R-NH-Ar-P
P-Ar (tyrosine)		

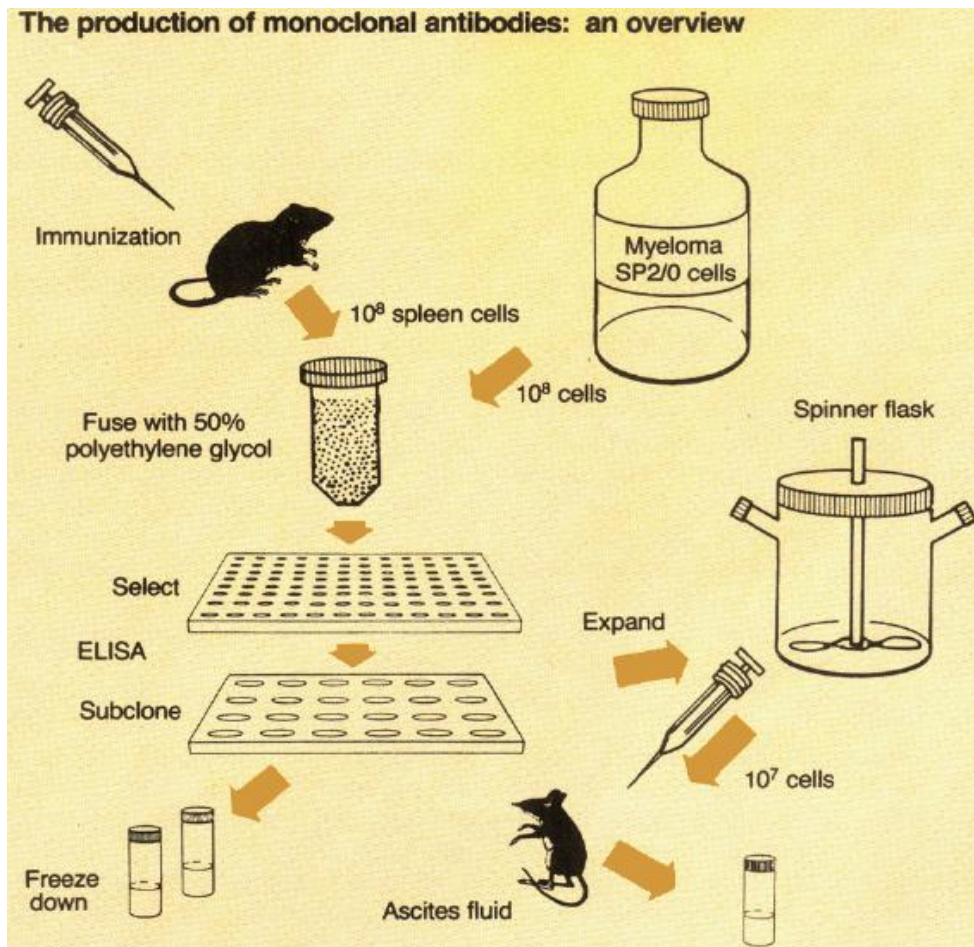
Ref: (Marco *et al.*, II, 1995)

In this context, the effect of the resulting hapten-protein ratio in the conjugates should be noted. Usually it is considered that a high ratio of hapten per protein increases the strength and specificity of the immune response, but for competitors (an enzyme, protein or derivatised solid surface) a moderate value is more desirable, favouring the sensitivity of the resulting competitive immunoassay (IA). Theoretically, when the amount of hapten in the competitor is limited, less analyte in solution is needed to compete for the specific Ab. There is also a risk that a high degree of substitution could affect the activity of enzymes or antibodies when these are the labelled immunoreagents (Marco *et al.*, II, 1995).

1.4.2.5 Immunisation, fusion and hybridoma

For obtaining antibodies, essentially any vertebrate can be used. Sheep, goats and cows offer the possibility of obtaining larger amounts of Ab; but rabbits, mice and rats are used because they are easy to care for and produce moderate amounts of serum.

Figure 8 Monoclonal antibody production



Ref: (Vanderlaan *et al.*, 1988)

The production of polyclonal Abs is relatively simple but monoclonal antibodies offer the advantage of containing a defined Ab type and being produced by established cell lines, yielding unlimited quantities of antibodies as long as the hybridoma line is stable. However, for both research and commercial purposes, polyclonal antibodies are often sufficient and reduce costs of the research. Nevertheless, the quality of the antibodies (either polyclonal or monoclonal) depends mainly on the animal's immune system, the immunogen, and the immunisation schedule or protocol used. A number of immunisation procedures has been described but, because of animal variability and the diversity of immunogens used, no conclusion can be drawn on which are the more efficient methods (Marco *et al.*, II, 1995).

In 1975 George Köhler and Cesar Milstein revolutionised the production of antibodies by developing a method for culturing the particular lymphocytes that secrete antibodies (Figure 8) (Köhler & Milstein, 1975). Briefly, after several weeks of immunisation, a rat/mouse is sacrificed and its spleen cells are used as the source of antibody-secreting lymphocytes. Even

though these cells normally do not grow in culture, antibody secreting cell lines could be created by fusing them with cells that do grow in culture-in this case, myeloma tumor cells. Spleen cells and tumor cells are mixed in the presence of polyethylene glycol, where they fuse into a new cell type, called a hybridoma, which grows in culture like the tumor cell and produces antibodies like the spleen cells. Hybridomas are seeded at roughly one colony per well in multi-well plates for cloning (Vanderlaan *et al.*, 1988).

The greatest task in making monoclonal antibodies is the rapid screening of hybridomas to find the 1-10 per spleen that produce the best antibodies. Each hybridoma secretes its own monoclonal antibody in to the cell culture medium of its well, and medium samples are screened by immunoassay. Once selected, the clones are expanded into the larger wells of a 24-well plate and then to bulk spinner flasks. There is at least a three month period from the time of fusion until large quantities of antibodies are available. During this time, there are continuous rounds of subculturing the cells, assaying the media from wells, selecting the desired clones, and expanding the culture to ensure that, in the end, the cells are stable and uniform and each cell is secreting the best antibody. These antibodies are called monoclonal antibodies (mAbs) because they are produced from a single strain of B-cells. Before Köhler and Milstein, the only means of obtaining monoclonal antibodies was to purify them from the polyclonal serum of immunized animals (Vanderlaan *et al.*, 1988).

Antibodies can be used as serum or ascites fluid, or well purified. The most commonly used purification methods include ammonium sulphate purification and affinity purification. Once the affinity of the resulting sera or ascites fluid for the target analyte has been proven by titration experiments, the purified antisera can be used directly for the preparation of immunoaffinity columns or direct immunosensors (Marco *et al.*, II, 1995).

1.4.3 Immunoassay and different formats

Immunoassay (IA) is based on the use of labels to detect the immunological reaction. Although fluorescent and chemiluminescent labels have become more popular, enzyme labels such as horseradish peroxidase or alkaline phosphatase are still the most popular non-isotopic labels, alongside the use of radioisotopes in radioimmunoassay formats. Among the enzyme immunoassays, those based on heterogeneous conditions are most commonly employed and are referred to as enzyme-linked immunosorbent assays (ELISAs). For ELISAs, either Abs or Ags are immobilised on a solid phase to facilitate the separation of free and bound fractions.

1.4.3.1 Enzyme-tracer format ELISA

An equilibrium is established between the Ab bound to the solid surface (either directly or through orientating reagents such as anti-IgG or protein G, protein A), the analyte, and the analyte-enzyme tracer which are in solution. After the main incubation step the unbound reagents are washed away and the amount of enzyme bound to the solid phase by the Ab is measured.

1.4.3.2 Coating antigen format ELISA

This format is based on the competition between the immobilised Ag (or surface derivatised analyte) and the analyte for a fixed small amount of labelled Ab. The concentration of the analyte is measured indirectly by the quantification of bound Ab with a second Ab which is covalently labelled with an enzyme or other markers (Marco *et al.*, II, 1995).

The coating antigen and enzyme-tracer format ELISAs are both competitive assays thus the signals are inversely proportional to analyte concentration.

1.4.3.3 Sandwich ELISA

In this case, an excess of labelled Ab is used to detect the analyte captured by another Ab bound to the solid surface. This configuration is restricted by the fact that the analyte must have multiple Ab binding sites (Marco *et al.*, II, 1995). This assay format is very commonly used in the clinical field for big molecules detections like proteins or peptides. Differently to competitive assays, sandwich ELISAs present proportional signals to analyte concentration.

1.4.4 Optimisation of immunoassays

The final goal of an immunoassay development is to establish a specific, sensitive and stable assay, which fulfils the demand of target analyte detection. Due to the multiple steps of assays and their variability of material and methods, many aspects have to be considered for assay-optimisation.

1.4.4.1 Test sensitivity

A plenty of test systems require a very high sensitivity of assays, because the natural occurrence of some targeting substances is in a very low concentration range, e.g. in nano molar or pico molar. If the working range of assays could not reach the demanding sensitivity,

the assays are then not able to detect the required analytes in samples. Thus the different assay conditions should be tested to obtain more sensitive assays.

1.4.4.2 Reagents

Generally for ELISA tests, all buffers, blocking solutions and standards are strongly recommended to be prepared freshly. The chemical or biological reagents should be carefully stored to avoid the changing or losing of their chemical or biological activity. To minimise the freeze-thaw process, it is recommended to aliquot the reagents. A high quality assay can be achieved only, when the antibody and antigen could perform the best binding. For this purpose, the assay format, coating of microtiter plate, e.g. the antigen-conjugates, must be tested. Also the blocking of the plate, the buffers for reagents set up, the different incubation times should be considered.

Besides the conditions described above, a correct dilution of antibody plays an essential role on assay sensitivity. The antibody dilutions are only appreciated, if they could show the concentration dependent signals. A zero (only buffer) and a high concentration of analyte should be compared for the same antibody concentration and a decreased optical signal must be seen with the addition of high amount of analytes if the antibody dilution is in dynamic range. Thus, a two dimensional titration is very useful to obtain the best dilution combinations of antibodies, coating antigen, enzyme-tracer, secondary antibodies or analytes dependent on assay formats.

1.4.4.3 Hapten conjugates

It was discussed in the previous section (1.4.2.4) that the hapten-conjugates have strong influence on immunoassays because they directly affect the resulting antibody properties. In assays the hapten-protein and the hapten-tracer conjugates would have an effect on the performance of assays in different formats. Despite the selection of haptens, the hapten density, which means the hapten amount on one carrier macromolecule, is essential for assays sensitivity. It was mentioned that a high conjugation density (many epitopes) is required for the hapten-protein conjugates for immunisation purpose. However, for coating antigen assays, a reduced hapten density is preferred due to the binding competition with analytes to antibodies. But the hapten amount could not be too low that there is no more binding of antigen to antibodies. Similarly, a low hapten density of hapten-tracer conjugation was recommended for more sensitive enzyme-tracer assay. Therefore, different conjugation rates should be compared to get most sensitive assays.

1.4.4.4 Buffers and blocking systems

Not only the primary antibody, the secondary antibody, coating antigen and enzyme-tracer influence the assay sensitivity, the buffers and blocking solutions also have drastic effect on ELISAs. The important buffers are standard buffer, buffer for sample and conjugation dilution, wash buffer, coating and blocking buffer. A correct physiological condition is very important for ELISAs according to the biological natures of the antibodies and enzymes. The buffer must fulfil the criteria like pH, salt content, buffer range, viscosity, etc. correspondingly to the assays. The goal of buffer selection is to obtain stable and sensitive assays with low standard deviation and low background. In order to reduce unspecific binding on coated plate, a blocking was very often performed with addition of different kinds of proteins or protein mixtures. Albumin is commonly used as blocking substance and also smaller proteins like casein for example were used for blocking. Effective blocking could significantly reduce the unspecific binding but a blocking could also cause increased background. In general, the blocking substance should not interfere with the ELISA system. For example, BSA should not be used as blocking agent, if the antibody was generated with hapten-BSA conjugate.

Not only the in-lab prepared but also the commercially purchased buffers should always be controlled, because a small change of the buffer composition could have huge effect on assays.

1.4.4.5 Immobilisation on the surface of microtiter plate

Depending on ELISA format, the surface of microtiter plate can be immobilised (coated) with antigens, antibodies, hapten-protein-conjugates or some other materials like streptavidin. There are different kinds of specialised microtiter plates available, using optimised adsorptive surface. Lipophilic substances, proteins or sugars could be immobilised on the surface. A high purity of the coating substance is required because the biological products might contain other proteins in matrix, which could also bind on the plate surface besides the target coating substance.

1.4.5 Immunoassay evaluation

Accuracy describes the exactness of the assay to measure a known, true value of analyte and to measure it repeatedly. Accuracy is expressed as the per cent error between the assay-determined value and the assigned value for that sample. A per cent error of $\leq 20\%$ is an

acceptable level of accuracy for an enzyme immunoassay (O'Connell *et al.*, 1993). Precision, a measure of the degree of repeatability of an assay under normal operating conditions, is expressed as the coefficient of variation of the concentrations calculated for the standard reference curve dilutions within a single assay plate (intra-assay precision) and between different assay plates (inter-assay precision) determined over time and controlling for different operators. Acceptable levels of intra-assay and inter-assay precision are 10% and 20%, respectively (O'Connell *et al.*, 1993), and these can be used to define the range of the assay and the upper and lower limits of determination (LOD). The working range of the assay is the interval between the upper and lower levels of analyte that have been demonstrated to be determined with these levels of precision and accuracy.

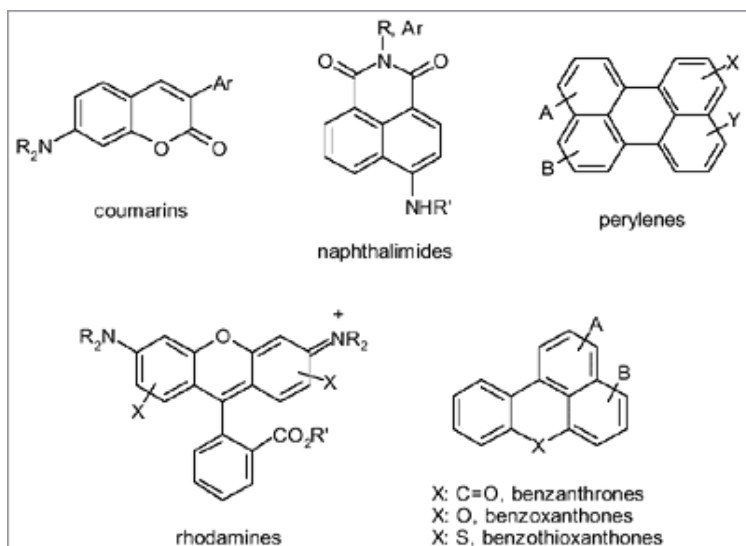
The “goodness of fit” of the assay is, for comparative purposes, an indication of how closely the data points of the reference serum standard curve fit the four parameter model. Goodness of fit is expressed as the regression coefficient (R^2) of the standard curve. An R^2 value is indicative of a good fit for the data to the curve (Quinn *et al.*, 2002).

1.4.6 Fluorescence in immunochemistry

1.4.6.1 Fluorescence

Fluorescence is the emission of visible light from fluorophore substance at electronic excited states after excitation with shorter wavelength light. It includes excitation and emission process of fluorophores, which means receiving and releasing of energy. There are different kinds of fluorescent substances and the typical structures of fluorescent dyes are shown in Figure 9. Fluorescence phenomena have been widely applied in the chemical and biological sciences, e.g. fluorescence immunoassay, fluorescence microscopy, confocal laser scanning microscopy (LSM), fluorescence *in situ* hybridisation (FISH) etc. The measurement of fluorescence can provide information on a wide range of molecular processes, including the interactions of solvent molecules with fluorophores, conformational changes, and binding interactions (Lakowicz, 2006).

Figure 9 Chemical structures of typical fluorescent dyes



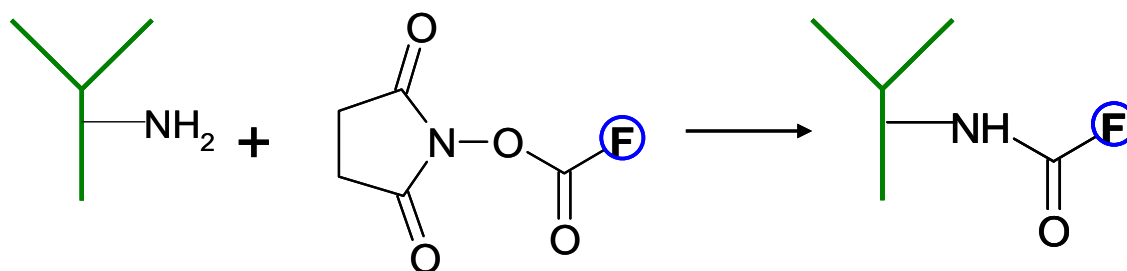
Ref: (<http://www.dyepigments.com/fluorescent-dyes.html>)

The invention of water soluble cyanine fluorescent dye is a revolutionary step of the fluorescent technology, and now the cyanine dyes are becoming the most popular fluorescent dyes for biological science. Commercially, cyanine dyes are differently termed, which include CyDye, Cy2, Cy3 and Cy5 from Amersham Bioscience UK Ltd., Alexa Fluor and Texas red from Molecular Probes Inc., and Oyster from Denovo Biolabels GmbH (Raem & Rauch, 2007).

1.4.6.2 Fluorescent dye conjugation to antibody

For fluorescence immunoassays a dye-antibody conjugation is normally required, and the carrying Ab can then serve as primary antibody or secondary antibody. Numerous companies offer ready to use fluorescent labelled antibodies. But for many primary antibodies, the users have to do the labelling themselves. A serious consideration must be taken to choose the suitable method for labelling due to the big amounts of commercially available dyes and variable conjugation methods. The conjugation of dyes using activated ester residues on NH_2 - (lysine) of proteins is a very commonly used method (scheme see Figure 10). In this study, all conjugation experiments were performed using this reaction.

Figure 10 Fluorescent dye conjugation using activated amino groups on lysine residues of proteins



As discussed previously, due to the change of fluorescence through conjugation to protein, optimising steps must be processed to achieve the aimed applications. To check the quality of fluorescent dye conjugation, a determination of label degree, which indicates the molar ratio of dye and protein, is recommended. The label degree over 10 is reachable, however, in praxis a label degree between one and five is preferred. The high amount of protein bound dyes might modify the lysine in antigen binding domains and consequently reduce the antibody antigen binding affinity (Raem & Rauch, 2007).

1.4.6.3 Tyramide Signal Amplification (TSA)

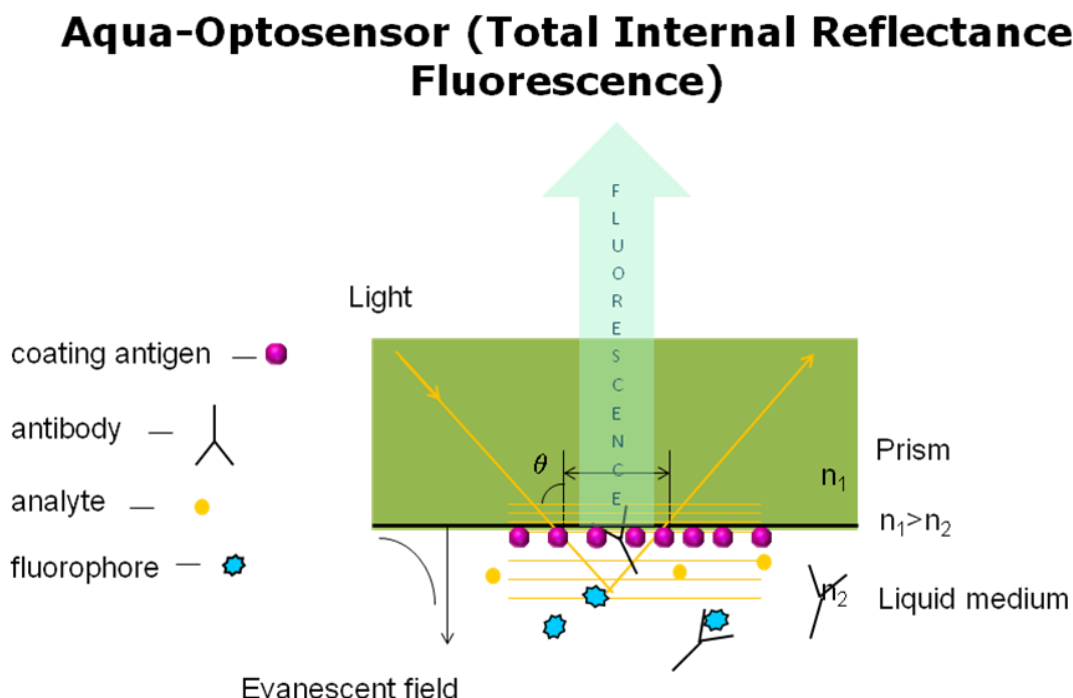
TSA signal amplification, also named CARD, was introduced by Bobrow *et al.*, (1989, 1991, 1992) for use in immunoblotting and ELISAs and is based on the deposition of a large number of haptenised tyramine molecules by peroxidase activity. Tyramine is a phenolic compound and HRP can catalyse the dimerisation of such compounds when they are present at high concentrations, probably by the generation of free radicals (Zaitse & Ohkura, 1980). If applied in lower concentrations, such as those used in the signal amplification reaction, the probability of dimerisation is reduced, whereas the binding of the highly reactive intermediates to electron-rich moieties of proteins, such as tyrosine, at or near the site of the peroxidase binding site is favored (Speel *et al.*, 1999). Visualisation of deposited tyramides can be performed either directly after the TSA reaction with fluorescence microscopy, if fluorochrome-labelled tyramides are used, or indirectly with either fluorescence or brightfield microscopy, if biotin, digoxigenin, or di- or trinitrophenyl are used as haptens. This can act as further binding sites for anti-hapten antibodies or (strept)avidin conjugates (in the case of biotinylated tyramides, Speel *et al.*, 1999).

1.4.7 Aqua-Optosensor (AOS)

Aqua-Optosensor is an optical immunosensor based on total internal reflectance fluorescence (TIRF). The sensor system consists of a disposable sensor chip and an optical readout device

(Sensor device see Figure 18, page 69). The chip is built up from a ground and cover plate with in- and outlet and, between, of an adhesive film with a capillary aperture of 50 μm . The ground plate serves as a solid phase for the immobilisation of bio-components e.g. the capture antibody or hapten conjugate. In the readout device, an evanescent field is generated at the surface of the ground plate by total internal reflection of a laser beam (principle see Figure 11). This field is used for the excitation of fluorophore markers. The generated fluorescence light is detected by a simple optical setup using a photomultiplier tube and the voltage signal increase in time is directly proportional to the amount of fluorophore bound to the surface of the flow channel (Schult *et al.*, 1999).

Figure 11 Principle of the Aqua-Optosensor



Principle of total internal reflectance fluorescence, figures supplied from Karin Wöllner (presentation file, 2010)

For the excitation of the fluorophores the evanescent field of the laser light is used which is generated by total internal reflection of the laser beam at an interface between the high-refractive (n_1 , PMMA, poly- (methyl methacrylate)) and the low-refractive (n_2 , liquid sample) material. The intensity of this field decreases exponentially with increasing distance from the interface in the half-space of the low refractive (n_2) medium. Theoretical prediction and experimental results show that this increase is linear in the case of small analyte concentration and/or short times which always hold for the sensor setup presented here. Consequently, the slope of the linear increase is directly proportional to the concentration of

the analyte. From the increase of the fluorescence signal the initial slope (sensitivity), as mV/s, is calculated. In general, every kind of immunochemical assay can be performed with this setup (Schult *et al.*, 1999).

1.5 Outline of goal and tasks for this work

Reviewing the current AHL detection methods, both of bioreporter assays and conventional chemical analyses have the advantages and disadvantages. According to this background, the development of a new sensitive AHL molecule detection system, based on anti-AHL antibodies, was set to be the goal of this study. The idea was to offer an additional AHL analytical method, which might also be possible for *in situ* detection of AHLs.

As noticed in section 1.4, the key of an immunochemical technology is the antibody quality, which has direct influence on the assay sensitivity. Therefore the antibody establishment was the focus of this study. The tasks consisted of four main steps. A) The preparation of the immunisation, which contained the selection, synthesis of the AHL hapten and further conjugation to protein carriers. B) Production and screening of anti-AHL antibodies. C) Further characterisation of the antibodies and optimising of the immunoassays. D) Application of the assays for detection of QS molecules in biological samples from different biological origins.

2 Materials and methods

2.1 Chemicals, standards and proteins

Adipic acid, adipic acid dichloride, aluminium oxide, potassium hydroxide, toluene, benzyl bromide, tetrabutyl ammonium bromide, sebacid acid, Meldrum's acid, dichloromethane, 4-dimethylaminopyridine, triethylamine, acetonitrile, (*S*)-2-amino-4-butyrolactone hydrobromide and sodium cyanoborohydrid were purchased from Sigma-Aldrich (Taufkirchen, Germany). Ethyl acetate, cyclohexane, ammonium chloride and acetonitrile (chromasolv) were purchased from Riedel-de-Haën (Seelze, Germany). Dimethylformamide, pyridine, hydrochloric acid, sodium hydroxide, sodium chloride, and sodium hydrogen carbonate were purchased from Merck (Darmstadt, Germany). Hexane was purchased from Promochem (Wesel, Germany).

Table 4 Commercially purchased HSL standards

HSLs	Company
C4-HSL	Cayman chemical, USA
3oxo-C4-HSL	Nottingham University, UK
3OH-C4-HSL	Nottingham University, UK
C6-HSL	Cayman chemical, USA
C6-HSL (DL isomer)	Sigma Aldrich, Germany
3oxo-C6-HSL	Sigma Aldrich, Germany
3OH-C6-HSL	Nottingham University, UK
C8-HSL	Cayman chemical, USA
3oxo-C8-HSL	Sigma Aldrich, Germany
3OH-C8-HSL	Nottingham University, UK
C10-HSL	Cayman chemical, USA
3oxo-C10-HSL	Sigma Aldrich, Germany
3OH-C10-HSL	Nottingham University, UK
C12-HSL	Sigma Aldrich, Germany
3oxo-C12-HSL (in ethanol)	Cayman chemical, USA
3oxo-C12-HSL	Cayman chemical, USA
3OH-C12-HSL	Nottingham University, UK

All substances in powder form and L isomer if not noticed.

The haptens *N*-(11-carboxy-3-oxoundecanoyl)-L-homoserine lactone (HSL1), *N*-(5-carboxypentanoyl)-L-homoserine lactone (HSL2), *N*-(11-carboxy-3-hydroxyundecanoyl)-L-homoserine lactone (HSL3), and *N*-(9-carboxynonanoyl)-L-homoserine lactone (HSL4) were synthesised in house.

The HSL standards were purchased from different companies (Table 4). The homoserine molecules (HS), the hydrolysis products of HSLs, were prepared in house. Briefly, 1 mg of HSL substances was solved in 900 μ L ACN and 100 μ L 1M NaOH was added to the solution at room temperature and shaken for 15 min. The homoserine lactone rings were supposed to be completely opened according to (Engelmann *et al.*, 2007) and ready for use as stock solution for assays.

For conjugations, *N*-hydroxysuccinimid (NHS), 1,3-dicyclohexylcarbodiimide (DCC), *N,N*-dimethylformamide 99% (DMF), ovalbumin from chicken egg white (OVA), albumin from bovine serum (BSA), and sodium tetraborate were purchased from Sigma-Aldrich (Taufkirchen, Germany). Horseradish peroxidase (HRP) was purchased from Serva Electrophoresis (Heidelberg, Germany). Boric acid was from Riedel-de-Haën (Seelze, Germany). SuperFreeze peroxidase stabilizer was purchased from Pierce/Perbio (now Thermo Fisher Scientific, Bonn, Germany).

For ELISAs, protein G from *Streptococcus* and skim milk powder, hydrogen peroxide (H_2O_2) and 3,3',5,5'-tetramethylbenzidine (TMB) were purchased from Sigma-Aldrich (Taufkirchen, Germany). Mouse anti-rat IgGs (TIB170, TIB 172, TIB 173 and TIB 174) are in house clones (E. Kremmer, IMI, HMGU). They are commercially available from ATCC (American Type Culture Collection, Manassas, USA). Goat anti-rat antibody (GAR) conjugated with HRP was obtained from Dianova (Hamburg, Germany). Dimethylsulfoxide (DMSO), 99%, was purchased from Fluka (now Sigma-Aldrich). Buffer salts (sodium dihydrogen phosphate monohydrate, disodium hydrogen phosphate dehydrate and sodium chloride, sodium acetate, sodium carbonate, citric acid mono hydrate), Tween 20 and sulphuric acid, 95-97%, were purchased from Merck (Darmstadt, Germany).

2.2 Instruments for hapten syntheses

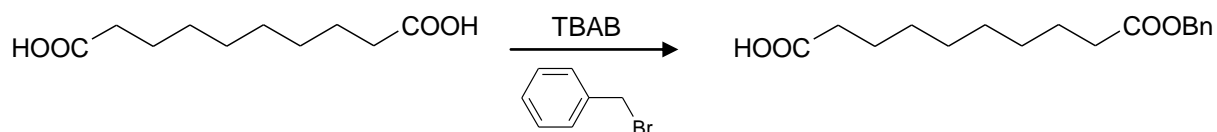
NMR spectra were acquired on solutions containing 0.4-0.7 mg HSL substances in 0.5-0.75 mL $CDCl_3$. 1H and ^{13}C NMR spectra were obtained at 303 K with a 5mm z-gradient $^{13}C/^1H$ dual cryogenic probe using 90° excitation pulses on a Bruker DMX 500 spectrometer

(Rheinstetten, Germany) operating at 500 MHz. Chemical shifts (ppm) were reported relative to internal CDCl_3 (^1H , 7.24 ppm and ^{13}C , 77.00 ppm).

UPLC-MS measurements were carried out with a NanoAcquity UPLC system (Waters, Milford, USA) coupled to a Q-TOF2 mass spectrometer (Waters-Micromass, Manchester, UK) using negative electrospray ionisation. After injection of 0.5 μL sample volume, the analytes were trapped for preconcentration on a symmetry C18 column (5 μm , 180 μm x 20 mm) for 4 min at a flow rate of 4 $\mu\text{L min}^{-1}$ and separated subsequently at 0.4 $\mu\text{L min}^{-1}$ and 30°C on an Atlantis C18 nano-column, (3 μm , 75 μm x 150 mm, both Waters, Milford, USA) with an initial mobile phase composition of 95% of eluent A (methanol/water 10:90 v/v, 2 mM ammonium acetate and 5% eluent B (methanol, 2 mM ammonium acetate). The eluent gradient started after a delay of 2 min increasing to 30% B within 5 min. A final gradient increase to 100% B followed by further 15 min holding this composition for 4 min. Then immediate switching to initial conditions was done followed by an equilibration time of 9 min until the end of the cycle after 35 min in total. Thus the retention time of 17.6 min for HSL3 and 18.2 for the co-product was measured. Voltage of PicoTip electrospray emitter (10 μm orifice, New Objective, USA) was set to 1.8 kV, MS cone voltage 17 V, collision energy 8 eV, MCP detector 2.3 kV and scan time was 2 sec from m/z 120 – 500. The analytes were detected as mono-deprotonated (M-1)-molecular ions with m/z 328.2 and m/z 360.2.

2.3 Synthesis of HSL haptens

2.3.1 Synthesis of sebacic acid monobenzyl ester (1)



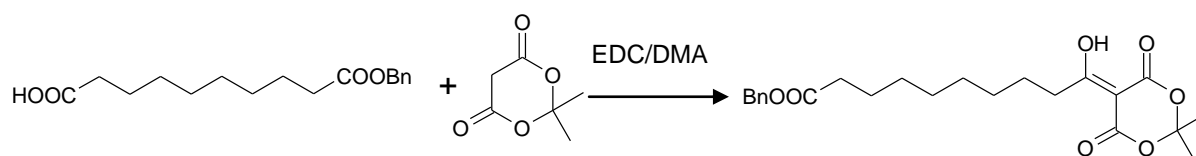
Sebacic acid ($\text{HOOC}-(\text{CH}_2)_8-\text{COOH}$, MW=202) [20 mmol] was reacted with a potassium hydroxide solution (KOH, MW=56 [20 mmol] in 40 mL distilled water under stirring for 1 h at 40°C. Ethanol was added and the azeotrope was evaporated to dryness. 60 mL of toluene were added and mixed with 2 mmol tetrabutyl ammonium bromide (TBAB, MW=322) and 20 mmol of benzyl bromide (MW=171). The reaction was stirred under reflux for 5 h. After cooling down to RT, the solvent was removed.

The residue was purified on silica gel column chromatography using a gradient of



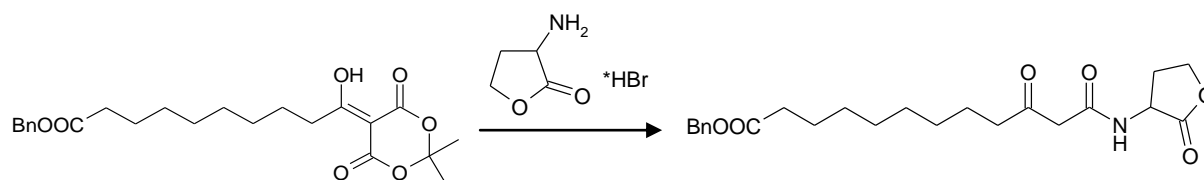
as eluent.

2.3.2 Synthesis of N-(9-benzylcarboxyl-1-hydroxy)-Meldrum's acid (2)



4.05 mmol of the purified sebacic acid monobenzyl ester (MW=292, 1 Eq), Meldrum's acid (MW=144, 1 Eq), and dimethyl aminopyridine (DMAP, MW=122, 1.05 Eq) were dissolved in 47 mL dry CH_2Cl_2 . The reaction mixture was cooled down with an ice bath (4°C) and EDC (MW=191, 1.1 Eq) was added. The mixture was stirred for 1 h at 4°C then overnight at RT. The solvent was evaporated off and the crude residue dissolved in 75 mL ethyl acetate (EA) and washed twice with 20 mL (2 x 20 mL) 2N HCl. The aqueous phases were joined and washed with 25 mL ethyl acetate. The EA phases were joined and dried over Na_2SO_4 . Na_2SO_4 was filtered off and the solvent was removed. The crude product was used without further purification.

2.3.3 Synthesis of N-(11-benzylcarboxy-3-oxoundecanoyl)-L-homoserine lactone (3)



6.86 mmol of **2** (MW=292, 1 Eq), α -amino- γ -butyrolactone hydrobromide (MW=182, 1Eq) and 1.145 mL triethylamine (MW=109, 1.2 Eq) were dissolved in 110 mL acetonitrile and stirred 2 h at RT then 3 h under solvent reflux.

Thereafter, the solvent was removed. The residue was dissolved in ethyl acetate (50 mL) and washed with:

1 x NaHCO₃ sat (30 mL)

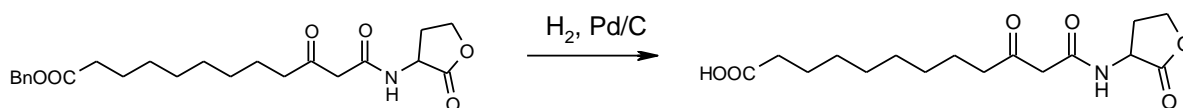
1 x NH₄Cl sat (30 mL)

1x NaCl sat (30 mL)

The organic phase was then dried over Na₂SO₄. Na₂SO₄ was filtered off and the solvent was removed.

The crude product was purified by column chromatography on silica gel using a mixture ethyl acetate (80%)-cyclohexane (20%) as eluent.

2.3.4 Synthesis of *N*-(11-carboxy-3-oxoundecanoyl)-*L*-homoserine lactone (HSL1) (4)



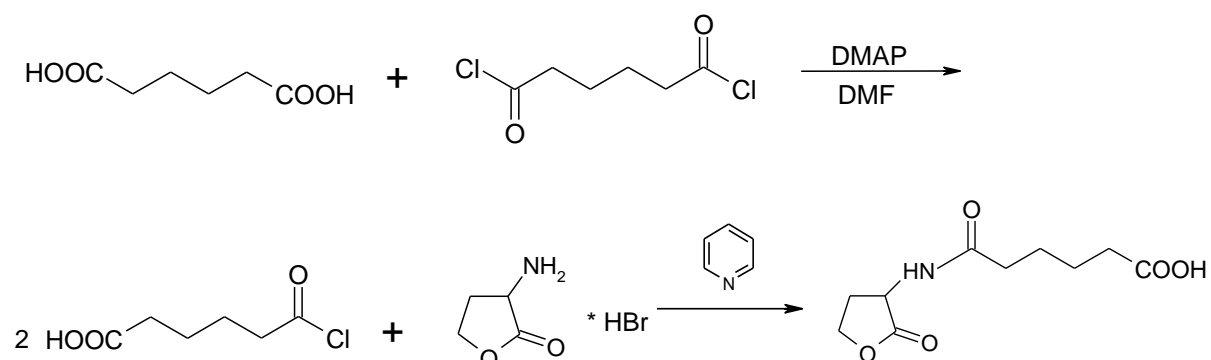
370 mg of **3** (MW=417, 1 Eq) and 37.4 mg Pd/C were dissolved in 11 mL absolute methanol. The atmosphere in the flask was purged with vacuum/N₂ and placed under H₂ atmosphere for 4 h. The catalyst was filtered out and the solvent evaporated off. The dried product had a weight of 266 mg and was used without further purification.

HSL1:

¹³C NMR (500 MHz, CDCl₃): δ = 206.49; 179.67; 172.17; 163.84; 66.06; 61.16; 49.65; 40.04; 33.98; 33.29; 29.53; 29.37; 29.14; 29.07; 24.81; 23.21.

¹H NMR (500 MHz, CDCl₃): δ = 9.85 (s, 2H); 4.45 (m, 1H); 4.39 (m, 1H); 4.26 (m, 1H); 3.58 (s, 2H); 2.52 (m, 1H); 2.31 (m, 2H); 2.30 (m, 2H); 2.26 (m, 1H); 1.59 (m, 2H); 1.54 (m, 2H); 1.52 (m, 2H); 1.28 (m, 2H); 1.27 (m, 2H); 1.23 (m, 2H).

2.3.5 Synthesis of *N*-(5-carboxypentanoyl)-L-homoserine lactone (HSL2) (5)



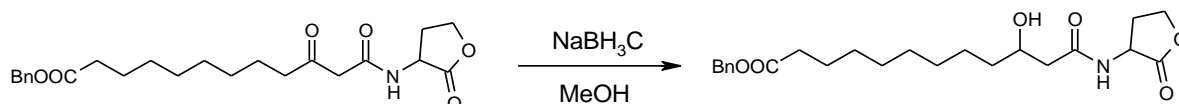
Adipic acid (MW = 146) 643 mg and 4-dimethylaminopyridine (MW = 122) 20 mg were solved in 0.35 mL dimethylformamide. Accordingly 0.6 mL adipic acid dichloride (4 mmol, MW = 183) were added and stirred for 4 days. After addition of 1.465 g (*s*)- α -amino- γ -butyrolactone hydrobromide (8 mmol, MW = 182) and 10 mL pyridine the mixture was stirred 2 days. After removal of the solvent with nitrogen flow, 3 mL H₂O was added and the mixture was extracted with ethyl acetate. The extract was purified with a short aluminum oxide column. After recrystallization in ethyl acetate/hexane solution, 1 g of raw product was gained (MW = 247, circa 50%).

HSL2:

¹³C NMR (500 MHz, CDCl₃): δ = 176.28; 174.3; 172.17; 66.06; 62.12; 36.77; 33.29; 33.00 24.00; 23.87.

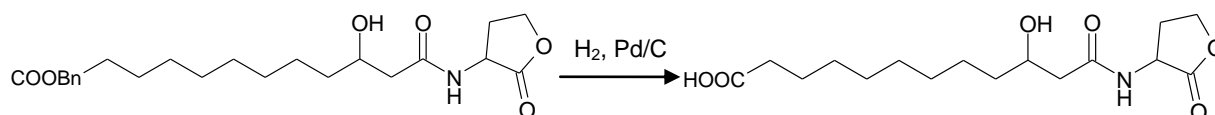
¹H NMR (500 MHz, CDCl₃): δ = 8.84 (s, 2H); 4.45 (m, 1H); 4.39 (m, 1H); 4.15 (m, 1H) 2.52 (m, 1H); 2.36 (m, 2H); 2.26 (m, 1H); 2.25 (m, 2H); 1.96 (m, 2H) 1.65 (m, 2H).

2.3.6 Synthesis of *N*-(11-benzylcarboxy-3-hydroxyundecanoyl)-*L*-homoserine lactone (**6**)



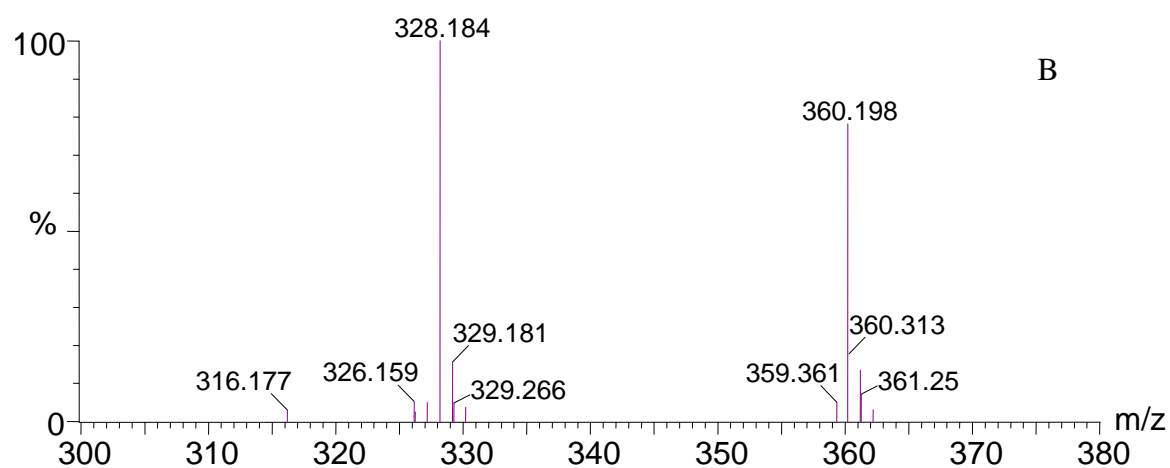
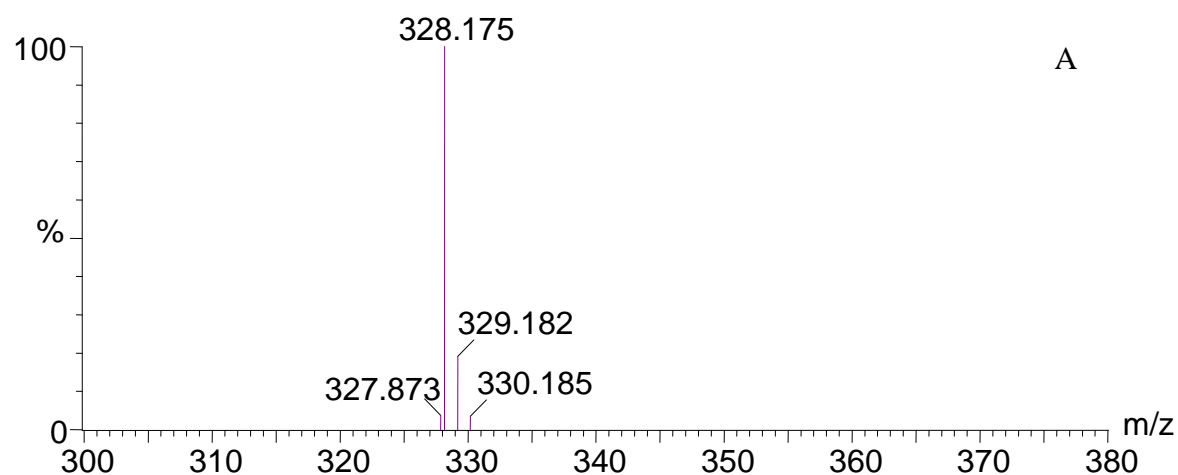
Sodium cyanoborohydride (2.9 mmol, MW=63, 1.5 Eq) was added to a solution of **3** (MW=417, 1 Eq) in 15 mL methanol. The reaction mixture was maintained at pH 3-4 by addition of 3% HCl in methanol. Three further additions of sodium cyanoborohydride (3 x 2.9 mmol) were made at 3 h intervals while the pH was kept at 3-4. The solvent was removed by rotary evaporation, and the residue was extracted with hot ethyl acetate (4 x 20 mL). The ethyl acetate extracts were combined and concentrated to yield the crude product, which was purified by silica column chromatography on silica gel using as eluent 10% MeOH in DCM.

2.3.7 Synthesis of *N*-(11-carboxy-3-hydroxyundecanoyl)-*L*-homoserine lactone (HSL3) (**7**)



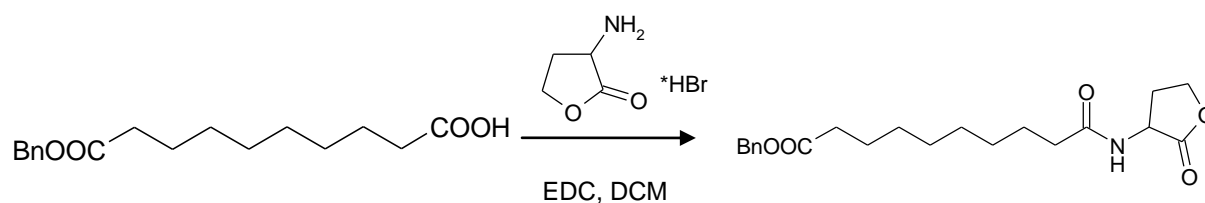
587 mg of **6** and 58.7 mg Pd/C were dissolved in 17 mL absolute methanol. The atmosphere in the flask was purged with vacuum/N₂ and placed under H₂ atmosphere for 2.5 h. The catalyst was filtered out and the solvent evaporated off. The dried product had a weight of 446 mg. Due to impurity of HSL3, further purification was performed by crystallization in 25% acetonitrile (v/v) at 4 °C over night. The purified HSL3 was characterised with NMR and LC-MS (Figure 12).

Figure 12 Mass spectrum (LC-MS) of HSL3



A: Purified HSL3 [(M-H) 328.175]; B: HSL3 [(M-H) 328.175]; and its containing the hydrolyzed byproduct [(M-H) 360.198] before purification

2.3.8 Synthesis of *N*-(9-benzylcarboxy nonanoyl)-*L*-homoserine lactone (8)



1.4 mmol of **1** (MW=292, 1.25 Eq), triethylamine (2.3 mmol, MW=101, 2 Eq), α -amino- γ -butyrolactone hydrobromide (1.1 mmol, MW=182, 1 Eq) were dissolved in 11 mL dry

dichloromethane. The reaction was cooled down with ice bath and kept under stirring for 1 h. EDC (1.7 mmol, MW=191, 1.5 Eq) was added and the mixture was stirred at RT for 48 h. DCM was removed by rotary evaporation. The residue was dissolved in ethyl acetate (30 mL) and washed with:

2 x 10 mL NaHCO₃ saturated

2 x 10 mL NH₄Cl saturated

1 x 10 mL NaCl saturated

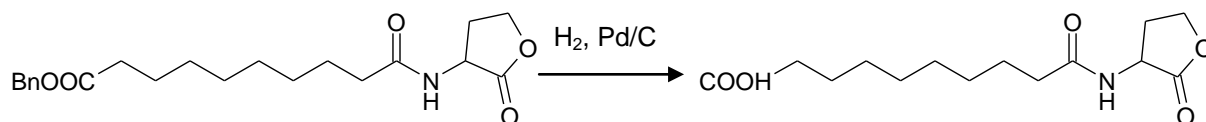
The organic phase was then dried over Na₂SO₄. Na₂SO₄ was filtered off and the solvent was removed. The crude product was purified by silica column chromatography on silica gel (ethyl acetate/cyclohexane: 80/20).

HSL3:

¹³C NMR (500 MHz, CDCl₃): δ = 179.05; 176.92; 172.17; 69.62; 66.06; 62.12; 41.62; 35.71; 34.23; 33.29; 29.44; 29.14; 29.03; 28.47; 24.81; 24.62.

¹H NMR (500 MHz, CDCl₃): δ = 7.10 (s, 3H); 4.45 (m, 1H); 4.39 (m, 1H); 4.15 (m, 1H); 3.84 (m, 1H); 2.52 (m, 1H); 2.31 (m, 2H); 2.29 (m, 1H); 2.26 (m, 1H); 2.10 (m, 1H); 1.52 (m, 2H); 1.46 (m, 1H); 1.30 (m, 2H); 1.28 (m, 2H); 1.27 (m, 1H); 1.26 (m, 2H); 1.25(m, 2H); 1.23 (m, 2H).

2.3.9 Synthesis of *N*-(9-carboxynonanoyl)-*L*-homoserine lactone **8** (HSL 4)



205 mg of **7** (MW=375) and 20.5 mg Pd/C were dissolved in 7 mL absolute methanol. The atmosphere in the flask was purged with vacuum/N₂ and placed under H₂ atmosphere for 3 h.

Thereafter, the catalyst was filtered out and the solvent was evaporated off. The dried product had a weight of 139 mg and was used without further purification.

HSL4:

^{13}C NMR (500 MHz, CDCl_3): $\delta = 179.67$; 176.28; 172.17; 66.06; 62.12; 36.56; 33.98; 33.29; 29.5; 29.18; 29.01; 26.76; 25.97; 24.81.

^1H NMR (500 MHz, CDCl_3): $\delta = 9.10$ (s, 2H); 4.45 (m, 1H); 4.39 (m, 1H); 4.15 (m, 1H); 2.52 (m, 1H); 2.29 (m, 2H); 2.26 (m, 1H); 2.10 (m, 2H); 1.60 (m, 2H); 1.52 (m, 2H); 1.42 (m, 2H); 1.35 (m, 2H); 1.34 (m, 2H); 1.23 (m, 2H).

2.4 Materials and instruments for ELISA

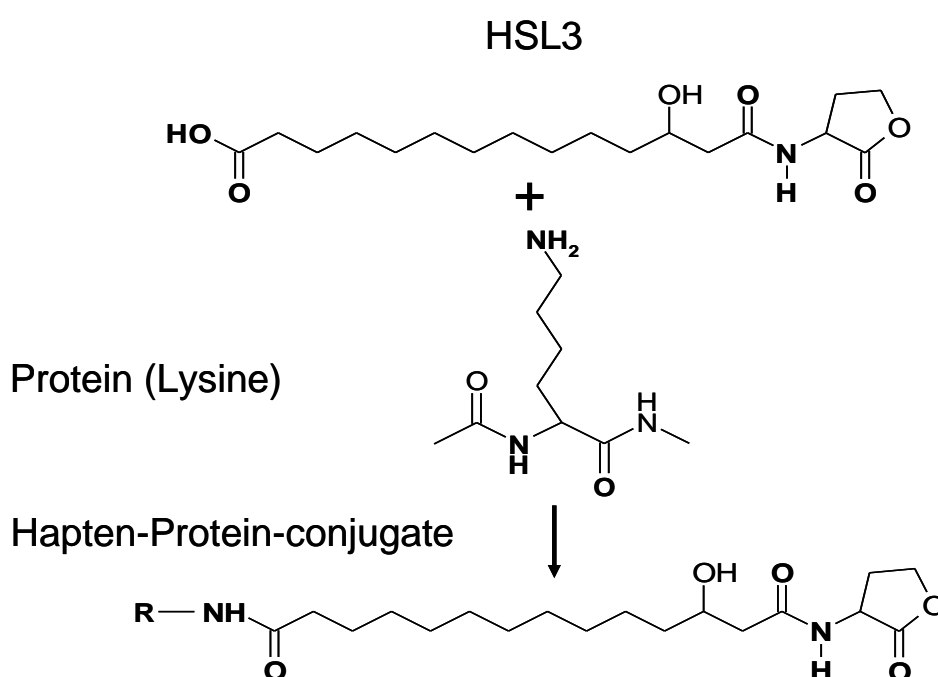
Ultra-pure water used for buffers and all other solutions, was prepared by Milli-Q filter system from Millipore (Eschborn, Germany). Nunc MaxiSorp™ 96-well microtiter plates and lids were purchased from Thermo Fisher Scientific (Schwerte, Germany) and Greiner 96-well U-shape medium binding plates were from Greiner Bio-One (Solingen-Wald, Germany). Washing steps in microtiter plates were performed with an automated microtiter plate washer from Bio-Tek Instruments (Bad Friedrichshall, Germany). Absorbance was read by a multi-detection reader Spectra Max M5^e from Molecular Devices (Palo Alto, USA, now part of Danaher Corporation, Washington, DC, USA). A heating-shaking-mixing system, Heidolph incubator 1000 from Metrohm (Herisau, Switzerland), was used for incubation or shaking. Centrifugation for conjugate preparations was performed with a Heraeus Sepatech Biofuge 1.5 (Hanau, Germany) in 500 μL protein low-bind tube from Eppendorf (Hamburg, Germany). During incubations, solutions were covered with parafilm (Pechiney Plastic Packaging, Menasha, USA).

2.5 Preparation of hapten-protein conjugates for immunogens and coating antigens

The haptens (HSL1, HSL2, HSL3, and HSL4) were conjugated to BSA and OVA according to the active ester method as described previously (Krämer, *et al.*, 2004, 2005). For example, for HSL1-BSA or HSL1-OVA, for each of the conjugates 47 μmol of NHS and 51 μmol of DCC were dissolved in 150 μL DMF, and the solution was added to 46 μmol of the hapten HSL1, respectively. This activation reaction was carried out for 4 h at RT with stirring. After that, the white precipitate urea was removed by centrifugation with 1400 rpm for 10 min. The

proteins BSA and OVA were solved in 40 mM PBS, pH 7.6 (15 mg in 1.5 mL), and the activated hapten solution was added slowly (10-20 μ L per 10 min) to the protein solutions. Approximately 140 μ L of hapten was added to each 1.5 mL protein solution. The conjugates were dialysed with 1 L 20 mM PBS buffer (pH 7.8) for 3 days in Slide-A-Lyser dialysis cassette (0.5-3 mL; 10 kDa MW cut-off) with buffer changes twice per day. For dialysis of all conjugations, Slide-A-Lyser dialysis cassettes, needles and syringes were purchased from Pierce/Perbio (now Thermo Fisher Scientific, Bonn, Germany)

Figure 13 Schematic protein conjugation process of HSL3.



Totally, eight conjugates were produced: HSL1-BSA, HSL1-OVA, HSL2-BSA, HSL2-OVA, HSL3-BSA, HSL3-OVA, HSL4-BSA, and HSL4-OVA for immunisations.

For the optimisation of the coating antigen ELISA format, HSL2-BSA-r1, HSL2-BSA-r2, HSL2-OVA-r2, HSL3-BSA-r1 and HSL3-BSA-r1 were conjugated with the analogous procedure as described above, but with a reduction in HSL hapten molecules per protein (Table 5).

Table 5 Preparation of hapten-protein conjugates for immunogens and coating antigens

Conjugate	Hapten	Protein	Hapten	NHS	DCC	DMF	Protein
HSL1-BSA	HSL1	BSA	46	47	51	150	15
HSL1-OVA	HSL1	OVA	46	47	51	150	15
HSL2-BSA	HSL2	BSA	46	47	51	150	15
HSL2-OVA	HSL2	OVA	46	47	51	150	15
HSL2-BSA-r1	HSL2	BSA	25	25	28	200	15
HSL2-BSA-r2	HSL2	BSA	20	25	28	300	15
HSL2-OVA-r2	HSL2	OVA	20	25	28	300	15
HSL3-BSA	HSL3	BSA	15	10	17	50	5
HSL3-OVA	HSL3	OVA	15	10	17	50	5
HSL3-BSA-r1	HSL3	BSA	4	3	4	13	5
HSL3-OVA-r1	HSL3	OVA	4	3	4	13	5
HSL4-BSA	HSL4	BSA	92	93	102	300	15
HSL4-OVA	HSL4	OVA	92	93	102	300	15

2.6 Characterisation of hapten protein conjugates with UV absorbance spectra

The haptens, proteins and conjugates were diluted in 40 mM PBS and 250 μL well⁻¹ of the prepared solution were pipette into the wells of a UV-star 96-well plate (Greiner Bio-one, Monroe, USA). The absorbance of the UV spectra of the HSL1, HSL2 and HSL4 conjugates were determined with a SAFIRE II microplate reader (Tecan, Switzerland) from 240-500 nm. Differently HSL3 conjugates were performed with the Spectra Max M5^e microplate reader (Molecular Devices, USA) with the same preparation procedure described above. The spectra were recorded and visualised automatically with the corresponding software of the instruments. Additionally, coating antigen format ELISAs were also used for determination of the binding of antibody-conjugates. The concentrations used for UV measurement of the conjugates, haptens and proteins are listed in Table 6.

Table 6 Concentration of haptens, proteins and conjugates for UV absorbance spectra

Hapten [mg mL ⁻¹]	Protein		Conjugate	
	[mg mL ⁻¹]		[mg mL ⁻¹]	
HSL1	BSA	OVA	HSL1-BSA	HSL1-OVA
0.1	2.5	2.5	2.5	2.5
HSL2	BSA	OVA	HSL2-BSA	HSL2-OVA
0.1	2.5	2.5	2.5	2.5
HSL3	BSA	OVA	HSL3-BSA	HSL3-OVA
0.1	3	3	3	3
HSL4	BSA	OVA	HSL4-BSA	HSL4-OVA
0.1	1.25	1.25	1.25	1.25

2.7 Preparation of enzyme-tracers

As enzyme-tracers, HSL1-HRP, HSL2-HRP, HSL3-HRP, and HSL4-HRP were prepared according to the method described by Schneider & Hammock (1992). Briefly, for each enzyme- tracer, 3 μmol of hapten (HSL1, HSL2, HSL3, or HSL4) were used. A solution with

NHS (15 μmol) and DCC (30 μmol) in 130 μL DMF was added to each hapten. The mixture was then stirred at RT for 4 h and further for 12 h at 4°C. The solution was then centrifuged to remove the precipitates and the clear supernatants of the activated haptens were slowly added (10 μL per 10 min) to 3 mL of HRP solution (2 mg HRP in 3 mL 40 mM PBS, pH 7.6). After complete addition of hapten supernatants, the hapten-HRP mixtures were stirred for 12 h at 4°C. After that, the conjugates were dialysed for 3 days in 1 L 20 mM PBS buffer (pH 7.6), using Slide-A-Lyser cassette (0.5-3 mL; 10 kDa MW cut-off), with a minimum of one buffer change per day. Finally, the HSL-HRPs were stored at 4 °C for use or partly at -20 °C with a 1:3 dilution in SuperFreeze peroxidase stabilizer. Only HSL1-HRP and HSL3-HRP could be used for enzyme-tracer format assays. That was because HSL2-HRP and HSL4-HRP showed either weak binding or no inhibition, thus it's difficult to obtain sensible assays.

Table 7 Materials for enzyme-tracer production

Enzyme-Tracer	Date	Hapten [μmol]	NHS [μmol]	DCC [μmol]	DMF [μL]	HRP [mg]	Buffer [mL]
HSL1-HRP	08022008	HSL1, 3 μmol	15	30	130	3	3 (130 mM NaHCO ₃)
HSL1-HRP	05062009	HSL1, 3 μmol	15	30	130	3	3 (130 mM NaHCO ₃)
HSL2-HRP	08022008	HSL2, 3 μmol	15	30	130	3	3 (130 mM NaHCO ₃)
HSL3-HRP	09052009	HSL3, <3 μmol	15	30	130	3	3 (130 mM NaHCO ₃)
HSL3-HRP	25042008	HSL3(impure), 3 μmol	15	30	130	3	3 (40 mM PBS)
HSL3-HRP	06102009	HSL3, 3 μmol	15	30	130	3	3 (40 mM PBS)
HSL4-HRP	25042008	HSL4, 3 μmol	15	30	130	3	3 (40 mM PBS)

2.8 Production of anti-HSL monoclonal antibodies

Approximately 50 μg of each immunogen conjugate was injected intraperitoneally and subcutaneously in to LOU/C rats using CPG2006 (TIB MOLBIOL, Berlin, Germany) as adjuvant. After 2 months a final boost was given 3 days before fusion. Fusion of the myeloma

cell line P3X63-Ag8.653 with the rat (or mouse) immune spleen cells was performed according to standard procedure (Kremmer *et al.*, 1995). Hybridoma supernatants were tested in a solid-phase immunoassay using HSL-BSA conjugates adsorbed on polystyrene microtiter plates. After incubation with culture supernatant for 1 h, bound mAbs were detected using HRP-labelled goat-anti-rat IgG+IgM antibodies (Dianova) and o-phenylenediamine as chromogen in the enzyme reaction. A hapten-BSA conjugate, which was prepared in the same way, but with an unrelated hapten structure, was used as negative control (Performed by Kremmer, IMI; HMGU).

2.9 Determination of immunoglobulin type

The immunoglobulin (Ig) type of the mAbs was determined using biotinylated mAbs specific for IgM, IgG subclasses, and light chains (α -IgG1, α -IgG2a, α -IgG2b, α -kappa (ATCC), α -IgM (Zytomed, Berlin, Germany), α -IgG2c, α -lambda (Ascenion, Munich, Germany). HRP-labelled avidin (Alexis, Grünberg, Germany) was used to visualize the bound biotinylated mAbs. The mAbs present in this study were all IgG2a, κ antibodies (determined by Kremmer, IMI, HMGU).

2.10 Purification of monoclonal antibodies and determination of protein concentration

Protein G or protein A was used for purification of mAbs. A culture supernatant was added to protein G-Sepharose 4 Fast Flow (Amersham Pharmacia Biotech, Uppsala, Sweden), and the antibodies were eluted from the column with 0.1 mol L⁻¹ citrate buffer, pH 2.7. Dialysis was performed against 40 mM PBS, pH 7.6, three times, each time with 100 times the antibody volume. Antibody solutions were sterile filtered with a 0.2- μ m filter and stored at 4°C until used. The determination of protein concentrations of the antibodies was carried out with a spectrophotometer, on the basis of absorbance measurements at 235 nm and 280 nm (Whitaker & Granum, 1980) (performed by Kremmer, IMI, HMGU).

2.11 Characterisation of HSL antibodies (anti-HSL mAbs) with enzyme-linked immunosorbent assay (ELISA)

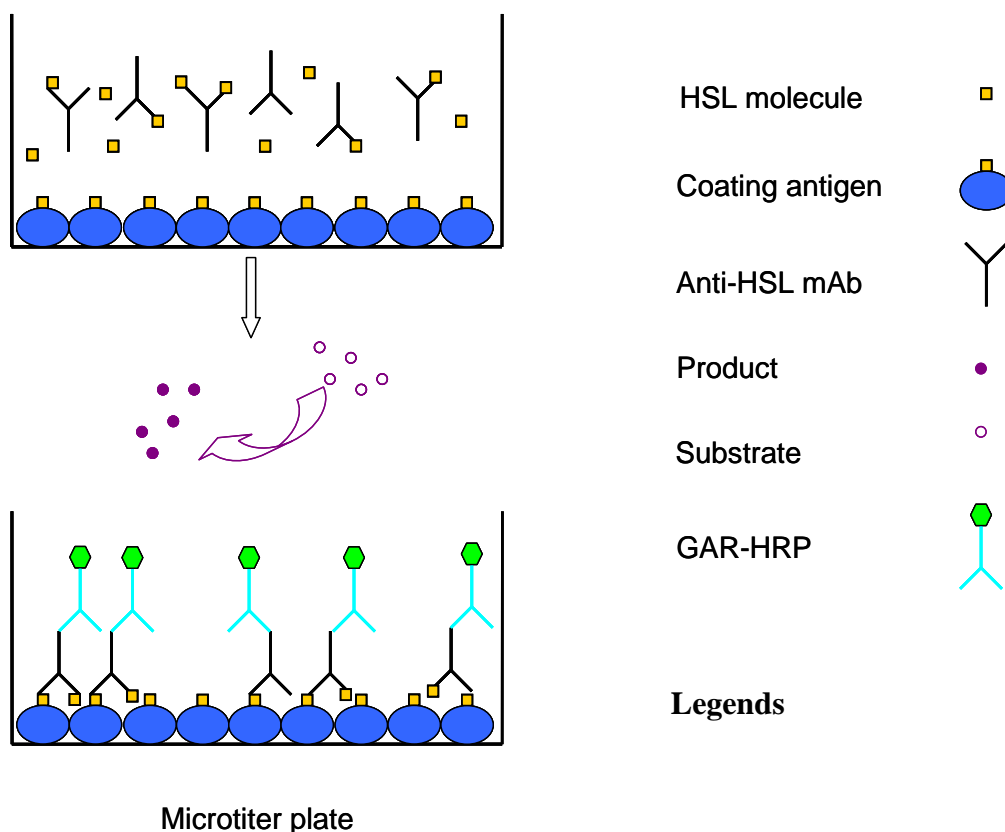
The antibody binding was determined against numerous HSL substances using coating antigen and enzyme-tracer format. Further antibody selection and application were all based on the characterisation of the antibodies.

2.11.1 Standard procedure of coating antigen format ELISA

For antibody screening, HSL2-BSA was diluted to $2 \mu\text{g mL}^{-1}$ in 50 mM carbonate buffer, (100 μL per well, pH 9.6) for coating on MaxiSorp microtiter plate at 4°C , overnight. The next day, the plate was washed, 200 μL per well slim milk powder solution were added (1% in 40 mM PBS, 1 h) to block the unsaturated plate surface. During the time for blocking, 75 μL analyte per well (commercially purchased HSL analogues in 40 mM PBS, pH 7.6) and 75 μL mAb per well (in 40 mM PBS) were pre-incubated in Greiner Bio-One U-shape plate (concentrations please see Table 14). The U-shape plates, containing 150 μL per well of analyte-mAb mixture, were covered with lids and shaken by Heidolph incubator 1000 for 1 h. Then the analyte-mAb (100 μL per well) mixture was transferred from U-shape plate to the blocked MaxiSorp plate after washing. The mixture was incubated for 1 h on the coated MaxiSorp plate. After the plate was washed again, 100 $\mu\text{L well}^{-1}$ of a mixture of biotinylated mouse anti-rat mAbs (named TIBmix: biotinylated TIB 172 (mouse anti-rat kappa light chain), TIB173 mouse anti-rat IgG2a (Fc)), TIB174 (mouse anti-rat IgG2b (Fc)), TIB 170 (mouse anti-rat IgG1 (Fc)) mixed with same portion of each, provided by E. Kremmer, IMI, HMGU) was added to plate for 1 h. After another washing step, 100 μL per well of streptavidin-HRP was used for the biotin-streptavidin reaction with 1 h incubation. The plate was washed and 100 μL TMB substrate (200 μL of 1% H_2O_2 and 800 μL of 6 mg mL^{-1} TMB (in DMSO) per well dissolved in 50 mL 100 mM sodium acetate buffer, pH 5.5) was added for the enzyme reaction. Finally, the reaction was stopped by the addition of 50 μL of 2 M H_2SO_4 per well after 5-25 min, depending on the color intensity on the plate. Alternatively, the steps of TIB mix and streptavidin could be replaced with the labelled secondary antibody GAR-HRP (100 $\mu\text{L well}^{-1}$, in 40 mM PBS, 1 h) while the rest of the procedure remained unchanged (Figure 15). In optimised coating antigen format assays HSL2-BSA-r1 and HSL2-BSA-r2, which contained reduced number of HSL2 molecules on BSA, were used for coating. The concentrations of antibodies, coating antigen, and the labelled secondary antibody are given in Table 14 (Page 92).

The optimising of the coating antigen format assay was including different tests of buffers (Hepes, PBS), incubation surfaces (glass, low bind tube et.), blocking solutions (BSA, Tween 20 etc.) incubation time etc. The details and results of the assay optimising can be found in the master thesis of Mandy Starke (Starke, 2009, unpublished study).

Figure 14 Scheme of coating antigen format ELISA



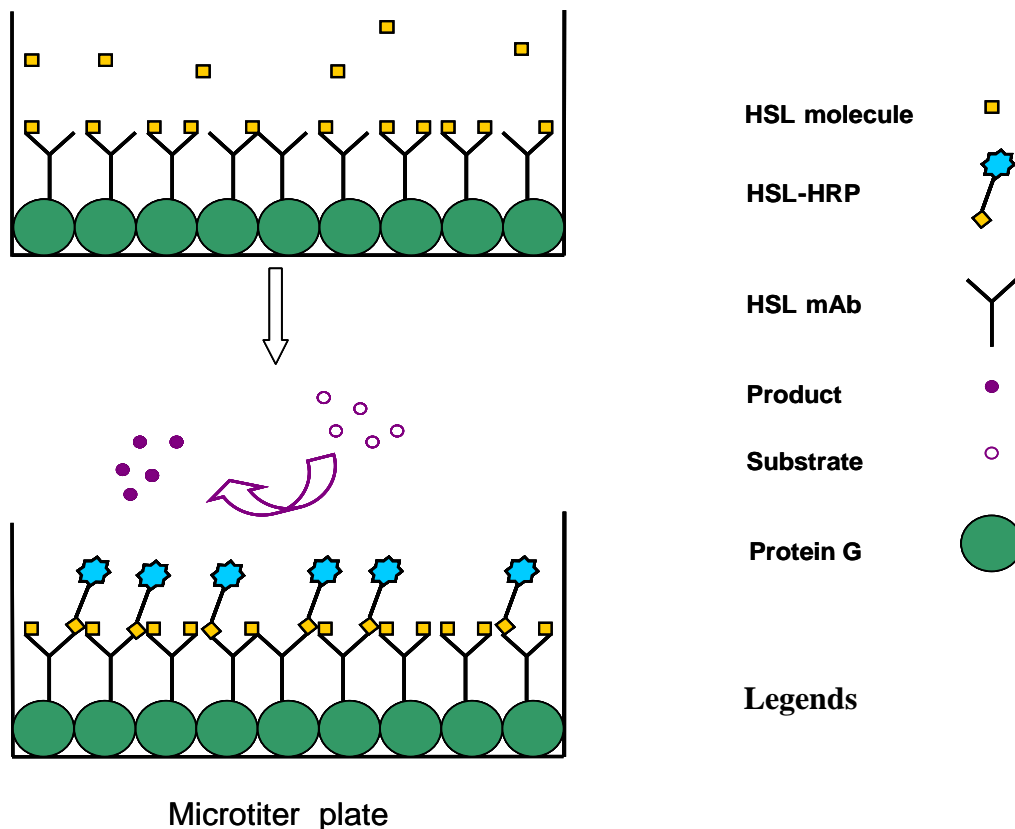
2.11.2 ELISA in the enzyme-tracer format

For coating on MaxiSorp plate, 200 $\mu\text{L well}^{-1}$ of Protein G solution with a concentration of 2 $\mu\text{g mL}^{-1}$ in 50 mM carbonate buffer (pH 9.6) was used (4°C, overnight, Figure 15). The next day, the plate was washed and 150 $\mu\text{L well}^{-1}$ of mAb solution was added for 2 h. Then, the plate was washed again, and 100 $\mu\text{L well}^{-1}$ of analyte solution was added (1 h). As a competitor and enzyme-tracer, 50 $\mu\text{L well}^{-1}$ of the prepared HSL1-HRP or HSL3-HRP solution was directly added to the plate wells, which still contained analyte solutions. The mixture was incubated with shaking for 1 h and the plate was washed (the concentrations of antibodies and dilutions of HSL-HRP tracers are summarised in Table 15). As described for the coating antigen format, TMB substrate (150 $\mu\text{L well}^{-1}$) was used for the enzymatic reaction. Finally, the reaction was stopped after 5-25 min with the addition of 50 $\mu\text{L well}^{-1}$ 2M H_2SO_4 .

The wash programme for both formats was the same, and it included 3 times washing with 200 $\mu\text{L well}^{-1}$, 4 mM PBST (40 mM PBS 1:10 diluted plus 0.05% Tween 20, pH 7.2) buffer. The incubation temperature was $25\pm 3^\circ\text{C}$. The optimised concentrations of all described solutions were determined by 2D titrations (results not shown). All ELISA absorbance

measurements were performed with a Spectra Max M5[°] microplate reader (Molecular Devices) at 450 nm (reference 650 nm).

Figure 15 Scheme of enzyme-tracer format ELISA



2.11.3 Titration and screening against HSL substances

To obtain the most sensitive assays, a titration process is necessary to find out the best combination of the assay relevant substances and concentrations. In coating antigen format, the HSL conjugates, anti-HSL antibody, HSL analyte and secondary antibody need to be tested. While in enzyme tracer format, coating protein (e.g. Protein G), anti-HSL antibody and HSL enzyme-tracer should be taken into consideration. For better understanding, an example of the template (experiment design in 96-well microtiter plate) is given in Figure 16. This is a coating antigen format assay for titration of HSL2-BSA concentration and the antibody dilutions. Three HSL2-BSA concentrations at $1 \mu\text{g mL}^{-1}$, $2 \mu\text{g mL}^{-1}$ and $4 \mu\text{g mL}^{-1}$ were coated, and 2 dilutions of antibody supernatants (1:50, 1:200) were applied, but only GAR-HRP dilution of 1:20000 was used for the assay. The variations are dependent on the factors, which are needed to be optimised for certain assays.

Figure 16 A template example for titration in coating antigen format

HSL2-BSA 1 µg mL ⁻¹				HSL2-BSA 2 µg mL ⁻¹				HSL2-BSA 4 µg mL ⁻¹				
PBS	C8-HSL	C4-HSL	PBS, no Ab	PBS	C8-HSL	C4-HSL	PBS, no Ab	PBS	C8-HSL	C4-HSL	PBS, no Ab	Ab 1:200
C												Ab 1:50
D												
E												Ab 1:200
F												
G												Ab 1:50
H												

Goat anti rat HRP 1:20000

Employing the optimal combination of the assay from titration, a series of selected HSL substances were tested to each single HSL antibody in both assay formats. The % control was calculated, using the formula below:

$$\text{Control (\%)} = (A/A_0) \times 100,$$

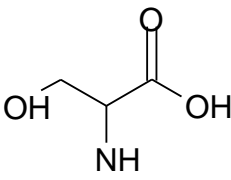
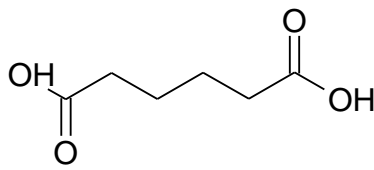
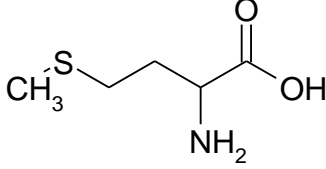
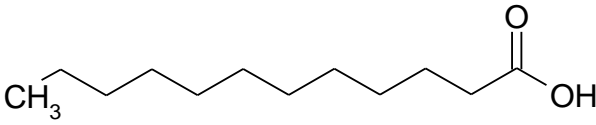
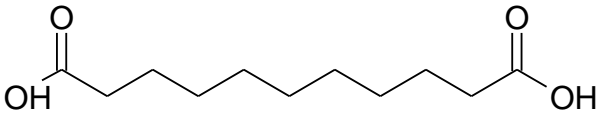
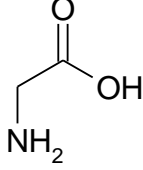
where A is the value of the absorbance for each standard or sample and A_0 is the value of absorbance for the zero standard (only 40 mM PBS). The less the % control values the higher is the binding affinity of the tested HSL to the antibody, because the ELISAs in this study are both competitive assays. The determination of % control values are the important process for the antibody characterisation because these results indicate how good the binding is between the antibody and HSL molecules. The screening of the first antibody supernatants was only performed with this method and standard curves were additionally tested for the second antibody screening.

2.11.4 Binding test to a few possible HSL degradation substances

Due to the high recognition to HSs of the mAbs, it was considered if the antibodies showed affinities to other possible HSL degradation products, e.g. serine. A few serine analogues and HSL acyl side chain similar esters (see Figure 17) have been selected for specific binding test. The 1 mg mL⁻¹ stock solutions were prepared in ACN or methanol and then further diluted to 1000 µg L⁻¹ in 40 mM PBS for immunoassay. The substances were determined with enzyme-

tracer format using mAb HSL1/2-2C10 in 200 ng mL⁻¹ and enzyme tracer HSL1-HRP 1:1000. The % control was calculated using the formula described in last paragraph (2.11.3).

Figure 17 Tested HSL/HS analogues

HSL fragment analogues	Molecular structure
Serine	
Adipic acid	
Methionine	
Dodecanoic acid	
Dodecandiacid	
Glycine	

2.11.5 Standard curves

The standard curves for the HSL analytes were set up in 40 mM PBS, ranging from 0 (only PBS) to 20000 or 50000 µg L⁻¹. Both the coating antigen and the enzyme-tracer format are competitive formats, which reveal (absorbance) signals that are inversely proportional to the analyte concentration. A blank, consisting of all buffers, was subtracted from all values, and was used in the corresponding reagents, addition of substrate for the enzyme reaction, and the stop solution. Usually, the blank value was in the same absorbance range as the highest HSL standard concentration of the standard curve.

Curve fitting of the standard curve was performed with SOFTmax Pro 5.2 (Molecular Devices) or SigmaPlot 11 (Systat Software, Inc., Chicago, IL, USA), using the four-parameter curve fit according to:

$$y = \frac{A - D}{1 + \left(\frac{x}{C}\right)^B} + D$$

Where A is the y-value corresponding to the asymptote at low values of the x-axis and D is the y-value corresponding to the asymptote at high values of the x-axis. The coefficient C is the x-value corresponding to the midpoint between A and D (e.g. $\mu\text{g L}^{-1}$; test midpoint (IC_{50})). The coefficient B describes how rapidly the curve makes its transition from the asymptotes in the centre of the curve.

Standard curves were normalised to % control as described above (Section 2.11.3). From these normalised standard curves, the limit of detection (LOD) of the assays was determined between 15- 85 % or 10-90 % of control (Harrison *et al.*, 1989).

2.11.6 Determination of cross reactivity

Using the optimised immunoassays, cross reactivities (CR) of 16 substances were determined, including twelve HSLs and four HSs (hydrolysed compounds of HSLs). In addition, all four haptens used in immunogens and/or enzyme-tracers were tested as cross-reactants. Usually, on each microtiter plate, the main analyte (3oxo-C10-HSL or C8-HSL) was used as reference in duplicate determination, whereas cross-reactants were determined in duplicate or triplicate. Standards for the cross reactants were set up in 40 mM PBS, pH 7.6, ranging from 0 (only PBS), and 0.5 to 20000 or 50000 $\mu\text{g L}^{-1}$, according to their expected CR.

CR% was calculated by use of the formula:

$$\text{CR (\%)} = (\text{IC}_{50} \text{ for the main analyte}) / (\text{IC}_{50} \text{ for the compound tested}) \times 100$$

2.12 Detection of HSLs in biological samples with ELISA

After full characterisation of the HSL mAbs, the application of the developed antibodies was followed by the detection of HSLs in different biological samples with ELISA. Since the operation procedure is very similar between different samples, the method will be described below using the example of HSL detection in *B. cepacia* LA3 culture supernatant (Chen *et al.*, 2010b).

2.12.1 Standard curves in matrix: determination of matrix effects

The *B. cepacia* LA3 was growing in ABC medium (components given in Attach. 2, page 144), thus the OD and IC₅₀ values of the main analyte were compared in PBS or in ABC medium. Only enzyme-tracer format with mAb HSL1/2-2C10 and HSL1/2-4H5 was used for detection of HSLs in real samples (only HSL1/2-2C10 was used for other biological samples), because of the higher sensitivity in this format than coating antigen format. The assays were carried out as described in section (2.11.2). For the determination of the matrix effect, standard solutions of the main analyte (3oxo-C10-HSL) were set up in ABC medium though, ranging from 0 (only ABC medium), 0.5 to 20000 µg L⁻¹. For better comparison of both assays (with mAbs HSL1/2-2C10 and HSL1/2-4H5, respectively), the same enzyme-tracer, namely HSL3-HRP was used here, diluted 1:600 and 1:400, respectively. As mentioned above, the change of OD, and the shifting of IC₅₀ and working ranges between immunoassays in PBS and in different media indicate the matrix effect of the assays (Chen *et. al.*, 2010b).

2.12.2 Standard curves in ABC Medium: determination of HSL in *B. cepacia* LA3 supernatants

As described in the previous section (2.12.1), different concentrations of 3oxo-C10-HSL in ABC medium were used for the set-up of the standard curve for *B. cepacia* LA3 supernatant measurements. Concentrations of 3oxo-C10-HSL and each LA3 supernatant sample were at least determined in duplicate wells on one plate, and the mean values with standard deviations were taken for final results. Depending on the working range of the assays, the samples were used undiluted or prepared in a dilution of 1:5, 1:10, or 1:20 before and after hydrolysis to obtain the best reliable results. For control purpose, 50 µg L⁻¹ (and 25 µg L⁻¹) of 3oxo-C10-HS were spiked to each hydrolysed sample. The biological samples were calculated by SOFTmax Pro and results were expressed as 3oxo-C10-HSL equivalents (Chen *et. al.*, 2010b).

2.13 Preparation of biological samples

All the biological samples in this study were prepared *in vitro* using the corresponding developed standard procedures. The preparation procedures will be thus described separately below.

2.13.1 Preparation of *Burkholderia cepacia* culture supernatants

B. cepacia strain LA3, a bacterial isolate from the rhizosphere of rice (Jha *et al.*, 2009), was cultivated in ABC minimal medium (Clark & Maaloe, 1967) (A and B modified using 20% glucose as C-source) with a pH of 6.8 (pH meter, pH 523, WTW, Weilheim, Germany). Two baffled flasks A and B (100 mL, Schott AG, Mainz, Germany), each contained 50 mL of the medium, were separately inoculated 1:1000 with an overnight culture. The flasks were incubated and shaken at 30°C and 175 rpm using an incubator shaker (Innova 4200, New Brunswick Scientific, Edison, NJ, USA). Cell cultures were sampled directly after inoculation and after 4, 8, 12, 24, 32 and 48h from flasks A and B in parallel. The OD_{436nm} was measured with a spectrophotometer (CE3021, Cecil Instruments Ltd., Cambridge, UK) at the sampling time points. To obtain cell free supernatants, samples were centrifuged at 4°C and 15000 g for 30 minutes (Sorvall Evolution RC, Thermo Fisher Scientific, Bonn, Germany). Subsequently, the supernatants were filtered through nitrocellulose filters (filter type 0.22 µm GSWP, Millipore, Schwalbach, Germany), frozen at -80°C for 1h and stored at -20°C until measurement. All chemicals were purchased from Sigma-Aldrich (Taufkirchen, Germany). The hydrolysis of *B. cepacia* culture supernatant samples was performed by addition of NaOH. Briefly, 100 µL of 1M NaOH was added to 800 µL sample in a glass tube, which then was shaken for 15 min at RT. The solution was neutralized to pH 7 by titration of 1M HCl and ABC medium was added to get a final volume of 1 mL, taking the amount of HCl used for titration into consideration. The control sample did not receive the NaOH but was instead dissolved in ABC medium (Chen *et al.*, 2010b).

2.13.2 Preparation of *Pseudomonas putida* culture supernatants

Preparation of culture supernatant of *P. putida* strains IsoF (Steidle *et al.*, 2001), F117 (an AHL-negative ppuI mutant of IsoF) and KT2440 (Steidle *et al.*, 2002) were grown in ABC minimal medium (Clark & Maaloe, 1967) (A B medium modified using the only carbon source C of 10 mM sodium citrate). The medium was buffered to a pH of 6.8 to avoid abiotic degradation of AHLs (Englmann *et al.*, 2007). The pH was measured after each sampling and was never found to be above 7.2. Cells were shaken at 30 °C and 175 rpm in 500-mL baffled flasks with 200 mL of medium. The medium was inoculated 1:1000 with an overnight grown bacterial culture and samples were taken 24h after inoculation. The bacterial culture samples were centrifuged at 15000 g at 4 °C for 15 min and the supernatant was filtered through Millipore nitrocellulose filters (0.22 mm, type GSWP) with a vacuum pump to remove the bacterial cells. Then the samples were quenched by shock frosting with liquid nitrogen and

stored at -20 °C until measured. The samples were measured undiluted or diluted with factors of 1:2 and 1:5.

2.13.3 Preparation of 1,2,4-TCB-mineralising bacterial biofilm community samples

The TCB degrading bacteria community and clay were prepared as described in (Wang et al., 2010). Totally 4 treatments in three replicates were performed:

Blank (B): medium+clay+TCB;

Community (C): medium+community+TCB;

Sterilised clay (S): medium+sterilised clay+TCB;

Established biofilm (E): medium+biofilm on clay+ TCB.

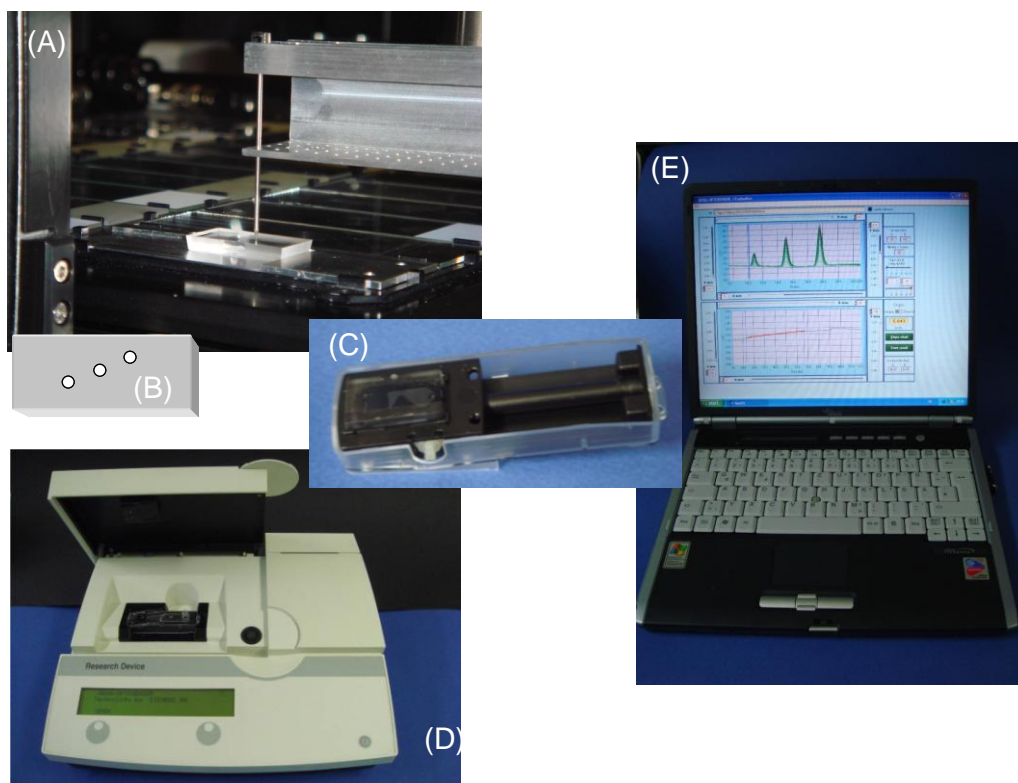
Three replicates were examined on days 1, 4, 7, 14, 21 and 28. The clay particles and the liquid medium were separated. The liquid medium was centrifuged at 6000 rpm for 30 min. 2×0.5 mL of the supernatant was taken for immunoassay analysis of AHLs, 45 mL for AHLs extraction and the left for pH measurement (Wang, unpublished manuscript).

The prepared supernatants and the extraction from clay were directly used to measure HSLs. The hydrolysis of the samples was performed using 0.1 M NaOH as prepared for *B. cepacia* LA3 samples. Considering the detection range of the immunoassay, the original and hydrolysis treated samples were prepared undiluted or diluted with factors of 1:5, 1:10, and 1:20 in TCB containing mineral medium.

2.14 HSL antibody characterisation with Aqua-Optosensor (AOS)

Alternatively to the coating antigen format ELISA, an immunosensor, called Aqua-Optosensor (Siemens AG, München, Germany), which uses TIRF as transduction principle, was applied for the characterisation of HSL mAbs. Due to the limited number of available chips in lab, only HSL1/2-2C10 was characterised with AOS for standard curves. The chips were coated with a polymethyl methacrylate (PMMA) matrix.

Figure 18 Aqua-Optosensor instruments



A: prism in spotter; B: PMMA prism chip with spots; C: sensor chip; D: reader; E: laptop with evaluation software. Pictures from Petra Krämer (Presentation file).

The coating-antigen HSL2-BSA-r2 was spotted via Microarray-Spotter Microgrid II (BioRobotics, UK, now Genomic Solutions, Ann Arbor, USA) onto the prism. Through Contact-Spotting method three accurate spots (each $\leq 1 \mu\text{L}$) of HSL2-BSA-r2 with concentrations of 3, 2 and 1 mg mL^{-1} were transferred from a 384-well microtiter plate (Greiner Bio-One GmbH, Frickenhausen, Germany) to the prism. A 50 mM carbonate buffer with 0.05% (v/v) Tween 20 (pH 9.6) was used for spotting. To enhance the immobilisation of the coating antigen, the spotted chips were further incubated over night at 4°C .

For determination of antibody-analyte binding on AOS, $150 \mu\text{L}$ of mAb HSL1/2-2C10-Oyster645 ($48 \mu\text{g mL}^{-1}$) and the same volume of analyte (3oxo-C10 HS or C10-HS) were prepared. The mAb HSL1/2-2C10-Oyster645 was firstly diluted in 40 mM PBS, which also contained 0.05% (v/v) Tween 20 (pH 7.6) and 1% BSA up to $75 \mu\text{L}$ as total amount. Then an additional $75 \mu\text{L}$ of Low Cross-buffer (CANDOR Bioscience GmbH, Weißensberg, Germany) was added to the antibody solution with a final mAb concentration of $48 \mu\text{g mL}^{-1}$. The analytes standards were prepared in the similar way as antibodies with concentrations ranging from 0 (only buffer) to $5000 \mu\text{g L}^{-1}$, only the buffer was 40 mM PBS without Tween

or BSA. After 300 μL antibody-analyte mixture was incubated in a vial for 20 min at 27°C, 280 μL of the it was pipetted into the chip container. The incubation step was performed on a shaker. The fluorescent signal was measured automatically by AOS at 35.5°C. The results were evaluated with the provided AOS software (Wöllner *et. al.*, 2010).

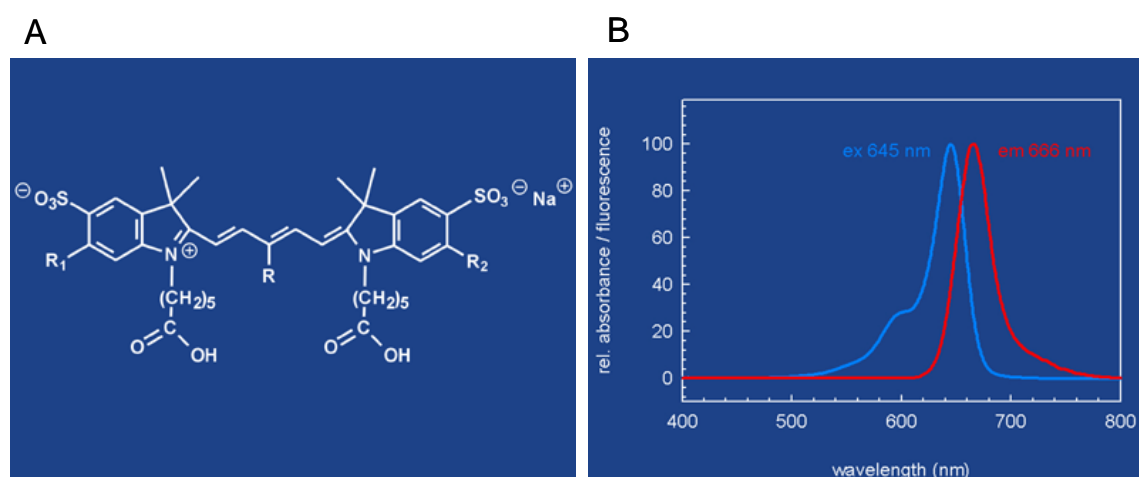
2.15 Optimisation of fluorescent labelling

The conjugation and label degree determination methods were optimised according to the protocol of labelling of antibodies from Denove Biolabels (Biolabels, 2005) (now Luminartis, Münster, Germany). A serial of conjugates with label degrees (moles fluorophore or dye per mol protein, D/P) of 1, 2, 5, 10 and 20 were produced.

2.15.1 Antibody-dye conjugation

The ester activated dye Oyster645-NHS was dissolved by addition of *N,N*-dimethylformamide (DMF) in original packed plastic tube. The purified mAbs were prepared in 40 mM PBS buffer (pH 7.6) with a concentration of about 1.5 mg mL^{-1} in Eppendorf protein lowbind tubes. The antibodies were diluted if their original concentrations were higher than 1.5 mg mL^{-1} . Then the diluted Oyster645-NHS (1 eq.) was added to the antibody solution (1 eq./label ratio) and incubated with shaking for 10, 20 or 40 min at room temperature.

Figure 19 Chemical structure and fluorescent spectra and of Oyster-645



A: molecular structure of Oyster-645; B: fluorescent spectra of Oyster 645. Ref: (www.biolabels.com)

The amount of antibody and dye was calculated with the formulas:

$$\text{*label degree} = \frac{n_{dye}}{n_{antibody}}$$

$$\text{*}n = \frac{CV}{M}$$

IgG antibody has a molecular weight of 150 kD and Oyster645-NHS has a molecular weight of 1 kD. The corresponding concentrations of mAbs were determined after purification.

To block the activated ester on fluorophore, a 10 % glycine solution (≥ 1 eq. Oyster645-NHS solution) in MilliQ water was added to the antibody-dye mixture. For purification of the antibody-dye conjugation, a dialysis was performed in 20 mM PBS buffer with Slide-A-Lyser cassette (0.5-3 ml; 10 kDa MW cut-off, Thermo Fisher Scientific, Bonn, Germany) for 3 days. Finally, the labelled mAbs were removed from slides to brown glasses with syringes and stored at -4°C . The final concentrations of labelled antibodies were calculated correspondingly to their final volumes after dialysis.

2.15.2 Determination of the label degree

For the determination of the label degree, the conjugates were diluted to a concentration of 0.2 mg mL^{-1} in 20 mM PBS. The solution was filled in 96-well UV-plate with $70 \mu\text{L}$ per well and the absorbance was measured by a multi-detection reader Spectra Max M5^e at $\lambda=280 \text{ nm}$ and $\lambda=650 \text{ nm}$. The label degree was calculated by the formulas below:

$$\text{*} C_{\text{protein}} = \frac{A_{280} - (Cf_{280} \times A_{\text{max}})}{\epsilon_{\text{protein}}} \quad \text{*} C_{\text{fluorophore}} = \frac{A_{\text{max}}}{\epsilon_{\text{dye}}}$$

$$\text{* Label degree (D/P)} = \frac{C_{\text{fluorophore}}}{C_{\text{protein}}}$$

A_{280} is the absorbance at $\lambda=280 \text{ nm}$; A_{max} is the absorbance of the dye at its absorbance maximum (λ_{max}); ϵ is extinction coefficient ($\text{cm}^{-1} \times \text{M}^{-1}$), $\epsilon_{\text{protein}} = 210000 \text{ cm}^{-1} \times \text{M}^{-1}$ for a typical IgG (which corresponds to A_{280} of 1.4 for a 1 mg mL^{-1} solution and Cf_{280} is expressed as correction factor by the absorbance of the fluorophore at $\lambda=280 \text{ nm}$. The spectra factors of Oyster[®]-645 is listed below in Table 8.

Table 8 Spectra characteristics of the Oyster-645, Ref: www.biolabels.com

Dye	ϵ ($\text{cm}^{-1} \times \text{M}^{-1}$)	A_{max} (nm)	Em (nm)	Cf_{280}
Oyster-645	250000	649	666	0.08

2.15.3 Affinity test of fluorophore labelled antibodies

The fluorophore labelled antibodies were tested with AOS and coating antigen format ELISA to determine their affinities after conjugation. The processes were described above in the sections (2.11.1 and 2.14).

2.16 *In situ* experiments

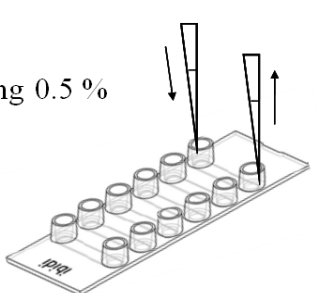
2.16.1 *B. cepacia* biofilm in flow chamber system-ibidi slide

The *B. cepacia* LA3 was transferred from NB (rich medium) plate to M9 medium (minimal medium) with a cell density of 10^9 cells per mL and 150 μL of bacterial suspension was filled to ibidi slide per channel (6 channels, 1 $\mu\text{-Slide VI ibiTreat}$, from ibidi, Munich, Germany). The slide was covered in petri dish with moisturised tissue under the slide and the whole petri dish was sealed with parafilm and incubated for 24h at 30°C. After incubation the autoclaved plastic tubes were connected to the ibidi slide device and M9 medium was pumped with a flow rate of 3 mL per hour per channel with peristaltic pump (Ismatec IPC-12, Glattbrugg, Switzerland) for 24 h at 30°C. Then the plastic tubes were taken off, sterilised, and the slides were ready for further antibody treatment.

Figure 20 Antibody treatment of biofilm on ibidi slide

- Established biofilm on slide
- Wash the slide with PBS, 100 $\mu\text{L} \times 2$
- Blocking with 1 M BSA, 100 μL , 30 min
- Wash the slide with PBS, 100 $\mu\text{L} \times 2$
- Addition of fluorescent labelled HSL mAb (containing 0.5 % glycine), 100 μL , 40 min
- Wash the slide with PBS, 100 $\mu\text{L} \times 2$
- Add 50 μL PBS
- LSM

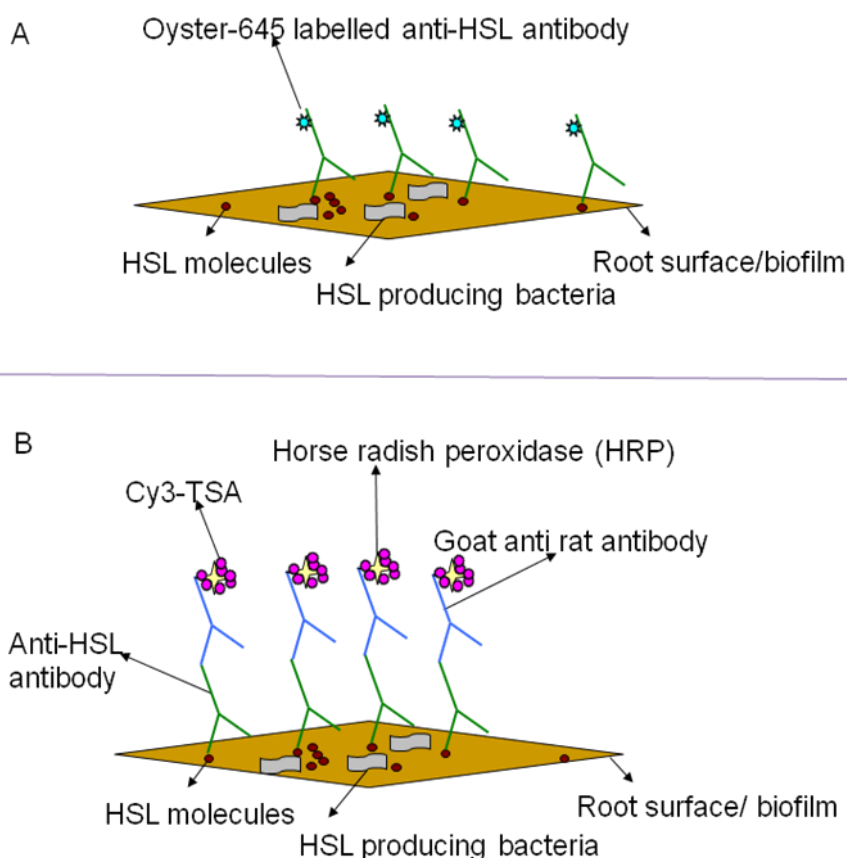
a. Process of mAb treatment



b. Pipette on slide channels

The optimised antibody treatment of the biofilm on ibidi slide is illustrated in (Figures 20 and 21). First, the ibidi slide was washed twice and incubated with 100 μL per channel 1M BSA for 30 min at RT for blocking. The slide was washed twice and 100 μL per channel of fluorescent labelled antibody solution was added and incubated for 45 min. Finally the slide was washed twice and filled with 50 μL 40 mM PBS per channel for microscopy. The wash steps were performed with 100 μL 40 mM PBS using pipette and the in- and outlet sides remained unchanged during the whole process. The fluorescent labelled mAbs HSL1/2-2C10, HSL1/2-4H5 with concentration from 0.05 to 0.2 $\mu\text{g mL}^{-1}$ were used for this experiment. To avoid unspecific binding activated NHS on the Oyster-645 during fluorescent conjugation, 5 μL of 10% glycine was added to each 100 μL antibody solution and incubated for 10 min. The experiment was obtained at $25\pm 3^\circ\text{C}$. Using the 6 separate channels, different treatments were able to be performed.

Figure 21 *In situ* experiment design with Oyster-645 labeled HSL antibody and Cy3-TSA

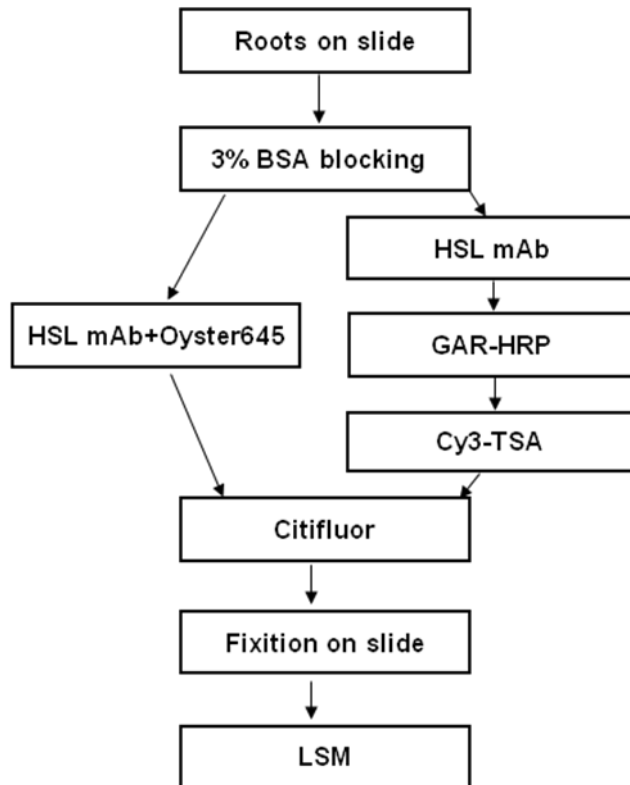


A (top): experiment design with Oyster-645 labelled mAb; B (below): experiment design with Cy3-TSA

Instead of fluorescent labelled HSL mAbs, the Cy3 labelled TSA was applied to enhance the fluorescent signal. In this case, unlabelled HSL mAbs were used and followed with incubation with GAR-HRP for 30 min and addition of TSA solution for 5-10 min. The

channels were washed twice with 100 μ L 40 mM PBS. The principle of the *in situ* experiment is presented in Figure 22.

Figure 22 Antibody treatments of roots



Left procedure: treatment with Oyster645 labelled antibody; right procedure: treatment with Cy3-TSA.

The fluorescence of Oyster-645 and Cy3 were detected using a confocal laser scanning microscope (LSM510 Meta, Zeiss, Oberkochen, Germany). An argon ion laser supplied the wavelength of 488 nm for excitation of Oyster-645. Two helium neon lasers provided excitation wavelengths of 543 nm and 633 nm, producing only unspecific autofluorescence of the root material enabling visualisation of the root structure. The three signals were combined and depicted as RGB (red green blue)-image. Additionally, specific Oyster-645 fluorescence could be verified by scanning the characteristic wavelength spectrum of a signal in question with the implemented function of the LSM510 Meta system. An optical sectioning of the biofilm was achieved by moving the focus position deeper into the sample in 1 μ m steps producing *z*-stacks of individual pictures from the same *xy*-area with a penetration depth of up to 60 μ m. The resulting set of pictures was displayed as an orthogonal view with the help of the LSM510 software package provided by Zeiss (the ibidi-slides were prepared by M. Rothballer).

2.16.2 *Pseudomonas putida* IsoF on the root of barley

2.16.2.1 Preparation of the plant roots inoculated with *P. putida* IsoF

The *gfp*-tagged *P. putida* strain IsoF (Steidle *et al.*, 2001) harbouring the plasmid pJBA28 (Andersen *et al.*, 2001) was inoculated to summer barley cultivar Barke seeds and the plants were grown in sealed glass tubes filled with quartz sand. Two weeks after planting, whole barley plants were taken out of the glass tubes. Roots were carefully shaken to remove adhering quartz sand particles, gently washed in sterile 1 x PBS in Petri dishes and separated from the shoot. For antibody treatment 2 cm root pieces were removed from the older basal part of the root close to the seed and then briefly air-dried on glass slides. The process is shown in the Figure 22. Washing with 40 mM PBS was performed between all steps before Citifluor addition (the plant roots were prepared by Buddrus-Schiemann).

2.16.2.2 HSL antibody treatment on the barley root

The principle of the experiment was introduced in Figure 21. Different from ibidi slide system, plant roots were more complex surfaces, which contained multiple proteins, carbohydrate polymers, lipid compounds and salts from plant origin or from the environment. The treatment procedure is shown in Figure 22 and the root was rinsed once with ca. 2 mL 40 mM PBS using injector between all the steps.

After the washing step, the root pieces were transferred to glass slides, air-dried, embedded in Citifluor (Citifluor Ltd., Canterbury, United Kingdom) and then covered with a cover slip. Bacterial root colonization and antibody treatment were followed using a confocal laser scanning microscope LSM510 Meta (same as for ibidi slide) that was equipped with two helium neon lasers for excitation of the fluorophores Cy3 and Cy5 at wavelengths of 543 and 633 nm, and an argon laser for excitation of the *gfp*-signal at a wavelength of 488 nm. Bacterial cells were localized with a 63x water immersion objective.

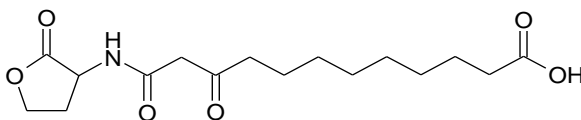
3 Results

3.1 Selection of hapten for immunisations

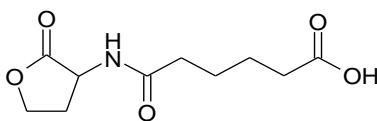
Considering the structural similarity and the homoserine lactones of interest, four haptens named HSL1, HSL2, HSL3 and HSL4 were chosen for the development of anti-HSL mAbs. As shown in Figure 23, HSL1 and HSL3 have the same side chain length, but differ in the C3 position: HSL1 contains an oxo functional group whereas HSL3 contains an OH group. In comparison, both HSL2 and HSL4 contain only a hydrogen atom at the C3 position. HSL2 has the shortest chain length, while HSL4 has a chain length between HSL1/HSL3 and HSL2. For immunisations, all four haptens were conjugated to BSA and OVA, resulting in the following conjugates: HSL1-BSA, HSL1-OVA, HSL2-BSA, HSL2-OVA, HSL3-BSA, HSL3-OVA, HSL4-BSA and HSL4-OVA. These eight immunogens were used for the immunisation of rats and for assay development. During the first screening, anti-HSL1/2 mAbs recognised both hapten-protein conjugates equally well and were named therefore HSL1/2. All other mAbs had a preference to only one hapten-protein conjugate.

Figure 23 HSL hapten structures (detailed chemical names see section 2.3, page 47-53)

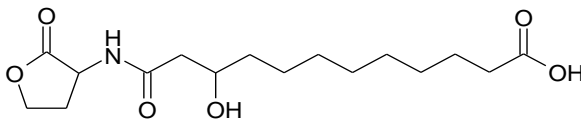
HSL1
(MW=327)



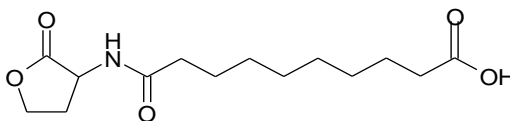
HSL2
(MW=229)



HSL3
(MW=329)



HSL4
(MW=285)



3.2 Hapten-protein conjugate characterisation with UV absorbance spectrum

The shift of the absorbance peak and its slope change could generally be observed from all conjugates (see Figures 24-26). HSL1 was the only hapten, which showed slight UV absorbance at a wavelength of 277 nm with OD of 0.1516 (Figure 25 top left) and no peak was shown in the spectra of HSL2, HSL3 and HSL4 haptens (top right of Figure 24, top of Figure 26 and top of Figure 25). The 2.5 mg mL⁻¹ BSA and OVA presented absorbance peaks at 279 nm and 280 nm with ODs >0.9 (Figure 24 middle left and right). After conjugation, the HSL1-BSA shifted the peak to 277 nm and HSL1-OVA had a peak at 269 nm (Figure 24 bottom left and right) and the slope of both left peak shoulders reduced significantly compared to pure BSA and OVA. Thus the conjugations of HSL1 to BSA/OVA were confirmed to be successful.

Figure 24 UV spectra of HSL1 and HSL2 conjugates

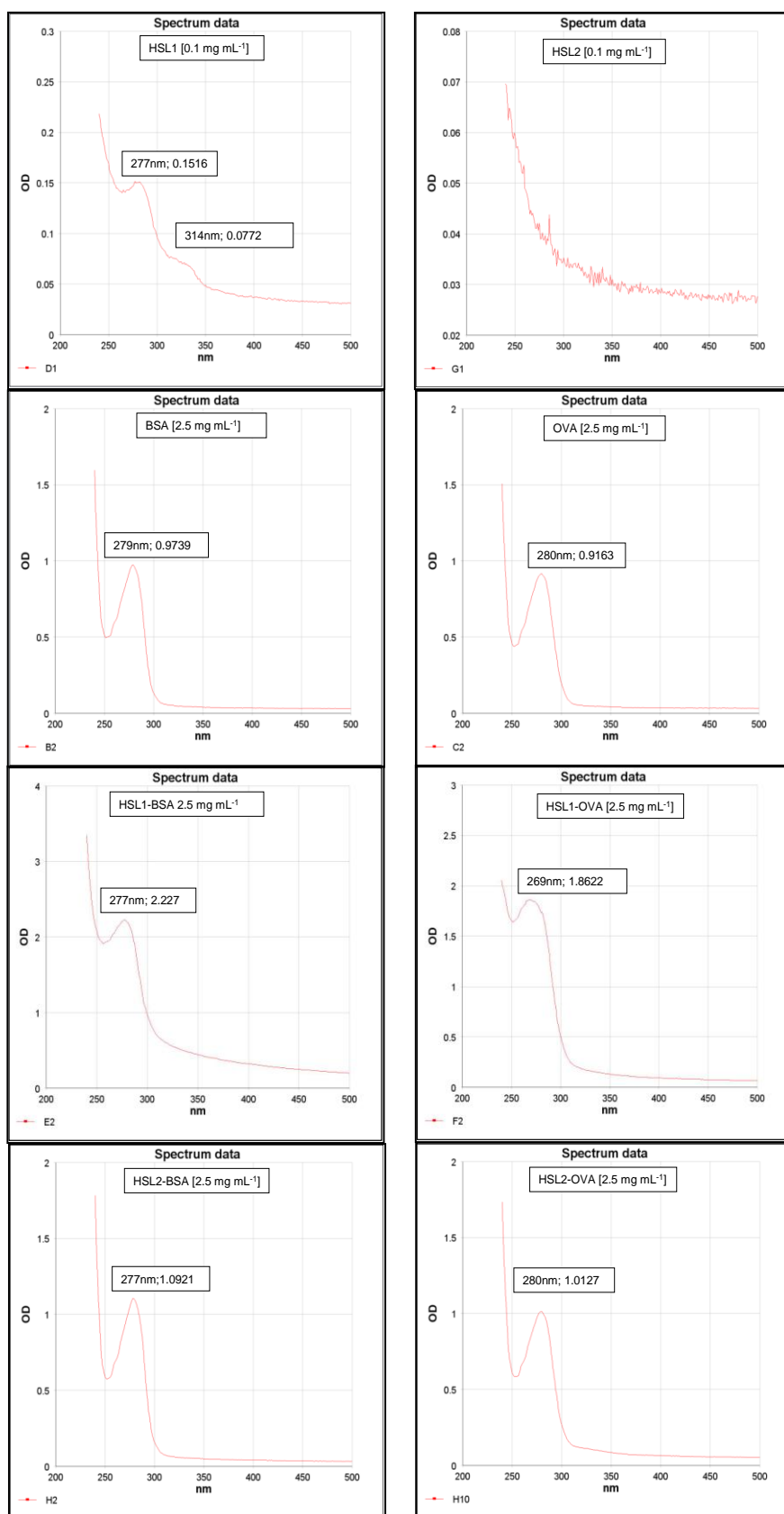
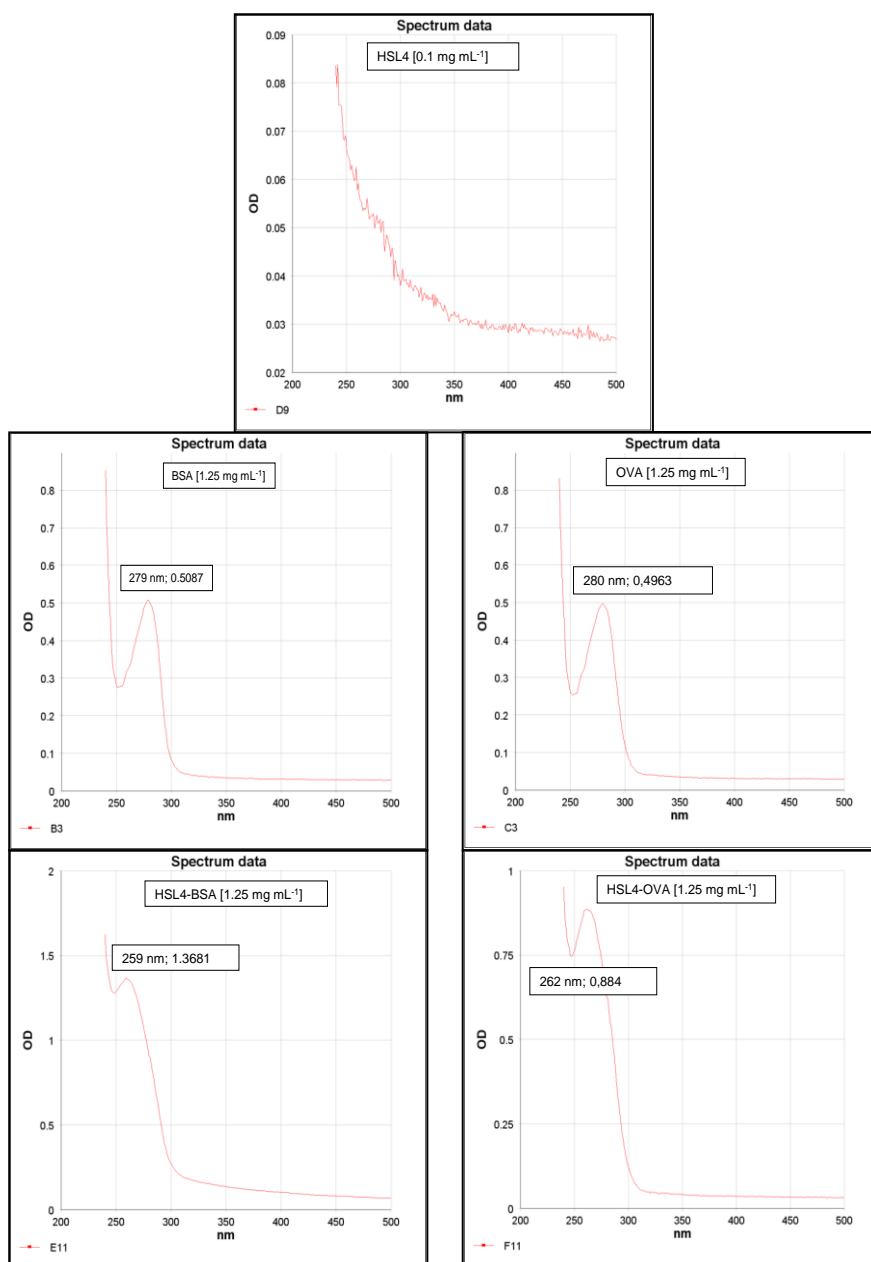


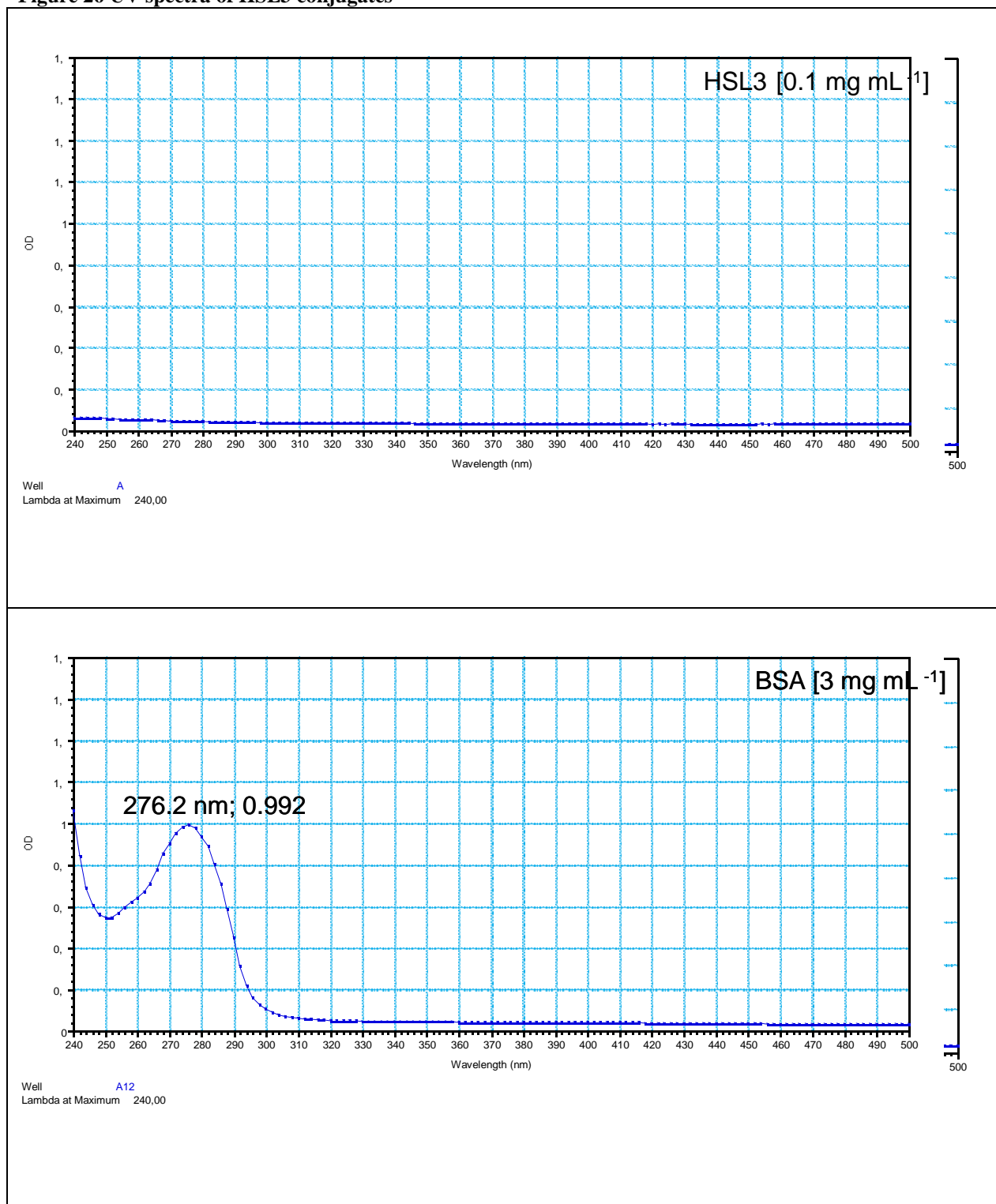
Figure 25 UV spectra of HSL4 conjugates

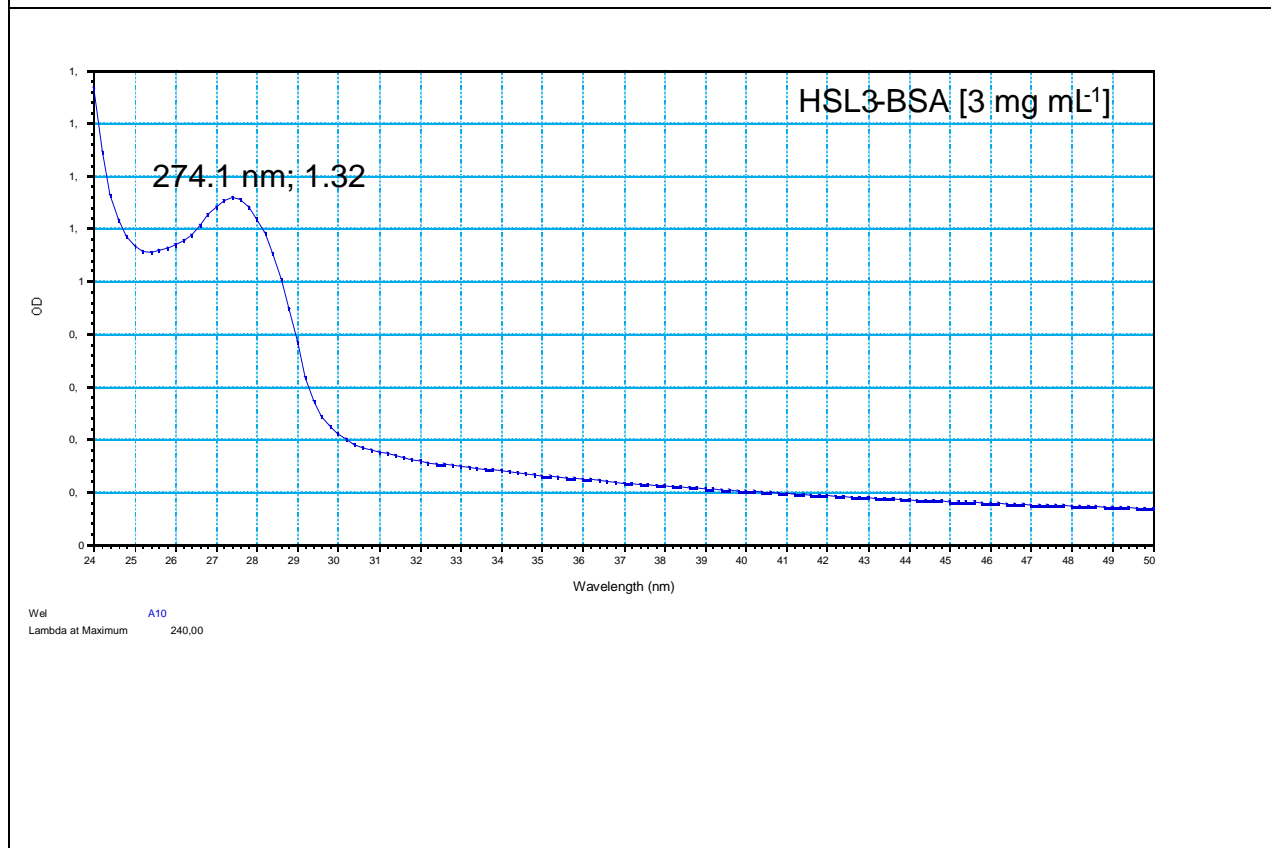
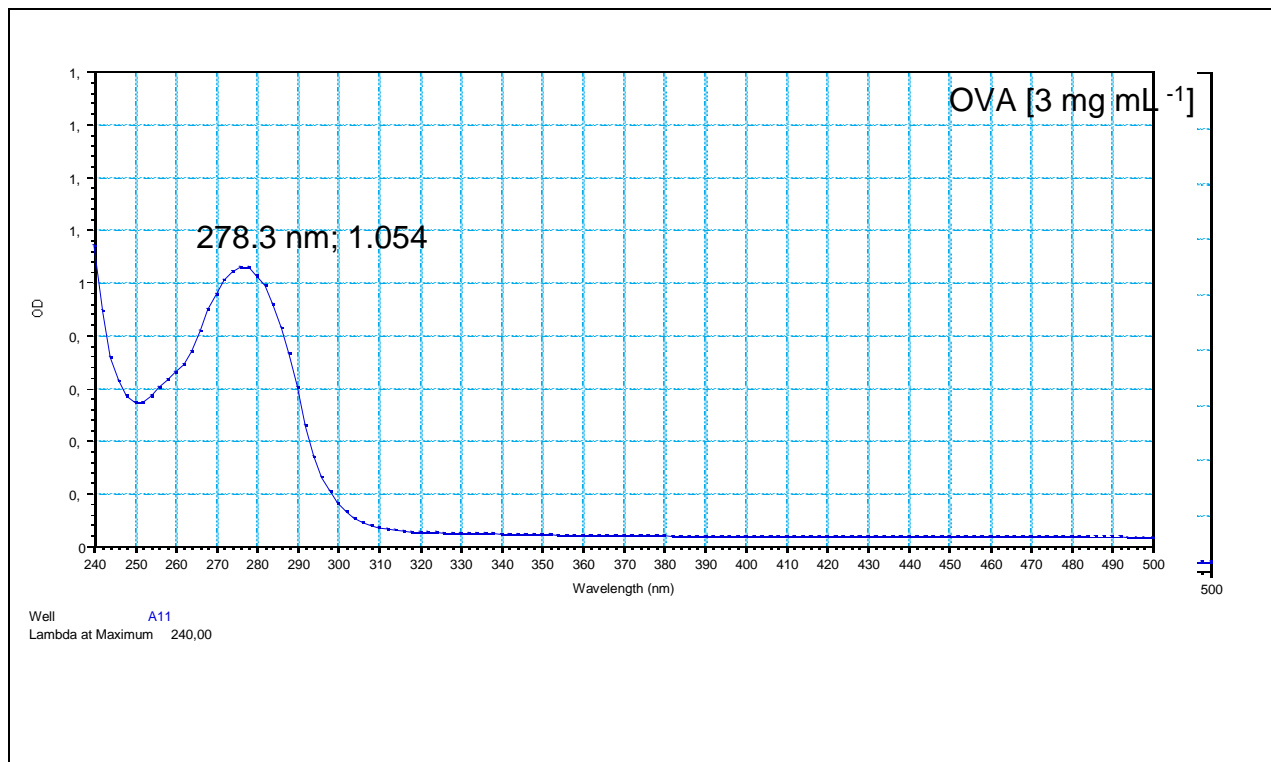


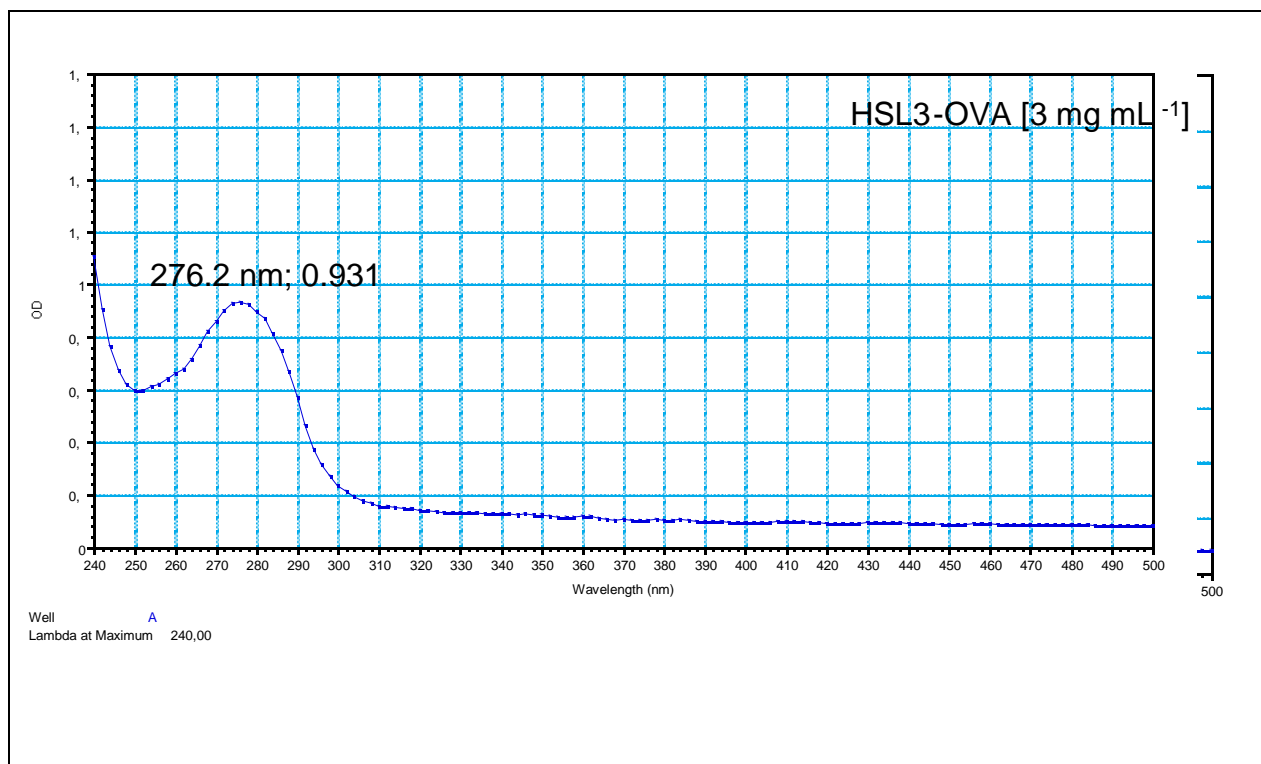
Significant shift of peaks and change of the slope have been observed from the HSL4-BSA (259 nm) and HSL4-OVA (262 nm) after conjugation (see Figure 25), though the HSL4 itself did not show any peak. However, HSL2 and HSL3 conjugates did not have that significant difference compared to HSL1 and HSL4 conjugates. HSL2-BSA had a slight shift of 2 nm, while HSL2-OVA had the same absorbance wavelength as OVA at 280 nm (Figure 24). The shifts of HSL3-BSA and HSL3-OVA compared to the original proteins were both approximately 2 nm (Figure 26). But the left peak shoulders of hapten conjugates were less steep than the pure proteins in all conjugates. The conjugates were all tested with ELISA in

the coating antigen format and the binding of the antibody to the HSL-protein-conjugates was thus able to confirm the success of conjugation indirectly (data not shown).

Figure 26 UV spectra of HSL3 conjugates







3.3 Coating antigens and enzyme-tracers selection

In coating antigen format, all eight HSL-protein conjugates were tested as coating antigens, and HSL2-BSA was suitable for almost all antibodies (partly presented in Table 9). Additionally following a strategy already employed earlier (Krämer *et al.*, 2010) - conjugates with a reduced amount of hapten molecules per protein (HSL2-BSA-r1 and HSL2-BSA-r2) were produced and used for optimised assays (production details in Table 5, page 56). They both resulted in more sensitive assays than HSL2-BSA due to the reduced HSL2 molecules on BSA.

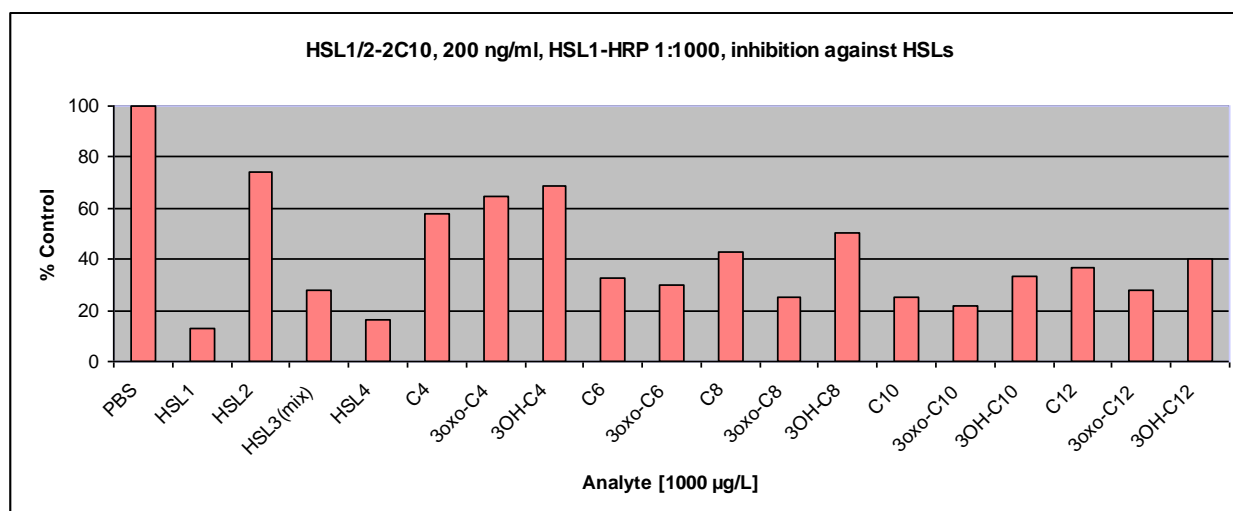
As enzyme-tracers, the four HSL haptens were conjugated to HRP for their usage in the enzyme-tracer format. HSL1- and HSL3-HRP were used as enzyme-tracers in combination with HSL1, HSL1/2 and HSL4 antibodies, while with HSL2- and HSL4-HRP it was less suitable to obtain an assay in the enzyme-tracer format due to high background (HSL2-HRP) or less sensitivity (HSL4-HRP). However, a recent test revealed that the assays could be potentially optimised with further diluted HSL4-HRP (data not shown).

3.4 Antibody screening

In total, 192 hybridoma culture supernatants (59 with anti-HSL1 and anti-HSL2 antibodies, 133 with anti-HSL4 antibodies) were tested in the first screening using coating antigen format ELISA (procedures present in section 2.11.1, page 60). The affinity and selectivity of the

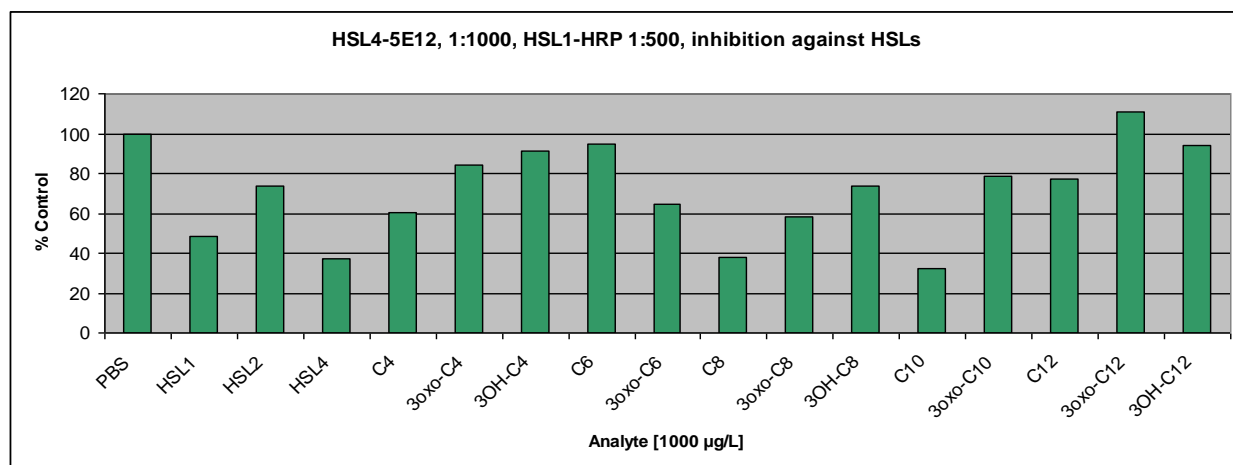
antibodies to the HSL standards, which were presented as % control (formula see 2.11.3, page 62) inhibition, were the main criteria of screening. With coating antigen format in a second round for inhibition with HSLs. HSL3 mAbs are not present in this study, because the antibody production and characterisation is not completed yet.

Figure 27 HSL1/2-2C10 inhibition test against HSL substances in enzyme-tracer format



After the first screening, two anti-HSL1 mAbs, eleven anti-HSL1/2 mAbs and 15 anti-HSL4 mAbs were selected for further characterisation (Tables 9 and 10). The antibodies were named according to the first screening process, where the haptens were used for antibody binding test. For example, HSL1-mAb showed binding to HSL1 and HSL1/2 had binding to both HSL1 and HSL2.

Figure 28 HSL4-5E12 inhibition tests against HSL substances in enzyme-tracer format



As examples for antibody screening and characterisation, the Figures 27 and 28 present the inhibition tests of mAbs against all selected HSLs from C4 to C12 and without or with 3oxo-, 3-hydroxy substitutions on C3 atom. The OD of PBS was set as 100% and the OD of the

Figures 27 and 28 of the HSL substances were calculated (formula described in section 2.11.3, page 62). The lower the bars, the better are the recognition of the antibodies to the substance, since the assays were competitive. In Figure 27, 28, the hapten HSL1 and HSL4 were the best recognised substances from all, while HSL2 was very less recognised. The % control of each antibody and analyte were taken into consideration for antibody selection and further characterisation. The second screening of HSL1, HSL1/2 and HSL4 antibodies are listed in Tables 9 and 10.

Table 9 Selected HSL1 and HSL1/2 antibodies and characterisation with coating antigen format

Antibody	Subclass	Coating	HSL 1	HSL 2	C ₄ -HSL	C ₆ -HSL	3oxo-C ₆ -HSL	3oxo-C ₈ -HSL	3oxo-C ₁₂ -HSL
HSL1/2-1F6	IgG-2c	HSL1-BSA	++	-	-	-	-	+	-
HSL1/2-2C10	IgG-2a	HSL2-BSA	++	+	-	++	++	++	+
HSL1/2-2G10	IgG-2a	HSL2-BSA	+	+	-	+	-	++	-
HSL1/2-3C12	IgG-2a	HSL2-BSA	+	-	-	+	-	-	-
HSL1/2-4A7	IgG-2a	HSL2-BSA	++	-	-	-	+	+	+
HSL1/2-4B12	IgG-2a	HSL2-BSA	++	-	-	+	-	-	-
HSL1/2-4C10	IgG-2a	HSL2-BSA	+	-	-	+	-	-	+
HSL1/2-4G11	IgG-2a	HSL2-BSA	+	-	-	+	-	-	-
HSL1/2-4H5	IgG-2a	HSL2-BSA	++	-	-	++	++	++	+
HSL 1/2-8F4	IgG-2c	HSL1-BSA	-	-	-	-	-	+	-
HSL1-1A5	IgG-2a	HSL2-BSA	++	-	+	+	+	++	+
HSL1-8E1	IgG-2a	HSL2-BSA	++	-	-	-	+	++	+

In coating antigen format, as a competitive assay, the signal of the assays inversely indicates the affinity of the antibodies. The higher the affinity, the lower is the signal and thus lowers % control. Symbols in table: ++: % control ≤ 30%; +: % control 30%-60%; -: % control ≥ 60%.

Table 10 Selected HSL4 antibodies and characterisation with coating antigen format

Antibody	Subclass	Coating antigen	HSL2	C4-HSL	3oxo-C4-HSL	3OH-C4-HSL	C6-HSL	C6-3oxo-HSL	C8-HSL	C8-3oxo-HSL	3OH-C8-HSL	C10-HSL	3oxo-C10-HSL	C12-HSL	C12-3oxo-HSL	3OH-C12-HSL
HSL4-2F12	IgG-2a	HSL2-OVA 2 µg mL ⁻¹	-	+	-	-	-	-	++	+	-	-	-	-	-	-
HSL4-4B5	IgG-2a	HSL2-BSA 1 µg/ml	-	+	-	-	-	-	++	+	-	+	-	+	-	-
HSL4-4B12	IgG-2a	HSL2-BSA 1 µg/ml	-	+	-	-	+	-	++	-	-	++	+	+	+	-
HSL4-4C9	IgG-2a	HSL2-BSA 1 µg/ml	-	+	-	-	-	-	++	+	+	+	-	+	-	-
HSL4-5E4	IgG-2a	HSL2-BSA 1 µg/ml	-	+	-	-	+	+	+	+	-	++	+	+	+	-
HSL4-5E12	IgG-2a	HSL2-OVA 2 µg/ml	-	+	-	-	+	-	++	+	-	+	+	+	+	-
HSL4-5H3	IgG-2a	HSL2-OVA 2 µg/ml	-	+	+	-	+	+	++	-	-	++	-	+	-	-
HSL4-6D3	IgG-2a	HSL2-BSA 1 µg/ml	-	+	-	-	+	+	++	+	-	++	+	+	+	+
HSL4-6H8	IgG-2c	HSL2-OVA 2 µg/ml	-	++	-	-	-	-	+	-	-	-	-	-	-	-
HSL4-8B8	IgG-2a	HSL2-OVA 2 µg/ml	-	+	-	-	+	-	++	+	-	+	+	+	+	+
HSL4-8D8	IgG-2a	HSL2-OVA 2 µg/ml	+	+	-	-	+	+	++	+	-	++	+	+	+	+
HSL4-8H10	IgG-2a	HSL2-OVA 2 µg/ml	-	+	+	-	+	+	++	+	-	++	+	+	+	-

In coating antigen format, as a competitive assay, the signal of the assays inversely indicates the affinity of the antibodies. The higher the affinity, the lower is the signal and thus lowers % control. Symbols in table: ++: % control ≤ 30%; +: % control 30%-60%; -: % control ≥ 60%.

3.5 Antibody subclass determination and purification

Most HSL1, HSL1/2 and HSL4 mAbs were IgG-2a antibodies and a few of them were IgG-2c (reported in Tables 9 and 10) antibodies. Within the purified antibodies, only a part of HSL1-1A5 was processed with protein A affinity column, the rest were all purified with protein G columns. However, the immunoassays did not show any difference between protein A and G processed HSL1-1A5 antibody (data not shown). The purified antibodies are listed in Table 11.

Table 11 Purified HSL antibodies

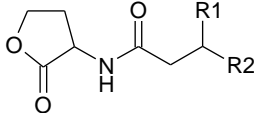
Antibody	Concentration [mg mL ⁻¹]	Purified with
HSL1-1A5	1.4	Protein A
	2.4	Protein G
	6.3	Protein A
HSL1-8E1	0.8	Protein G
	unknown	Protein G
HSL1/2-2C10	0.7	Protein G
	1.5	Protein G
	2.8	Protein G
HSL1/2-4H5	0.8	Protein G
HSL1/2-4G11	0.4	Protein G
HSL4-4C9	1.3	Protein G
HSL4-5E12	3.0	Protein G
HSL4-5H3	1.0	Protein G
HSL4-6D3	2.0	Protein G

3.6 Anti-HSL antibody characterisation with ELISAs

With the selected antibodies standard curves for twelve HSL and four HS compounds of the four HSL haptens were carried out in the coating antigen and/or in the enzyme-tracer format. The CRs for all HSL and HS compounds with the selected antibodies are listed in Table 12

(coating antigen format) and Table 13 (enzyme-tracer format). The assay conditions e.g. antibody concentration, tracer dilution, coating antigens etc. are given in Table 14 (coating antigen format) and Table 15 (enzyme-tracer format). The bold written analyte (3oxo-C10-HSL and C8 HSL) in the tables were the main analytes for the corresponding assays. Only three mAbs were characterised with the enzyme-tracer format, because all other mAbs showed either too high background or unacceptable standard deviations within this format. The reason for this phenomenon remains unknown.

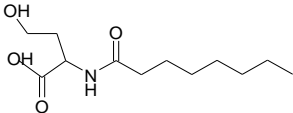
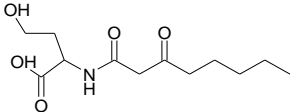
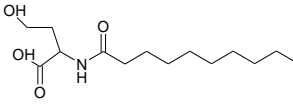
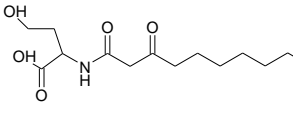
Table 12 Cross reactivity of mAbs in coating antigen format



MAb

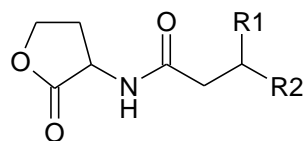
Cross reactivity %

Analyte (Short form)	MAb									
	R1	R2	HSL1-1A5	HSL1-8E1	HSL1/2-2C10	HSL1/2-4H5	HSL4-4C9	HSL4-5E12	HSL4-5H3	HSL4-6D3
Coating Antigen	HSL2-BSA-r2									
C4-HSL	H	CH ₃	8	6	14	21	9	39	13	19
3-oxo-C4-HSL	O	CH ₃	13	3	12	12	8	11	34	3
3-OH-C4-HSL	OH	CH ₃	5	0	8	0	3	15	0	6
C8-HSL	H	(CH₂)₄CH₃	17	10	73	110	100	100	100	100
3-oxo-C8-HSL	O	(CH ₂) ₄ CH ₃	44	54	89	76	12	46	16	46
3-OH-C8-HSL	OH	(CH ₂) ₄ CH ₃	8	5	23	20	0	14	9	10
C10-HSL	H	(CH ₂) ₆ CH ₃	14	4	55	27	37	38	70	100
3-oxo-C10-HSL	O	(CH₂)₆CH₃	100	100	100	100	5	117	38	29
3-OH-C10-HSL	OH	(CH ₂) ₆ CH ₃	16	0	38	61	5	24	3	31

C12-HSL	H	(CH ₂) ₈ CH ₃	2	5	23	3	9	8	41	30
3-oxo-C12-HSL	O	(CH ₂) ₈ CH ₃	18	34	43	35	4	33	14	44
3-OH-C12-HSL	OH	(CH ₂) ₈ CH ₃	8	2	26	20	4	17	4	12
C8-HS			511	258	1587	843	1360	714	-	-
3-oxo-C8-HS			630	1021	1052	782	584	178	-	-
C10-HS			545	39	498	869	566	1838	1517	5239
3-oxo-C10-HS			1935	1760	1780	1140	837	905	317	909
HSL1	O	(CH ₂) ₈ COOH	143	159	315	166	5	78	22	120
HSL2	H	(CH ₂) ₂ COOH	<0.1	<0.1	3	<0.1	1	3	72	33
HSL3	OH	(CH ₂) ₈ COOH	21	4	51	9	1	27	5	10
HSL4	H	(CH ₂) ₆ COOH	70	20	354	151	73	259	67	167

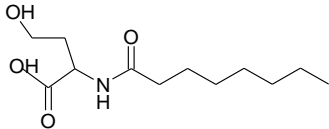
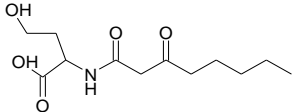
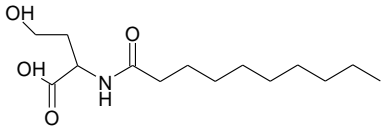
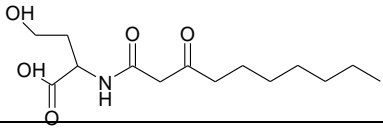
“-” means not determined; assay conditions listed in Table 14. Published results (Chen *et al.*, 2010 a)

Table 13 Cross reactivity of mAbs in enzyme- tracer format



Mab
Cross reactivity %

Analyte (short form)	R1	R2	Mab		
			HSL1/2-2C10	HSL1/2-4H5	HSL4-5E12
Enzyme Tracer			HSL1-HRP	HSL3-HRP	HSL3-HRP
C4-HSL	H	CH ₃	13	11	12
3-oxo-C4-HSL	O	CH ₃	8	7	4
3-OH-C4-HSL	OH	CH ₃	5	11	4
C8-HSL	H	(CH₂)₄CH₃	71	156	100
3-oxo-C8-HSL	O	(CH ₂) ₄ CH ₃	79	70	19
3-OH-C8-HSL	OH	(CH ₂) ₄ CH ₃	16	18	6
C10-HSL	H	(CH ₂) ₆ CH ₃	41	56	46
3-oxo-C10-HSL	O	(CH₂)₆CH₃	100	100	39
3-OH-C10-HSL	OH	(CH ₂) ₆ CH ₃	39	33	15

C12-HSL	H	(CH ₂) ₈ CH ₃	34	12	71
3-oxo-C12-HSL	O	(CH ₂) ₈ CH ₃	39	52	14
3-OH-C12-HSL	OH	(CH ₂) ₈ CH ₃	18	24	11
C8-HS			3820	1119	4183
3-oxo-C8-HS			383	-	-
C10-HS			1531	2268	841
3-oxo-C10-HS			1813	1667	1053
HSL1	O	(CH ₂) ₈ COOH	263	191	37
HSL2	H	(CH ₂) ₂ COOH	4	6	4
HSL3	OH	(CH ₂) ₈ COOH	22	30	9
HSL4	H	(CH ₂) ₆ COOH	362	292	68

“-” means not determined; assay conditions listed in Table 15. Published results (Chen *et al.*, 2010 a)

Table 14 Test midpoints (IC₅₀) of main analytes using coating antigen format

Main Analyte						
(short form)	mAb Concentration	Coating Antigen Conc.	Secondary Ab Conc.	IC₅₀[μg L⁻¹]	STD [μg L⁻¹]	n
3oxo-C10-HSL	HSL1-1A5 [200 ng mL ⁻¹]	HSL2-BSA-r2 [2 μg mL ⁻¹]	GAR-HRP [20 μg mL ⁻¹]	455	213	12
3oxo-C10-HSL	HSL1-8E1 [800 ng mL ⁻¹]	HSL2-BSA-r2 [2 μg mL ⁻¹]	GAR-HRP [20 μg mL ⁻¹]	1278	519	12
3oxo-C10-HSL	HSL1/2-2C10 [400 ng mL ⁻¹]	HSL2-BSA-r2 [1 μg mL ⁻¹]	GAR-HRP [20 μg mL ⁻¹]	669	182	18
3oxo-C10-HSL	HSL1/2-4H5 [100 ng mL ⁻¹]	HSL2-BSA-r1 [1 μg mL ⁻¹]	GAR-HRP [40 μg mL ⁻¹]	1377	435	20
C8-HSL	HSL4-4C9 [200 ng mL ⁻¹]	HSL2-BSA-r1 [2 μg mL ⁻¹]	GAR-HRP [40 μg mL ⁻¹]	518	218	22
C8-HSL	HSL4-5E12 [400 ng mL ⁻¹]	HSL2-BSA-r2 [2 μg mL ⁻¹]	GAR-HRP [40 μg mL ⁻¹]	1478	591	18
C8-HSL	HSL4-5H3 (CS) 1:1000	HSL2-BSA-r2 [2 μg mL ⁻¹]	GAR-HRP [20 μg mL ⁻¹]	455	113	7
C8-HSL	HSL4-6D3 (CS) 1:200	HSL2-BSA-r2 [2 μg mL ⁻¹]	GAR-HRP [20 μg mL ⁻¹]	447	197	4

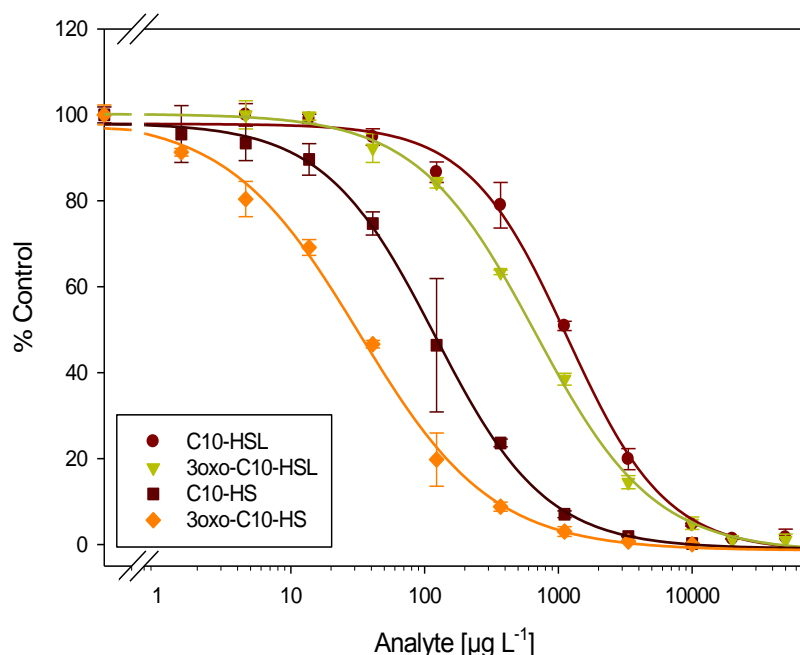
Table 15 Test midpoints (IC₅₀) of main analytes using enzyme-tracer format

Main Analyte					
(Short form)	mAb Concentration	Enzyme-Tracer Dilution	IC₅₀ [µg L⁻¹]	STD [µg L⁻¹]	n
3oxo-C10-HSL	HSL1/2-2C10 [400 ng mL ⁻¹]	HSL1-HRP 1:1000	134	30	53
3oxo-C10-HSL	HSL1/2-4H5 [200 ng mL ⁻¹]	HSL3-HRP 1:400	253	44	19
C8-HSL	HSL4-5E12 [400 ng mL ⁻¹]	HSL3-HRP 1:400	646	114	19

3.6.1 Comparison of ELISA in the coating antigen and in the enzyme-tracer formats

Although the design of both ELISA formats is different (schemata see Figure 14, page 61 and 15, page 62) and although the haptens in the conjugates differ (HSL2 in the coating antigen format, HSL1 or HSL3 in the enzyme-tracer format), the assays showed generally similar results. This reflects the recognition of the mAbs, which should not differ, even if the competition within the assays is changed. As illustrated in Figures 29 and 30, the IC₅₀ values revealed the same recognition pattern in both assay formats: 3-oxo-C10-HS < C10-HS < 3-oxo-C10-HSL < C10-HSL.

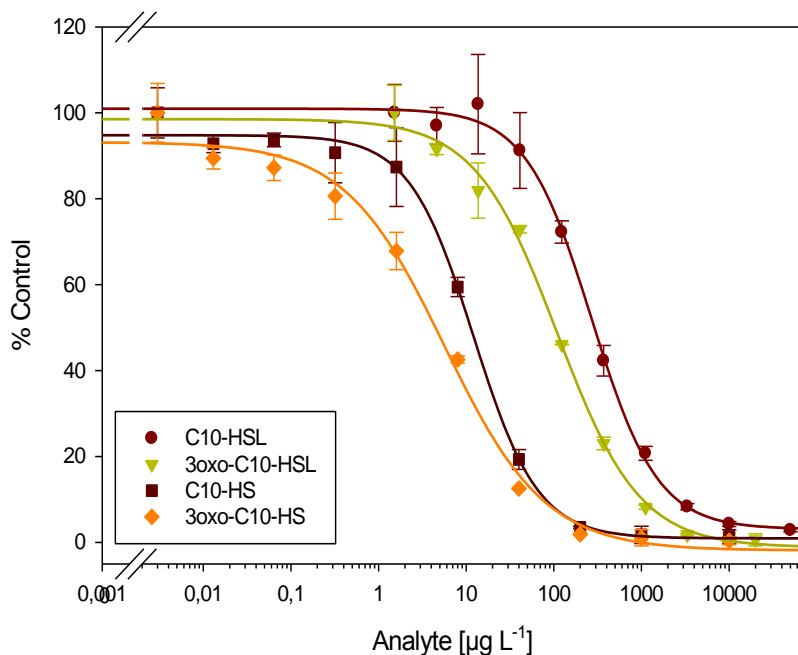
Figure 29 HSL1/2-2C10 coating antigen format standard curves



Standard curves for C10-HSL, 3-oxo-C10-HSL, C10-HS and 3-oxo-C10-HS using mAb HSL1/2-2C10 and HSL2-BSA-r2. Assay conditions: HSL1/2-2C10 400 ng mL⁻¹, HSL2-BSA-r2 1 µg mL⁻¹, GAR-HRP 40 ng mL⁻¹. Four parameter curve-fitting data are given in parentheses: *red circles* C10-HSL (A 97.9, B 1.17, C 1169 µg L⁻¹, D -1.58, R² 0.998), *yellow green inverted triangles* 3-oxo-C10-HSL (A 100.2, B 0.98, C 672.7 µg L⁻¹, D -1.7, R² 0.999), *brown squares* C10-HS (A 98.2, B 1.05, C 119.5 µg L⁻¹, D -0.95, R² 0.999), and *orange rhombuses* 3-oxo-C10-HS (A 99.4, B 0.88, C 32.6 µg L⁻¹, D -1.37, R² 0.997).

However, all three antibodies, tested with both assay formats, presented lower test midpoints for the corresponding main analyte in the enzyme-tracer format than in the coating antigen format (Tables 12 and 13). For example, mAb HSL1/2-2C10 had an IC₅₀ of 134±30 µg L⁻¹ (n=53) in the enzyme-tracer format and an IC₅₀ of 669±182 µg L⁻¹ (n=18) in the coating antigen format.

Figure 30 HSL1/2-2C10 enzyme-tracer format standard curve

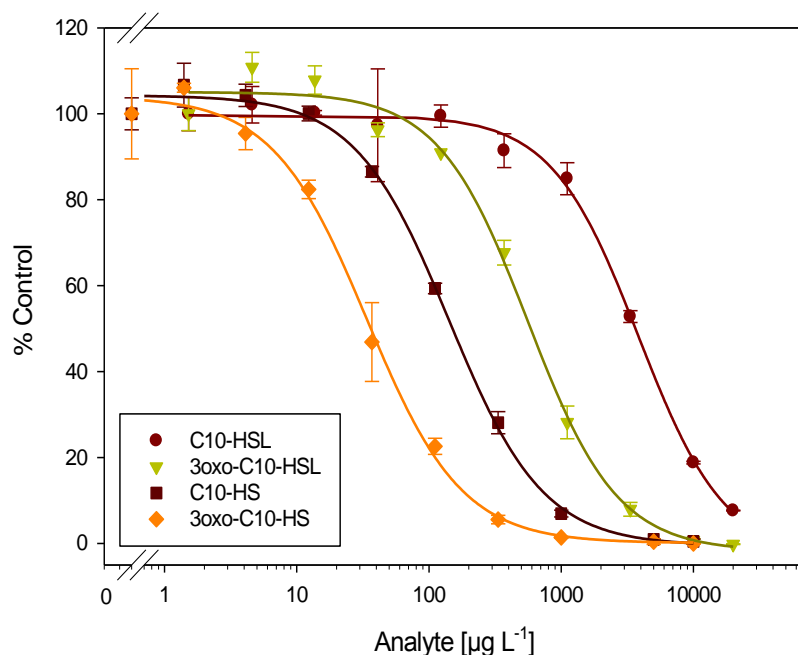


Standard curves for C10-HSL, 3-oxo-C10-HSL, C10-HS and 3-oxo-C10-HS using mAb HSL1/2-2C10 and HSL1-HRP. Assay conditions: HSL1/2-2C10 400 ng mL⁻¹, HSL1-HRP 1:1000, Protein G 2 µg mL⁻¹. Four parameter curve-fitting data are given in parentheses: *red circles* C10-HSL (A 100.9, B 1.16, C 270.5 µg L⁻¹, D 3.1, R² 0.998), *yellow green inverted triangles* 3-oxo-C10-HSL (A 97.7, B 0.93, C 111.7 µg L⁻¹, D -1.2, R² 0.998), *brown squares* C10-HS (A 94.8, B 1.18, C 12.2 µg L⁻¹, D 0.95, R² 0.998), and *orange rhombus* 3-oxo-C10-HS (A 93.2, B 0.76, C 5.7 µg L⁻¹, D -1.8, R² 0.993).

3.6.2 Difference in selectivities of anti-HSL1-, anti-HSL1/2-, and anti-HSL4 mAbs to HSL compounds

The selected antibodies showed different selectivities against the HSL compounds, which differ in the side chain length and in the functional group on the C3 position. For better comparability, the assays described in this paragraph were all carried out in the coating antigen format. Similar to mAb HSL1/2-2C10, anti-HSL1 mAb HSL1-1A5 had a higher affinity to HSLs with the 3oxo-group in the C3 position, but the difference in CR between with or without 3oxo-group was more significant (Table 12, Figures 29 and 31).

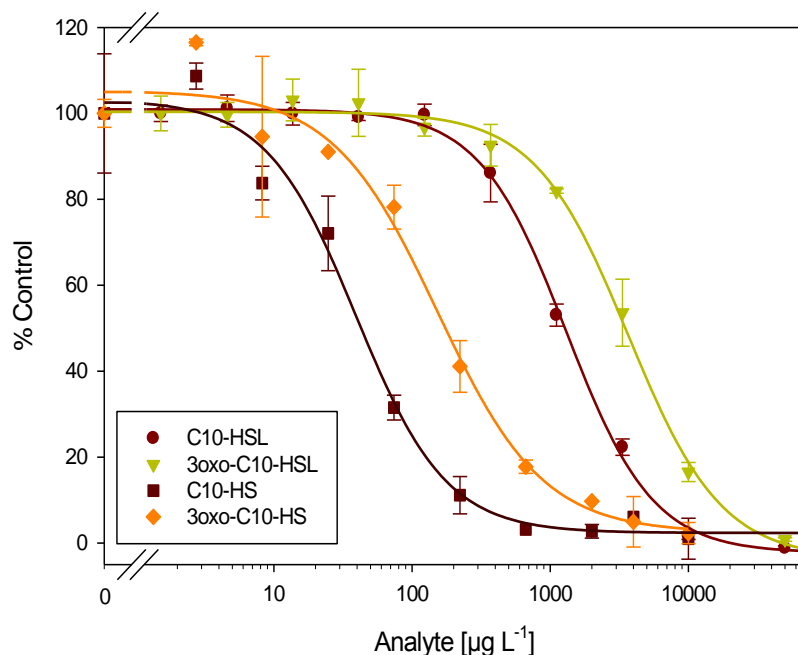
Figure 31 HSL1-1A5 coating antigen format standard curves



Standard curves for C10-HSL, 3-oxo-C10-HSL, C10-HS, and 3-oxo-C10-HS using mAb HSL1-1A5 and HSL2-BSA-r2. Assay conditions: HSL1-1A5 200 ng mL⁻¹, HSL2-BSA-r2 2 $\mu\text{g mL}^{-1}$, GAR-HRP 40 ng mL⁻¹. Four parameter curve-fitting data are given in parentheses: *red circles* C10-HSL (A 99.7, B 1.32, C 3840 $\mu\text{g L}^{-1}$, D -3.2, R² 0.997); *yellow green inverted triangles* 3-oxo-C10-HSL (A 105, B 1.29, C 561 $\mu\text{g L}^{-1}$, D -1.8, R² 0.994); *brown squares* C10-HS (A 104, B 1.2, C 142 $\mu\text{g L}^{-1}$, D -0.54, R² 0.998), and *orange rhombuses* 3-oxo-C10-HS (A 104, B 1.21, C 34 $\mu\text{g L}^{-1}$, D 0.08, R² 0.998).

For HSL1 and HSL1/2 antibodies, 3-oxo-C10-HSL was used as the main analyte for cross reactivity tests (described in section 2.11.6, page 65). C10-HSL had a CR of 14% for mAb HSL1-1A5, while 55% to mAb HSL1/2-2C10 (Table 12). In contrast to anti-HSL1 and anti-HSL1/2 mAbs, anti-HSL4 mAbs showed higher sensitivity against HSLs without the oxo-group in the C3 position. For example, using mAb HSL4-5H3 C10-HSL had a CR of 70% and 3-oxo-C10-HSL a CR of 38%. Here, C8-HSL was used as the main analyte (Table 12 and Figure 32). Additionally, after hydrolysis, the recognition of HS with or without 3-oxo- group of mAbs remained the same trend as for their original HSL forms for most mAbs (exception: mAb HSL4-4C9, the antibody with the highest selectivity, standard curves see attachments).

Figure 32 HSL4-5H3 coating antigen format standard curves



Standard curves for C10-HSL, 3-oxo-C10-HSL, C10-HS, and 3-oxo-C10-HS with the coating antigen format, using mAb HSL4-5H3 and HSL2-BSA-r2. Assay conditions: HSL4-5H3 culture supernatant 1:1000, HSL2-BSA-r2 2 $\mu\text{g mL}^{-1}$, GAR-HRP 40 ng mL^{-1} . Four parameter curve-fitting data are given in parentheses: *red circles* C10-HSL (A 100.9, B 1.38, C 1303 $\mu\text{g L}^{-1}$, D -2.3, R^2 0.999), *yellow green inverted triangles* 3-oxo-C10-HSL (A 100.4, B 1.3, C 3674 $\mu\text{g L}^{-1}$, D -3.7, R^2 0.997), *brown squares* C10-HS (A 103.2, B 1.33, C 39.4 $\mu\text{g L}^{-1}$, D 2.3, R^2 0.99), and *orange rhombuses* 3-oxo-C10-HS (A 105.3, B 1.14, C 152.9 $\mu\text{g L}^{-1}$, D 2.4, R^2 0.986).

3.6.3 Recognition of HSL and HS

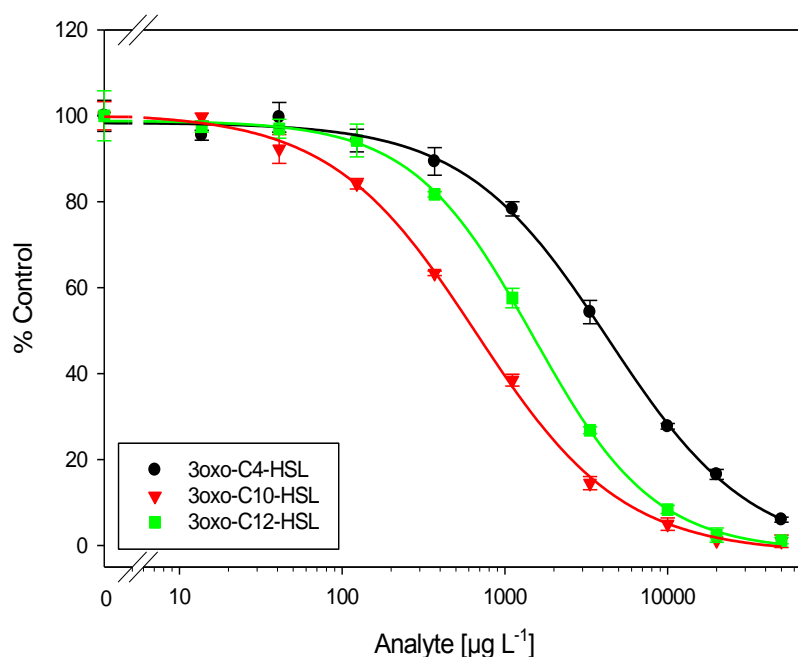
Interestingly, all our HSL mAbs proved to be more sensitive against homoserines (HSs, hydrolysed HSLs) than HSLs, no matter which analyte and which assay format were used. For example, 3oxo-C10-HS has a CR of 1935% and C10-HS has a CR of 545% to mAb HSL1-1A5 in the coating antigen format and similar trends were observed for other anti-HSL mAbs. The detection of tested HSs is in the low $\mu\text{g L}^{-1}$ range in all assays (e.g., 3oxo-C10-HS had an IC_{50} of 5.7 $\mu\text{g L}^{-1}$ using mAb HSL1/2-2C10 in enzyme-tracer format, Figure 30). Probably, the HSL antigens used for immunisation were hydrolysed to the HS-form at the physiological conditions in the rat.

3.6.4 Recognition of HSL side chain length

The side chain length of HSLs plays an important role for the antibodies recognition. When the functional group on the C3 position is not taken into account, all antibodies showed the best recognition of HSLs with side chain length of C8 or C10, the shorter chain length (C4) and longer chain length (C12) were comparatively less recognised by the HSL mAbs. Most

HSL1 and HSL1/2 mAbs recognised 3oxo-C10-HSL the best, and most HSL4 mAbs had best affinity towards C8-HSL (Tables 13 and 14). That was also the reason why they were chosen as main analytes for CR assays. As shown in Figure 33, the assay with mAb HSL1/2-2C10 has the lowest IC₅₀ for 3oxo-C10-HSL, followed by 3oxo-C12-HSL, and then 3oxo-C4-HSL. Anti-HSL4 mAbs were slightly better than HSL1 and HSL1/2 mAbs for short chain HSL recognition. This trend was observed from other mAbs as well; despite there were small differences between different antibodies.

Figure 33 HSL1/2-2C10 recognition of different chain length



Standard curves for HSL compounds with different chain length: 3-oxo-C4-HSL, 3-oxo-C10-HSL and 3-oxo-C12-HSL using mAb HSL1/2-2C10 and HSL2-BSA-r2. Assay conditions: HSL1/2-2C10 400 ng mL⁻¹, HSL2-BSA-r2 1 $\mu\text{g mL}^{-1}$, GAR-HRP 40 ng mL⁻¹. Four parameter curve-fitting data are given in parentheses: *black circles* 3-oxo-C4-HSL (A 98.4, B 0.99, C 4293 $\mu\text{g L}^{-1}$, D -2.1, R²0.999), *red inverted triangles* 3-oxo-C10-HSL (A 100.3, B 0.98, C 671.5 $\mu\text{g L}^{-1}$, D -1.7, R²0.999), and *green squares* 3-oxo-C12-HSL (A 98.9, B 1.17, C 1487 $\mu\text{g L}^{-1}$, D -1.3, R²0.999).

3.6.5 Recognition of haptens

All four haptens (HSL1, HSL2, HSL3 and HSL4, Figure 23) were tested also as analytes with all assays to characterise the antibodies. HSL2 and HSL3 were generally less recognised than HSL1 and HSL4 for all tested mAbs. In addition, all mAbs could clearly distinguish between HSL1 and HSL3, which have the identical chain length and differ only in the C3 position (oxo- versus hydroxyl group). The best discrimination of the functional group in this position is shown with mAb HSL1-8E1, which recognises the oxo- group 40 times better than the hydroxyl group. HSL1 mAbs had CRs in the order HSL1>HSL4>HSL3>HSL2, and the CR

of HSL1 was about 150% and for HSL2 below 0.1%. Similarly, as described in section 3.6.2, the anti-HSL1 antibodies were able to distinguish the side chain length and functional group in the C3 position significantly. Slightly differently, HSL1/2 antibodies had nearly identical high CRs to HSL1 and HSL4. Again HSL2 was the least recognised. The CR from HSL1 to HSL3 dropped also significantly. As expected, all anti-HSL4 mAbs showed best recognition for HSL4. This was followed by the recognition of HSL1. Interestingly, the mAbs HSL4-5E12, HSL4-5H3 and HSL4-6D3 showed relatively higher CR to HSL2 compared to all other mAbs (Tables 13 and 14). This special property of these HSL4 antibodies offers better binding opportunity to short chain HSLs than other mAbs. (The standard curves of mAbs HSL1-8E1, HSL4-4C9 HSL4-5E12 and HSL4-6D3 are supplied in Attach. 5-8, page 155-158).

3.7 HSL detection in biological samples

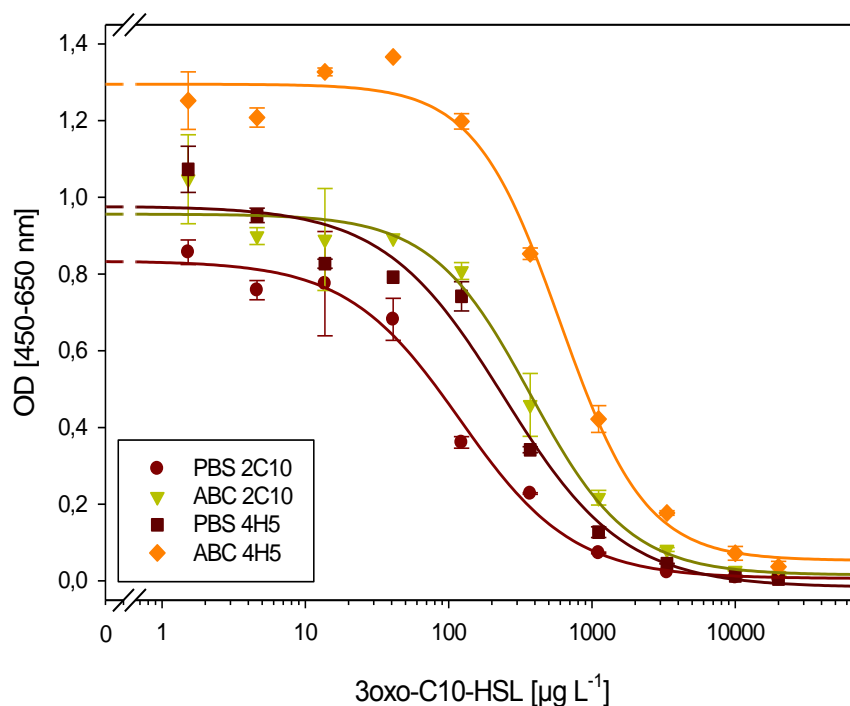
In this study, three kinds of biological samples were selected for HSL detection in the bacterial supernatant with the developed immunoassays. They were *Burkholderia cepacia* LA3, TCB degradation bacterial community, and *Pseudomonas putida* (wild type IsoF, mutant F117 and negative strain KT2440).

3.7.1 *Burkholderia cepacia* isolate LA3

3.7.1.1 Matrix effects in ABC medium

For *B. cepacia* LA3 samples, the matrix effects were determined by comparing the 3oxo-C10-HSL standard curves in 40 mM PBS buffer and ABC medium. A slight OD increase (about 0.2) in ABC medium was observed for both ELISAs, but the signal was still in an acceptable range in both buffers. In addition, a shift of standard curves to the right (to higher concentration) was clearly visible and is shown in Figure. 34. Both ELISAs performed with a lower sensitivity in ABC medium than in PBS buffer. The ABC/PBS factor of IC_{50} for 3oxo-C10-HSL is 3.1 using mAb HSL1/2-2C10 and 2.5 using mAb HSL1/2-4H5. Noticing this matrix effect, the standard curve of 3oxo-C10-HSL was set up in ABC medium as a reference for culture supernatant samples. The working range was taken from 15% to 85% control of the standard curve (Brady, 1995). According to the standard curves it was 21–585 $\mu\text{g L}^{-1}$ (78–2,170 nM) in the assay with PBS buffer and 50–1,500 $\mu\text{g L}^{-1}$ (186– 5,576 nM) in the assay with ABC medium (Figure 34; mAb HSL1/2-2C10, enzyme tracer HSL3-HRP). This implies for the assay in ABC medium, that this assay has the lowest relative error between 50 and 1,500 $\mu\text{g L}^{-1}$ and correspondingly lower accuracy outside of this range (Harrison *et al.*, 1989).

Figure 34 Matrix effects in ABC medium.

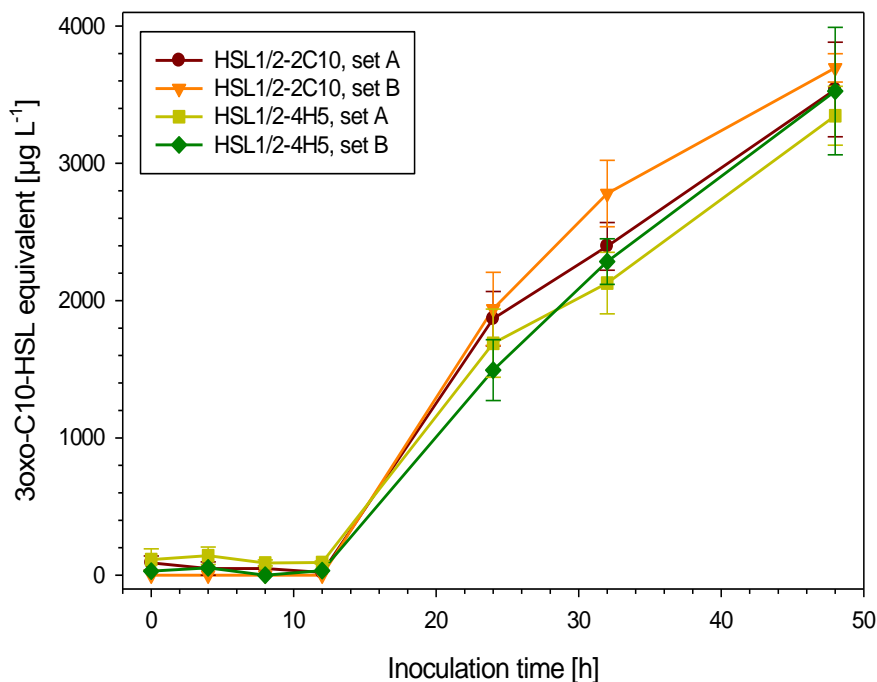


Standard curves for 3oxo-C10-HSL with mAbs HSL1/2-2C10 and HSL1/2-4H5 in PBS buffer and in ABC medium using HSL3-HRP as enzyme-tracer. Assay conditions: Protein G $2 \mu\text{g mL}^{-1}$; HSL1/2-2C10 400 ng mL^{-1} , HSL3-HRP 1:600; HSL1/2-4H5 200 ng mL^{-1} , HSL3-HRP 1:400. Four parameter curve fitting data are given in parentheses: *red circles* 3oxo-C10-HSL in PBS with HSL1/2-2C10 (A 0.834, B 1.1, C $120 \mu\text{g L}^{-1}$, D 0.006, R^2 0.991); *yellow green inverted triangles* 3oxo-C10-HSL HSL in ABC medium with HSL1/2-2C10 (A 0.956, B 1.25, C $373 \mu\text{g L}^{-1}$, D 0.015, R^2 0.989); *brown squares* 3oxo-C10-HSL in PBS with HSL1/2-4H5 (A 0.977, B 1.04, C $243 \mu\text{g L}^{-1}$, D -0.017, R^2 0.979); *orange rhombus* 3oxo-C10-HSL in ABC medium with HSL1/2-4H5 (A 1.29, B 1.45, C $601 \mu\text{g L}^{-1}$, D 0.054, R^2 0.992). Published results (Chen *et al.*, 2010 b)

3.7.1.2 Assay comparison with two mAbs and two setups with *B. cepacia* LA3 culture supernatants

Our previous work of this study had confirmed that the mAbs HSL1/2-2C10 and HSL1/2-4H5 have a very similar specificity pattern to HSLs and HSs (CRs see Tables 12 and 13). As listed in Table 15, mAb HSL1/2-2C10 has a lower IC_{50} for 3oxo-C10-HSL ($134 \mu\text{g L}^{-1}$) than HSL1/2-4H5 ($253 \mu\text{g L}^{-1}$), and the recognition of C8-HSL and C10-HSL was slightly different as well. In general, these antibodies showed significantly better recognition of the hydrolysed form of HSLs (HSs). Using mAb HSL1/2-2C10, C8-HS has a CR of about 3820%, C10-HS of 1531%, and 3oxo-C10-HS of 1813%. The similar high recognition for HSs was revealed with mAb HSL1/2-4H5.

Figure 35 Comparison of two ELISAs with different antibodies and set A and B of undiluted *B. cepacia* culture supernatants.

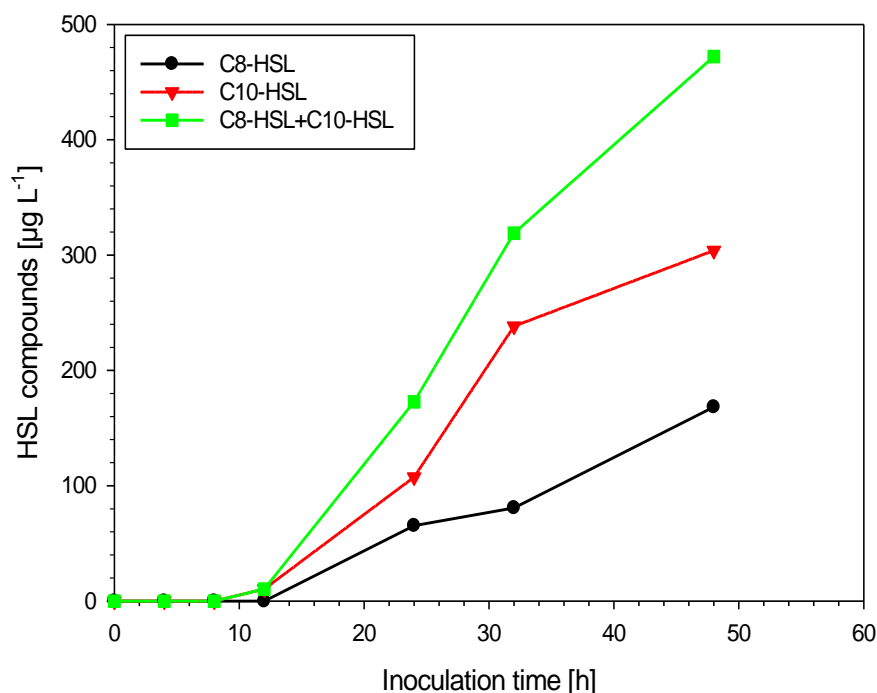


MAb HSL1/2-2C10 (400 ng mL^{-1}) and enzyme-tracer HSL3-HRP (1:600): set A *red circles*; set B *orange inverted triangles*. MAb HSL1/2-4H5 (200 ng mL^{-1}), HSL3-HRP (1:400): setup A *yellow-green squares*; setup B *green rhombus*. Published results (Chen *et al.*, 2010 b)

Undiluted *B. cepacia* culture supernatants were then analysed individually in set A and set B (in two different flasks set up in parallel) by ELISAs in the enzyme-tracer format using both mAbs, respectively. Although C8- and C10-HSL were expected to be the main HSLs for *B. cepacia*, in these experiments 3oxo-C10-HSL was used as the reference standard (= main analyte in our optimised assays), and results were then expressed as 3oxo-C10-HSL equivalents. All four assays (2 mAbs, 2 sets) showed very similar results for these *B. cepacia* culture supernatants (Figure 35). In summary, no HSLs were detected from samples taken from cultures grown less than 12h, and the HSL concentrations increased continuously from 12h to 48h. The maximum concentration of about $3500 \text{ } \mu\text{g L}^{-1}$ of 3oxo-C10-HSL equivalent was detected at 48h. Due to the fact that these two setups and two assays had reproducible results, the further experiments were performed only with mAb HSL1/2-2C10 and set A. Figure 36 presents the UPLC-MS measurement results of the parallel prepared sample. C10-HSL was the most detected signal molecule and followed by C8-HSL. To compare the ELISA results a summary of the both HSLs was additionally present (green curve). Very similar to ELISAs, almost no HSL was found before 12 h and the HSL concentration increased with the inoculation time (12 h-48h). However, the absolute concentrations, even the summarised

values, of detected HSLs were a lot lower than those from ELISAs. The max. HSL concentration detected in ELISA was about at 48h with $3500 \mu\text{g L}^{-1}$ (Figure 35) but the max. value from UPLC-MC was less than $500 \mu\text{g L}^{-1}$ (Figure 36).

Figure 36 HSLs detected with UPLC-MS in *B. cepacia* LA3 culture supernatant



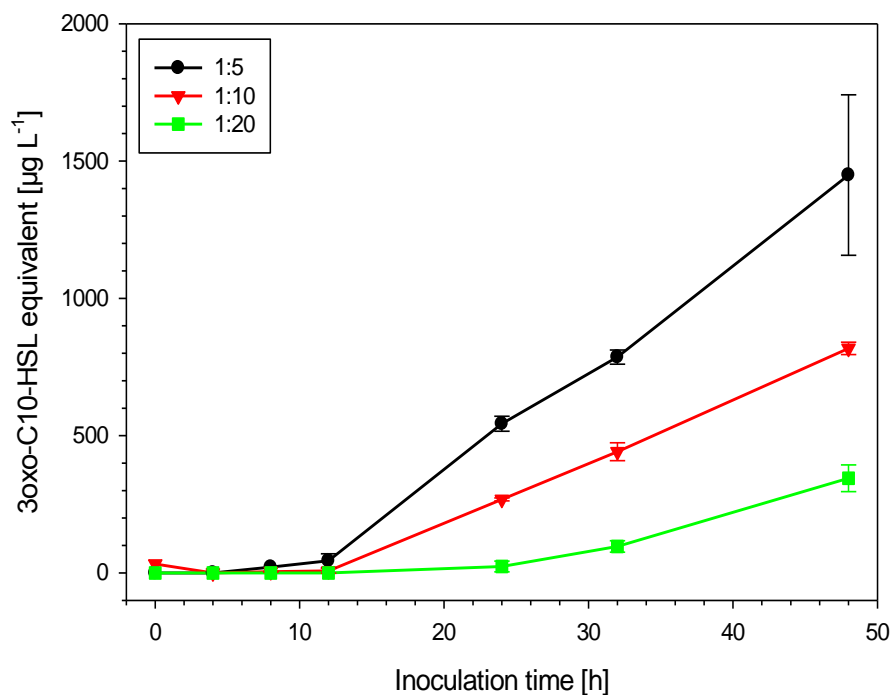
Green curve presents the summary of C8-HSL and C10-HSL, UPLC-MS measurement results supplied from Fekete 2010, unpublished.

3.7.1.3 Dilution control of *B. cepacia* LA3 culture supernatants

As mentioned before, the maximum concentration detected in *B. cepacia* LA3 culture supernatants at 48h was about $3500 \mu\text{g L}^{-1}$ 3oxo-C10-HSL equivalents. This was outside the assay's working range. Therefore the samples were diluted 1:5, 1:10, and 1:20 in ABC medium for the HSL determinations. Samples diluted 1:5 had the highest concentrations, and the 1:10 and 1:20 diluted samples showed correspondingly lower concentrations (Figure 37). Again, it was noticed that the LOD range of the assays had an effect on the accuracy of the detection, particularly the samples with higher concentrations. Thus, attention had to be paid to sample dilutions with careful consideration of the detection ranges of the assays. From the results shown in Figure 37, the 1:10 dilution was selected to be the most suitable for these measurements, because most of the values were within the working range. Additionally, the

samples with hydrolysing treatment were also diluted with the same factors as described for the untreated ones, and the final results were very well comparable (data not shown).

Figure 37 Dilution controls in ELISA using mAb HSL1/2-2C10 (400 ng mL⁻¹) and enzyme-tracer HSL3-HRP (1:600)



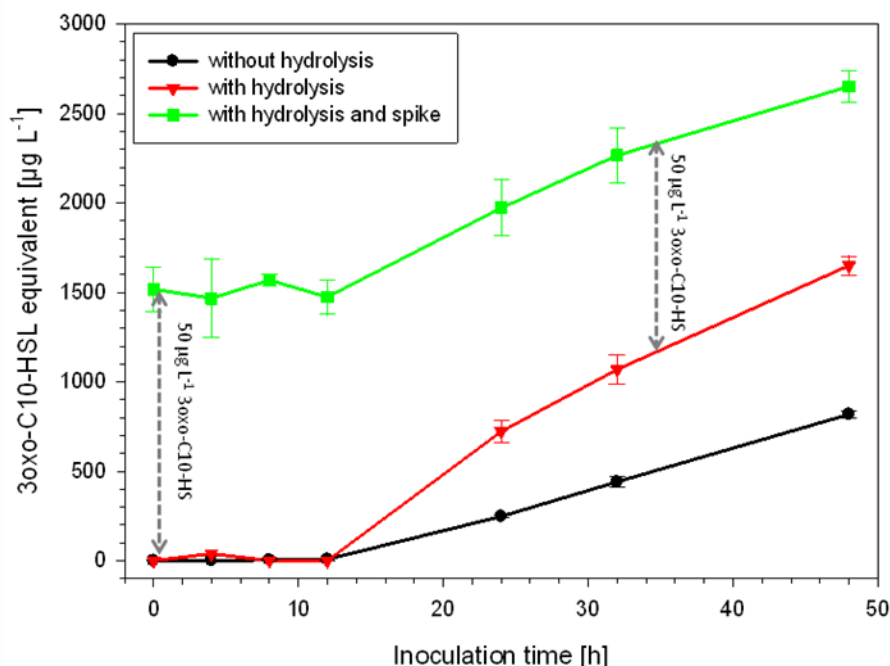
1:5 dilution: *black circles*; 1:10 dilution: *red inverted triangles*; 1:20 dilution: *green squares*. Published results (Chen *et al.*, 2010b)

3.7.1.4 Hydrolysis and spiking experiments

In natural environments, HSLs could be at least partially hydrolysed and HSs would be produced due to the lactone ring opening. However, analytic using mAbs and ELISA for HSLs in *B. cepacia* LA3 culture supernatants could not distinguish HSLs from HSs directly. In order to find out, whether HSLs of *B. cepacia* were already hydrolysed in the culture supernatants, measurements were carried out with the original sample and after effective hydrolysis. In addition, the hydrolysed samples were then spiked with $50 \mu\text{g L}^{-1}$ of 3oxo-C10-HS. Figure 38 shows only the 1:10 dilution of culture supernatants; but the dilutions 1:5 and 1:20 provided comparable results. The green curve (squares) in Figure 38 illustrates the concentration of hydrolysed samples which were spiked with $50 \mu\text{g L}^{-1}$ of 3oxo-C10-HS, respectively. The spike of $50 \mu\text{g L}^{-1}$ of 3oxo-C10-HS resulted in an average concentration of $1497 \pm 60 \mu\text{g L}^{-1}$ of 3oxo-C10-HSL equivalents (0 to 12h). This higher determination reflects the higher CR to 3oxo-C10-HS. For control purpose, the whole process was repeated with a

spiking concentration of $25 \mu\text{g L}^{-1}$ of 3oxo-C10-HS. Here, the spiked concentration of $25 \mu\text{g L}^{-1}$ of 3oxo-C10-HS was analysed as an average concentration of $669 \pm 76 \mu\text{g L}^{-1}$ of 3oxo-C10-HSL equivalents (0 to 12h).

Figure 38 Hydrolysis and spiking experiments with 1:10 diluted *B. cepacia* culture supernatants.



ELISA with mAb HSL1/2-2C10 400 ng mL^{-1} and enzyme-tracer HSL3-HRP 1:600. *Black circles*: 1:10 diluted culture supernatants. *Red inverted triangles*: 1:10 diluted culture supernatants after hydrolysis of HSLs. *Green squares*: 1:10 diluted culture supernatants after hydrolysis of HSLs and with a spiked concentration of $50 \mu\text{g L}^{-1}$ of 3oxo-C10-HS to each sample, the grey dash lines with arrows indicate the increasing of the detected 3oxo-C10-HSL signals due to the addition of $50 \mu\text{g L}^{-1}$ 3oxo-C10-HS. Published results (Chen *et al.*, 2010 b)

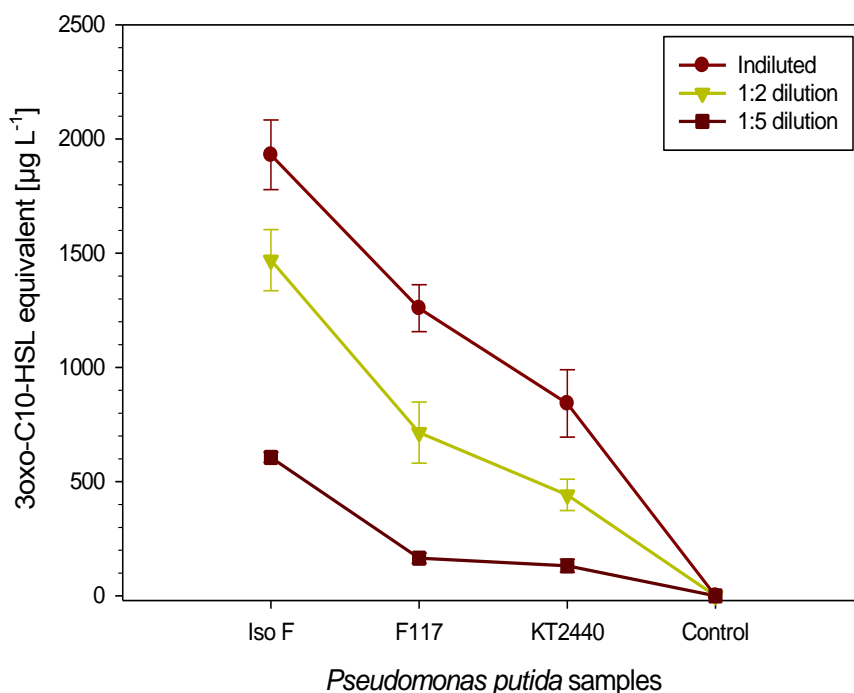
Assuming that C8- and C10-HSL were present in the *B. cepacia* LA3 culture supernatants (after 12h), the spiked concentration of 3oxo-C10-HS was still clearly visible (Figure 38). The spike of $50 \mu\text{g L}^{-1}$ of 3oxo-C10-HS resulted here in an average concentration of $1149 \pm 131 \mu\text{g L}^{-1}$ of 3oxo-C10-HSL equivalents (difference between measurements of 1:10 diluted culture supernatants after hydrolysis, without and with spike, 24-48h). The determined concentrations though were probably slightly influenced by the presence of C8-HS and C10-HS.

Although we could not give the distribution of HSLs and HSs in the *B. cepacia* culture supernatants, a clear increase of both compounds during the bacterial growth could be followed over time (12h to 48 h).

3.7.2 HSL detection in *Pseudomonas putida* cultural supernatant

In *P. putida* culture supernatants, the highest AHL concentration was detected from the wildtype IsoF and then followed by the negative mutant F117 and negative control KT2440. No signal was detected in the blank control samples (Figure 39). However the AHL concentration of the negative supernatant was in quite low level compared to the positive supernatant. The diluted samples showed comparable proportional factors (Figure 39).

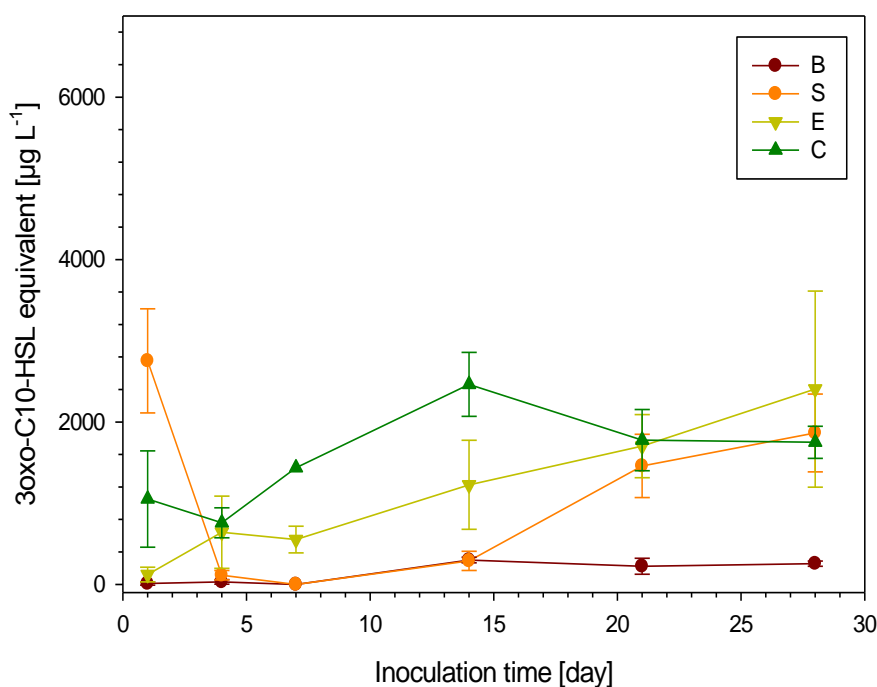
Figure 39 *P. putida* supernatants HSL detection with 24h inoculation time



3.7.3 HSL detection in TCB degradation bacterial community

In Figure 40 it is shown that the blank samples had only very low values. These values were, thought to be backgrounds. All samples showed an increase from day 7 to day 14. Not like the further increasing of S and E, the C samples showed slight decrease after two weeks. Interestingly, a particular high concentration of AHLs was detected of S sample of the day 1, which was different from all other sample series. The samples were also analysed by UPLC-MS and some HSLs were detected but the detailed evaluations are still not available at the moment (unpublished results, Fekete, 2010).

Figure 40 HSL detection TCB degrading bacterial communities supernatant



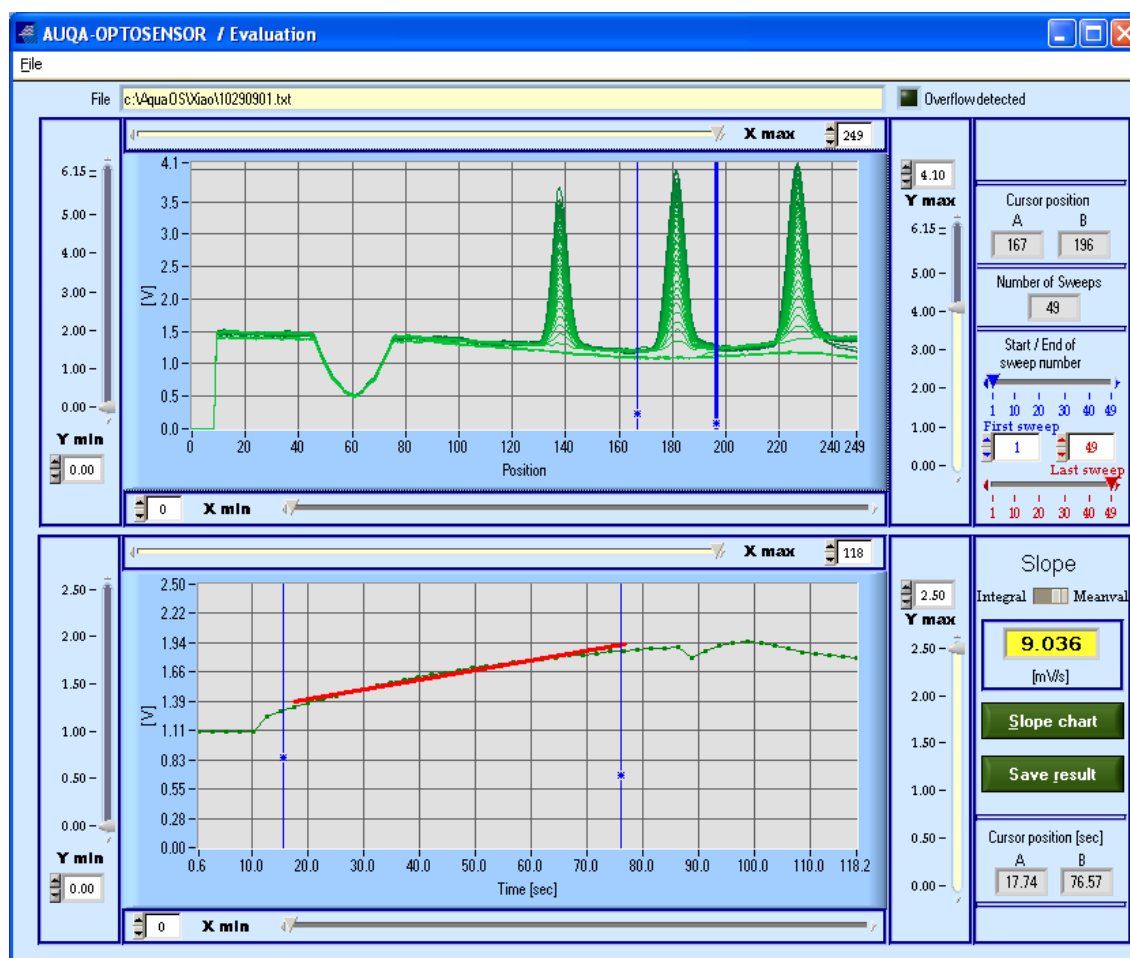
B: blank; C: community; S: sterilised clay; E: established biofilm on clay

3.8 AOS results of mAb HSL1/2-2C10

For comparison with ELISA, the mAb HSL1/2-2C10 was also characterised with AOS. Due to limited available sensor chips, no other mAb has been characterised with AOS. As discussed previously, the mAb HSL1/2-2C10 was well characterised with ELISA using both formats.

As an example, Figure 41 shows the directly measured and evaluated results of the AOS for the antibody HSL1/2-2C10 without analyte. The slope value of the second middle peak, which used the coating of 2 mg mL^{-1} of HSL2-BSA-r2, was obtained for further evaluation. As the competitive principle coating antigen format, the peaks become smaller (lower slope) with the increasing of the analyte concentration (data see Attach.9, page 159 and Attach.10, page 160).

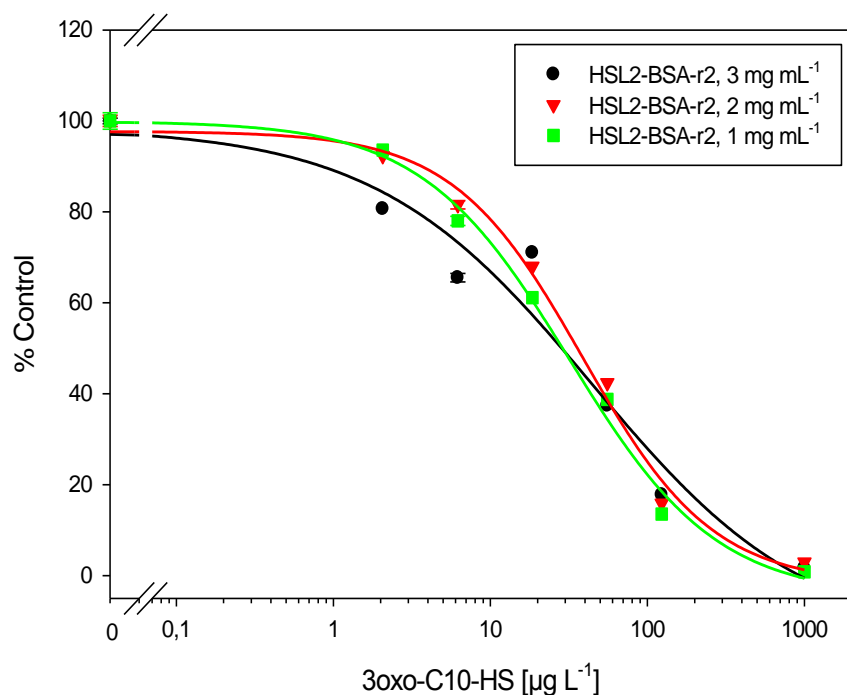
Figure 41 AOS peaks of Oyster-645 labelled mAb HSL1/2-2C10 without analyte



Assay condition: mAb HSL1/2-2C10 labelled with Oyster-645 (label degree 1:2), 48 ng mL⁻¹; spotting with HSL2-BSA-r2 in 50 mM carbonate buffer, pH = 9.6 + 0.05% (v/v) Tween 20, [3 mg mL⁻¹] for peak left, [2 mg mL⁻¹] for peak middle and [1 mg mL⁻¹] for peak right. Zero analyte addition. Slope value: peak left= 8.341 mV/s, peak middle= 9.036 mV/s (value in the figure), and peak right= 9.622 mV/s.

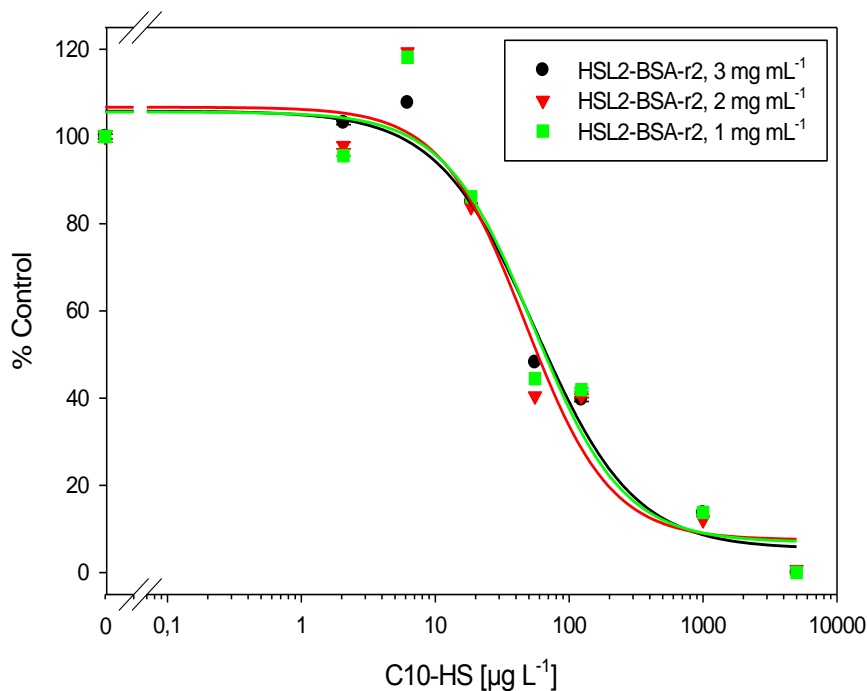
The Figure 42 and 43 are the standard curves for 3oxo-C10-HS and C10-HS measured by AOS using the antibody HSL1/2-2C10. No significant difference was observed between the coating concentrations of 1, 2 or 3 mg mL⁻¹ in both curves. The IC₅₀ of 3oxo-C10-HS was 38.8 µg L⁻¹, which is slightly lower than the IC₅₀ of C10-HS (54.3 µg L⁻¹).

Figure 42 Standard curves of 3oxo-C10-HS with AOS



AOS standard curves for 3oxo-C10-HS with different concentration of spotting antigen HSL2-BSA-r2, using mAb HSL1/2-2C10. Assay conditions: Oyster-645 labelled HSL1/2-2C10 (label degree 2), 48 ng mL⁻¹. Four parameter curve-fitting data are given in parentheses: *black circles* HSL2-BSA-r2, 3 mg mL⁻¹, (A 98.6, B -0.63, C 44.6 $\mu\text{g L}^{-1}$, D -14.5, R² 0.979), *red inverted triangles* HSL2-BSA-r2, 2 mg mL⁻¹, (A 97.7, B -1.04, C 38.8 $\mu\text{g L}^{-1}$, D -1.93, R² 0.996), and *green squares* HSL2-BSA-r2, 1 mg mL⁻¹, (A 99.9, B -9.23, C 31.8 $\mu\text{g L}^{-1}$, D -4.68, R² 0.997).

Figure 43 Standard curves of C10-HS with AOS



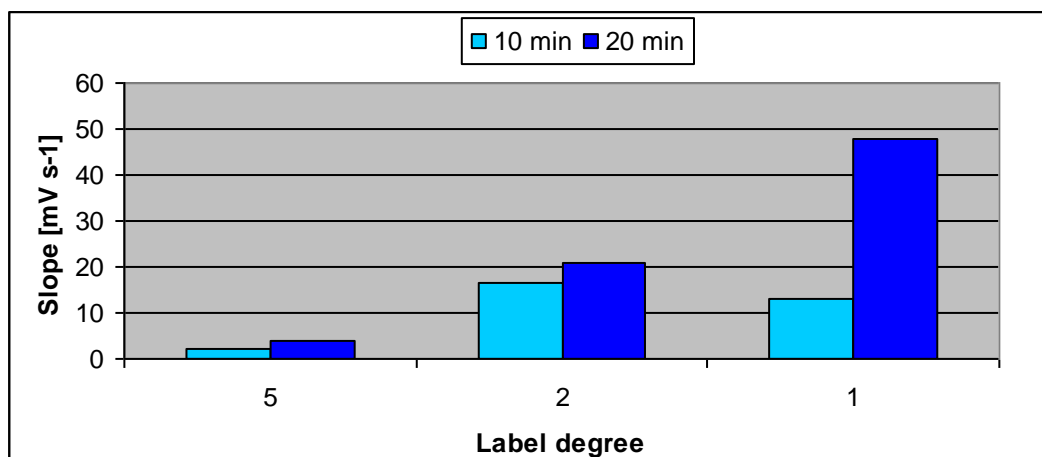
AOS standard curves for C10-HS with different concentration of spotting antigen HSL2-BSA-r2, using mAb HSL1/2-2C10. Assay conditions: Oyster-645 labelled HSL1/2-2C10 (label degree 2), 48 ng mL⁻¹. Four parameter curve-fitting data are given in parentheses: *black circles* HSL2-BSA-r2, 3 mg mL⁻¹, (A 105.8, B -1.18, C 56.2 $\mu\text{g L}^{-1}$, D 5.46, R² 0.989), *red inverted triangles* HSL2-BSA-r2, 2 mg mL⁻¹, (A 105.6, B -1.30, C 54.3 $\mu\text{g L}^{-1}$, D 6.94, R² 0.972), and *green squares* HSL2-BSA-r2, 1 mg mL⁻¹, (A 104.9, B -1.27, C 55.8 $\mu\text{g L}^{-1}$, D 6.03, R² 0.967).

3.9 Fluorophore labelled antibodies

It is possible that the chemical properties of antibodies are changed in some manners through the labelling with dyes. To obtain good fluorescence immunoassays, two aspects must be taken into consideration. First, a good affinity of the antibodies is still required for target analytes; secondly, the fluorescence signal should be strong enough to be detected. Using Oyster645-NHS as fluorescent dye for HSL antibodies, different label degrees and reaction times have been tested.

The increase of antibody-dye reaction time resulted in a slightly higher fluorescent signals (Figure 44) but reduced binding to the coating antigen (Figure 45), however, the difference was not very high.

Figure 44 AOS affinity determination of HSL1-1A5 after fluorescent labelling

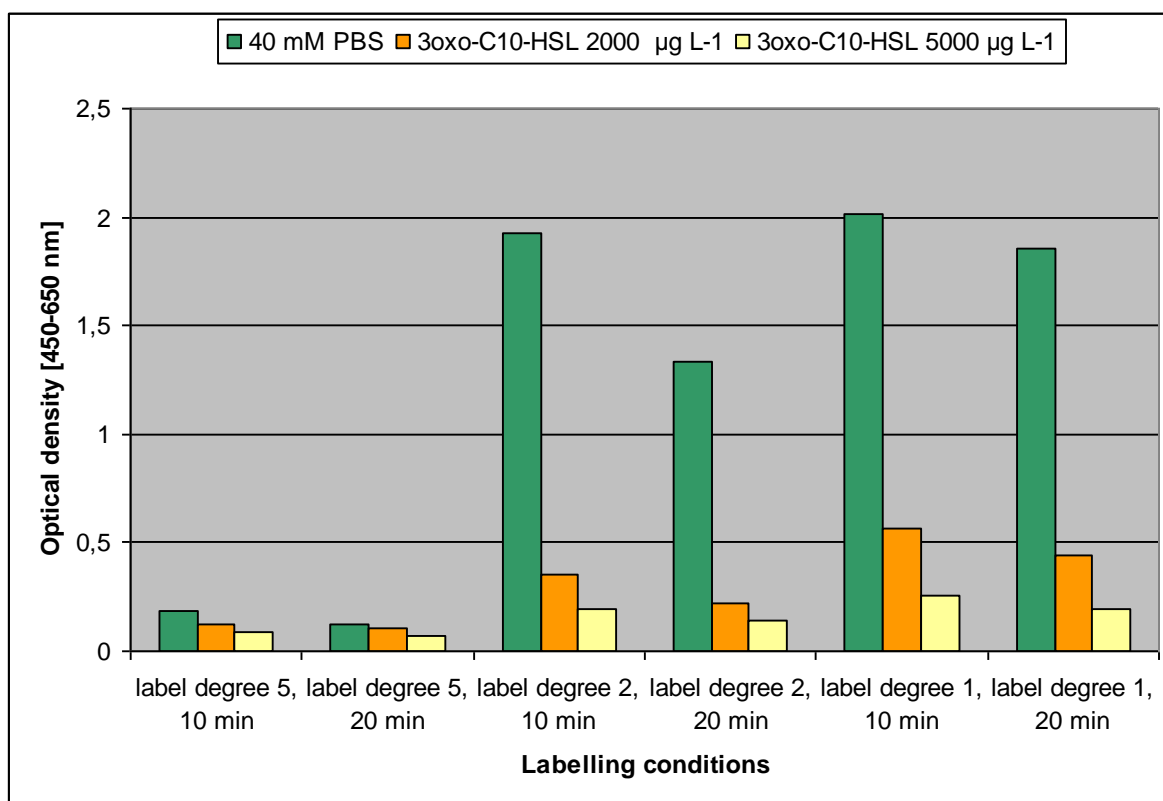


A representative figure for Oyster645 labelled HSL-mAb binding determined by AOS. Assay conditions: coating antigen HSL2-BSA-r2, 3 mg mL⁻¹ in 50 mM Carbonate-Puffer + 0.05 % (v/v) Tween 20; HSL1-1A5+Oyster 645, 48 ng L⁻¹ (measured by Miss Mandy Starke, 082009, IEC)

Interestingly, a strong influence to antibody affinities of label degrees has been observed from both methods. The antibody binding on coating antigen was almost completely inhibited with label degrees of 10 or 20 (results not shown) and only very small amount of binding was shown at label degree of 5 (Figures 44 and 45). The antibody-antigen binding sites could probably be blocked by the relative large amount of dye. Thus the reduced label rate resulted in significant increase of binding signal in AOS and more effective inhibition in ELISA. Based on the results discussed above, the antibodies with label degree of 2 and reaction time of 20 min were chosen for further applications, e.g. *in situ* experiments.

In addition to the fluorophore labelling protocol of Denovo Biolabels, the DMF volume was varied depending upon the dye amount needed for conjugations. Basically, the dye solution needed for individual antibody should be more than 1 μ L, which is aimed to reduce pipette error. This is particular important at small amount conjugations. Another important point was found to have enough glycine for complete blocking of activated ester on dye. A double or higher amount of glycine as dye is recommended to avoid unspecific binding of activated NHS.

Figure 45 Inhibition 2D tests of HSL1-1A5+Oyster645 with coating antigen format ELISA

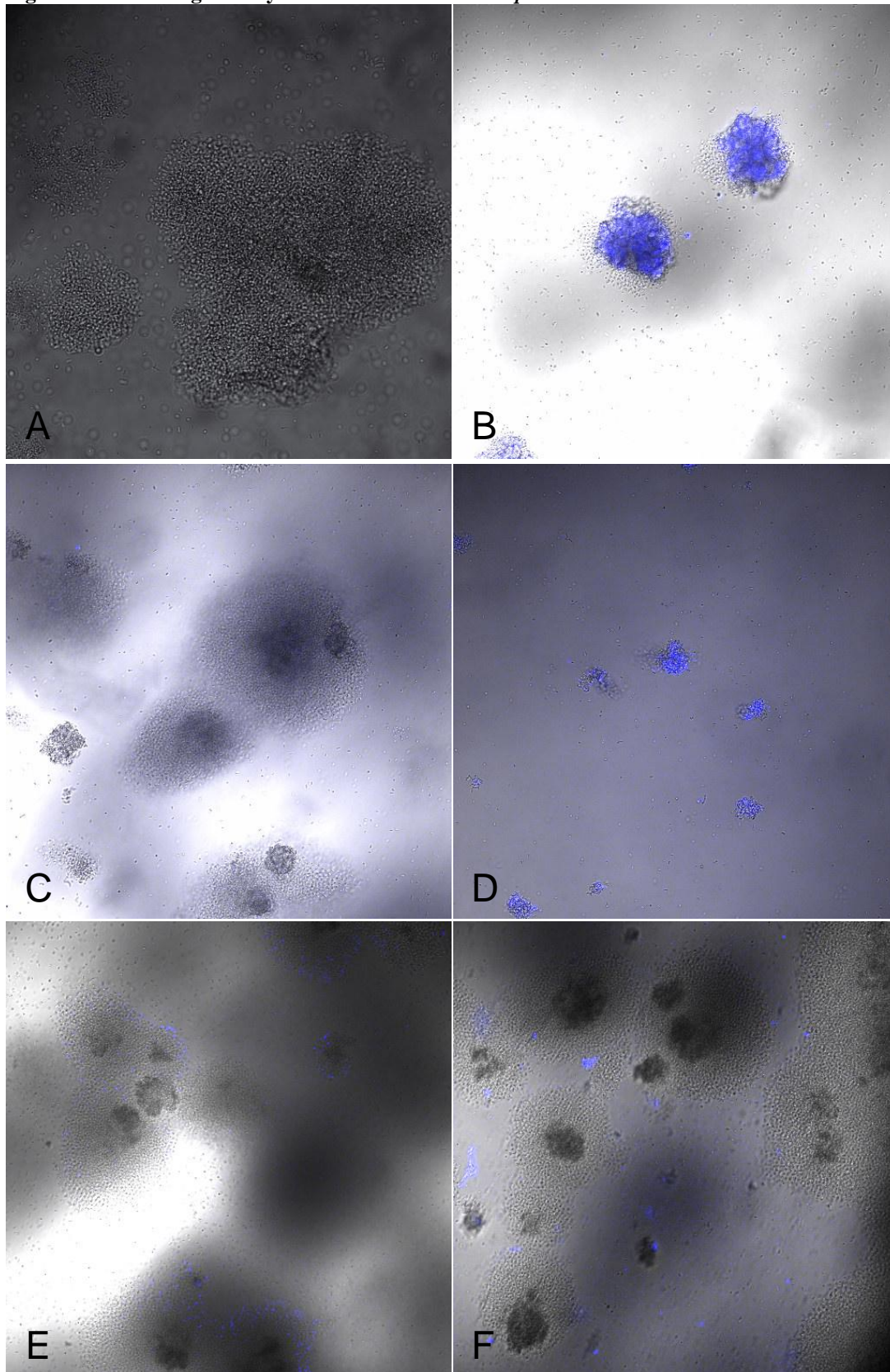


A representative figure evaluation of Oyster645-labelled HSL-mAb using two dimensional inhibition tests with the coating antigen format ELISA. Assay conditions: coating antigen HSL2-BSA-r2, 2 µg mL⁻¹; HSL1-1A5+Oyster 645, 400 ng mL⁻¹. The green bars are the OD without inhibition (only PBS), the orange and yellow bars are the OD with additional 30x0-C10-HSL as competitor of the binding to coating antigen. The more the difference to PBS, the better is the inhibition and the better is the sensitivity of the assay.

3.10 *In situ* experiments

The *in situ* experiments of bacterial biofilms on ibidi slides (Figure 46) and of bacterial colonisation of plant roots (Figure 47) were difficult due to the interference of the specific fluorophore label with the matrix autofluorescence and unspecific binding of the labelled antibodies. Figure 46 is showing biofilms/colonies of *B. cepacia* LA3 on ibidi slides. It is apparent, that without blocking with 10% glycine (0.5% glycine in final antibody solution) the Oyster645-staining binds un-specifically (Fig. 46B and 46C). Using Oyster-labelled HSL1/2-2C10 binding of the labelled antibody was visible (Fig. 46D) and less in Fig. 46F when less Ab-concentration was applied. However, low binding of Oyster645-labelled anti-DDT (as negative control) demonstrates still some degree of unspecific binding, which need to be reduced further by alternative blocking and more intense washing.

Figure 46 LSM-images of Oyster labeled mAb on *B. cepacia* LA3 biofilm in ibidi slide

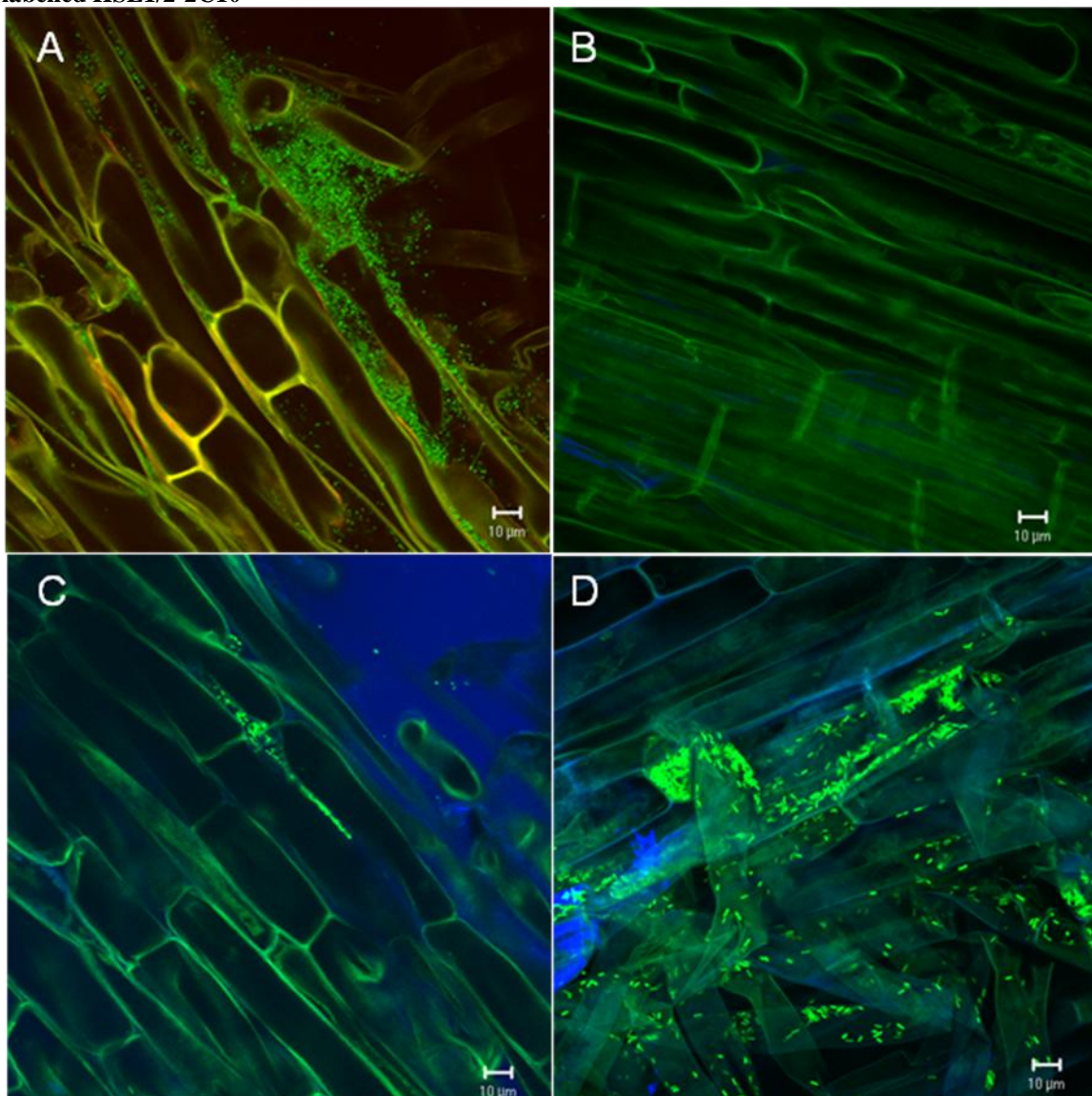


Experiment conditions: biofilm of *B.cepacia* LA3, mAb HSL1/2-2C10 labelled with Oyster645 in 40 mM PBS. A: only biofilm, no glycine; B: biofilm incubated with Oyster 645 solution, no glycine; C: biofilm incubated with 0.5% glycine treated Oyster 645; D: biofilm treated with Oyster 645-labelled HSL1/2-2C10, 0.3 mg mL⁻¹,

with 0.5% glycine E: biofilm treated with Oyster 645 labelled HSL1/2-2C10, 0.2 mg mL⁻¹, with 0.5% glycine; F: biofilm with Oyster645-labelled anti-DDT-mAb, with 0.5% glycine. Pictures from Rotballer, 2010.

In Figure 47 LSM-images of root surfaces of barley inoculated with *gfp*-labelled *Pseudomonas putida* IsoF are shown. The preincubation of 3% BSA was efficient to reduce drastically the unspecific background labeling with Oyster-645-labelled HSL 1/2-2C10 antibody (Fig. 47 B and C). In the presence of AHL-producing bacteria on the root surface, a strong “blue” antibody labeling was visible (Fig. 47D) – especially of the plant cell wall and intercellular spaces (upper left corner of 47D).

Figure 47 LSM-images of barley roots inoculated with *P. putida* IsoF and labelled with Oyster 645-labelled HSL1/2-2C10



The Oyster645 labelled antibody solutions were all treated with glycine (0.5% in final solution); A: root with GFP-labelled bacteria; B: uninoculated root, incubated with labelled antibody after blocking (then washed out) with 3% BSA; C: inoculated root treated with labelled antibody, without BSA blocking; D: inoculated root treated with labelled antibody after blocking (then washed out) with 3% BSA. Pictures from Buddrus-Schiemann, 2010.

4 Discussion

4.1 Selection of HSL haptens

Immunogens are structurally complex high molecular weight materials which cause an immune response in host animals (vertebrates) leading to antibody production. The hapten design is the most crucial step of immunoassay, because the properties of the haptens directly influence the antibody quality (more information see section 1.4.2.2 and 1.4.2.3). The HSL based haptens (Figure 23, page 76) selected in this study were aimed to obtain antibodies, which could distinguish the AHL side chain length, and the substitutions (oxo-, OH- or only hydrogen) on the C3 atom. Furthermore, the antibodies showed different selectivities to the D and L isomers of the HSL substances (Attach. 11, page 161). But a proper comparison was difficult because there are no pure D-form HSLs available and the experiments were only performed using Lisomeric HSLs and DL mixed HSLs.

4.2 Hapten conjugation and conjugates characterisation

Small molecules (MW<1000 Da) are usually not sufficient to trigger a vertebrates' immune system. In this study, the HSL molecules are too small (MW<1000 Da) and must be conjugated to carrier proteins to enable an immune response and consequently antibody production. Albumin (typically BSA and OVA) and keyhole limpet hemocyanin (KLH) are two very common carrier proteins. BSA is well suited as a carrier protein due to its high solubility in various buffers, moderate molecular weight (BSA, 66 kDa), and high content of available primary amines. Immunogens based on KLH have been frequently used; however, they are difficult to characterise due to poor solubility, variable mass of the starting protein, and inconsistencies in the purity. Thus BSA and OVA (45 kDa) were used as carrier proteins and confirmed to be a suitable choice for the resulting immunoassays. The haptens used for this work were produced with modification of a carboxyl functional group at the end of the HSL carbon side chain (Figure 24).

Several methods have been used to determine the hapten-protein conjugation. The UV absorbance spectrum of the synthesised conjugate is commonly used when the hapten or linker has a strong chromophore which differs from the carrier protein. Electrophoresis and fluorescence methods were also suggested to be very useful in detecting hapten-protein cross-linking while matrix-assisted laser desorption ionization mass spectrometry (MALDI-MS) and spectrophotometric detection provided qualitatively comparable hapten density (Adamczyk *et al.*, 1994, Singh *et al.*, 2004). In this study, the UV spectra of HSL haptens, BSA, OVA, and the conjugates were obtained to confirm the success of conjugation.

Unfortunately, HSL1 was the only hapten, which showed a peak in the UV spectra and no significant UV signal was detected of the rest three haptens (Figure 24-26). However, the shift of the peaks of BSA/OVA proteins after the conjugation indicated the success of the experiments. But the determination of the exact number of the HSL haptens per protein was not possible using this technology. MALDI-MS was tried to determine the hapten conjugate, but the experiment was not successfully because the detected molecular weight of proteins after coupling was very similar or even smaller compared to non-conjugated protein. The reason might be that the change of protein molecular weight caused by coupling of the small HSLs (MW<500) was not large enough for the instrumental sensitivity. MALDI-TOF-MS might be a more suitable method to the HSL conjugates characterisation for the BSA/OVA molecular size.

4.3 HSL-protein and HSL-HRP conjugates selection for ELISAs

The results of antibody screening and antibody characterisation showed that HSL2-BSA-r1 and HSL2-BSA-r2 with reduced hapten number had a higher sensitivity than HSL2-BSA with higher hapten number in the coating antigen format. The hapten amount per BSA molecule had the order of HSL2-BSA>HSL2-BSA-r1>HSL2-BSA-r2, and the sensitivity of the assays increased with the reduced hapten number. Marco *et al.* (II, 1995) and Raem & Rauch (2007) described that the hapten-protein ratio plays different roles for immunisation as compared to the immunoassay as coating antigen. A high hapten-protein ratio is commonly required to reach a high strength and specificity of the immune response, but for coating antigen assay (the HSLs on immunogen compete with the HSL in free solution for the antigen-binding sites of the antibody) a lower number is more desirable to obtain sensitive assays. In general, when the amount of hapten in the competitor (hapten-protein conjugate) is reduced, less analyte in solution is required to compete for the specific binding to mAb. However, a too low hapten-protein ratio could not be used as competitor since the binding to the antibody is too weak and therefore not sufficient for assays. From the four HSL-HRPs, HSL1-HRP and HSL3-HRP showed the best enzyme-tracer format assays and HSL2-HRP generally had very low or instable signals. Thus variable hapten-protein ratios for coating antigens and enzyme-tracers should be prepared to obtain most sensitive assays.

4.4 Antibody screening

Sensitivity, selectivity and signal intensity were the main criteria for antibody screening. For further characterisation of sub-cloned mAbs in culture supernatants or in purified solutions,

two-dimensional titrations were carried out and standard curves were used to check the combination which gave the highest sensitivity (lowest IC_{50}) and the lowest background with an acceptable binding signal (optical density > 0.3). The selectivity of antibodies against HSLs was also carefully considered to gain diverse antibodies. In the end, two HSL1 mAbs, two HSL1/2 mAbs and four HSL4 mAbs were chosen for purification regarding the results of optimised coating antigen and enzyme-tracer formats.

4.5 Comparison of coating antigen and enzyme-tracer format assays

All antibodies tested in this study showed less sensitivity in the coating antigen format than in the enzyme-tracer format, although similar tendency of cross-reactivity pattern was observed in general (Tables 12 and 13, page 88-90). This phenomenon of lower test midpoints in the enzyme-tracer format was already demonstrated in former ELISA developments (e.g., Krämer *et al.*, 2004, 2010). One explanation originates in the immunochemical reaction which is based on the law of mass action. As it was discussed above, more hapten molecules (per protein) will need more analyte molecules (higher concentration) in the competitive reaction to reveal the same signal. This implies particularly in applications when the same hapten is used for the coating antigen and for the enzyme-tracer conjugates and when mAbs are utilized in the assays (Krämer *et al.*, 2010). Generally, from six lysines in the HRP molecule, a maximum of three molecules show surface accessibility (Krämer *et al.*, 2004). The BSA molecule on the other hand has 59 lysine residues, 30-35 of which have primary amines capable of reacting with a conjugation reagent. Assuming that all accessible 30-35 lysine residues were occupied with haptens during our 'normal' conjugation process, the hapten-BSA conjugate with reduced hapten molecules, for which only half of the hapten quantity for conjugation was used (Table 5, page 56), approximately 15 hapten molecules per protein molecule are expected. This will lead to a less favourable inhibition for HSL compounds in the coating antigen format in comparison to the enzyme-tracer format.

4.6 Comparison of ELISA and AOS

The coating antigen format was used for both ELISA and AOS, however, there are a few differences between the two methods. The most important difference was the fluorophore labelling of the antibodies for AOS, while the antibodies for ELISA were unlabelled. The other differences referred to the incubation conditions (e.g. time, temperature, and concentrations) and immobilisation surface. These are the factors, which might affect the

sensitivity of the assays. As mentioned in the previous section of fluorophore conjugation (1.4.6.2, page 41), the antibody could be changed in some manner after conjugation with a fluorophore. The tendency of cross-reactivity pattern of the assays remained similar: the assays recognised 3oxo-C10-HS better than C10-HS. However, the AOS was slightly more sensitive than ELISA compared to the IC_{50} values of the analytes (Table 16). Another interesting point is that the ELISA distinguished the HS with or without –oxo group more significantly than AOS. In general, they are both very comparable characterisation methods for antibodies. But individual assay for different antibody and analyte is strongly recommended, because all molecules have their unique nature.

Table 16 IC_{50} and LOD comparison of ELISA and AOS

	ELISA		AOS	
	Coating antigen format		Coating antigen format	
Coating antigen	HSL2-BSA-r2 [1 $\mu\text{g mL}^{-1}$]		HSL2-BSA-r2 [2 mg mL^{-1}]	
mAb	HSL1/2-2C10 [400 ng mL^{-1}]		HSL1/2-2C10 labelled with Oyster-645 [48 ng mL^{-1}]	
Analyte	IC_{50} [$\mu\text{g L}^{-1}$]	LOD [$\mu\text{g L}^{-1}$]	IC_{50} [$\mu\text{g L}^{-1}$]	LOD [$\mu\text{g L}^{-1}$]
C10-HS	131 \pm 16, n=2	14 \pm 3, n=2	53 \pm 5, n=3	14 \pm 1, n=3
3oxo-C10-HS	37 \pm 6, n=2	4.7 \pm 3.5, n=2	38 \pm 6, n=3	2.4 \pm 1.4, n=3

4.7 Antibody recognition of homoserine lactone (HSL) and homoserine (HS) compounds

The selected antibodies showed distinguishing selectivities to the HSLs with varied chain length and functional groups on the C3 position corresponding to the immunised haptens. All antibodies showed best recognition of chain lengths of C8 or C10 and very low recognition of the hydroxy group on the C3 atom. HSL1 mAbs could significantly distinguish the HSLs with or without oxo- on C3 position, and long chain HSLs were preferred. HSL1/2 mAbs had very broad recognitions of HSLs with slightly better affinity for oxo- containing HSLs. In contrast

the HSL4 antibodies showed higher affinity to the HSL without any substitution on C3 position and the HSL4-4C9 was very specific to C8-HSL and showed much less recognition of other HSLs. The affinities of the antibodies to the HSL haptens showed very similar trends as obtained from HSL standards. These specificities of the antibodies confirmed a successful hapten design for targeting HSL molecules.

An unusual phenomenon was observed with six out of eight HSL-antibodies. The recognition of HSL2 was extremely low (CR<0.1 to 3%) although the HSL2-BSA conjugate was selected as the best coating antigen, meaning that HSL2 must have been recognised by the antibodies. One explanation for this might be that the linkage of HSL2 to the lysine group of the protein leads to an extension of the chain length. It seems that the peptide bond formed during covalent attachment of the HSL2 hapten to lysine is not so critical for recognition, and therefore the antibodies recognise a longer chain length than originally from HSL2. This is supported also by the good recognition seen of HSL4 and the very poor affinity of the HSL2 compound.

In this study, the newly developed anti-HSL mAbs were proven being more sensitive against homoserines (HSs, hydrolysed HSLs) than HSLs in both ELISA formats and biosensors. The initial goal of the study was to produce specific anti-HSL mAbs, which are relevant for quorum sensing. One explanation for this high specificity to HSs compounds might be that the HSLs were already hydrolysed during conjugation and immunisation processes which had $\text{pH} \geq 7$ and consequently, the antibodies were mostly developed to hydrolysed HSLs. Former publications have already stated the occurrence of abiotic hydrolysis of HSLs (lactone ring opens) under different conditions (Yates *et al.*, 2002; Frommberger *et al.*, 2005; Kaufmann *et al.*, 2006; Englmann *et al.*, 2007). Yates *et al.*, (2002) particularly revealed the mammalian physiological conditions (22°C or 37°C, pH 7) of hydrolysis in a temperature, pH and chain length dependent manner. The hydrolysis enhanced with increased temperature and pH, but decreased chain length.

However, in order to distinguish HSLs and HSs in samples, the assay conditions were carefully considered. This could be accomplished, for example, by the measurements of a sample before and after chemical hydrolysis of the HSLs (using alkaline conditions, lactonolysis). Also, the preliminary analysis of the samples with a conventional method prior to the screening of corresponding samples by immunoassay will give information about the distribution of HSLs and potential appearance of HSs. This method was successfully applied

for the analysis of HSLs in *Burkholderia cepacia* culture supernatants with the established immunoassays.

Furthermore a few of HSL/HS analogues (Figure 17, page 64), including serine, methionine and fatty acids with different chain length, were tested against HSL1/2-2C10. None of the tested substances showed binding in assays. This result can prove the specificity of the antibodies, that they recognise HSL/HS but not some degradation products, even serine. Of course it is still difficult to confirm with 100% security, because so many other analogues were not determined.

4.8 Biological relevance of HSL and HS

Regarding the affinity and selectivity of the antibodies, the developed immunoassays were used for the detection of HSLs and HSs in bacterial cultural supernatants. But the broad recognition of HSLs and even higher sensitivity of HSs were the main factors, which needed to be considered. Similar to bioreporter assays, the immunoassays are not able to distinguish single individual molecules, but only report the sum of all the HSLs and HSs. The challenging question is what and how exactly could we see with the immunoassays? Taking the 10% control of the standard curves as LODs, the values ranged from low μM to nM depending on assay format and antibody. This sensitivity is enough for most HSLs in real samples reported with other analytical methods e.g. with UPLC, LC-MS (Li *et al.*, 2006; Fekete *et al.*, 2010). The LODs of HSs could even come down to pM, e.g. 3oxo-C10-HS had an LOD of ca. 250 pM in enzyme-tracer format assay with mAb HSL1/2-2C10.

Though the HSLs are the known quorum sensing molecules, the co-appearance of HSLs and HSs were reported in many publications (Englmann *et al.*, 2007; Uroz *et al.*, 2009; Fekete *et al.*, 2010). Fekete *et al.*, (2010) demonstrated the dynamic curves of production and degradation of C10-HSL and C10-HS in *P. putida* IsoF cultural supernatant (see Figure 4, page 23). In *B. cepacia* LA3 cultural supernatant, 6.33 μM C10-HSL and 3 μM C10-HS were determined in the same sample using UPLC. As one of the main degradation pathways of HSLs, hydrolysis seems to have not fully discovered meaning of the QS regulation. In a recent review of quorum quenching (Uroz *et al.*, 2009), the QS inhibition mechanisms and the potential biological applications were extensively discussed, which included the therapeutic strategies against QS related disease. Beside the abiotic hydrolysis, a few lactone-degrading enzymes (named lactonase) were identified for hydrolysis of HSLs in natural environments and a few bacteria (e.g. *Agrobacterium*) owned HSL synthase and lactonase as well (Dong *et*

al., 2000; Uroz *et al.*, 2009). Thus, the significant sensitivity against HSs of these newly developed mAbs allows the detection of HSs at low concentrations and may help to reveal quorum quenching processes. On the other hand, the assay conditions must be carefully considered, due to the high CRs to HSs.

4.9 Development of QQ innovative biological tools

4.9.1 Immunotherapy

The 3oxo-C12-HSL has been shown not only to mediate bacterial QS, but also to exert cytotoxic effects on mammalian cells. These findings allowed the development of new strategies to combat microbial infections by targeting the QS signalling molecules. Kaufmann *et al.* (2006, 2008) reported an immunopharmacotherapeutic approach for the attenuation of AHL-dependent QS in the Gram-negative human pathogen *P. aeruginosa*. Monoclonal antibodies (mAbs) raised against the 3oxo-C12-HSL hapten demonstrated an affinity (K_d range between 150 nM and 5 mM) *in vitro* for 3oxo-C12-HSL, and may exhibited high specificity as these antibodies did not recognise any of the short-chain 3oxo-AHLs. These mAbs exerted a clear inhibitory effect on the production of phyocyanin by *P. aeruginosa*, a QS-controlled virulence factor. More recently, Park *et al.* (2007) have reported a similar immunotherapeutic approach for the attenuation of QS in the Gram-positive human pathogen *Staphylococcus aureus*. Remarkably, the antibody that was raised against the peptidic QS signal suppressed *S. aureus* pathogenicity in an abscess-formation mouse model *in vivo*, and provided complete protection against an otherwise lethal *S. aureus* challenge. These findings provide a strong foundation for further investigations of immunotherapy for the treatment of bacterial infections in which QS controls the expression of virulence factors.

4.9.2 QQ bacterial strains as biocontrol agents

When expressed in a heterologous system, such as *Burkholderia glumae*, *Pectobacterium carotovora*, *Pseudomonas aeruginosa* or *Agrobacterium tumefaciens*, some of the known AHL-degrading enzymes have been shown to limit or abolish the accumulation of AHL in the environment. As a consequence, this process also significantly reduces the expression of QS-regulated functions of the host bacterium (Uroz *et al.*, 2008). Therefore, in these systems, the expression of an AHL-degradation enzyme by an AHL-producing strain led to the same phenotype as a luxI null-mutation. However, this approach is barely exploitable in biological control experiments. A more suitable approach is based upon the selection of bacteria that are naturally able to degrade AHL or AHL analogues either as single isolates or as consortia. Co-

inoculation experiments involving the AHL-producing pathogen and the AHL-degrading quencher(s) revealed that this approach is often able to significantly reduce, and in some cases abolish, the expression of the QS-regulated function of the pathogens (Uroz *et al.*, 2003; Cirou *et al.*, 2007). AHL-degrading strains might therefore have great potential as biocontrol agents to protect plants from pathogens (Uroz *et al.*, 2009).

4.10 Comparison of the current methods for HSL and HS analysis

Compared to conventional analysis, the developed immunoassays are faster, more cost-effective, and easier to carry out. Another valuable advantage is the low sample volume requirement, which is lower than 1 mL. A comparison of different analytical methods for HSLs is presented in Table 17. It has to be pointed out though that a proper assessment of these different methods is not easy. Conventional methods on the one hand use, for example, a well-adapted sample pretreatment before the analytical procedure. On the other hand bioreceptor-based assays often use long incubation times, have an internal amplification system, and need specialised laboratories (genetically modified organisms) for their execution. Considering the sample pretreatment, the volume of sample needed, the analysis time and costs, and the ease of operation, immunoassays are certainly a truly competitive analytical method for HSLs.

Table 17 Comparison of analytical methods for HSL compounds

Analytical method	Description	Analyte	Samples extraction and pre-concentration	Real sample volume [mL]	Limit of detection [nM]	Working range [nM]	Reference
Immunoassay	mAb HSL1/2-2C10 / enzyme-tracer format	3-oxo-C10-HSL	no	0.5 ⁽¹⁾	31	31-3200	This study
	mAb HSL4-4C9 / coating antigen format	C8-HSL	no	0.5 ⁽¹⁾	476	476-12500	This study
	mAb RS2-1G9 / coating antigen format	3-oxo-C12-HSL	no	Not reported	15 ⁽²⁾	15-1500 ⁽²⁾	(Kaufmann <i>et al.</i> , 2006)
3-oxo-C6-HSL				>10000 ⁽²⁾	Not reported		
Conventional methods	GC-MS	3-oxo-C12-HSL	yes	2	67 ⁽³⁾	Not reported	(Charlton <i>et al.</i> , 2000)
		3-oxo-C10-HSL			74 ⁽³⁾	Not reported	
	GC/EI-MS	C10-HSL	yes	50	3600	Not reported	(Cataldi <i>et al.</i> , 2007)
		C6-HSL			5100	Not reported	
	SPE,UPLC, FT-ICR-MS	C10-HSL	yes	10-50	400	400-90000	(Li <i>et al.</i> , 2006)
		C8-HSL			400	400-90000	

	UPLC, FT-ICR-MS, SDME	L-C10-HSL	yes ⁽⁴⁾	2	391	Not reported	(Malik <i>et al.</i> , 2009)
		L-C8-HSL			439	Not reported	
Bioreporter assay	<i>Agrobacterium tumefaciens</i> A 136 (pMV26)(pCF218)	3-oxo-C10-HSL	yes	0.05-0.5	0.00002	Not reported	(Chambers <i>et al.</i> , 2005) ⁽⁵⁾
		C10-HSL			25	Not reported	
	<i>Escherichia coli</i> JM109 (pSB1075)	C12-HSL	no	0.3 ⁽⁶⁾	1	1-10000	(Kumari <i>et al.</i> , 2006)
		C4-HSL			100	100-100000	
	<i>Escherichia coli</i> ROlux2	3-oxo-C6-HSL	no	2	3	3-390	(Yan, <i>et al.</i> 2007)

⁽¹⁾ For quadruplicate determination

⁽²⁾ Not given, working range was calculated as a factor of 10 below and above the IC₅₀.

⁽³⁾ Not given, calculated from the lowest detected HSL (1 ng tube⁻¹), sample volume (50 µL tube⁻¹) and molecular weight of HSL compound.

⁽⁴⁾ Extraction and pre-concentration was included in the process of SDME.

⁽⁵⁾ Concentration measured is from the extracted and pre-concentrated sample.

⁽⁶⁾ For triplicate determination

Published results (Chen *et al.*, 2010 a)

4.11 Matrix effects

Initially, the assays were developed in a specific buffer system. Biological samples though have usually very different background substances, called matrix, which can contribute to changes in assay performance. The matrix of a sample can interfere with antibodies and enzymes (in the enzyme-tracer) and have an influence on the antibody-analyte binding. Thus, the matrix effects must be considered carefully for any biological samples determination in immunoassays. In extreme cases, the matrix effects could entirely inhibit the immunoassay (Krotzky & Zeeh, 1995).

Table 18 Matrix effects of different media

Assay	Buffer/medium	OD	IC ₅₀ of 3oxo-C10-HSL [$\mu\text{g L}^{-1}$]	Medium OD/PBS OD	Medium IC ₅₀ /PBS IC ₅₀
1	40 mM PBS	0.83	120	1.15	3.11
	ABC medium	0.96	373		
2	40 mM PBS	1.51	99	1.16	3.20
	Mineral medium +TCB	1.75	316		
3	40 mM PBS	1.09	143	1.32	2.79
	M9 medium	1.44	399		
4	40 mM PBS	1.18	103	0.14	-
	NB medium*	0.17	-		

Due to the standard deviation between the plates, the matrix effect was compared in one plate with PBS and the corresponding medium. * The test in NB medium obtained almost no binding signals, thus the IC₅₀ in NB was not given.

In Table 18, the matrix effects of 4 media were present compared to PBS buffer. Except NB medium, all these 3 media showed increased OD and reduced sensitivity (increased IC₅₀). But the changing factors are slightly different (listed in Table 18). Differently, NB medium showed much lower OD (0.17) compared to PBS (1.18) and it was not possible to obtain evaluable assay. This phenomenon might be due to the high interfering with the contents in NB medium (detailed composition of buffer/medium, see Attach. 2, page 143).

4.12 Possible problems and suggestions of immunoassays

There are a few key facts which should be pointed out while working with these immunoassays:

A) The matrix interference with assays of the biological samples should be tested and optimised before real sample determination. In some cases, sample preparation procedures like extraction might be required to reduce or avoid the matrix effect.

B) Broad recognition HSLs and HSs, but the affinities are very dependent on the individual antibodies and HSL molecular structures. A suitable combination of antibodies and analytes is essential for good assays.

C) The antibodies are unable to distinguish HSLs and HSs in a mixture, but it is possible to check the relative presence of HSLs through the hydrolysis treatment due to their dramatically higher sensitivity for HSs.

D) Identification of individual molecules is basically not possible with immunoassays and must be performed by using chemical analysis such as HPLC, MS, NMR and etc.

E) The antibodies recognition might be influenced by some unknown AHL-mimic substances, which cannot be absolutely excluded.

4.13 Difficulties and solutions of fluorescence based *in situ* experiments

The aim of the *in situ* tests was to visualise the localisation of HSL molecules on QS regulated biofilms. Different to planktonic cell culture, biofilms are understood as highly complex structures. Within them the accumulated HSLs can reach particularly high concentrations on some spots (Charlton *et al.*, 2000).

Initially, there were two strategies for *in situ* experiments. One was with HSL QS regulated biofilms on plastic flow chambers (ibidi slides), and the other was on living plant roots inoculated with HSL producing bacteria. Two types of fluorescence labels were used for these two experiments. The first type was fluorophore Oyster-645 which was labelled to anti-HSL mAbs and these directly labelled mAbs were used for most experiments. Later on, the Cy3-TSA system (Perkin Elmer, Boston, USA) was employed in order to get enhanced fluorescence signals. With this method, fluorescent signals could be catalysed and amplified by the HRP on secondary goat anti rat antibody (schema see Figure 21, page 73).

In both experimental setups, the occurrence of background signals was unfortunately the main problem of the tests. It is quite well known that fluorophores could react with environmental matrices and possibly cause unspecific signals. However, this interference can be inhibited by using appropriate quenching solutions. A lot of factors could influence the fluorescent performance, e.g. hydrophobicity, temperature, viscosity, salt content, pH value in the corresponding environment. It was reported that a conjugation of fluorescent dye to protein would change the fluorescent behaviour and would not be identical to free dye (Raem & Rauch, 2007). Additionally, the common existing auto-fluorescence in many biological samples could disturb the targeted fluorescent signals as well. In this study, strong auto-fluorescence was observed on barley root at different wavelengths under the laser scanning microscope (Figure 46, page 112 and Figure 47, page 113). AHL molecules are low molecular compounds, which lead to the consequence of being easily removed during washing steps. Even assuming that the HSL molecules are immobilised somewhere on biofilm or plant root structures, the fluorophore labelled antibodies might not be able to reach the targeted location due to their big molecular size. All these aspects must be taken into consideration for *in situ* HSL detection. The searching of other new suitable visualising signal systems may help to enable the *in situ* idea in the future.

5 Summary

Quorum Sensing (QS) is a process that enables bacteria to communicate via chemical signalling molecules, which are called autoinducers (AI). When a threshold concentration of QS molecules is reached, the bacteria start their QS regulated gene expression e.g. bioluminescence (*Vibrio fischeri*), virulence factor secretion (*Pseudomonas aeruginosa*), biofilm formation (*Burkholderia cepacia*), sporulation, and mating. It was found that many Gram-negative bacteria use acylated homoserine lactones (AHLs or HSLs) as autoinducers. Due to the broad biological functions of HSLs, the interest in detection and analysis of HSLs is increasing for medical, biotechnological and agricultural applications. In the past years, numerous analytical methods have been developed for HSLs. Conventional analysis, which usually combines chromatography, mass spectrometry (MS), and nuclear magnetic resonance (NMR) has been very successfully applied for identification and quantification of HSLs. But normally, conventional analysis requires many steps of sample preparation, e.g. extraction, pre-concentration and optimisation of conditions to separate individual HSL molecules. In addition, many sensitive bioreporter assays have been developed using different *LuxR* responsive promoters, which contain *LuxR* family functional proteins but lack the HSL synthase. A combination of different bioassays is strongly recommended, since no bioreporter is sensitive to all HSLs.

Alternatively, in this study, an anti-HSL antibody based immunochemical detection method has been successfully developed and established. HSL molecules consist of a homoserine lactone ring and an acyl side chain (4-18 carbon atoms), and they differ only from side chain length and substitution at C3 atom. Regarding the variation of the molecule structures, four HSL haptens, named HSL1, HSL2, HSL3 and HSL4, were designed for antibody and assay development. HSL1 and HSL3 have a long chain (C11-COOH), but HSL1 has an -oxo and HSL3 has an -OH functional group at the C3 position. In comparison, HSL2 (C5-COOH) and HSL4 (C9-COOH) have shorter side chains and no substitution on the C3 atom. The haptens were synthesised and were covalently coupled to the C-terminal COOH-group of the NH₂-residues (lysines) of the carrier proteins (BSA/OVA). Using these HSL hapten-conjugates, rat and mouse anti-HSL monoclonal antibodies (mAbs) were produced, screened and further characterised with enzyme-linked immunosorbent assays (ELISAs). Corresponding to hapten structures, the antibodies showed different selectivities to HSLs with different substitution on C3 position and chain length.

Eight mAbs (HSL1-1A5, HSL1-8E1, HSL1/2-2C10, HSL1/2-4H5, HSL4-4C9, HSL4-5H3, HSL4-5E12 and HSL4-6D3) were selected from about 200 mAbs and characterised in detail using coating antigen and enzyme tracer formats. It was demonstrated that the new assays have HSL detection ranges from nM to low μ M, which is sensitive enough for detection of HSLs in natural samples according to literature. Interestingly but not surprisingly, AHLs mAbs have at least 20 times higher sensitivity against hydrolysed HSLs (named HSs) than original HSLs, because the conjugation and immunisation conditions, e.g. pH and temperature, for mAb development resulted in HSL hydrolysis. This property of antibodies additionally offers a new sensitive method to detect quorum quenching (QQ) relevant homoserines (HSs), which are important degradation products of HSLs. Comparable results have been obtained by Biacore and Aqua-Optosensor biosensors for HS (L) characterisation. Based on these properties of the mAbs, a detection method of HSLs and HSs in biological samples has been developed and optimised. With the comparison of the real samples before and after hydrolysis treatment, the assays could simply present the relative HSL- and HS-contents in the samples. Similar to bio-reporters, the identification or quantitation of single HSL molecules is not possible only using immunoassay due to the broad recognition of HSLs and HSs. For this purpose, a combination with conventional chemical analysis is a must. However, as a novel sensitive HSL and HS detection method, the developed immunoassays have the advantages of being fast, cost effective and having low sample volume requirement.

Using the direct or indirect fluorescence signals of fluorophore labelled anti-HSL mAbs, the *in situ* experiments with modified *Burkholderia cepacia* biofilm on ibidi slide (plastic flow chamber from ibidi GmbH) and *Pseudomonas putida* inoculated barley root have been carried out. Unfortunately, the *in situ* tests were not successful, mainly due to remaining unspecific background signals. Nevertheless, a few steps, e.g. fluorophore labelling, biofilm formation, and surface blocking have been optimised. The door of HSL *in situ* tests with the antibodies is still open, if a suitable specific visualising detection method could be found in the future. Certainly, the antibodies can also be broadly applied for many other immunochemical techniques, such as immunosensors or immunoaffinity columns for characterisation or pre-screening of HSLs/HSs, as have been demonstrated successfully.

6 Zusammenfassung

Quorum Sensing (QS) ist ein Prozess, welcher es den Bakterien ermöglicht, miteinander durch Signalmoleküle zu kommunizieren. Die Signalmoleküle werden auch als Autoinducer (AI) bezeichnet. Wenn eine bestimmte Konzentration der QS-Moleküle erreicht ist, starten die QS-Bakterien die Regulation mit einer Genexpression, was z.B. zur Biolumineszenz (*Vibrio fischeri*), zur Virulenzfaktorensekretion (*Pseudomonas aeruginosa*) oder zur Ausbildung von Biofilmen (*Burkholderia cepacia*) führt. Es wurde für einen Großteil der Gram-negativen Bakterien nachgewiesen, dass *N*-acylierte Homoserinlaktone (abgekürzt als AHL oder HSL) als Autoinducer verwendet werden. Aufgrund der vielfältigen biologischen Funktion der HSL-Moleküle ist das Interesse an der Detektion und der Analyse von HSL für medizinische, biotechnologische und agrarwissenschaftliche Anwendungen deutlich angestiegen. Während der letzten Jahre sind viele unterschiedliche Methoden zur HSL-Analyse entwickelt worden. Konventionelle analytische Methoden kombinieren häufig die Chromatographie mit der Massenspektroskopie (MS) und der kernmagnetischen Resonanzspektroskopie (NMR) und werden sehr erfolgreich für die Identifizierung und Quantifizierung der HSL angewandt. Hierbei sind jedoch viele Probenvorbereitungsschritte, wie z.B. die Probenextraktion, die Vorkonzentrierung und die Optimierung der individuellen HSL-Trennung, notwendig. Weiterhin wurden viele sensitive Bioreporter-Assays entwickelt, welche mit dem Einsatz der unterschiedlichen *LuxR*-ansprechbaren Promoter arbeiten. Diese funktionellen Proteine der *LuxR*-Familie besitzen aber keine HSL-Produzenten. Eine Kombination von mehreren Bioassays ist empfehlenswert, weil kein einziger Bioreporter für alle HSL ausreichend sensitiv und selektiv ist.

Als eine Alternative zu den genannten Methoden werden in dieser Arbeit auf anti-HSL monoklonalen Antikörpern (mAk) basierende immunochemische Detektionsmethoden erfolgreich eingeführt. Es wurde berücksichtigt, dass HSL-Moleküle aus einem Homoserinlacton-Ring bestehen und eine Seitenkette (mit 4 bis 18 Kohlenstoffatomen) besitzen, welche sich nur durch die Kettenlänge und die Substitution am C3-Atom unterscheiden. Auf dieser Grundlage wurden vier HSL-Derivate, die als HSL1, HSL2, HSL3 und HSL4 bezeichnet wurden, synthetisiert und für die Antikörper- und die Assay-Entwicklungen eingesetzt. HSL1 und HSL3 besitzen dieselbe Kettenlänge (C11-COOH); HSL1 zeichnet sich jedoch durch eine oxo- und HSL3 durch eine OH-Gruppe an der C3-Position aus. Im Vergleich dazu haben HSL2 (C5-COOH) und HSL4 (C9-COOH) eine

kürzere Kettenlänge und besitzen keine Substitution am C3-Atom. Diese Haptene (HSL Derivate) wurden synthetisiert und über ihre C-terminale COOH-Gruppe mit der NH₂-(Lysin) Gruppe der Trägerproteine (BSA/OVA) kovalent gekoppelt. Mit den HSL-Hapten-Protein-Konjugaten wurden Ratten und Mäuse immunisiert. Dadurch wurden die anti-HSL mAk produziert, welche weiter mit Hilfe von Enzyme-linked Immunosorbent Assays (ELISAs) ‚gescreent‘ und charakterisiert wurden. Im Zusammenhang mit den Hapten-Strukturen können die entsprechenden Antikörper die unterschiedlichen Substitutionen an der C3-Position und die Kettenlänge erkennen.

Von ca. 200 monoklonalen Antikörpern wurden acht ausgewählt (mAk HSL1-1A5, HSL1-8E1, HSL1/2-2C10, HSL1/2-4H5, HSL4-4C9, HSL4-5H3, HSL4-5E12 und HSL4-6D3) und detailliert mittels ELISA im Coating Antigen und Enzym Tracer Format charakterisiert. Der Detektionsbereich der neuen Assays befindet sich im nM bis unterem µM Bereich; dieser ist sensitiv genug für den Nachweis der HSL-Moleküle in Realproben. Interessanterweise weisen die HSL mAk eine mindestens 20-mal höhere Sensitivität gegenüber hydrolysierten HSL (Homoserine genannt) als den originalen HSL auf. Die Bedingungen während der Konjugation und der Immunisierung, z.B. die Temperatur und der pH Wert, könnte die Hydrolyse der HSL-Moleküle verursacht haben. Diese Eigenschaft der Antikörper bietet eine neue sensitive Methode für Quorum Quenching (QQ) der relevanten Homoserine (HS), welche eine der wichtigsten Abbauprodukte der HSL sind. Außer mit ELISA wurden vergleichbare Ergebnisse für die HSL-Charakterisierung mit Hilfe der Biosensoren Biacore und Aqua-Optosensor erzielt.

Aufgrund der gefundenen Eigenschaften der Antikörper wurde eine Nachweismethode der HSL- und HS- Moleküle in biologischen Proben entwickelt und optimiert. Mit dem Vergleich der Realproben vor und nach der Hydrolysebehandlung konnten die Assays den relativen HSL- und HS- Inhalt aufzeigen. Ähnlich wie bei den Bioreporter Assays ist es nicht möglich die Identifizierung und Quantifizierung für einzelne Moleküle allein mit dem ELISA durchzuführen. Die immunochemische Analyse muss mit konventionellen chemischen Analysen kombiniert werden, weil die Assays breitere Erkennungen von HSL und HS besitzen. Die neu entwickelten Assays stellen aber eine sensitive Detektionsmethode für HSL/HS dar, welche schnell und kostengünstig mit einer geringen Probenmenge durchgeführt werden kann.

Mithilfe der direkten oder indirekten Fluoreszenzsignale der an anti-HSL mAk konjugierten Fluorophore wurden *in situ* Tests entweder mit einem modifizierten *Burkholderia cepacia*-Biofilm an Ibidi Slides oder an einer mit *Pseudomonas putida* inokulierten Weizenwurzel durchgeführt. Leider waren die *in situ* Experimente nicht erfolgreich, hauptsächlich aufgrund der noch verbliebenen unspezifischen Hintergrundsignale. Trotzdem konnten einige Schritte wie die Fluorophor-Koppelungsrate an mAk, die Biofilmbildung und die Absättigung der Oberfläche optimiert werden. Die Möglichkeit der HSL *in situ* Detektion ist immer noch gegeben, wenn ein passender Signalstoff gefunden wird. Die Antikörper können für viele weitere immunochemische Techniken verwendet werden, wie z.B. für Immunosensoren und Immunoaffinität für die Charakterisierung und das , Screening' der HSL/HS.

7 References

- [1] Adamczyk M, Buko A, Chen YY, Fishpaugh JR, Gebler JC, Johnson DD. (1994) Characterization of protein-hapten conjugates. 1. Matrix-assisted laser desorption ionization mass spectrometry of immuno BSA-hapten conjugates and comparison with other characterization methods. *Bioconjugate Chemistry* **5**: 631-635.
- [2] Andersen JB, Heydorn A, Hentzer M, Eberl L, Geisenberger O, Christensen BB, Molin S, Givskov M. (2001) gfp-based N-acyl homoserine-lactone sensor systems for detection of bacterial communication. *Applied and Environmental Microbiology* **67**: 575-585.
- [3] Arevalo-Ferro C, Reil G, Görg A, Eberl L, Riedel K. (2005) Biofilm formation of *Pseudomonas putida* IsoF: the role of quorum sensing as assessed by proteomics. *Systematic and Applied Microbiology* **28**: 87-114.
- [4] Bassler BL & Losick R (2006) Bacterially Speaking. *Cell* **125**: 237-246.
- [5] Bevivino A, Dalmastrì C, Tabacchioni S & Chiarini L (2000) Efficacy of *Burkholderia cepacia* MCI7 in disease suppression and growth promotion of maize. *Biology and Fertility of Soils* **31**: 225-231.
- [6] Bevivino A, Sarrocco S, Dalmastrì C, Tabacchioni S, Cantale C & Chiarini L (1998) Characterization of a free-living maize-rhizosphere population of *Burkholderia cepacia*: effect of seed treatment on disease suppression and growth promotion of maize. *FEMS Microbiology Ecology* **27**: 225-237.
- [7] www.biolabels.com/Oyster645-spectra.htm.
- [8] www.biolabels.com
- [9] Bobrow MN, Shaughnessy KJ, Litt GJ (1991) Catalyzed reporter deposition, a novel method of signal amplification. II. Application to membrane immunoassays. *Journal of Immunological Methods*. **137**: 103-112.
- [10] Bobrow MN, Harris TD, Shaughnessy KJ & Litt GJ (1989) Catalyzed reporter deposition, a novel method of signal amplification application to immunoassays. *Journal of Immunological Methods* **125**: 279-285.
- [11] Bobrow MN, Litt GJ, Shaughnessy KJ, Mayer PC & Conlon J (1992) The use of catalyzed reporter deposition as a means of signal amplification in a variety of formats. *Journal of Immunological Methods* **150**: 145-149.
- [12] Boyen F, Eeckhaut V, Van Immerseel F, Pasmans F, Ducatelle R & Haesebrouck F (2009) Quorum sensing in veterinary pathogens: Mechanisms, clinical importance and future perspectives. *Veterinary Microbiology* **135**: 187-195.
- [13] Brady JF. (1995) Interpretation of Immunoassay Data. *Immunoanalysis of agrochemicals* P: 266-287, American Chemical Society, Washington, DC.
- [14] Brelles-Mariño G, Bedmar EJ (2001) Detection, purification and characterisation of quorum-sensing signal molecules in plant-associated bacteria. *Journal of Biotechnology* **91**: 197-209.
- [15] Byers JT, Lucas C, Salmond GPC, Welch M (2002) Nonenzymatic turnover of an *Erwinia carotovora* quorum-sensing signaling molecule. *Journal of Bacteriology*. **184**: 1163-1171.

- [16] Cataldi TRI, Bianco G, Frommberger M, Ph S-K (2004) Direct analysis of selected N-acyl-L-homoserine lactones by gas chromatography/mass spectrometry. *Rapid Communications in Mass Spectrometry* **18**: 1341-1344.
- [17] Cataldi TRI, Bianco G, Palazzo L, Quaranta V (2007) Occurrence of N-acyl-l-homoserine lactones in extracts of some Gram-negative bacteria evaluated by gas chromatography-mass spectrometry. *Analytical Biochemistry* **361**: 226-235.
- [18] Chambers CE, Visser MB, Schwab U, Sokol PA (2005) Identification of N-acylhomoserine lactones in mucopurulent respiratory secretions from cystic fibrosis patients. *FEMS Microbiology Letters* **244**: 297-304.
- [19] Charlton ST, Nys R, Netting A, Kumar N, Hentzer M, Givskov M, Kjelleberg S (2000) A novel and sensitive method for the quantification of N-3-oxoacyl homoserine lactones using gas chromatography-mass spectrometry: application to a model bacterial biofilm. *Environmental Microbiology* **2**: 530-541.
- [20] Chen X, Kremmer E, Gouzy MF, Clausen E, Starke M, Wöllner K, Pfister G, Hartmann A, Krämer MP. (2010) Development and characterisation of rat monoclonal antibodies for N-acylated homoserine lactones. *Analytical and Bioanalytical Chemistry* **398**: 2655-2667
- [21] Chen X, Buddrus-Schiemann K, Rothballer M, Krämer PM, Hartmann A (2010). Detection of AHL quorum sensing molecules in *Burkholderia cepacia* culture supernatants with enzyme-linked immunosorbent assays, *Analytical Bioanalytical Chemistry*, vol. 398, 2669-2676
- [22] Chevrot R, Rosen R, Haudecoeur E, Cirou A, Shelp BJ, Ron E, Faure D (2006) GABA controls the level of quorum-sensing signal in *Agrobacterium tumefaciens*. *Proceedings of the National Academy of Sciences of the United States of America* **103**: 7460-7464.
- [23] Chiarini L, Bevivino A, Dalmastrì C, Tabacchioni S, Visca P (2006) *Burkholderia cepacia* complex species: health hazards and biotechnological potential. *Trends in Microbiology* **14**: 277-286.
- [24] Cirou A, Diallo S, Kurt C, Latour X, Faure D (2007) Growth promotion of quorum-quenching bacteria in the rhizosphere of *Solanum tuberosum*. *Environmental Microbiology* **9**: 1511-1522.
- [25] Clark DJ, Maaloe O (1967) DNA replication and the division cycle in *Escherichia coli*. *Journal of Molecular Biology* **23**: 99-112.
- [26] Coenye T, Vandamme P (2003) Diversity and significance of *Burkholderia* species occupying diverse ecological niches. *Environmental Microbiology* **5**: 719-729.
- [27] Dance ABD (2002) Melioidosis. *Current Opinion in Infectious Diseases* **15**: 127-132.
- [28] Delalande L, Faure D, Raffoux A, Uroz S, D'Angelo-Picard C, Elasri M, Carlier A, Berruyer R, Petit A, Williams P, Dessaux Y. (2005) N-hexanoyl-l-homoserine lactone, a mediator of bacterial quorum-sensing regulation, exhibits plant-dependent stability and may be inactivated by germinating *Lotus corniculatus* seedlings. *FEMS Microbiology Ecology* **52**: 13-20.
- [29] Diggle SP, Crusz SA, Cámara M (2007) Quorum sensing. *Current Biology* **17**: R907-R910.
- [30] Diggle SP, Cornelis P, Williams P, Cámara M (2006) 4-Quinolone signalling in *Pseudomonas aeruginosa*: Old molecules, new perspectives. *International Journal of Medical Microbiology* **296**: 83-91.

- [31] Diggle SP, Winzer K, Chhabra SR, Worrall EK, Cámara M, Williams P (2003) The *Pseudomonas aeruginosa* quinolone signal molecule overcomes the cell density-dependency of the quorum sensing hierarchy, regulates rhl dependent genes at the onset of stationary phase and can be produced in the absence of LasR. *Molecular Microbiology* **50**: 29-43.
- [32] Dong Y-H, Xu J-L, Li X-Z, Zhang L-H (2000) AiiA, an enzyme that inactivates the acylhomoserine lactone quorum-sensing signal and attenuates the virulence of *Erwinia carotovora*. *Proceedings of the National Academy of Sciences of the United States of America* **97**: 3526-3531.
- [33] Dong Y-H, Wang L-H, Xu J-L, Zhang H-B, Zhang X-F, Zhang L-H (2001) Quenching quorum-sensing-dependent bacterial infection by an N-acyl homoserine lactonase. *Nature* **411**: 813-817.
- [34] Eberhard A, Burlingame AL, Eberhard C, Kenyon GL, Nealson KH, Oppenheimer NJ (1981) Structural identification of autoinducer of *Photobacterium fischeri* luciferase. *Biochemistry* **20**: 2444-2449.
- [35] Eberl L (2006) Quorum sensing in the genus *Burkholderia*. *International Journal of Medical Microbiology* **296**: 103-110.
- [36] Englmann M, Fekete A, Kuttler C, Frommberger M, Li X, Gebefügi I, Fekete J, Schmitt-Kopplin P. (2007) The hydrolysis of unsubstituted N-acylhomoserine lactones to their homoserine metabolites: Analytical approaches using ultra performance liquid chromatography. *Journal of Chromatography A* **1160**: 184-193.
- [37] Fekete A, Rothballer M, Hartmann A, Schmitt-Kopplin P (2010) Identification of bacterial autoinducers. In: *Bacterial Signaling*, Wiley Publisher, Weinheim, Germany 95-111.
- [38] Fekete A, Kuttler C, Rothballer M, Hense BA, Fischer D, Buddrus-Schiemann K, Lucio M, Müller J, Schmitt-Kopplin P, Hartmann T (2010) Dynamic regulation of N-acyl-homoserine lactone production and degradation in *Pseudomonas putida* IsoF. *FEMS Microbiology Ecology* **72**: 22-34.
- [39] Fiore A, Laevens S, Bevivino A, Dalmastrì C, Tabacchioni S, Vandamme P, Chiarini L (2001) *Burkholderia cepacia* complex: distribution of genomovars among isolates from the maize rhizosphere in Italy. *Environmental Microbiology* **3**: 137-143.
- [40] Fries MR, Forney LJ, Tiedje JM (1997) Phenol- and Toluene-Degrading Microbial Populations from an Aquifer in Which Successful Trichloroethene Cometabolism Occurred. *Applied and Environmental Microbiology* **63**: 1523-1530.
- [41] Frommberger M, Hertkorn N, Engelmann M, Jakoby S, Hartmann A, Kettrup A, Schmitt-Kopplin P (2005) Analysis of N-acylhomoserine lactones after alkaline hydrolysis and anion-exchange solid-phase extraction by capillary zone electrophoresis-mass spectrometry. *Electrophoresis* **26**: 1523-1532.
- [42] Frommberger M, Schmitt-Kopplin P, Menzinger F, Albrecht V, Schmid M, Eber L, Hartmann A, Kettrup A. (2003) Analysis of N-homoserine lactones produced by *Burkholderia cepacia* with partial filling micellar electrokinetic chromatography - electrospray ionization-trap mass spectrometry. *Electrophoresis* **24**: 3067-3074.
- [43] Geisenberger O, Givskov M, Riedel K, Høiby N, Tümmler B, Eberl L (2000) Production of N-acyl-homoserine lactones by *P. aeruginosa* isolates from chronic lung infections associated with cystic fibrosis. *FEMS Microbiology Letters* **184**: 273-278.

- [44] Gotschlich A, Huber B, Geisenberger O, Tögl A, Steidle A, Riedel K, Hill P, Tümmler B, Vandamme P, Middleton B, Camara M, Williams P, Hardman A, Eberl L. (2001) Synthesis of Multiple N-Acylhomoserine Lactones is Wide-spread Among the Members of the *Burkholderia cepacia* Complex. *Systematic and Applied Microbiology* **24**: 1-14.
- [45] Götz C, Fekete A, Gebefügi I, Sándor T, Fuksová K, Li X, Englmann M, Gryndler M, Hartmann A, Matucha M, Schmitt-Kopplin P, Schröder P (2007) Uptake, degradation and chiral discrimination of N-acyl-D/L-homoserine lactones by barley (*hordeum vulgare*) and yam bean (*Pachyrhizus erosus*) plants. *Analytical and Bioanalytical Chemistry* **389**: 1447-1457.
- [46] Harrison RO, Braun AL, Gee SJ, O'brien DJ, Hammock B (1989) Evaluation of an enzyme-linked immunosorbent assay (ELISA) for the direct analysis of Molinate (Ordram) in rice field water. *Food & Agricultural Immunology* **1**: 37-51.
- [47] Hense BA, Kuttler C, Müller J, Rothballer M, Hartmann A, Kreft JU (2007) Does efficiency sensing unify diffusion and quorum sensing? *Nature* **5**: 230-239.
- [48] Heungens K, Parke JL (2000) Zoospore Homing and Infection Events: Effects of the Biocontrol Bacterium *Burkholderia cepacia* AMMDR1 on Two Oomycete Pathogens of Pea (*Pisum sativum* L.). *Applied Environmental Microbiology* **66**: 5192-5200.
- [49] <http://www.dyespigments.com/fluorescent-dyes.html>
- [50] Huber B, Riedel K, Hentzer M, Heydorn A, Gotschlich A, Givskov M, Molin S, Eberl L (2001) The *cep* quorum-sensing system of *Burkholderia cepacia* H111 controls biofilm formation and swarming motility. *Microbiology* **147**: 2517-2528.
- [51] Hughes DT, Sprendio V (2008) Inter-kingdom signalling: communication between bacteria and their hosts. *Nature reviews* **6**: 111-120.
- [52] Jha B, Thakur MC, Gontia I, Albrecht V, Stoffels M, Schmid M, Hartmann A (2009) Isolation, partial identification and application of diazotrophic rhizobacteria from traditional Indian rice cultivars. *European Journal of Soil Biology* **45**: 62-72.
- [53] Jiang CY, Sheng XF, Qian M, Wang QY (2008) Isolation and characterization of a heavy metal-resistant *Burkholderia* sp. from heavy metal-contaminated paddy field soil and its potential in promoting plant growth and heavy metal accumulation in metal-polluted soil. *Chemosphere* **72**: 157-164.
- [54] Kaufmann GF, Park J, Mee JM, Ulevitch RJ, Janda KD (2008) The quorum quenching antibody RS2-1G9 protects macrophages from the cytotoxic effects of the *Pseudomonas aeruginosa* quorum sensing signalling molecule N-3-oxo-dodecanoyl-homoserine lactone. *Molecular Immunology* **45**: 2710-2714.
- [55] Kaufmann GF, Sartorio R, Lee SH, Roger CJ, Meijler MM, Moss JA, Clapham B, Brogan AP, Dickerson TJ, Janda KD (2005) Revisiting quorum sensing: Discovery of additional chemical and biological functions for 3-oxo-N-acylhomoserine lactones. *Proceedings of the National Academy of Sciences of the United States of America* **102**: 309-314.
- [56] Kaufmann GF, Sartorio R, Lee SH, Mee JM, Altobelli LJ, III, Kujawa DP, Jeffries E, Clapham B, Meijler MM, Janda KD (2006) Antibody interference with N-Acyl homoserine lactone-mediated bacterial quorum sensing. *Journal of the American Chemical Society* **128**: 2802-2803.
- [57] Köhler G, Milstein C (1975) Continuous cultures of fused cells secreting antibody of predefined specificity. *Nature* **256**: 495-497.

- [58] Krämer PM, Goodrow MH & Kremmer E (2004) Enzyme-linked immunosorbent assays based on rabbit polyclonal and rat monoclonal antibodies against isoproturon. *Journal of Agricultural and Food Chemistry* **52**: 2462-2471.
- [59] Krämer PM, Weber CM, Forster S, Rauch P, Kremmer E (2010) Analysis of DDT isomers with enzyme-linked immunosorbent assay and optical immunosensor based on rat monoclonal antibodies as biological recognition elements. *Journal of AOAC International* **93**: 44-58.
- [60] Krämer PM, Kremmer E, Weber CM, Ciumasu IM, Forster S, Kettrup AA (2005) Development of new rat monoclonal antibodies with different selectivities and sensitivities for 2,4,6-trinitrotoluene (TNT) and other nitroaromatic compounds. *Analytical Bioanalytical Chemistry* **382**: 1919-1933.
- [61] Kremmer E, Kranz BR, Hille A, Klein K, Eulitz M, Hoffmann-Fezer G, Feiden W, Herrmann K, Delecluse HJ, Delsol G, Bornkamm GW, Mueller-Lantzsch N, Grässert FA (1995) Rat monoclonal antibodies differentiating between the epstein-barr virus nuclear antigens 2A (EBNA2A) and 2B (EBNA2B). *Virology* **208**: 336-342.
- [62] Krotzky AJ, Zeeh B (1995) Immunoassays for residue analysis of agrochemicals: proposed guidelines for precision, standardization and quality control. *Pure and Applied Chemistry* **67**: 2065-2088.
- [63] Kumari A, Pasini P, Deo SK, Flomenhoft D, Shashidhar H, Daunert S (2006) Biosensing systems for the detection of bacteria quorum signaling molecules. *Analytical Chem.* **78**: 7306-7609.
- [64] Lakowicz RJ (2006) *Principles of fluorescence spectroscopy* Springer, New York, USA Third Edition.
- [65] Lee EY (2003) Continuous treatment of gas-phase trichloroethylene by *Burkholderia cepacia* G4 in a two-stage continuous stirred tank reactor/trickling biofilter system. *Journal of Bioscience and Bioengineering* **96**: 572-574.
- [66] Lewenza S, Sokol PA (2001) Regulation of Ornibactin Biosynthesis and N-Acyl-L-Homoserine Lactone Production by CepR in *Burkholderia cepacia*. *Journal of Bacteriology* **183**: 2212-2218.
- [67] Lewenza S, Conway B, Greenberg EP, Sokol PA (1999) Quorum Sensing in *Burkholderia cepacia*: Identification of the LuxRI Homologs CepRI. *Journal of Bacteriology* **181**: 748-756.
- [68] Li X, Fekete A, Englmann M, Götz C, Rothballer M, Frommberger M, Buddrus K, Fekete J, Cai CP, Schröder P, Hartmann A, Chen GN, Schmitt-Kopplin P (2006) Development and application of a method for the analysis of N-acylhomoserine lactones by solid-phase extraction and ultra high pressure liquid chromatography. *Journal of Chromatography A* **1134**: 186-193.
- [69] Malik AK, Fekete A, Gebefügi I, Rothballer M, Schmitt-Kopplin P (2009) Single drop microextraction of homoserine lactones based quorum sensing signal molecules, and the separation of their enantiomers using gas chromatography mass spectrometry in the presence of biological matrices. *Microchimica Acta* **166**: 101-107.
- [70] Marco MP, Gee S & Hammock BD (1995) Immunochemical techniques for environmental analysis II. Antibody production and immunoassay development. *Trends in Analytical Chemistry* **14**: 415-425.

- [71] Marco MP, Gee S, Hammock BD (1995) Immunochemical techniques for environmental analysis I. Immunosensors. *Trends in Analytical Chemistry* **14**: 341-350.
- [72] Master ER, Lai VWM, Kuipers B, Cullen WR, Mohn WW (2002) Sequential anaerobic-aerobic treatment of soil contaminated with weathered aroclor 1260. *Environmental Science and Technology* **36**: 100-103.
- [73] McClean KH, Winson MK, Fish L, Taylor A, Chhabra SR, Camara M, Daykin M, Lamb JH, Swift S, Bycroft BW, Stewart GS, Williams P (1997) Quorum sensing and *Chromobacterium violaceum*: exploitation of violacein production and inhibition for the detection of N-acylhomoserine lactones. *Microbiology* **143**: 3703-3711.
- [74] McKenney D, Brown KE, Allison DG (1995) Influence of *Pseudomonas aeruginosa* exoproducts on virulence factor production in *Burkholderia cepacia*: evidence of interspecies communication. *Journal of Bacteriology* **177**: 6989-6992.
- [75] Miller SCM, LiPuma JJ, Parke JL (2002) Culture-based and non-growth-dependent detection of the *Burkholderia cepacia* complex in soil environments. *Applied and Environmental Microbiology* **68**: 3750-3758.
- [76] Mosby (2009) *Mosby's Medical Dictionary*, 8th Edition. Elsevier.
- [77] Nealson KH, Platt T, Hastings JW (1970) Cellular Control of the Synthesis and Activity of the Bacterial Luminescent System. *Journal of Bacteriology* **104**: 313-322.
- [78] O'Connell MA, Belanger BA, Haaland PD (1993) Calibration and assay development using the four-parameter logistic model. *Chemometrics and Intelligent Laboratory Systems* **20**: 97-114.
- [79] Park J, Jagasia R, Kaufmann GF, Mathison JC, Ruiz DI, Moss JA, Meijler MM, Ulevitch RJ, Janda KD (2007) Infection control by antibody disruption of bacterial quorum sensing signaling. *Chemistry & Biology* **14**: 1119-1127.
- [80] Peix A, Mateos PF, Rodriguez-Barrueco C, Martinez-Molina E, Velazquez E (2001) Growth promotion of common bean (*Phaseolus vulgaris* L.) by a strain of *Burkholderia cepacia* under growth chamber conditions. *Soil Biology and Biochemistry* **33**: 1927-1935.
- [81] Pesci EC, Milbank JB, Pearson JP, Mcknight S, Kende AS, Greenberg EP, Iglewski BH (1999) Quinolone signaling in the cell-to-cell communication system of *Pseudomonas aeruginosa* *Biochemistry* **96**: 11229-11234.
- [82] Qazi SNA, Counil E, Morrissey J, Rees CED, Cockayne A, Winzer K, Chan WC, Williams P, Hill PJ (2001) *agr* Expression precedes escape of internalized *Staphylococcus aureus* from the host endosome. *Infection and Immunity* **69**: 7074-7082.
- [83] Quinn CP, Senenova VA, Elie CM, Romero-Steiner S, Greene C, Li H, Stamey K, Steward-Clark E, Schmidt DS, Mothershed E, Pruckler J, Schwartz S, Benson RF, Helsel LO, Holder PF, Johnson SE, Kellum M, Messmer T, Thacker WL, Besser L, Plikaytis BD, Taylor TH, Jr, Freeman AE, Wallace KJ, Dull P, Sejvar J, Bruce E, Moreno R, Schuchat A, Lingappa JR, Marano N, Martin SK, Walls J, Bronsdon M, Carlone GM, Bajani-Ari M, Ashford DA, Stephens DS, Perkins BA (2002) Specific, sensitive, and quantitative enzyme-linked immunosorbent assay for human immunoglobulin G antibodies to anthrax toxin protective antigen. *Emerging Infectious Diseases* **8**: 1103-1110.
- [84] Raem AM, Rauch P (2007) *Immunoassays*. Elsevier, Munich, Germany.
- [85] Redfield RJ (2002) Is quorum sensing a side effect of diffusion sensing? *Trends in Microbiology* **10**: 365-370.

- [86] Riedel K, Hentzer M, Geisenberger O, Steidle A, Wu H, Høiby N, Givskov M, Molin S, Eberl L (2001) N-Acylhomoserine-lactone-mediated communication between *Pseudomonas aeruginosa* and *Burkholderia cepacia* in mixed biofilms. *Microbiology* **147**: 3249-3262.
- [87] Schaefer AL, Hanzelka BL, Parsek MR, Greenberg EP (2000) Detection, purification, and structural elucidation of the acylhomoserine lactone inducer of *Vibrio fischeri* luminescence and other related molecules. *Methods in enzymology* **305**: 288-301.
- [88] Schaefer AL, Val DL, Hanzelka BL, Cronan JE, Greenberg EP (1996) Generation of cell-to-cell signals in quorum sensing: acyl homoserine lactone synthase activity of a purified *Vibrio fischeri* LuxI protein. *Proceedings of the National Academy of Sciences of the United States of America* **93**: 9505-9509.
- [89] Schneider P, Hammock BD (1992) Influence of the ELISA format and the hapten-enzyme conjugate on the sensitivity of an immunoassay for S-triazine herbicides using monoclonal antibodies. *Journal of Agricultural and Food Chemistry* **40**: 525-530.
- [90] Schroll R, Brahushi F, Dörfler U, Kühn S, Fekete J, Munch JC (2004) Biomineralisation of 1,2,4-trichlorobenzene in soils by an adapted microbial population. *Environmental Pollution* **127**: 395-401.
- [91] Schult K, Katerkamp A, Trau D, Grawe F, Cammann K, Meusel M (1999) Disposable Optical Sensor Chip for Medical Diagnostics: New Ways in Bioanalysis. *Analytical Chemistry* **71**: 5430-5435.
- [92] Shaw PD, Ping G, Daly SL, Cha C, Cronan JE, Jr, Rinehart KL, Farrand SK (1997) Detecting and characterizing N-acyl-homoserine lactone signal molecules by thin-layer chromatography. *Proceedings of National Academy of Sciences of the United States of America* **94**: 6036-6041.
- [93] Singh KV, Kaur J, Varshney GC, Raje M, Suri C (2004) Synthesis and characterization of hapten-protein conjugates for antibody production against small molecules. *Bioconjugate Chemistry* **15**: 168-173.
- [94] Sokol PA, Malott RJ, Riedel K, Eberl L (2007) Communication systems in the genus *Burkholderia*: global regulators and targets for novel antipathogenic drugs. *Future Microbiology* **2**: 555-563.
- [95] Speel EJM, Hopman AHN, Komminoth P (1999) Amplification Methods to Increase the Sensitivity of In Situ Hybridization: Play CARD(S). *Journal of Histochemistry and Cytochemistry* **47**: 281-288.
- [96] Starke M (2009) Immunochemische Untersuchungen zu HSL-Molekülen. Master thesis, unpublished.
- [97] Steidle A, Allesen-Holm M, Riedel K, Givskov M, Molin S, Eberl L (2002) Identification and characterization of an N-acylhomoserine lactone-dependent quorum sensing system in *Pseudomonas putida* strain IsoF. *Applied and Environmental Microbiology* **68**: 6371-6382.
- [98] Steidle A, Sigl K, Schuegger R, Ihring A, Schmid M, Gantner S, Stoffels M, Riedel K, Givskov M, Hartmann A, Langebartels C, Eberl L (2001) Visualization of N-Acylhomoserine Lactone-Mediated Cell-Cell Communication between Bacteria Colonizing the Tomato Rhizosphere. *Applied and Environmental Microbiology* **67**: 5761-5770.
- [99] Swift S, Winson MK, Chan PF, Bainton NJ, Birdsall M, Reeves J, Rees CED, Chhabra SR, Hill PJ, Throup JP, Bycroft BW, Salmond GPC, Williams P, Stewart GSAB. (1993) A

novel strategy for the isolation of luxI homologues: evidence for the widespread distribution of a LuxR:LuxI superfamily in enteric bacteria. *Molecular Microbiology* **10**: 511-520.

[100] Tomasz A (1965) Control of the competent state in *Pneumococcus* by a hormone-like cell product: an example for a new type of regulatory mechanism in bacteria. *Nature* **208**: 155-159.

[101] Uroz S, Dessaux Y, Oger P (2009) Quorum sensing and quorum quenching: the Yin and Yang of bacterial communication. *ChemBioChem* **10**: 205-216.

[102] Uroz S, Oger PM, Chapelle E, Adeline MT, Faure D, Dessaux Y (2008) A *Rhodococcus* qsdA-encoded enzyme defines a novel class of large-spectrum quorum-quenching lactonases. *Applied and Environmental Microbiology* **74**: 1357-1366.

[103] Uroz S, D'Angelo-Picard C, Carlier A, Elasri M, Sicot C, Petit A, Oger P, Faure D, Dessaux Y (2003) Novel bacteria degrading N-acylhomoserine lactones and their use as quenchers of quorum-sensing-regulated functions of plant-pathogenic bacteria. *Microbiology* **149**: 1981-1989.

[104] Vanderlaan M, Watkins BE, Stanker L (1988) ES&T Critical Review: Environmental monitoring by immunoassay. *Environmental Science and Technology* **22**: 247-254.

[105] Vanlaere E, Baldwin A, Gevers D, Henry D, De Brandt E, LiPumma JJ, Mahenthiralingam E, Speert DP, Dowson C, Vandamme P (2009) Taxon K, a complex within the *Burkholderia cepacia* complex, comprises at least two novel species, *Burkholderia contaminans* sp. nov. and *Burkholderia lata* sp. nov. *International Journal of Systematic and Evolutionary Microbiology* **59**: 102-111.

[106] Vermis K, Brachkova M, Vandamme P, Nelis H (2003) Isolation of *Burkholderia cepacia* Complex Genomovars from Waters. *Systematic and Applied Microbiology* **26**: 595-600.

[107] Wang F, Grundmann S, Schmid M, Dörfler U, Roherer S, Munch JC, Hartmann A, Jiang X, Schroll R (2007) Isolation and characterization of 1,2,4-trichlorobenzene mineralizing *Bordetella* sp. and its bioremediation potential in soil. *Chemosphere* **67**: 896-902.

[108] Whitaker JR, Granum PE (1980) An absolute method for protein determination based on difference in absorbance at 235 and 280 nm. *Analytical Biochemistry* **109**: 156-159.

[109] Williams P, Winzer K, Chan WC, Cárama M (2007) Look who's talking: communication and quorum sensing in the bacterial world. *Philosophical transactions of the royal society B* **362**: 1119-1134.

[110] Winson MK, Swift S, Fish L, Throup JP, Jørgensen F, Chhabra SR; Bycroft BW, Williams P, Stewart GS (1998) Construction and analysis of luxCDABE-based plasmid sensors for investigating N-acyl homoserine lactone-mediated quorum sensing. *FEMS Microbiology Letters* **163**: 185-192.

[111] Winson MK, Camara M, Latifi A, Foglino M, Chhabra SR, Daykin M, Bally M, Chaptin V, Salmond GP, Bycroft BW (1995) Multiple N-acyl-L-homoserine lactone signal molecules regulate production of virulence determinants and secondary metabolites in *Pseudomonas aeruginosa*. *Proceedings of the National Academy of Sciences of the United States of America* **92**: 9427-9431.

[112] Winzer K, Hardie KR, Williams P (2002) Bacterial cell-to-cell communication: Sorry, can't talk now - gone to lunch! *Current Opinion in Microbiology* **5**: 216-222.

[113] Wöllner K, Chen X, Kremmer E, Krämer PM (2010) Comparative SPR and ELISA characterisation of a monoclonal antibody with N-acyl homoserine lactones. *Analytica Chimica Acta* **683**: 113-118.

[114] Wöllner K, Starke M, Chen X, Kremmer E, Krämer PM, Two optical immunosensors for the detection of homoserine molecules with newly developed monoclonal antibodies, *Sensors and Actuators B*, submitted

[115] www.virology.ws.

[116] Yan L, Allen MS, Simpson ML, Saylor GS; Cox CD (2007) Direct quantification of N-(3-oxo-hexanoyl)-l-homoserine lactone in culture supernatant using a whole-cell bioreporter. *Journal of Microbiological Methods* **68**: 40-45.

[117] Yates EA, Philipp B, Buckley C, Atkinson S, Chhabra SR, Sockett RE, Goldner M, Dessaux Y, Cámara M, Smith H, Williams P (2002) N-Acylhomoserine Lactones Undergo Lactonolysis in a pH-, Temperature-, and Acyl Chain Length-Dependent Manner during Growth of *Yersinia pseudotuberculosis* and *Pseudomonas aeruginosa*. *Infection and Immunity* **70**: 5635-5646.

[118] Zaitsev K & Ohkura Y (1980) New fluorogenic substrates for horseradish peroxidase: Rapid and sensitive assays for hydrogen peroxide and the peroxidase. *Analytical Biochemistry* **109**: 109-113.

[119] Zhu J, Beaber JW, More MI, Fuqua C, Eberhard A & Winans SC (1998) Analogs of the autoinducer 3-oxooctanoyl-homoserine lactone strongly inhibit activity of the TraR protein of *Agrobacterium tumefaciens*. *Journal of Bacteriology* **180**: 5398-5405.

8 Publications

Paper:

- **Chen X**, Kremmer E, Gouzy MF, Clausen E, Starke M, Wöllner K, Pfister G, Hartmann A, Krämer PM (2010), Development and characterisation of rat monoclonal antibodies for *N*-acylated homoserine lactones, *Analytical Bioanalytical Chemistry*, DOI: 10.1007/s00216-010-4017-9, vol. 398, 2655-2667
- **Chen X**, Buddrus-Schiemann K, Rothballe M, Krämer PM, Hartmann A (2010). Detection of AHL quorum sensing molecules in *Burkholderia cepacia* culture supernatants with enzyme-linked immunosorbent assays, *Analytical Bioanalytical Chemistry*, , DOI: 10.1007/s00216-010-4045-5, vol. 398, 2669-2676
- Wöllner K, **Chen X**, Kremmer E, Krämer PM (2010), Comparative SPR and ELISA characterisation of a monoclonal antibody with *N*-acyl homoserine lactones, *Analytica Chimica Acta*, , DOI: 10.1016/j.aca.2010.10.015, vol. 683: 113-118
- Wöllner K, Starke M, **Chen X**, Kremmer E, Krämer PM (2010), Two optical immunosensors for the detection of homoserine molecules with newly developed monoclonal antibodies, *Sensors and Actuators B*, submitted

Oral presentation:

- **Chen X**, Kremmer E, Gouzy MF, Clausen E, Kleinschmidt U, Hartmann A, Krämer PM, Developing of anti-homoserine lactone monoclonal antibodies and their characterisation with enzyme-linked immunosorbent assay (ELISA), Nov 2009, 1st Bio-sensing Technology Conference, Bristol, UK

Poster:

- Wöllner K, **Chen X**, Keß M, Clausen E, Kremmer E, Krämer PM, SPR-based immunosensor for the detection of homoserine lactones, Nov 2009, 1st Bio-sensing Technology Conference, Bristol, UK

9 Acknowledgements

I would like to take the opportunity here to thank all the people who have supported me and helped me in different ways for the duration of my PhD study. Without any of them, I could not have come so far in my doctoral studies. First of all, I would like to thank PD. Dr. Petra M. Krämer and Prof. Anton Hartmann for their excellent supervision and guidance during my PhD study. It was not always about having good antibodies or assays, but also about how to be a proper scientist! They set a great example to me and showed me the importance of being conscientious, open and flexible as a scientist.

Secondly, I would like to thank my colleagues in the Biosensor group, Dr. Karin Wöllner, Ms. Ulrike Kleinschmidt, Ms. Melanie Kess, Mrs. Ana Nowak, Ms. Mandy Starke, Dr. Marie Gouzy and Mr. Stephan Oxynus for the endless support (experiment, data treatment, ideas and encouragements) and the great fun we had together. You all made my time in Helmholtz Zentrum München more colourful and unforgettable.

I also want to thank all the (non-biosensors) cooperation partners in my study. I thank Dr. Elisabeth Kremmer and her group for their great work on HSL antibodies production. I am also very grateful for my great cooperation with Dr. Michael Rothballer, Dr. Katharina Buddrus-Schiemann, Ms. Tina Riedel, Ms. Dan Li and Dr. Fang Wang for application of antibodies and for the very helpful suggestions you gave me. And I thank Dr. Ernst Clausen, Dr. Gerd Pfister, Dr. Agnes Fekete, Dr. Norbert Hertkorn, Dr. Andrea Bauer, and Mr. Konrad Hinderland for their synthesis work. Without your work, I would have nothing to work on.

Many thanks for my father, mother and brother for their long term support. Although the time zone is 6-7 hours different, I know you are there for me all the time. Finally I would like to thank my laogong Barry, for his encouragement, love and the sharing of the pain.

10 Attachments

Attach. 1 Chemicals for synthesis

Chemicals	MW	MF	Company
Sodium cyanoborohydride	62.8	NaBH ₃ CN	Sigmal aldrich,Steinheim Germany
Potassium hydroxide	56.1	KOH	Fluka,Steinheim Germany
Toluene	92.1	C ₇ H ₈	Fluka,Steinheim Germany
Benzyl bromide	171.0	C ₇ H ₇ Br	Fluka,Steinheim Germany
Tetrabutylammonium bromide	322.4	C ₁₀ H ₃₆ BrN	Fluka,Steinheim Germany
Sebacid acid	202.3	C ₁₀ H ₁₈ O ₄	Fluka,Steinheim Germany
Ethyl acetate	88.1	C ₄ H ₈ O ₂	Riedel de Haen, Seelze, Germany
Meldrum's acid	144.1	C ₆ H ₈ O ₄	Fluka,Steinheim Germany
Dichloromethane (dry)	84.93	CH ₂ Cl ₂	Fluka,Steinheim Germany
4-Dimethylaminopyridine	122.2	C ₇ H ₁₀ N ₂	Fluka,Steinheim Germany
Cyclohexane	84.2	C ₆ H ₁₂	Riedel de Haen, Seelze, Germany
Hydrochloric acid 32%	36.5	HCl	Merck, Darmstadt, Germany
Sodium chloride	58.4	NaCl	Merck, Darmstadt, Germany
Sodium hydrogen carbonate	84.0	NaHCO ₃	Merck, Darmstadt, Germany
Ammonium chloride	53.5	NH ₄ Cl	Riedel de Haen, Seelze, Germany
Triethylamine	101.2	C ₆ H ₁₅ N	Fluka,Steinheim Germany
Acetonitrile	41.1	C ₂ H ₃ N	Fluka,Steinheim Germany
(S)-2-Amino-4-butyrolactone hydrobromide	182.0	C ₄ H ₇ NO ₂ .HBr	Fluka,Steinheim Germany
Acetonitrile Chromasolv 34851	41.1	C ₂ H ₃ N	Riedel de Haen, Seelze, Germany

Attach. 2 Buffers and media used in this study

Buffer/medium	pH	Composition for 1 L buffer	
40 mM PBS	7.6	NaH ₂ PO ₄	0.689 g
		Na ₂ HPO ₄	6.23 g
		NaCl	5.84 g
		MilliQ H ₂ O	1000 mL
<hr/>			
200 mM PBS	7.5-7.8	NaH ₂ PO ₄	3.45 g
		Na ₂ HPO ₄	31.15 g
		NaCl	5.84 g
		MilliQ H ₂ O	1000 mL
<hr/>			
20 mM PBS dialysis buffer	7.8	200 mM PBS	100 mL
		MilliQ H ₂ O	900 mL
<hr/>			
4 mM PBST wash buffer	7.8	40 mM PBS	100 mL
		Tween 20	500 µL
		MilliQ H ₂ O	900 mL
<hr/>			
50 mM carbonate coating buffer	9.6-9.8	Na ₂ CO ₃	1.59 g
		NaHCO ₃	2.94 g
		MilliQ H ₂ O	1000 mL
<hr/>			
100 mM sodiumacetat substrate buffer	5.5	C ₂ H ₃ NaO ₂	8.2 g
		adjust with 1% (w/v) citric acid to pH 5.5	ca. 100 mL
		MilliQ H ₂ O	1000 mL (final volume)

10 mM HEPES with 2.5 mM CaCl₂	7.4	1M HEPES	10 mL	
		0.5M CaCl ₂ Solution	5 mL	
		adjust with 0.1M NaOH to pH 7.4	variable	
		MilliQ H ₂ O filled	1000 mL (final volume)	
10 mM HEPES	7.4	1M HEPES	10 mL	
		adjust with 0.1M NaOH to pH 7.4	variable	
		MilliQ H ₂ O filled	1000 mL (final volume)	
1 mM HEPES washbuffer	7.4	10 mM HEPES (with or without CaCl ₂)	100 mL	
		Tween 20	500 µL	
		MilliQ H ₂ O	900 mL	
0.2 M borate buffer	7.8	0.2 M boric acid	250 mL	
		0.05 M borax	24.5 mL	
		MilliQ H ₂ O	1000 mL (final volume)	
ABC medium modified from (Clark & Maaloe, 1967) 10 mL	6.8	A	(NH ₄) ₂ SO ₄ 2 g	100 mL
			Na ₂ HPO ₄ 6 g	
			KH ₂ PO ₄ 3 g	
			NaCl 3 g	
			H ₂ O _{dest} 100 mL	
		B	1 M MgSO ₄ x 6 H ₂ O 2 mL	900 mL
0.5 M CaCl ₂ x 2 H ₂ O 0.2 mL				

			0.01 M FeCl ₃ x 6 H ₂ 0.3 mL	
			H ₂ O _{dest} 900 mL	
		C	1M sodium citrate for <i>P. putida</i>	10 mL
			20 % (W/V) glucose for <i>B. cepacia</i>	10 mL
Mineral medium				
	7.0		Na ₂ HPO ₄ •2H ₂ O	2.9 g
			KH ₂ PO ₄	1.5 g
			NH ₄ NO ₃	1g
			MgSO ₄ •7H ₂ O	100 mg
			Ca(NO ₃) ₂ •4H ₂ O	50 mg
			MilliQ H ₂ O	1000 mL (final volume)
M9 medium				
	6.9		1M KH ₂ PO ₄	22 mL
			10% (W/V) NH ₄ Cl	10mL
			1M CaCl ₂	100 µL
			1M MgSO ₄	2 mL
			20 % (W/V) glucose	9 mL
			MilliQ H ₂ O	1000 mL (final volume)
NB (nutrient broth) medium				
	7.0		Pepton	5 g
			Meatextract	3 g
			MilliQ H ₂ O	1000 mL

Attach. 3 First screening of HSL1 and HSL1/2 antibodies with coating antigen format

No.	Mabs	Coating antigen [1 µg mL ⁻¹]	Analyte						
			HSL 1	HSL 2	C4-HSL	C6-HSL	3oxo-C6-HSL	3oxo-C8-HSL	3oxo-C12-HSL
1	HSL1/2-1A5	HSL 1-BSA	-	-		-	-	-	-
		HSL 2-BSA	-	-		-	-	-	-
2	HSL1/2-1C7	HSL 1-BSA	-	-		-	-	-	-
		HSL 2-BSA	-	-		-	-	-	-
3	HSL1/2-1D5	HSL 1-BSA	-	-		-	-	-	-
		HSL 2-BSA	-	-		-	-	-	-
4	HSL1/2-1D12	HSL 1-BSA	-	-		-	-	-	-
		HSL 2-BSA	-	-		-	-	-	-
5	HSL1/2-1E6	HSL 1-BSA	-	-		-	-	-	-
		HSL 2-BSA	-	-		-	-	-	-
6	HSL1/2-1F6	HSL 1-BSA	++	-		-	-	+	-
		HSL 2-BSA	-	-		-	-	-	-
7	HSL1/2-1F10	HSL 1-BSA	-	-		-	-	-	-
		HSL 2-BSA	-	-		-	-	-	-
8	HSL1/2- 1G4	HSL 1-BSA	-	-	-	-	-	-	-
		HSL 2-BSA	-	-	-	-	-	-	-
9	HSL1/2- 2A9	HSL 1-BSA	-	-	-	-	-	-	-
		HSL 2-BSA	-	-	-	-	-	-	-
10	HSL1/2-2A10	HSL 1-BSA	-	-		-	-	-	-
		HSL 2-BSA	-	-		-	-	-	-
11	HSL1/2-2C1	HSL 1-BSA	-	-	-	-	-	-	-
		HSL 2-BSA	-	-	-	-	-	-	-
12	HSL1/2-2C10	HSL 1-BSA	+	-	-	-	-	+	-

		HSL 2-BSA	++	+	-	++	++	++	+
13	HSL1/2-D11	HSL 1-BSA	-	-		-	-	-	-
		HSL 2-BSA	-	-		-	-	-	-
14	HSL1/2-2E2	HSL 1-BSA	-	-		-	-	-	-
		HSL 2-BSA	-	-		-	-	-	-
15	HSL1/2-2E5	HSL 1-BSA	-	-		-	-	-	-
		HSL 2-BSA	-	-		-	-	-	-
16	HSL1/2-2F6	HSL 1-BSA	-	-	-	-	-	-	-
		HSL 2-BSA	-	-	-	-	-	-	-
17	HSL1/2-2G8	HSL 1-BSA	-	-		-	-	-	-
		HSL 2-BSA	-	-		-	-	-	-
18	HSL1/2-2G10	HSL 1-BSA	-	-		-	-	+	-
		HSL 2-BSA	+	+		+	-	++	-
19	HSL1/2-3A5	HSL 1-BSA	-	-	-	-	-	-	-
		HSL 2-BSA	-	-	-	-	-	-	-
20	HSL1/2-3A7	HSL 1-BSA	-	-	-	-	-	-	-
		HSL 2-BSA	+	-	-	-	-	-	-
21	HSL1/2-3A11	HSL 1-BSA	-	-	-	-	-	-	-
		HSL 2-BSA	-	-	-	-	-	-	-
22	HSL1/2-3A12	HSL 1-BSA	-	-	-	-	-	-	-
		HSL 2-BSA	-	-	-	-	-	-	-
23	HSL1/2-3B11	HSL 1-BSA	-	-	-	-	-	-	-
		HSL 2-BSA	-	-	-	-	-	-	-
24	HSL1/2-3C4	HSL 1-BSA	-	-	-	-	-	-	-
		HSL 2-BSA	+	-	-	-	-	-	-
25	HSL1/2-3C11	HSL 1-BSA	-	-	-	-	-	-	-
		HSL 2-BSA	-	-	-	-	-	-	-

26	HSL1/2-3C12	HSL 1-BSA	-	-	-	-	-	-	-
		HSL 2-BSA	+	-	-	+	-	-	-
27	HSL1/2-3D2	HSL 1-BSA	-	-	-	-	-	-	-
		HSL 2-BSA	-	-	-	-	-	-	-
28	HSL1/2-3E7	HSL 1-BSA	-	-	-	-	-	-	-
		HSL 2-BSA	-	-	-	-	-	-	-
29	HSL1/2-3F10	HSL 1-BSA	-	-	-	-	-	-	-
		HSL 2-BSA	-	-	-	-	-	-	-
30	HSL1/2-4A2	HSL 1-BSA	-	-	-	-	-	-	-
		HSL 2-BSA	+	-	-	-	-	-	-
31	HSL1/2-4A7	HSL 1-BSA	-	-	-	-	-	-	-
		HSL 2-BSA	++	-	-	-	+	+	+
32	HSL1/2-4B12	HSL 1-BSA	-	-	-	-	-	-	-
		HSL 2-BSA	++	-	-	+	-	-	-
33	HSL1/2-4C3	HSL 1-BSA	-	-	-	-	-	-	-
		HSL 2-BSA	+	-	-	-	-	-	-
34	HSL1/2-4C10	HSL 1-BSA	-	-	-	-	-	-	-
		HSL 2-BSA	+	-	-	+	-	-	+
35	HSL1/2-4E6	HSL 1-BSA	-	-	-	-	-	-	-
		HSL 2-BSA	-	-	-	-	-	-	-
36	HSL1/2-4G6	HSL 1-BSA	-	-	-	-	-	-	-
		HSL 2-BSA	-	-	-	-	-	-	-
37	HSL1/2-4G7	HSL 1-BSA	-	-	-	-	-	-	-
		HSL 2-BSA	-	-	-	-	-	-	-
38	HSL1/2-4G11	HSL 1-BSA	-	-	-	-	-	-	-
		HSL 2-BSA	+	-	-	+	-	-	-
39	HSL1/2-4H1	HSL 1-BSA	-	-	-	-	-	-	-

		HSL 2-BSA	-	-	-	-	-	-	-
40	HSL1/2-4H5	HSL 1-BSA	+	-	-	-	-	-	-
		HSL 2-BSA	++	-	-	++	++	++	+
41	HSL1/2-6C5	HSL 1-BSA	-	-	-	-	-	-	-
		HSL 2-BSA	-	-	-	-	-	-	-
42	HSL1/2-6D6	HSL 1-BSA	-	-	-	-	-	-	-
		HSL 2-BSA	-	-	-	-	-	-	-
43	HSL1/2-7A8	HSL 1-BSA	-	-	-	-	-	-	-
		HSL 2-BSA	+	-	-	-	-	-	-
44	HSL1/2-7B2	HSL 1-BSA	-	-	-	-	-	-	-
		HSL 2-BSA	-	-	-	-	-	-	-
45	HSL1/2-8C6	HSL 1-BSA	-	-	-	-	-	-	-
		HSL 2-BSA	-	-	-	-	-	-	-
46	HSL1/2-8E5	HSL 1-BSA	-	-	-	-	-	-	-
		HSL 2-BSA	+	-	-	-	-	-	-
47	HSL1/2-8F4	HSL 1-BSA	-	-	-	-	-	+	-
		HSL 2-BSA	-	-	-	-	-	-	-
48	HSL1/2-10E1	HSL 1-BSA	-	-	-	-	-	-	-
		HSL 2-BSA	-	-	-	-	-	-	-
49	HSL1/2-11D10	HSL 1-BSA	-	-	-	-	-	-	-
		HSL 2-BSA	-	-	-	-	-	-	-
50	HSL1/2-12C7	HSL 1-BSA	-	-	-	-	-	-	-
		HSL 2-BSA	+	-	-	-	-	-	-
51	HSL1/2-12E6	HSL 1-BSA	-	-	-	-	-	-	-
		HSL 2-BSA	-	-	-	-	-	-	-
52	HSL1-1A5	HSL 1-BSA	-	-	-	-	-	-	-
		HSL 2-BSA	++	-	+	+	+	++	+

53	HSL1-3D6	HSL 1-BSA	-	-	-	-	-	-	-
		HSL 2-BSA	-	-	-	-	-	-	-
54	HSL1-8A7	HSL 1-BSA	-	-	-	-	-	-	-
		HSL 2-BSA	-	-	-	-	-	-	-
55	HSL1-8E1	HSL 1-BSA	-	-	-	-	-	-	-
		HSL 2-BSA	++	-	-	-	+	++	+
56	HSL1-9E9	HSL 1-BSA	-	-	-	-	-	-	-
		HSL 2-BSA	-	-	-	-	-	-	-
57	HSL1-11D1	HSL 1-BSA	-	-	-	-	-	-	-
		HSL 2-BSA	-	-	-	-	-	-	-
58	HSL1-11F9	HSL 1-BSA	-	-	-	-	-	-	-
		HSL 2-BSA	-	-	-	-	-	-	-
59	HSL1-12E6	HSL 1-BSA	-	-	-	-	-	-	-
		HSL 2-BSA	-	-	-	-	-	-	-
60	HSL2-10A6	HSL 1-BSA	-	-	-	-	-	-	-
		HSL 2-BSA	-	-	-	-	-	-	-

The symbols in table: ++: % control \leq 30%; +: % control 30%-60%; -: % control \geq 60%.

Attach. 4 Characterisation of selected HSL4 mAbs with enzyme-tracer format

Antobody	Enzyme-Tracer	C4-HSL	C8-HSL	3oxo-C8-HSL	C10-HSL
HSL4-2F12	HSL1-HRP 1:500	-	+	-	+
	HSL1-HRP 1:1000	-	+	-	+
	HSL3-HRP 1:500	-	-	-	-
	HSL3-HRP 1:1000	-	-	-	+
HSL4-4B5	HSL1-HRP 1:500	-	-	-	+
	HSL1-HRP 1:1000	-	-	-	+
	HSL3-HRP 1:500	-	-	-	-
	HSL3-HRP 1:1000	-	-	-	-
HSL4-4B12	HSL1-HRP 1:500	-	-	-	-
	HSL1-HRP 1:1000	-	-	-	-
	HSL3-HRP 1:500	-	-	-	-
	HSL3-HRP 1:1000	-	-	-	-
	HSL1-HRP 1:2000	-	-	-	+
	HSL1-HRP 1:4000	-	+	-	+
	HSL3-HRP 1:2000	-	-	-	+
	HSL3-HRP 1:4000	-	+	-	+
HSL4-4C9	HSL1-HRP 1:500	+	+	+	+
	HSL1-HRP 1:1000	-	+	-	+
	HSL3-HRP 1:500	-	+	-	+
	HSL3-HRP 1:1000	-	+	-	+
HSL4-5D6	HSL1-HRP 1:500	-	-	-	-
	HSL1-HRP 1:1000	-	-	-	-
	HSL3-HRP 1:500	-	-	-	-
	HSL3-HRP 1:1000	-	-	-	-
	HSL1-HRP 1:2000	-	-	-	+
	HSL1-HRP 1:4000	-	+	-	+
	HSL3-HRP 1:2000	-	-	-	-
	HSL3-HRP 1:4000	-	-	-	-

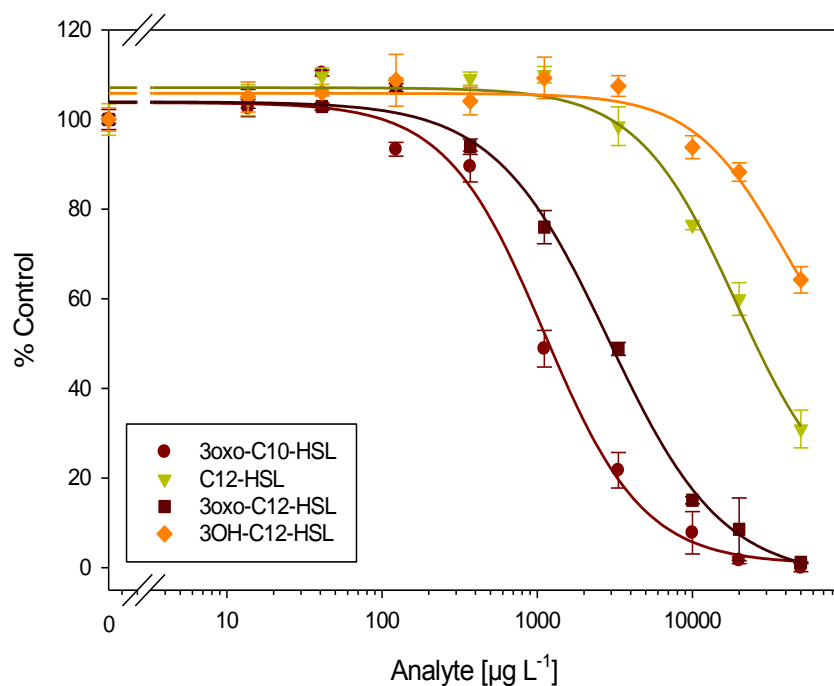
HSL4-5D7	HSL1-HRP 1:500	-	-	-	-
	HSL1-HRP 1:1000	-	-	-	+
	HSL3-HRP 1:500	-	-	-	+
	HSL3-HRP 1:1000	-	-	-	+
HSL4-5E4	HSL1-HRP 1:500	-	-	-	-
	HSL1-HRP 1:1000	-	-	-	-
	HSL3-HRP 1:500	-	-	-	-
	HSL3-HRP 1:1000	-	-	-	-
HSL4-5E12	HSL1-HRP 1:500	-	-	-	-
	HSL1-HRP 1:1000	-	-	-	-
	HSL3-HRP 1:500	-	-	-	-
	HSL3-HRP 1:1000	-	-	-	-
	HSL1-HRP 1:2000	-	-	-	+
	HSL1-HRP 1:4000	-	+	-	+
	HSL3-HRP 1:2000	-	-	-	-
	HSL3-HRP 1:4000	-	-	-	+
HSL4-5H3	HSL1-HRP 1:500	-	+	-	-
	HSL1-HRP 1:1000	-	+	-	+
	HSL3-HRP 1:500	+	+	-	+
	HSL3-HRP 1:1000	+	+	-	+
HSL4-6D3	HSL1-HRP 1:500	-	-	-	+
	HSL1-HRP 1:1000	-	+	-	+
	HSL3-HRP 1:500	-	-	-	-
	HSL3-HRP 1:1000	-	-	-	-
	HSL1-HRP 1:2000	-	+	-	+
	HSL1-HRP 1:4000	-	+	-	+
	HSL3-HRP 1:2000	-	+	-	+
	HSL3-HRP 1:4000	-	+	-	+
HSL4-6F6	HSL1-HRP 1:500	-	+	-	+
	HSL1-HRP 1:1000	-	+	-	+
	HSL3-HRP 1:500	-	-	-	+

	HSL3-HRP 1:1000	-	+	-	+
HSL4-6H8	HSL1-HRP 1:500	+	+	+	-
	HSL1-HRP 1:1000	-	-	-	+
	HSL3-HRP 1:500	+	-	+	+
	HSL3-HRP 1:1000	+	+	+	+
HSL4-8B8	HSL1-HRP 1:500	-	-	-	-
	HSL1-HRP 1:1000	-	-	-	-
	HSL3-HRP 1:500	-	-	-	-
	HSL3-HRP 1:1000	-	-	-	-
	HSL1-HRP 1:2000	-	-	-	+
	HSL1-HRP 1:4000	-	+	-	+
	HSL3-HRP 1:2000	-	-	-	-
	HSL3-HRP 1:4000	-	-	-	-
HSL4-8D8	HSL1-HRP 1:500	+	-	-	-
	HSL1-HRP 1:1000	-	-	-	+
	HSL3-HRP 1:500	-	-	-	-
	HSL3-HRP 1:1000	+	-	-	-
	HSL1-HRP 1:2000	-	+	-	+
	HSL1-HRP 1:4000	-	-	-	+
	HSL3-HRP 1:2000	-	-	-	+
	HSL3-HRP 1:4000	-	+	-	+
HSL4-8E2	HSL1-HRP 1:500	-	-	-	-
	HSL1-HRP 1:1000	-	-	-	-
	HSL3-HRP 1:500	-	-	-	-
	HSL3-HRP 1:1000	-	-	-	+
	HSL1-HRP 1:2000	-	-	-	-
	HSL1-HRP 1:4000	-	-	-	-
	HSL3-HRP 1:2000	-	-	-	-
	HSL3-HRP 1:4000	-	-	-	-
HSL4-8H10	HSL1-HRP 1:500	-	-	-	-
	HSL1-HRP 1:1000	-	-	-	-

HSL3-HRP 1:500	-	-	-	-
HSL3-HRP 1:1000	-	-	-	-
HSL1-HRP 1:2000	-	-	-	+
HSL1-HRP 1:4000	-	-	-	+
HSL3-HRP 1:2000	-	-	-	-
HSL3-HRP 1:4000	-	-	-	-

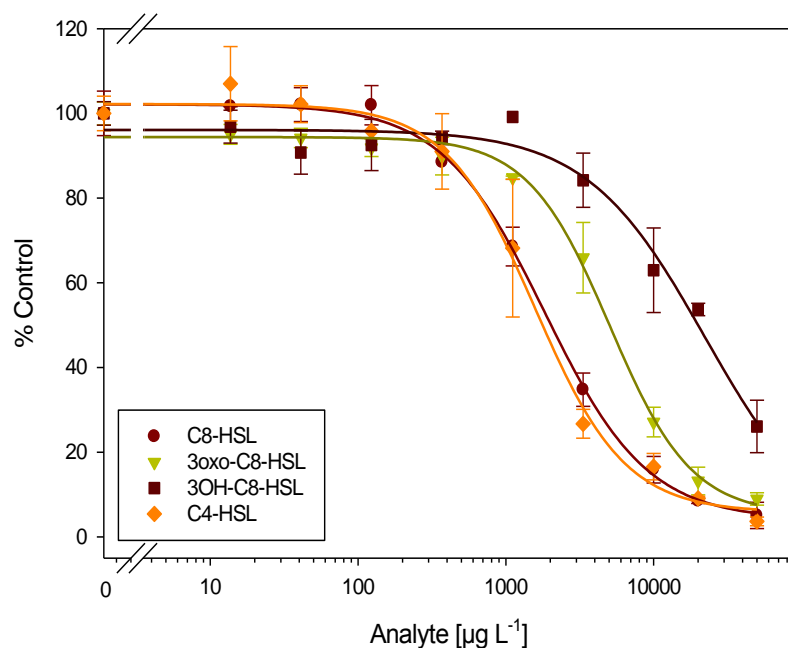
Coating with $2 \mu\text{g mL}^{-1}$ protein G, antibody cultural supernatant was 1:50 or 1:100 diluted in PBS, the symbols in table: ++: % control $\leq 30\%$; +: % control 30%-60%; -: % control $\geq 60\%$.

Attach. 5 HSL1-8E1 coating antigen format standard curves



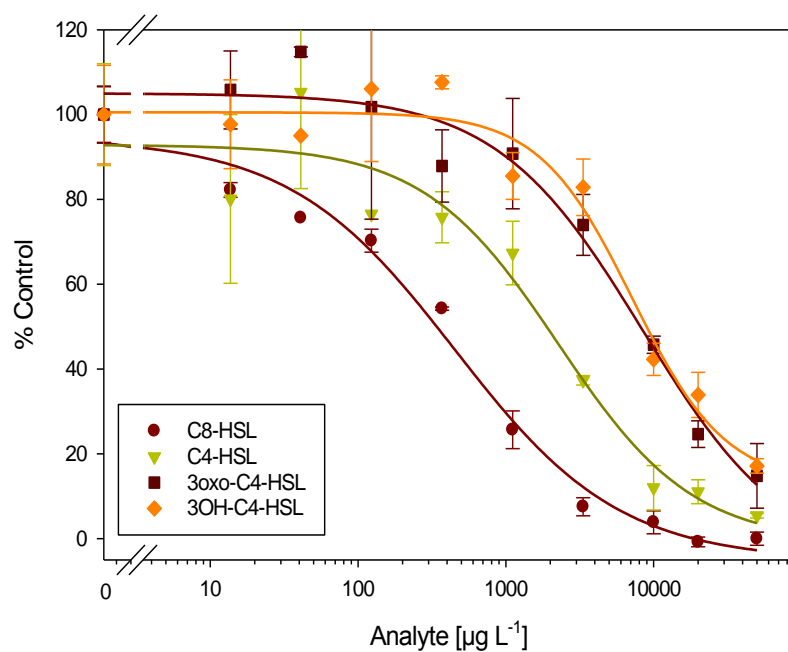
Standard curves for 3-oxo-C10-HSL, C12-HSL, 3-oxo-C12-HSL, and 3-OH-C12-HSL with the coating antigen format, using mAb HSL1-8E1 and HSL2-BSA-r2. Assay conditions: HSL1-8E1 800 ng mL^{-1} , HSL2-BSA-r2 $2 \mu\text{g mL}^{-1}$, GAR-HRP 40 ng mL^{-1} . Four parameter curve-fitting data are given in parentheses: *red circles* 3-oxo-C10-HSL (A 103.7, B -1.36, C $1112 \mu\text{g L}^{-1}$, D 0.84, R^2 0.996), *yellow green inverted triangles* C12-HSL (A 107.1, B -1.36, C $19250 \mu\text{g L}^{-1}$, D 10.8, R^2 0.992), *brown squares* 3-oxo-C12-HSL (A 103.9, B -1.18, C $2886 \mu\text{g L}^{-1}$, D -2.35, R^2 0.999), and *orange rhombuses* 3-OH-C12-HSL (A 105.8, B -1.46, C $39292 \mu\text{g L}^{-1}$, D 35.3, R^2 0.974).

Attach. 6 HSL4-5E12 coating antigen format standard curves



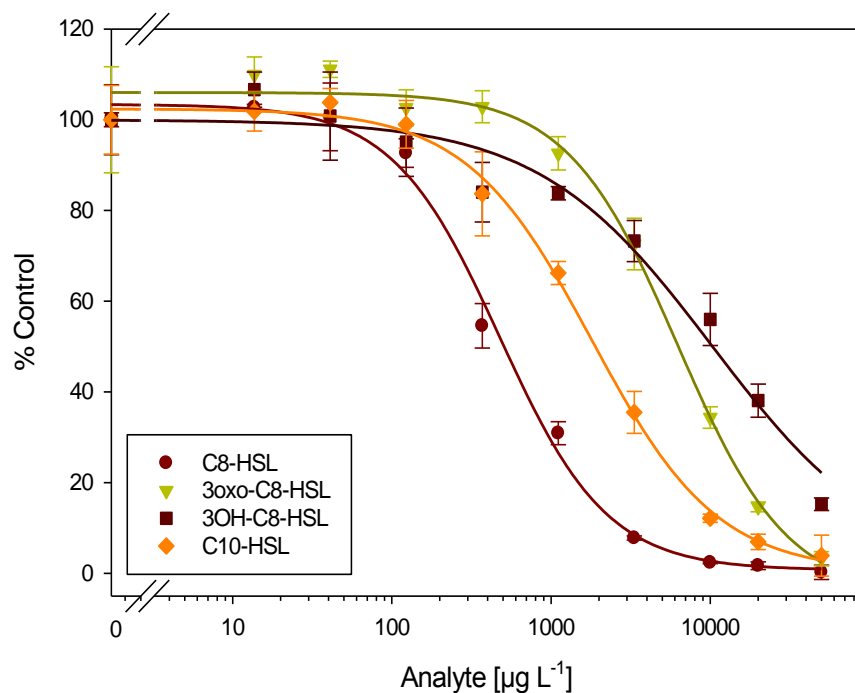
Standard curves for C8-HSL, 3-oxo-C8-HSL, 3-OH-C8-HSL, and C4-HSL with the coating antigen format, using mAb HSL4-5E12 and HSL2-BSA-r1. Assay conditions: HSL4-5E12 400 ng mL⁻¹, HSL2-BSA-r1 2 µg mL⁻¹, GAR-HRP 20 ng mL⁻¹. Four parameter curve-fitting data are given in parentheses: *red circles* C8-HSL (A 102.1, B -1.25, C 1829 µg L⁻¹, D 4.04, R² 0.999), *yellow green inverted triangles* 3-oxo-C8-HSL (A 94.4, B -1.57, C 5054 µg L⁻¹, D 5.23, R² 0.996), *brown squares* 3-OH-C8-HSL (A 96.1, B -1.08, C 22214 µg L⁻¹, D -1.68, R² 0.988), and *orange rhombuses* C4-HSL (A 102.2, B -1.42, C 1577 µg L⁻¹, D 5.78, R² 0.997).

Attach. 7 HSL4-6D3 coating antigen format standard curves



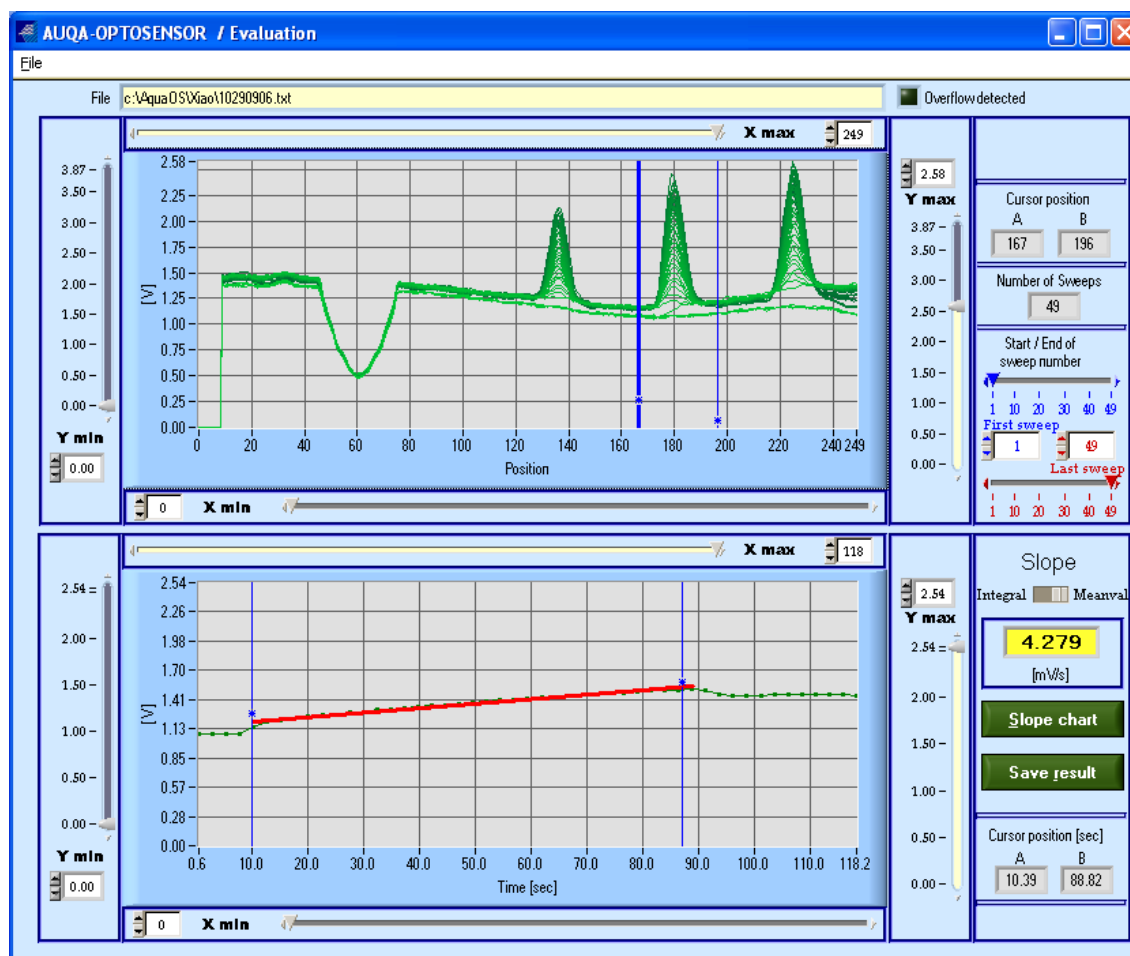
Standard curves for C8-HSL, C4-HSL, 3-oxo-C4-HSL, and 3-OH-C4-HSL with the coating antigen format, using mAb HSL4-6D3 and HSL2-BSA-r2. Assay conditions: HSL4-6D3 cultural supernatant 1:200, HSL2-BSA-r2 2 $\mu\text{g mL}^{-1}$, GAR-HRP 20 ng mL^{-1} . Four parameter curve-fitting data are given in parentheses: *red circles* C8-HSL (A 94.4, B -0.78, C 451.5 $\mu\text{g L}^{-1}$, D -5.23, R^2 0.993), *yellow green inverted triangles* C4-HSL (A 92.9, B -0.95, C 2267 $\mu\text{g L}^{-1}$, D -1.05, R^2 0.976), *brown squares* 3-oxo-C4-HSL (A 105.0, B -0.88, C 8421 $\mu\text{g L}^{-1}$, D -6.65, R^2 0.987), and *orange rhombuses* 3-OH-C4-HSL (A 100.5, B -1.38, C 7175 $\mu\text{g L}^{-1}$, D 12.8, R^2 0.985).

Attach. 8 HSL4-4C9 coating antigen format standard curves



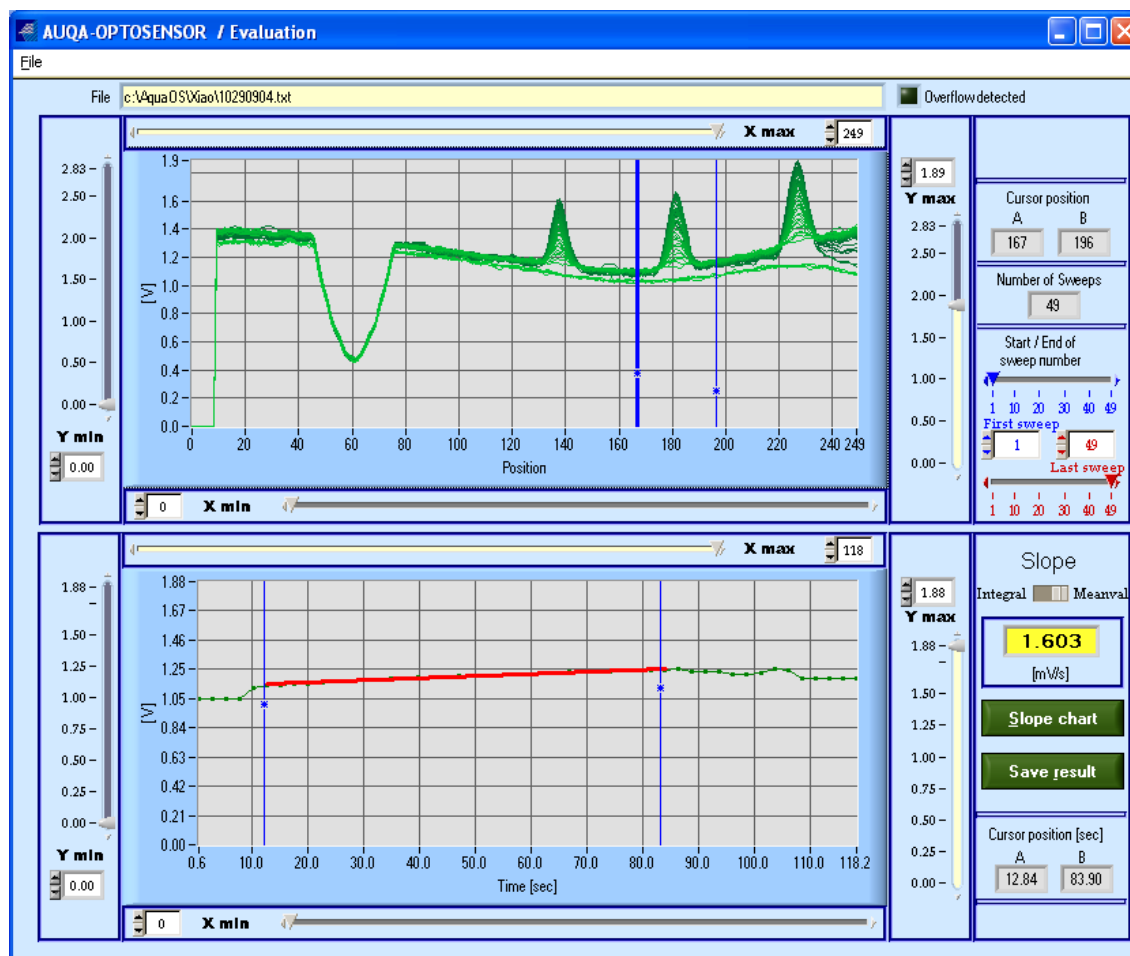
Standard curves for C8-HSL, 3-oxo-C8-HSL, 3-OH-C8-HSL, and C10-HSL with the coating antigen format, using mAb HSL4-4C9 and HSL2-BSA-r1. Assay conditions: HSL4-4C9 200 ng mL⁻¹, HSL2-BSA-r1 2 µg mL⁻¹, GAR-HRP 40 ng mL⁻¹. Four parameter curve-fitting data are given in parentheses: *red circles* C8-HSL (A 103.4, B -1.29, C 476 µg L⁻¹, D 0.71, R² 0.998), *yellow green inverted triangles* 3-oxo-C8-HSL (A 106.0, B -1.25, C 6227 µg L⁻¹, D -5.16, R² 0.997), *brown squares* 3-OH-C8-HSL (A 100.0, B -0.80, C 10349 µg L⁻¹, D 0, R² 0.986), and *orange rhombuses* C10-HSL (A 102.4, B -1.10, C 1807 µg L⁻¹, D 0.32, R² 0.999).

Attach. 9 AOS peaks of Oyster-645 labelled mAb HSL1/2-2C10 with analyte 3oxo-C10-HS concentration of $[55.5 \mu\text{g L}^{-1}]$



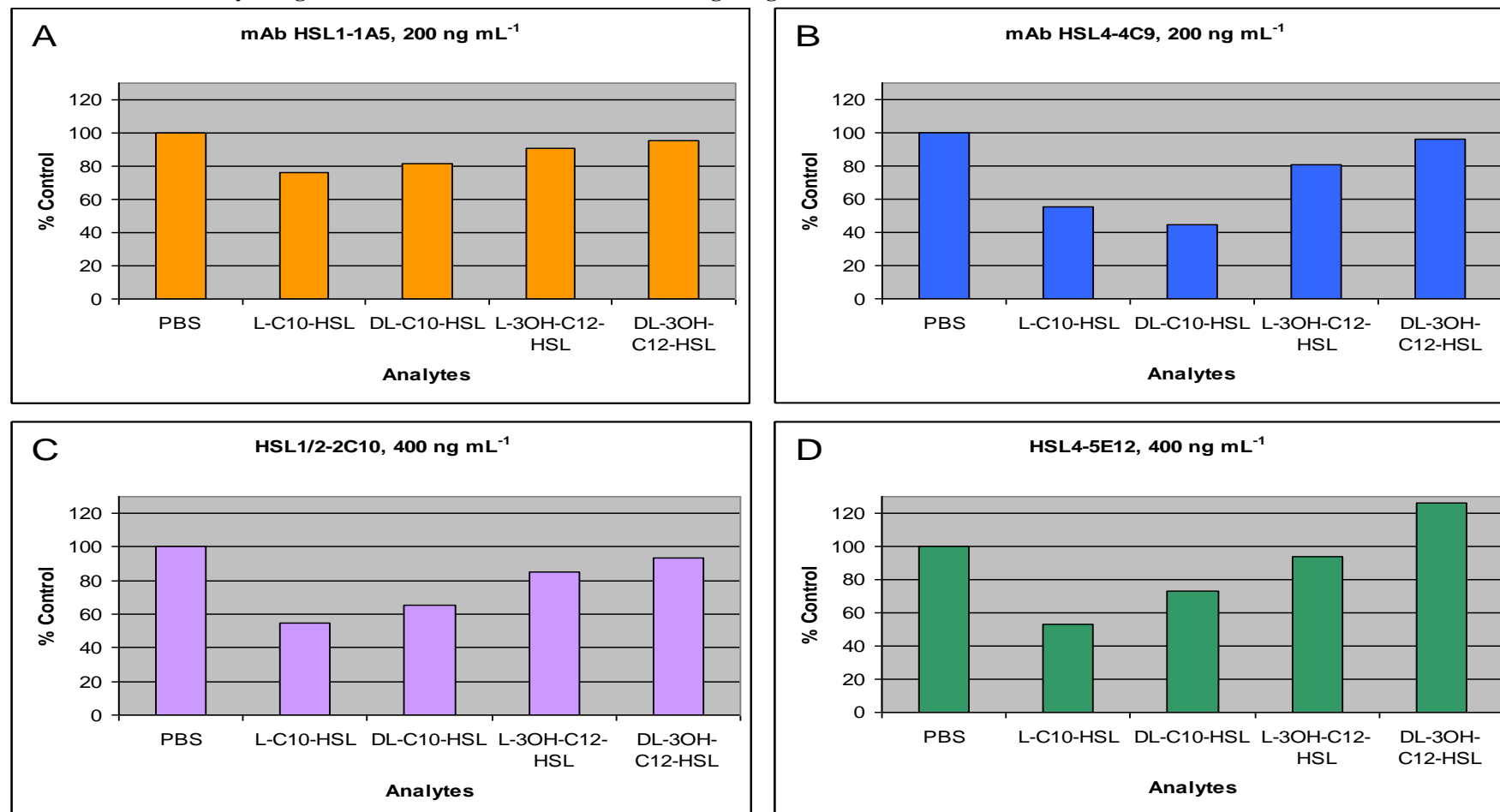
Assay condition: mAb HSL1/2-2C10 labelled with Oyster-645 (label degree 1:2), 48 ng mL^{-1} ; spotting with HSL2-BSA-r2 in 50 mM carbonate buffer, $\text{pH} = 9.6 + 0.05\%$ (v/v) Tween 20, $[3 \text{ mg mL}^{-1}]$ for peak left, $[2 \text{ mg mL}^{-1}]$ for peak middle and $[1 \text{ mg mL}^{-1}]$ for peak right; analyte 3oxo-C10-HS, $55 \mu\text{g L}^{-1}$. Slope value: peak left= 3.050 mV/s , peak middle 4.279 mV/s (value in the figure), and peak right= 4.337 mV/s .

Attach. 10 AOS peaks of Oyster-645 labelled mAb HSL1/2-2C10 with analyte 3oxo-C10-HS concentration of [123.3 $\mu\text{g L}^{-1}$]



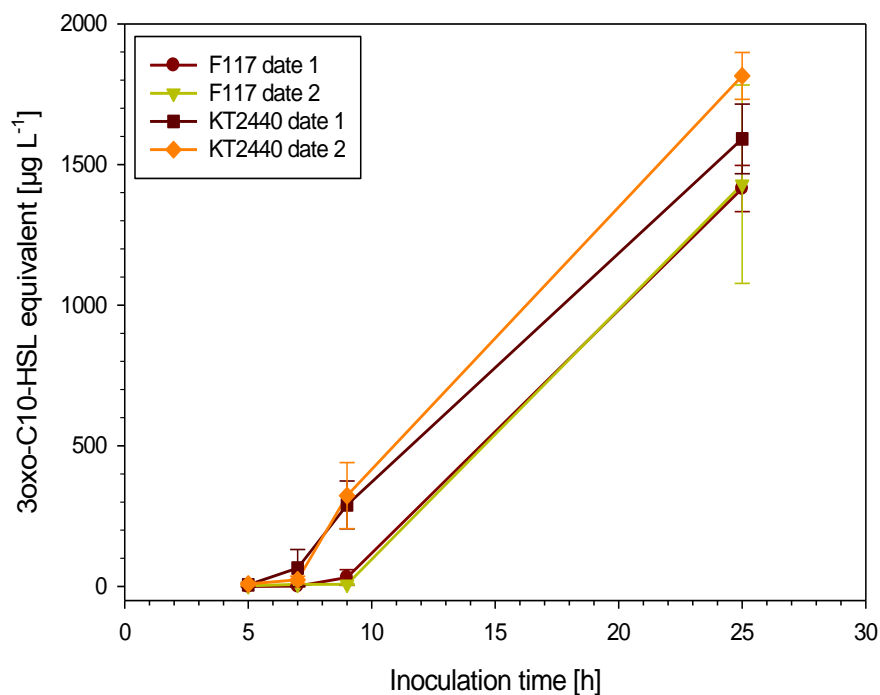
Assay condition: mAb HSL1/2-2C10 labelled with Oyster-645 (label degree 1:2), 48 ng mL⁻¹; spotting with HSL2-BSA-r2 in 50 mM carbonate buffer, pH = 9.6 + 0.05% (v/v) Tween 20, [3 mg mL⁻¹] for peak left, [2 mg mL⁻¹] for peak middle and [1 mg mL⁻¹] for peak right; analyte 3oxo-C10-HS, 123.3 $\mu\text{g L}^{-1}$. Slope value: peak left= 1.447 mV/s, peak middle 1.603 mV/s (value in the figure), and peak right= 1.515 mV/s.

Attach. 11 HSL antibody recognition of DL and L HSL isomers in coating antigen format ELISA



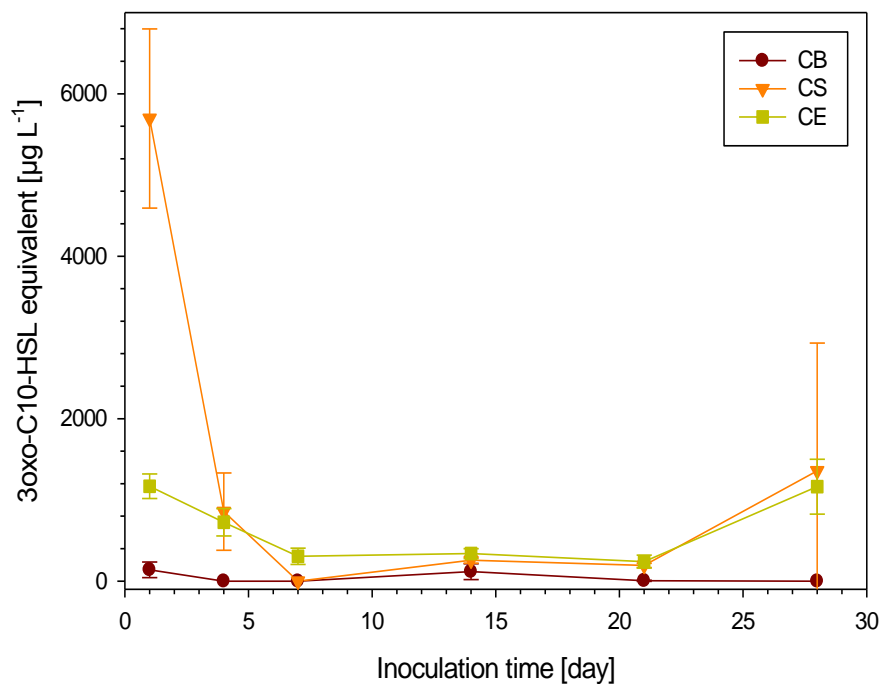
A: mAb HSL1-1A5 200 ng mL⁻¹, B: mAb HSL4-4C9 200 ng mL⁻¹, C: HSL1/2-2C10 400 ng mL⁻¹, D: HSL4-5E12 400 ng mL⁻¹. General assay condition: coating with HSL2-BSA-r2 2 μg mL⁻¹, GAR-HRP 20 ng mL⁻¹, all analytes 2000 μg L⁻¹

Attach. 12 *P. putida* IsoF and strain KT2440 supernatants HSL detection with different sampling time



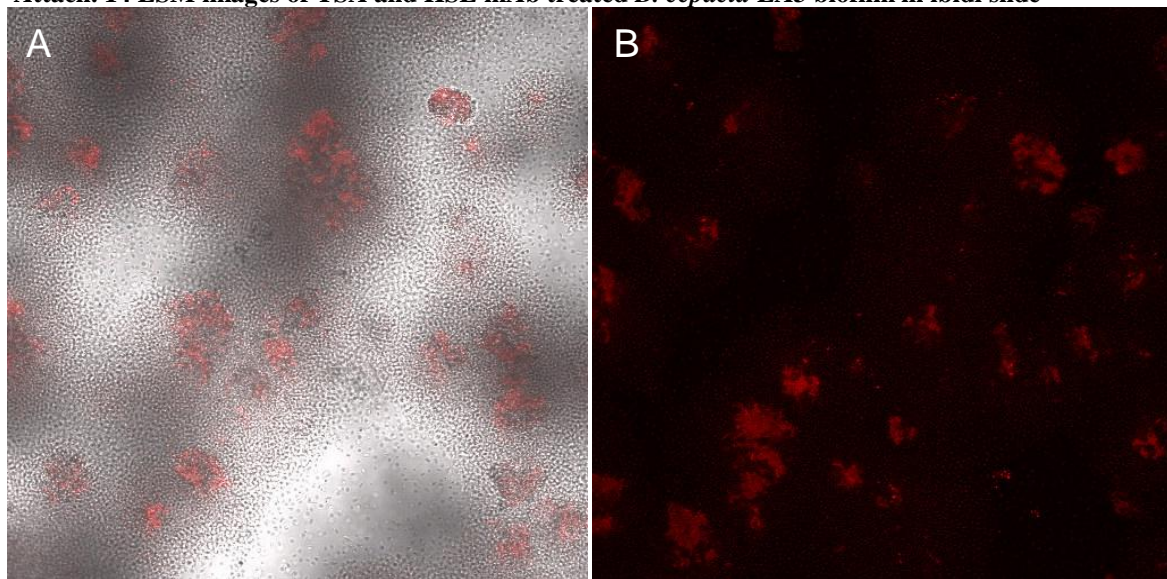
ELISA results with mAb HSL1/2-2C10 400 ng mL^{-1} in enzyme-tracer format.

Attach. 13 HSL detection in extracted soil samples with inoculated TCB community



B: blank, S: sterilised clay; S; E: established biofilm

Attach. 14 LSM images of TSA and HSL mAb treated *B. cepacia* LA3 biofilm in ibidi slide



A: biofilm incubated with 1:50 diluted TSA without HRP and HSL mAb; B: TSA signals on the biofilm with HSL1/2-2C10 but without GAR-HRP treatment. Pictures captured from Dr. Michael Rotballer.

Attach. 15 HSL3 antibody list

Antibody	Animal for immunisation	Subclass
HSL3-1D2	rat	IgG-2a
HSL3-2D11	rat	IgG-2a
HSL3-2F4	rat	IgG-2a
HSL3-8F6	rat	IgG-2c
HSL3-13F8	rat	IgG-2a
HSL3-2C4	mouse	IgG-2b
HSL3-4A1	mouse	IgG-2a
HSL3-4F7	mouse	IgG-2a

Curriculum Vitae

Personal data

Name/family name	Xiao Chen
Date of birth	04-May-1980
Place of birth	Wenling, China
Nationality	Chinese

Education

Doctoral

Apr 2007-May 2011	PhD student in Helmholtz Centre Munich, Institute of Ecological Chemistry; registered in Ludwig Maximilian University of Munich, department Biology
	Topic: developing and characterisation of an immunochemical test system for the determination of bacterial signal molecules (quorum sensing molecules)

Masters

Oct 2004-Sep 2007	Technical University of Munich, Weihenstephan
	Major: Environmental Ecology
	Master thesis: black carbon in soil after forest fire

Bachelor

Sep 1998-Jun 2002	Zhejiang University, China
	Major: Environment and Resource Management

Second degree

Sep 1999-Jun 2001	Zhejiang University, China
	Tourism Management Certification

German language school

Dec 2003-Mar 2004	Language School Colón, Hamburg
Apr 2004-Jun 2004	Sprachbörse, Munich

Part time work

Nov 2005-Feb 2007	Student assistant in chair of soil science, TUM
Dec 2006-Feb 2007	Student assistant in chair of plant nutrition, TUM